University of Liège
Faculty of Medicine
GIGA-Cancer

Metastasis Research Laboratory
Pr. Vincent Castronovo

Role of carbonyl stress in breast cancer progression and metastases development

Marie-Julie Nokin

Thesis submitted in support of the candidature to the PhD degree in Biomedical and Pharmaceutical Sciences

Promoters: Dr. Akeila Bellahcène and Pr. Vincent Castronovo

Academic year 2015-2016

University of Liège
Faculty of Medicine
GIGA-Cancer

Metastasis Research Laboratory
Pr. Vincent Castronovo

Role of carbonyl stress in breast cancer progression and metastases development

Marie-Julie Nokin

Thesis submitted in support of the candidature to the PhD degree in Biomedical and Pharmaceutical Sciences

Promoters: Dr. Akeila Bellahcène and Pr. Vincent Castronovo

Academic year 2015-2016

Imagination is more important than knowledge

Albert Einstein

Remerciements

Au terme de ces 4 années, je tiens, au travers de ces quelques lignes, à remercier toutes les personnes qui ont, de près ou de loin, contribué à la réalisation de cette thèse de doctorat.

Dans un premier temps, je remercie le Professeur **Vincent Castronovo** de m'avoir donné l'opportunité de travailler au sein de son Laboratoire. Votre exigence et votre rigueur resteront pour moi deux qualités indissociables du métier de chercheur. Je garderai toujours le souvenir de cette thèse comme d'une formidable aventure.

Je tiens à exprimer ma plus profonde reconnaissance au Docteur **Akeila Bellahcène** qui a supervisé jour après jour l'entièreté de ce travail. Akeila, merci pour la confiance de plus en plus importante que vous m'avez accordée ainsi que pour votre soutien, votre patience, vos conseils et votre disponibilité. Vous n'avez jamais hésité à me consacrer du temps dans votre bureau pour discuter, réfléchir et corriger nos écrits (parfois même au détriment de votre vie personnelle). Au travers de tout ce que nous avons traversé durant ces quatre années, vous m'avez transmis votre passion pour la recherche scientifique.

Je tiens également à remercier le Docteur **Olivier Peulen** pour ses conseils avisés et pour les heures passées à analyser statistiquement les résultats.

Merci aussi au Docteur **Andrei Turtoi** pour ses nombreuses remarques au cours des réunions qui ont contribué à l'amélioration de ce travail.

Un grand merci au Docteur **Paul Peixoto**, mon « papa du labo ». Merci pour ta gentillesse, ta disponibilité, tes conseils, ta pédagogie et tes indéniables qualités humaines. Tu resteras un modèle pour moi pour la transmission des techniques et des connaissances aux plus jeunes.

Je remercie également le Docteur **Arnaud Blomme**. Tes conseils, tes remarques et les discussions que nous avons échangées m'ont été d'une aide précieuse. Merci aussi pour ton perpétuel optimisme.

Merci à **Florence Durieux**. Je suis heureuse et fière de t'avoir guidée lors de ton mémoire. Merci pour ton aide précieuse, ta sympathie et tes conseils. Je sais que je peux toujours compter sur toi et j'espère être à la hauteur pour te rendre la pareille.

Je remercie également toutes les filles de la « MG team ». Merci à **Barbara Chiavarina** pour son aide et ses conseils. Merci à **Aurélie Henry** pour son aide et tous les bons moments que nous avons partagés. Merci à **Maude Gabriel** et **Christine Monseur** pour leur aide précieuse ces derniers mois.

Un tout grand merci aux techniciens du Laboratoire, **Naïma Maloujahmoum** et **Vincent Hennequière**. Merci à toi, Naïma, pour ton écoute, ton soutien, ta serviabilité et ton humour. Vincent, notre MacGyver du Labo, merci pour ton aide, tes conseils enrichissants et constructifs et ta disponibilité à toutes heures. Durant ces 4 années de thèse, j'ai toujours pu compter sur vous et je vous en suis très reconnaissante.

Je remercie également **Véronique Goffin** pour son aide logistique ainsi que tous les autres membres du Laboratoire de Recherche sur les Métastases. Une pensée toute particulière pour **Brunella Costanza** pour son coup de main avec les souris. Merci aussi à tous ceux dont j'ai croisé la route au Laboratoire et qui ont rendus ces 4 années inoubliables.

Mes remerciements vont aussi aux membres des différentes plateformes du GIGA, aux collaborateurs et aux membres du jury d'avoir consacré de leur temps à la lecture de ce travail.

Je remercie également mes amis pour leur présence et leur soutien durant toutes ces années. Je pense tout particulièrement à **Angélique**, **Anneline**, **Christelle**, **Delphine**, **Julie** et **Tania**. Je suis heureuse et fière d'avoir fait votre connaissance durant nos études universitaires et d'avoir toujours garder contact avec vous. Vous êtes des amies en or… Merci pour tout.

Je tiens à remercier tous les membres de ma famille et tout particulièrement mes parents. Merci, **Maman** et **Papa**, pour l'éducation et les valeurs que vous m'avez transmis. Merci d'avoir toujours cru en moi et de m'avoir toujours soutenue et encouragée. Merci aussi à mon petit frère, **Erwan**, d'avoir toujours été là. Je suis très fière de toi. Je vous aime très fort.

Enfin je remercie du fond du cœur mon Amoureux, **Michaël**. Merci à toi pour ta patience, pour ton soutien incommensurable et pour ta complicité. C'est un vrai bonheur de partager ma vie avec toi et je me réjouis déjà de notre avenir…

Je vous remercie tous et vous souhaite le meilleur pour la suite.

Marie-Julie

Avec le soutien de l'Université de Liège, du Fonds National de la Recherche Scientifique, du Télévie, du Fond Léon Fredericq et du Centre Anti-Cancéreux.

Table of contents

List of abbreviations

- **3-DG** 3-deoxyglucosone
- **AG** Aminoguanidine
- **AGEs** Advanced Glycation End-products
- **BBGC** S-p-Bromobenzylglutathione Cyclopentyl diester
- **CAM** Chorioallantoic Membrane
- **CTGF** Connective Tissue Growth Factor
- **DHAP** Dihydroxyacetone Phosphate
- **EMT** Epithelial to Mesenchymal Transition
- **ER** Estrogen Receptor
- **GAP** Glyceraldehyde-3-phosphate
- **Glo1/2** Glyoxalase 1/2
- **GO** Glyoxal
- **GSH** Glutathione
- **HG** High glucose
- **HIF1α** Hypoxia-inducible Factor 1α
- **Hsp27/90** Heat Shock Protein 27/90
- **IHC** Immunohistochemistry
- **LATS1** Large Tumor Suppressor 1
- **LDH** Lactate dehydrogenase
- **LG** Low Glucose
- **MAGEs** MG-Advanced Glycation End-products
- **MG** Methylglyoxal
- **MG-H** Hydroimidazolones
- **NLS** Nuclear Localization Signal
- **Nrf2** Nuclear factor erythroid 2-related factor 2
- **NT** Non Target
- **PR** Progesteron Receptor
- **RAGE** Receptor for AGEs
- **ROS** Reactive Oxygen Species
- **STZ** Streptozotocin
- **TCA** Tricarboxylic Acid
- **TEAD** Transcriptional Enhancer Factor
- **TGFβ** Transforming Growth Factor Beta
- **TPI** Triose Phosphate Isomerase
- **YAP** Yes-associated Protein

I. Introduction

I. Introduction

1. Breast cancer

Cancer has been recognized as one of the main public health problem in more developed countries. In Europe, in 2012, 3.45 million new cancer patients have been diagnosed and 1.75 million patients died of cancer. In women, the most frequent cancers are breast, colorectal and lung cancers. In men, the most diagnosed cancers are prostate, lung and colorectal cancers. The most common causes of death from cancer are lung cancer in males and breast cancer in females. Thus, breast cancer is both the most commonly diagnosed cancer and the first leading cause of cancer death among women (Ferlay et al. 2013).

The presence of mammary glands is one of the major aspects to distinguish mammals from others organisms like birds, fish and insects. Both females and males develop breasts from the same embryological tissues. At puberty, estrogens, in conjunction with growth hormone, induce breast development in females. After pregnancy, mammary glands produce and secrete milk to feed infant. A healthy female breast is made up of 12–20 sections called lobes. Each of these lobes is made up of many smaller lobules, the gland that produces milk in nursing women. Both the lobes and lobules are connected by ducts that lead out to the nipple. These lobules and ducts are distributed throughout the background fibrous tissue and adipose tissue that make up the main mass of the breast (Figure 1). Most cancers of the breast arise from the cells forming the lobules and terminal ducts.

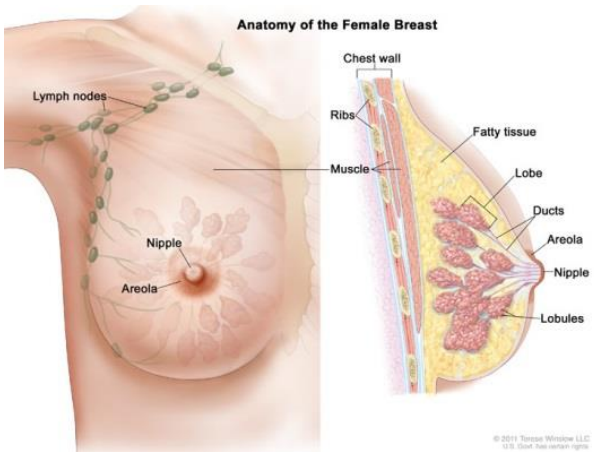

Figure 1: Anatomy of female breast. The nipple, areola, lymph nodes, lobes, lobules, ducts, and other parts of the breast are shown.

1.1. Risk factors for breast cancer

Breast cancer is a multifactorial disease associated with genetic and environmental risk factors.

Sixty five percent of breast cancers are sporadic carcinomas without significant family history. About 25% are familial breast cancers with mutations in multiple low penetrance genes such as ataxia telangiectasia mutated (*ATM)* and checkpoint kinase 2 (*CHEK2*), both involved in DNA repair process. The last 10% represent hereditary cancers in which many family members are affected by the disease. Mutations in high penetrance genes as *BRCA1* and *BRCA2*, *TP53* and *STK11* are a frequent feature of these tumors. Breast cancer 1, early onset (*BRCA1*) and breast cancer 2, early onset (*BRCA2*) are the 2 most common high penetrance breast cancer genes (Miki et al. 1994, Wooster et al. 1995). BRCA mutations are also found in patients with ovarian cancer. BRCA1 maintains genome integrity by participating in homologous repair, cell cycle checkpoint control and transcription regulation (Huen et al. 2010). BRCA2 plays an important role in double strand break homologous DNA repair system by regulating RAD51 recombinase protein (Davies et al. 2001). Other high penetrance genes are the transcription factor p53, encoded by Tumor protein 53 gene (*TP53*), playing a major role in cell-cycle regulation and *STK11*, formerly known as *LKB1*, encoding the Serine/threonine protein kinase 11 protein that regulates cell-cycle arrest pathways, notably via p53 (Karuman et al. 2001).

Lifestyle behaviors and environmental factors could also be involved in breast cancer development. Among these factors, some have a “general” cancer risk and some are more specific of breast neoplasia. It’s well known that the incidence of cancer is increasing with alcohol and tobacco consumption and with age (Hamajima et al. 2002, Pelucchi et al. 2011, Seitz et al. 2012, Reynolds 2013). A fat-diet and obesity are also associated with increased risk and poor outcome of breast cancer (Chlebowski et al. 2006, Goodwin and Stambolic 2015, Goodwin 2016). Recent meta-analyses reveal a 30% increased risk of recurrence or death in obese versus normal-weight women diagnosed with breast cancer (Protani et al. 2010). Several evidences exist to explain how obesity can be linked to cancer. Obesity (1) influences hormones production and growth factors secretion as insulin growth factor 1 (IGF1)

then (2) alters insulin/glucose homeostasis and (3) induces chronic inflammation (Goodwin 2015, Iyengar et al. 2015, Iyengar et al. 2016). Interestingly, obesity is associated with higher risk of triple-negative breast cancer in premenopausal women (Pierobon and Frankenfeld 2013). This could indicate an irreversible effect of obesity, given the poor prognosis of this breast cancer subtype. Moreover, physical activity is associated with better breast cancer outcomes (Ballard-Barbash et al. 2012).

The risk of breast cancer increases with younger age of menarche (Kelsey et al. 1993, McPherson et al. 2000). The use of oral contraceptives and its association to breast cancer is controversial. It has been reported that the use of oral contraceptives and its initiation before age 20 may be associated with increased breast cancer risk (Olsson et al. 1996). In addition, tumors of oral contraceptive pills users would be more likely to be highly differentiated compared to non-users (McPherson et al. 2000). An increased parity (number of times of woman has given birth to a fetus with a gestational age superior to 20 weeks) is mostly considered to be protective against breast cancer (Kelsey et al. 1993, McPherson et al. 2000). In general, an older age at first full-term pregnancy increase the risk of breast cancer (McPherson et al. 2000). Moreover, increasing age at menopause increases the risk of breast cancer. Menopausal hormone therapy is associated with higher risk, higher grade and poor outcome of breast cancer (Bond 2011). Conversely, another study demonstrated that menopausal hormone therapy, with estrogen only, reduces breast cancer risk (Chlebowski and Anderson 2012). The association between breast cancer and hormonal therapy is still unclear and further studies are needed.

1.2. Breast cancer classification

The term “breast cancer” comprises a set of different malignant tumors that develop within the breast. All these neoplasia are heterogeneous regarding progression and metastasis development, biological features and treatment response. This heterogeneity notably led pathologists to classify breast cancers according to four different criteria including histopathology, grade, stage and receptor status. These classifications are routinely used in clinical practice for breast cancer diagnostic and therapeutic decisions.

Histopathological classification is performed by pathologists after hematoxylin-eosin staining of biopsy samples. Most of breast tumors arise from the ductal

epithelium. Ductal in situ carcinomas are breast cancer which have not invaded deeper than the original site or spread through the body and, therefore, are associated with a low mortality rate. However, women with these types of lesions have an increased likelihood of developing invasive breast cancer in the future. Invasive ductal carcinoma is the most common histopathological subtype and accounts for 50-80% of all invasive breast cancers. They correspond to malignant lesions that originate in duct cells and then invade deeper into the breast, carrying the potential to form metastases. Invasive lobular carcinoma begins in the milk-producing lobule cells and represents 5-15% of all invasive breast tumors. Besides these two major types, other type of breast cancer such as tubular, mucinous, papillary or medullary carcinomas have been described and account for ~5% of all invasive breast cancers (Weigelt et al. 2005).

Grading systems focus on the appearance of cancer cells compared to normal tissues. Closer is the appearance of cancer cells to normal cells, better is the prognosis. The Nottingham or Elston-Ellis modification of the Scarff-Bloom-Richardson grading system is used to classify breast cancers. This grading system is based on tubule formation, degree of nuclear polymorphism and mitotic index. The 3 scores are grouped and translated into a grade that describes the outcome of the tumor. From low to high aggressiveness, grades 1, 2 and 3 correspond to well, moderately and poorly differentiated tumors, respectively (Elston and Ellis 2002).

The TNM stage is established in order to evaluate the tumor and its evolution at the time of diagnostic. Three factors are evaluated: T as the size of the primary tumor, N as the lymph nodes status and M as the occurrence of distant metastases. Lymph node status corresponds to number, size and location of lymph nodes infiltrated by cancer cells. For breast cancer, metastases are usually located in bone, brain, lung and liver (Weigelt et al. 2005). High stage values are associated with poor prognosis for breast cancer patients. Combined with the molecular classification and the overall health status of the patient, TNM stage is critical to determine the best therapeutic approach.

According to gene expression profiling studies (Perou et al. 2000), 4 major molecular subtypes of breast cancers have been identified: luminal A, luminal B, HER2 and basal-like types. These subtypes differ regarding their patterns of gene

expression, clinical features, treatment response and prognosis, as summarized in Table 1. The hormone receptor-positive cancers are divided in 2 groups, luminal A and B, according to HER2 or proliferative status. HER2 (Human Epidermal growth factor Receptor 2) or neu, encoded by the *ERBB2* gene, is amplified or overexpressed in 15% of breast cancer. Luminal A subtype shows high estrogen (ER) and progesterone (PR) receptors expression but no HER2 gene amplification. Luminal B breast cancers are ER positive, PR positive and/or HER2 positive and are associated with a high proliferation index (high Ki67). The HER2 and basal-like subtypes are the 2 major groups of hormone receptor-negative breast cancers. Those that display HER2 positivity are called HER2 type while those that are HER2 negative are basal-like or triple negative breast cancers. Basal-like breast carcinomas were identified as a separate breast cancer subtype before gene expression profiling experiments. In fact, pathologists characterized these tumors as poor prognosis breast cancers associated with expression of basal/myoepithelial cell specific markers (Dairkee et al. 1987, Santini et al. 1996). Most triple negative breast cancers are invasive ductal carcinomas with high histological grade, solid architecture, high mitotic rate, pushing borders, central necrosis and absence of tubule formation. Some of them present with a high expression of basal cytokeratins (cytokeratins 5 and 6) and are associated with a bad prognosis (van de Rijn et al. 2002). ER, PR and Ki67 status are evaluated by immunohistochemistry (IHC). HER2 overexpression/amplification is assessed by IHC and by fluorescent in-situ hybridization when IHC is highly positive.

Table 1: Molecular subtypes of breast cancers. Breast cancers are divided in 4 different molecular subtypes (Luminal A, Luminal B, HER2 and basal-like) associated with different gene expression pattern, biomarker profile, proportion, treatment response and prognosis.

		Luminal A	Luminal B (triple positive)	HER2	Basal-like (triple negative)
Gene expression pattern	**Estrogen receptor (ER)**	+	+	-	-
	Progesterone receptor (PR)	+	+	-	-
	HER2 overexpression	-	+	+	-
Biomarker profile		ER+ and/or PR+, HER2-, low Ki67 (<14%)	ER+ and/or PR+, HER2-, high Ki67 (>14%) Or ER+ and/or PR+, HER2+	ER-/PR-/HER2+	ER-, PR-, HER2- and CK5/6 and/or EGRF+
Proportion of invasive breast cancers		70%		15%	15%
Treatment		Hormonal therapy		Trastuzumab (Herceptin)	No response to hormonal therapy and Trastuzumab
Prognosis		Good	Intermediate	Poor (Better with Trastuzumab therapy)	Poor

1.3. Breast cancer therapies

Surgery is the main modality used for treatment of breast cancer patients. When possible, breast-conserving surgery is favored instead of mastectomy. The sentinel lymph node procedure is often used and positive lymph nodes are usually removed at the time as the primary tumor. Postoperative radiotherapy around the tumor site can be administered to eradicate possible residual cancer cells. A study has demonstrated that postoperative radiotherapy administered after breast-

conserving therapy halves the relative risk of recurrence (Darby et al. 2011). Next to surgery and radiotherapy, systemic treatments are also applied for breast cancer therapy. These treatments include chemotherapy, endocrine and anti-HER2 therapies. Standard chemotherapy regimens are combinations of several agents unselectively targeting dividing cells as anthracyclines, taxanes, cyclophosphamide and fluorouracil. For ER positive breast cancers, the blockade of the ER pathway is another possible treatment. Several strategies have been established to reduce estrogen effect: (1) blocking ER (tamoxifen), (2) inducing ER degradation (fulvestrant) or (3) inhibiting estrogen synthesis (aromatase inhibitor). For patients with HER2 positive tumors, a targeted therapy has been developed. Trastuzumbab (Herceptin®) is a monoclonal antibody directed against HER2 receptor. Several studies have demonstrated that trastuzumab decreases mortality by 30% and recurrence by 50% (Piccart-Gebhart et al. 2005, Romond et al. 2005, Smith et al. 2007). Nowadays, there is no specific treatment for patients with triple negative breast tumors.

2. Cancer metabolism

The development of cancer is a multistep process in which normal cells become malignant through a progressive series of alterations. Tumor initiation is described as genetic and/or epigenetic alterations of a single cells resulting in abnormal proliferation. Additional mutations and adaptation of the microenvironment such as extracellular matrix degradation and angiogenesis favor tumor progression. Cancer cells are characterized by several properties known as the hallmarks of cancer (Figure 2). Indeed, cancer cells can (a) proliferate independently of growth stimulating signals, (b) even in presence of growth suppressors and (c) with an unlimited replicative capacity, (d) can escape or alter the immune responses, (e) can promote a pro-tumoral inflammation, (f) are able to invade and metastasize, (g) can induce (lymph-)angiogenesis, (h) are able to maintain genomic instability, (i) are resistant to cell death and (j) are able to adapt their energetic metabolism (Hanahan and Weinberg 2011). Given accumulating researchers consider cancer as a metabolic disease in its own, the interest for studying the metabolic reprogramming of cancer cells has substantially increased in the last years (Coller 2014).

Figure 2: Hallmarks of cancer. Normal cells become malignant through a progressive series of alterations that are listed in the scheme. Adapted from (Hanahan and Weinberg 2011).

2.1. Cellular respiration

Metabolism represents all the biochemical reactions occurring in cells essential to sustain its homeostasis. Cellular maintenance involves energy consuming processes such as protein turnover, DNA repair, transcription and translation, vesicle trafficking and cytoskeletal dynamics. The required energy is provided through adenosine triphosphate (ATP) molecules. Cellular respiration is the classical way of ATP production and contains 4 main steps: glycolysis, pyruvate oxidation into acetyl-coA, tricarboxylic acid (TCA) cycle or Krebs cycle and oxidative phosphorylation (Figure 3). During this process, glucose is oxidatively metabolized to CO_2 and H_2O to generate large amounts of ATP as resumed by the following equation: $C_6H_{12}O_6 + 6\ O_2 \rightarrow 6\ CO_2 + 6\ H_2O + ATP$.

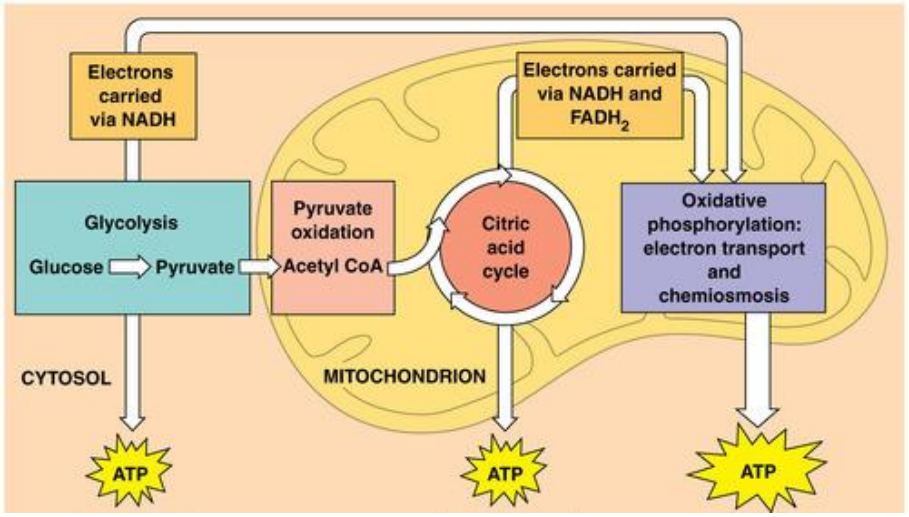

Figure 3: Schematic representation of the cellular respiration. Cellular respiration is composed of 4 main steps: glycolysis, pyruvate oxidation, citric acid cycle and oxidative phosphorylation. During this process, 36-38 ATP molecules are produced. Adapted from Biologie, Neil Campbell.

The first step of cellular respiration, glycolysis, occurs in the cytosol and transforms one molecule of glucose into 2 molecules of pyruvate, produces 2 molecules of ATP and requires 2 NAD^+ molecules. Glycolysis pathway represents a sequence of 10 enzyme-catalyzed reactions described in Figure 4.

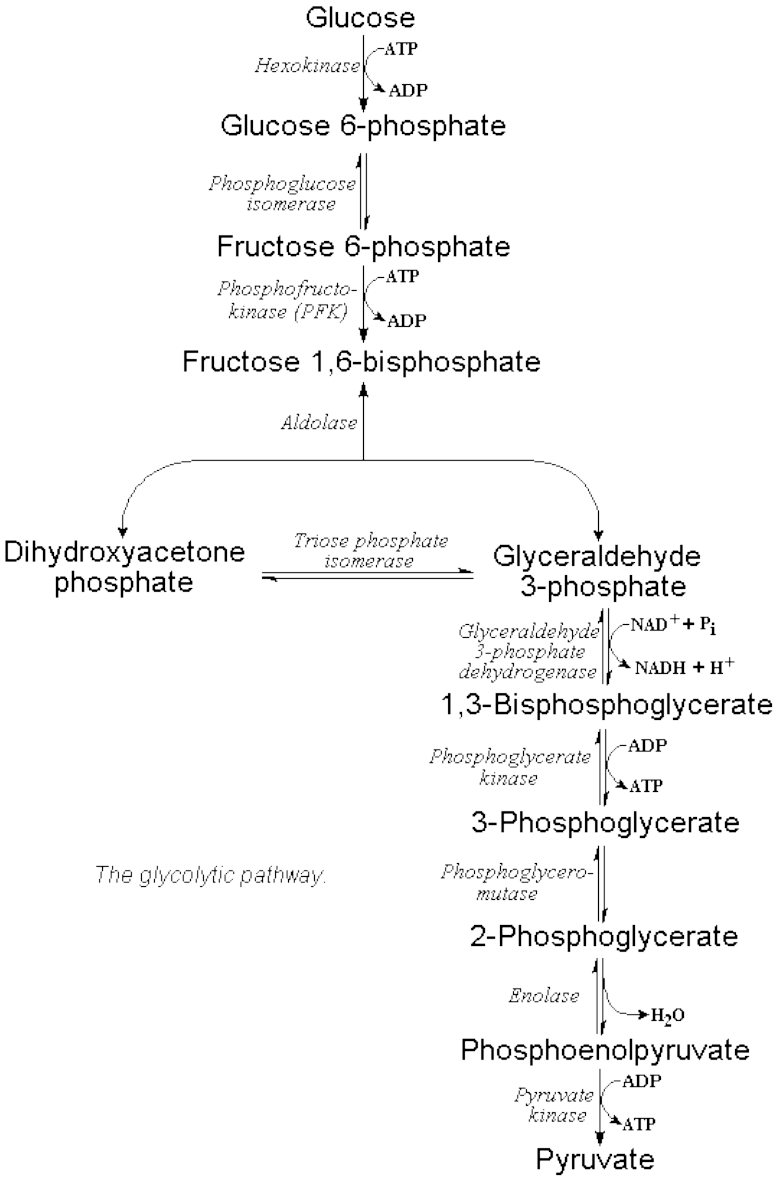

Figure 4: The 10 reactions of glycolysis. Oxidation of 1 molecule of glucose into 2 molecules of pyruvate occurs through a series of 10 reactions in the cytoplasm. Glycolysis requires 2 and produces 4 molecules of ATP per molecule of glucose. The net gain is, therefore, 2 molecules of ATP. Glycolysis generates also 2 NADH molecules which transport electrons to the electron transport chain in the mitochondria.

Then, pyruvate enters in the mitochondria matrix where it is oxidized into acetyl-coA. TCA cycle comprises 8 reactions and transforms acetyl-coA in CO_2 generating 2 ATP, 6 NADH and 2 $FADH_2$ molecules per molecule of glucose (Figure 5).

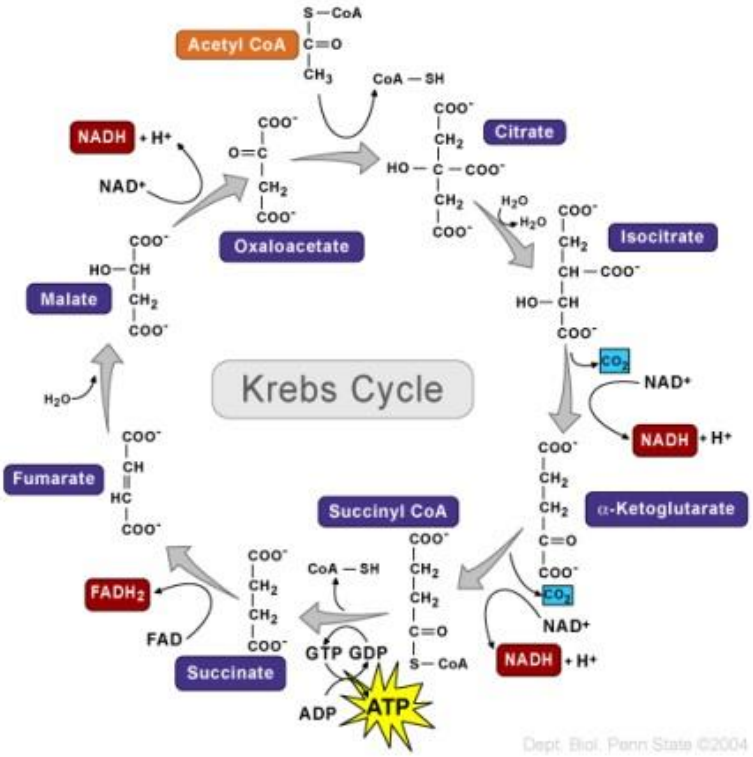

Figure 5: The Krebs or citric acid cycle. TCA cycle and comprises 8 reactions occurring in the mitochondrial matrix. During these reactions, acetyl-coA is transformed in CO_2 generating 1 ATP, 3 NADH and 1 $FADH_2$ molecules per molecule of pyruvate.

Some glycolysis and TCA steps are oxidoreduction reactions in which dehydrogenase enzymes transfer electrons from their substrate to NAD^+ generating NADH + H^+. Subsequently, the electrons transported by NADH and $FADH_2$ fuel the electron transport chain, composed of 4 protein complex, in the inner membrane of mitochondria. At the end of the chain, electrons react with H^+ and reduce O_2 in H_2O. The transport of electrons creates a proton gradient in the intermembrane space that in turn refluxes in the matrix and activates ATP synthase to produce ATP. This last step is called the chemiosmosis and, together with the electron transport chain, are considered as the oxidative phosphorylation (Figure 6). At the end of the four steps of cellular respiration, 36 to 38 ATP molecules are produced per molecule of glucose.

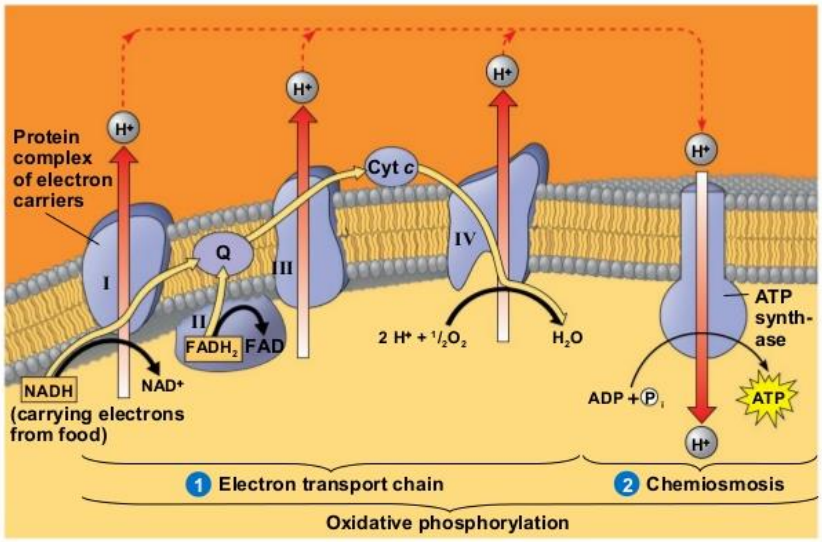

Figure 6: During oxidative phosphorylation, chemiosmosis couples electron transport to ATP synthesis. Following glycolysis and TCA cycle, NADH and FADH2 donate electrons to the electron transport chain located in the inner membrane of the mitochondria. The generated proton gradient activates the ATP production via ATP synthase.

As mentioned above, cellular respiration is a source of energy to maintain cell homeostasis. In addition to homeostasis maintenance, proliferating cells have additional energetic requirements for growth and division. These cells must uptake more nutrients, convert them into biosynthetic building blocks (amino acids, nucleotides, lipid precursors) and transform them into the macromolecules essential for creating a new cell. They have to regulate metabolic pathways in order to keep a balance between ATP production and biomass production. This adaptation is not restricted to cancer cells but applies also to normal proliferating cells and unicellular organisms. Thereafter, we will exclusively focus on cancer cells.

2.2. The Warburg effect

In 1924, Dr. Otto Warburg made the observation that cancer cells metabolize glucose in a different way compared to normal cells. Indeed, cancer cells consume more glucose than their normal counterparts and metabolize it mainly through glycolysis. Pyruvate is reduced to lactate through lactate dehydrogenase (LDH) rather than oxidized in acetyl-coA. Consequently, high levels of lactate are produced even in presence of oxygen (for review (Koppenol et al. 2011)). This phenomenon is known as the aerobic glycolysis or the Warburg effect. Several studies reported an association between increased glucose uptake and increased tumor invasiveness

and poor prognosis (Kunkel et al. 2003, Mochiki et al. 2004). Additionally, hypoxic tumors, which rely on aerobic glycolysis to survive, are usually more invasive and metastatic than normoxic tumors (Postovit et al. 2002, Buchler et al. 2003, He et al. 2004, Postovit et al. 2004). Consistently, the glycolytic rate in cultured cell lines seems to correlate with tumor aggressiveness. As an example, highly invasive MDA-MB-231 breast cancer cells consume more glucose and produce more lactate than non-invasive MCF7 breast cancer cells (Gatenby and Gillies 2004).

Warburg suggested that cancer cells shift to aerobic glycolysis to produce their energy due to the alteration of mitochondrial respiration. However, several groups reported in the last decade that mitochondrial function is not altered in cancer cells (Zu and Guppy 2004, Fantin et al. 2006, Moreno-Sanchez et al. 2007). Aerobic glycolysis is observed in cancerous and highly proliferating cells suggesting that aerobic glycolysis provides benefits for proliferation. The proliferative advantage of glycolytic cells is not directly evident. Indeed, glycolysis generates only 2 ATPs per molecule of glucose, whereas oxidative phosphorylation produces 36 ATPs per glucose. This observation raises the question of why a less efficient pathway, at least in terms of ATP production, is selected by proliferating cells. Moreover, cancer cells use the less active isoform of pyruvate kinase, PKM2, which catalyzes the last step of glycolysis generating ATP. Tsujimoto (Tsujimoto 1997) demonstrated that the loss of intracellular ATP induces cell death. ATP is necessary to sustain cell proliferation as a source for building blocks production. Actually, lipids and nucleotides synthesis and to a lower extent non-essential amino acids synthesis require ATP as a precursor (Lunt and Vander Heiden 2011). One explanation could be that aerobic glycolysis can compensate by increasing ATP production rate through the increased glucose uptake (Pfeiffer et al. 2001).

2.3. The advantages of aerobic glycolysis for cancer cells

The major advantage of aerobic glycolysis for cancer cells is the generation of biosynthetic precursors. Prior to cell division, cells have to replicate all the cellular contents, DNA, RNA, proteins and lipids. Glycolytic intermediates represent a large source for macromolecules building blocks production as summarized in Figure 7.

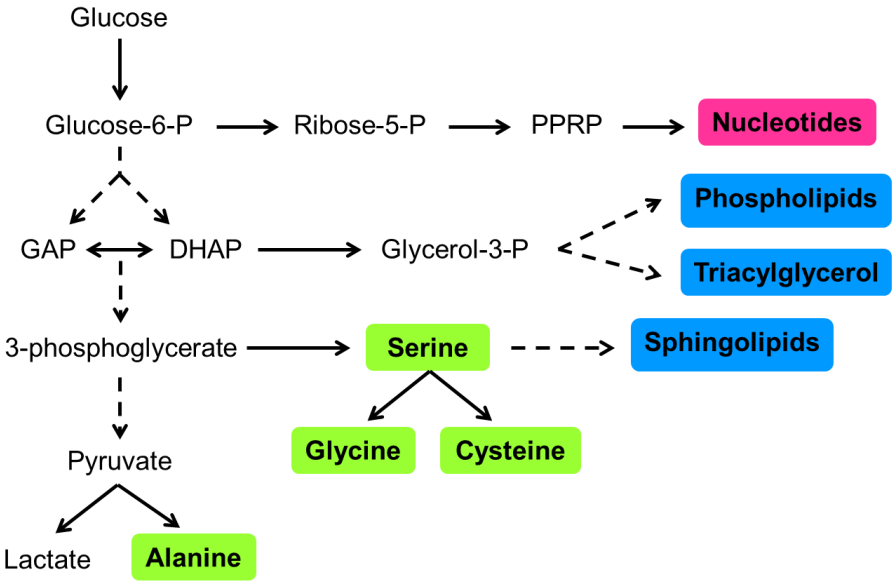

Figure 7: Glycolysis is a source for biosynthetic precursors. Several glycolytic intermediates lead to the formation of nucleotides, lipids precursors (in blue) and amino acids (in green). Adapted from (Lunt and Vander Heiden 2011).

Through glycolysis and pentose-phosphate-pathway, glucose is a carbon source for purine and pyrimidine nucleotides synthesis. Half of the 9 or 10 carbon atoms are derived from 5-phosphoribosyl-α-pyrophosphate (PRPP), an activated form of ribose-5-phosphate derived from glucose-6-phosphate. Interestingly, cells could grow in size when cultured in presence of glutamine only but were unable to proliferate unless glucose was added in the medium (Wellen et al. 2010). This supports the need of glucose for nucleic acid biosynthesis. In addition to nucleotide synthesis, glycolytic intermediates provide carbons for lipid precursors. Phospholipids and triacylglycerols, major lipid components of the cell membrane, are produced from glycerol-3-phosphate derived from dihydroxyacetone phosphate. Another glycolytic intermediate, 3-phosphoglycerate, is transformed into sphingolipids. These lipids are also important membrane components and are involved in several signaling pathways regulating cell growth, differentiation and apoptosis (Futerman and Hannun 2004, Ogretmen and Hannun 2004). Acetyl-CoA, indirectly derived from glycolysis, provides the carbon for fatty acyl chain components synthesis and also provides the carbon to synthesize mevalonate, a cholesterol precursor. In addition to nucleotide and lipids precursors, glucose is a carbon source for amino acids synthesis. Glycolytic intermediates, 3-phosphoglycerate and pyruvate, are precursors for cysteine, glycine and serine and alanine, respectively. Altogether, these observations

emphasize aerobic glycolysis as a carbon provider for the production of macromolecules to sustain high proliferation rate.

Pyruvate, the end product of glycolysis, is mainly transformed in L-lactate by lactate dehydrogenase (LDH) in cancer cells. In human glioma, only 10% of glucose uptake is used for biomass synthesis while 90% is metabolized in lactate and alanine (DeBerardinis et al. 2007). Lactate is excreted outside of the cells. If aerobic glycolysis is increased to generate macromolecule building blocks, then why cancer cells eliminate 3 carbons for each lactate molecule excreted? Actually, conversion of pyruvate into lactate via LDH regenerates NAD^+. As described in Figure 4, NAD^+ is important to maintain the glycolytic flux notably at step 6 between glyceraldehyde-3-phosphate and 1,3-biphosphoglycerate. NAD^+ is also required for the synthesis of nucleotides and amino acids. Lactic acid production and excretion induce a decrease of both intracellular and extracellular pH. Studies have demonstrated that acidosis leads to apoptosis through p53 and caspase-3 activation (Park et al. 1999, Williams et al. 1999). Among the beneficial adaptations, cancer cells increase proton transporters as Na^+/H^+ and H^+-ATPase to maintain a physiological pH (Ober and Pardee 1987, Martinez-Zaguilan et al. 1993, McLean et al. 2000). Furthermore, extracellular acidification has been shown to support tumor growth and invasion by suppressing immune response (Fischer et al. 2007) and by activating metalloproteinases to degrade extracellular matrix (Montcourrier et al. 1997). Acidosis can also be mutagenic and clastogenic, possibly through inhibition of DNA repair (Morita et al. 1992). Moreover, cellular metabolism is heterogeneous within a tumor mass and some cells can use lactate as a prominent substrate to fuel their oxidative metabolism (Sonveaux et al. 2008).

Mitochondria can produce large amount of ATP but are also the major source of Reactive Oxygen Species (ROS) such as superoxide anion (O_2^-), hydrogen peroxide (H_2O_2) and hydroxyl radical (OH•). ROS come from the binding of oxygen to electrons falling out of the electron transport chain. By damaging cellular macromolecules, ROS are highly toxic. Therefore, by favoring aerobic glycolysis rather than mitochondrial respiration, cancer cells protect themselves from ROS production and apoptosis (Kondoh 2008). However, recent studies demonstrated a more subtle effect of mitochondrial ROS: their production above pro-metastatic levels

would cause cell death whereas their moderate increase promotes tumorigenesis (Weinberg et al. 2010, Sena and Chandel 2012, Porporato et al. 2014).

2.4. The origin of aerobic glycolysis shift in cancer cells

During long time, it has been though that aerobic glycolysis is a simple adaptation to hypoxia. In 2004, Gatenby and Gillies (Gatenby and Gillies 2004) proposed a more sophisticated model for aerobic glycolysis as an important step in cancer progression (Figure 8). Aerobic glycolysis represents an evolved solution to common environmental growth constraints during carcinogenesis. In pre-malignant lesions, basement membrane is not impaired and blood vessels are confined in the stroma. Therefore, cancer initiation occurs in a poorly vascularized environment. Oxygen and glucose diffuse from the vessels across the basement membrane and through layers of tumor cells to be metabolized. Proliferation leads to a thickening of the epithelial layer, pushing cells further and further away from blood vessels. It has been demonstrated that oxygen concentrations decreased with distance from a capillary that does not exceed 150µm (Krogh 1919). Due to the oxygen diffusion limitation, pre-malignant lesions inevitably develop hypoxic regions. Although less dramatically than oxygen pressure, glucose availability also decreases with distance from blood vessels. Only cells which adapt to scarce oxygen and glucose resources survive in these harsh environmental conditions. Hypoxic stress leads to activation of the hypoxia-inducible factor 1α (HIF1α) (Semenza 1998). This transcription factor mediates a pleiotropic response to hypoxia by inducing survival genes expression as glucose transporters, glycolytic enzymes (hexokinase) and angiogenic factors (Vascular endothelial growth factor, VEGF). Together with genetic mutation, cyclic or persistent hypoxia favors aerobic glycolysis rather than oxidative phosphorylation. Therefore, cancer cells which switch to aerobic glycolysis and maintain their metabolic activities in absence of oxygen have a powerful growth advantage. The importance of the glycolytic phenotype is highlighted by several studies showing that increased glucose uptake coincide with the transition from pre-malignant lesions to invasive cancer (Younes et al. 1996, Yasuda et al. 2001). In addition, both VEGF production and microenvironment acidification promote cancer cell invasion and metastasis development. Interestingly, Rofstad and collaborators (Rofstad and Danielsen 1999) demonstrated that hypoxic melanoma cells displayed a higher metastatic potential compared to normoxic cells after injection in the tail vein of mice.

Altogether, these observations highlight the crucial role of aerobic glycolysis in tumor progression (Figure 8).

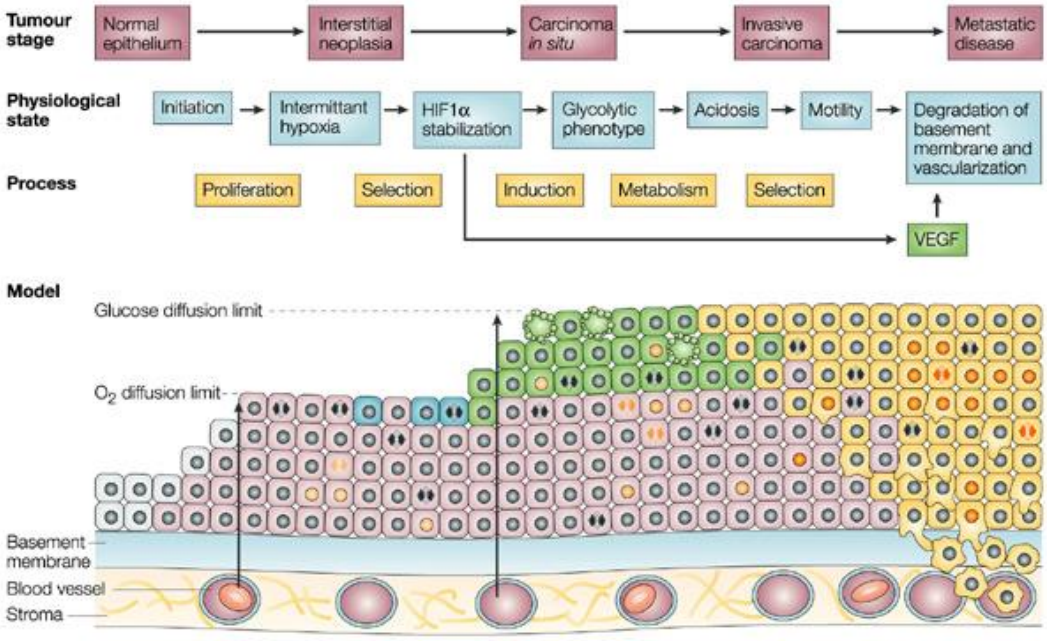

Figure 8: **Model of cancer progression and importance of aerobic glycolytic switch.** Normal epithelial cells (grey) become hyperproliferative (purple) following induction, mainly through genetic alterations (orange nuclei). As cancer progression proceeds, the mutations in cells increase. At initiation stage, blood vessels are restricted to the stroma compartment and pre-malignant cells are poorly vascularized. As they reach the oxygen diffusion limit, cancer cells become hypoxic (blue), which can either lead to cell death (apoptotic cells shown with blebbing) or adaptation of a glycolytic phenotype (green), which allows cells to survive. As a consequence of glycolysis, lesions become acidic, which selects for motile cells (yellow) that eventually breach the basement membrane. Following breakdown of the basement membrane, cells gain access to existing and newly formed blood and lymphatic vascular routes for metastasis. From (Gatenby and Gillies 2004).

The adapted phenotype of glycolytic cancer cells is accompanied by several genetic mutations and epigenetic modifications. It has been demonstrated that cancer cells frequently overexpress GLUT1 and GLUT3 glucose transporters, as well as hexokinase II and phosphofructokinase 1 (PFK1), the first and the third glycolysis enzyme, respectively. Various activating mutations have been reported in the phosphoinositide 3-kinase (PI3K) signaling pathway, a major regulator of glucose metabolism. For example, AKT activation, a downstream kinase of PI3K, increases glucose uptake by increasing GLUT1 glucose transporter expression and by preventing its internalization (Barthel et al. 1999, Vander Heiden et al. 2001, Wieman et al. 2007). As mentioned above, hypoxia promotes HIF1α transcription factor stabilization which induces glucose transporter and glycolytic enzymes expression.

For example, HIF1α upregulates pyruvate dehydrogenase kinase (PDK) expression that represses conversion of pyruvate to acetyl-CoA through pyruvate dehydrogenase (PDH) and, consequently, decreases pyruvate flux into Krebs cycle (Kim et al. 2006, Papandreou et al. 2006). Similar to HIF1α, the oncogene MYC promotes the expression of LDH (Semenza et al. 1994, Shim et al. 1997). Another important oncogene, RAS, promotes glucose uptake (Yun et al. 2009). Mutations of the tumor suppressor p53, widely implicated in cancer, suppress its pro-mitochondrial respiration function (Cheung and Vousden 2010, Levine and Puzio-Kuter 2010). Remarkably, cancer cells express the less efficient but highly regulated pyruvate kinase isoform, PKM2 which converts phosphoenolpyruvate into pyruvate (Mazurek et al. 2005, Christofk et al. 2008). Depending of the cellular needs, this variant offers the ability to switch rapidly from biosynthesis when PKM2 is inactive to high ATP production or lactate production when it is active. PKM2 activity is regulated by phosphorylation through tyrosine kinase receptor pathways (Christofk et al. 2008, Hitosugi et al. 2009). Interestingly, PKM2 isoform is not only expressed by cancer cells but is also found in rapidly proliferating tissues, notably during embryonic development. Besides PKM2, other proteins implicated in metabolic reprogramming of cancer cells such as HIF1α (Iyer et al. 1998) and Yes-associated protein (YAP) (Camargo et al. 2007, Mulvihill et al. 2014) are also involved in tissue development. Fast growth, rapid biomass synthesis and highly controlled resources management are three main features shared by tumorigenesis and embryogenesis.

Interestingly, the tendency of cancer cells to consume more glucose than normal cells is exploited for the diagnosis and monitoring of certain cancers. Indeed, the intravenous injection of ^{18}fluoro-deoxy-D-glucose is used for PET scan (Positron Emission Tomography) analysis. This glucose analogue is picked up by cells but is not metabolizable beyond the first step of glycolysis and is, therefore, sequestered in cancer cells due to their high avidity for glucose.

3. Methylglyoxal and carbonyl stress

3.1. Methylglyoxal production

The 2-oxoaldehyde methylglyoxal (MG), also called pyruvaldehyde or 2-oxopropanal, is an endogenous molecule with the formula $CH_3C(O)COH$. MG is a dicarbonyl compound composed of an aldehyde and a ketone group (Figure 9).

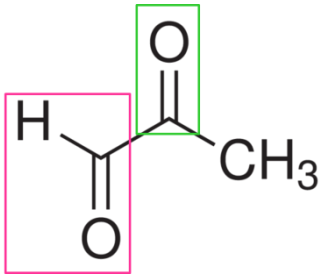

Figure 9: Chemical structure of methylglyoxal. Methylglyoxal is composed of two carbonyl groups, one aldehyde in pink and one ketone in green.

The main sources of MG are two triose phosphate glycolytic intermediates, glyceraldehyde-3-phosphate (GAP) and dihydroxyacetone phosphate (DHAP) (Figure 10). These intermediates are formed at the fourth step of glycolysis by aldolase and maintained in equilibrium by the triose phosphate isomerase (TPI). Non enzymatic spontaneous fragmentation and elimination of phosphate from GAP or DHAP contribute to MG formation (Phillips and Thornalley 1993, Richard 1993). GAP is eightfold more reactive than DHAP in the production of MG but DHAP is twenty fold more present in cells. Thus, both GAP and DHAP are important sources of MG (Phillips and Thornalley 1993). An important regulator of intracellular MG levels is the glyceraldehyde-3-phosphate dehydrogenase (GADPH). GAPDH catalyzes the transformation of triose phosphate into 1,3-diphosphoglycerate. Therefore, when GAPDH activity is low, triose phosphate intermediates tend to accumulate and to increase MG formation (Beisswenger et al. 2003). GAPDH activity is regulated by oxidative stress (Knight et al. 1996) and by MG modification (Lee et al. 2005) suggesting that MG is able to influence its own production. Although glycolysis is the major source for MG production, MG formation is a minor fate of triosephosphate. Indeed, it is considered that only 0.1% of glucose flux is converted to MG (Thornalley 1988) and this percentage can increase up to 1% in hyperglycemic conditions (Rabbani and Thornalley 2011). The rate of total cellular formation of MG is

approximatively 125 µmol/kg of cell mass per day which for an adult corresponds to a rate of MG formation of 3 mmol per day (Rabbani and Thornalley 2014).

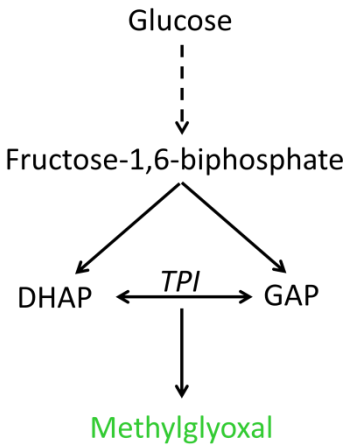

Figure 10: Glycolysis is the major source of methylglyoxal. MG is produced after the fifth step of glycolysis which correspond to the equilibrium between dihydroxyacetone phosphate (DHAP) and glyceraldehyde-3-phosphate (GAP) mediated by the triose phosphate isomerase (TPI). Non enzymatic fragmentation and elimination of phosphate from GAP or DHAP contribute to MG formation. Adapted from (Xue et al. 2011, Sousa Silva et al. 2013).

Besides glycolysis, MG can also be produced through oxidation of acetone in ketone bodies catabolism (Casazza et al. 1984) and through oxidation of aminoacetone during threonine metabolism (Lyles and Chalmers 1992). The degradation of glucose-glycated proteins and monosaccharides are also MG sources (Thornalley et al. 1999). MG can also be produced through the oxidative degradation of lipids (lipid peroxidation) (Esterbauer et al. 1982). These alternative pathways for MG production are summarized in Figure 11. In bacteria, MG may also arise from an enzymatic reaction through methylglyoxal synthase (Cooper and Anderson 1970). MG, under its non-hydrated hydrophobic form, can diffuse passively through cell membrane (Rabbani and Thornalley 2014).

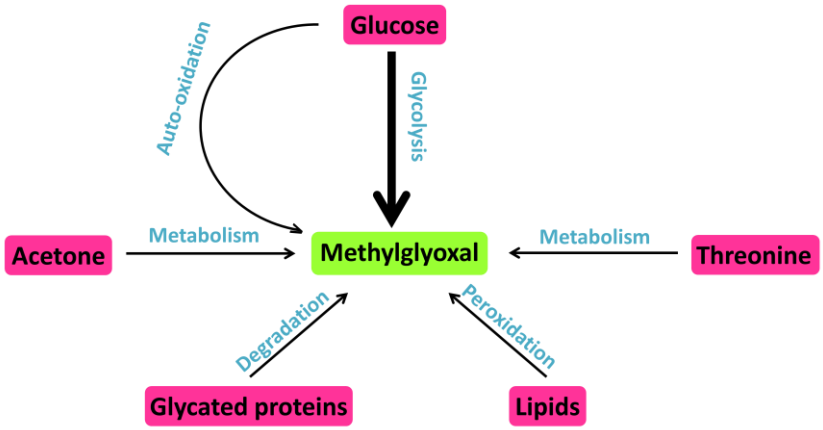

Figure 11: Methylglyoxal is produced through different pathways in human cells. The main source of MG is glycolysis. MG can also be produced via the auto-oxidation of glucose, the catabolism of acetone and threonine, the degradation of glycated proteins and the peroxidation of lipids. Adapted from (Maessen et al. 2015).

In addition to MG, two other major dicarbonyls, glyoxal (GO) and 3-deoxyglucosone (3-DG), have been characterized (Figure 12). GO and 3-DG are mainly formed by the non-enzymatic degradation of both glucose and glucose-glycated proteins (Thornalley et al. 1999). GO is also formed by lipid peroxidation and degradation of nucleotides (Thornalley 2005) whereas 3-DG can also be constituted in case of degradation of fructosamine-3-phosphate during the repair of early glycated proteins and degradation of fructose-3-phosphate (Lal et al. 1997, Delpierre et al. 2000).

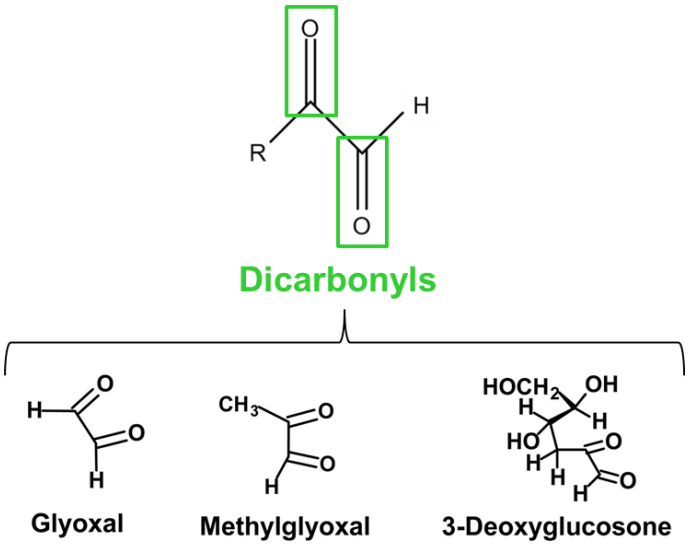

Figure 12: Chemical structures of the 3 dicarbonyls, glyoxal, methyglyoxal and 3-deoxyglucosone. The backbone structure of dicarbonyls with the 2 carbonyl groups highlighted in green is represented.

3.2. Glycation and MG-AGEs

In the 60-70s, it was discovered that MG and related aldehydes react with amino and guanido groups, although the pathophysiological significance of this reaction was not understood (Shapiro and Hachmann 1966, Takahashi 1968, Broude and Budowsky 1971). Now, MG has been implicated in ageing and in several diseases including diabetes and its vascular complications, obesity, renal failure, cardiovascular disease, neurological disorders, osteoarthritis and cancer (for review (Rabbani and Thornalley 2015)).

MG is a highly reactive dicarbonyl compound and a potent glycating agent. MG reacts with cellular macromolecules such as proteins, lipids and nucleic acids. Glycation has been first defined as “reactions that link a sugar to a protein or a peptide”. Later, the distinction between enzymatic modification of proteins forming glycoproteins (glycosylation) and non-enzymatic modification of proteins forming glycated proteins (glycation) was made (Lis and Sharon 1993). The term glycation refers now to non-enzymatic modification of proteins by saccharides and their derivatives. Glycation occurs through a series of sequential and parallel reactions known as the Maillard reaction. This latter has been named after Louis-Camille Maillard, a French pioneer physician and chemist, who discovered brown pigments after heating reaction between reducing sugars and amino acids (Finot 2005). The process involves multi-step non-enzymatic reactions between carbonyl-containing groups and amino groups leading to the formation of advanced glycation end-products (AGEs) (Brownlee et al. 1984).

The first step of the Maillard reaction involves nucleophilic attack by the nitrogen atom of the amino groups to the electrophilic carbonyl group of a sugar to form glycosylamines. After elimination of a water molecule, an unstable Schiff’s base is generated which undergoes a spontaneous rearrangement (called Amadori rearrangement) to form fructosamine or Amadori product (Hodge 1955). Glycosylamine, Schiff’s bases and fructosamine are all named “early stage glycation adducts” (Thornalley 2008). Fructosamine is then degraded into more stable adducts known as “advanced glycation end-products” (Figure 13). In addition, degradation of Schiff’s bases via a non-Amadori pathway (the Namiki pathway) forms dicarbonyls and subsequently leads to production of AGEs (Thornalley 2005, Thornalley 2008).

Indeed, the highly reactive α-oxoaldehydes, GO and MG, also directly react with proteins to form AGEs, not necessarily via early stage glycation adducts (Rabbani and Thornalley 2012). For example, incubation of 1µM of ^{14}C-MG with human plasma *ex vivo* at 37°C for 24h induced complete and irreversible binding of MG to plasma proteins (Thornalley 2005).

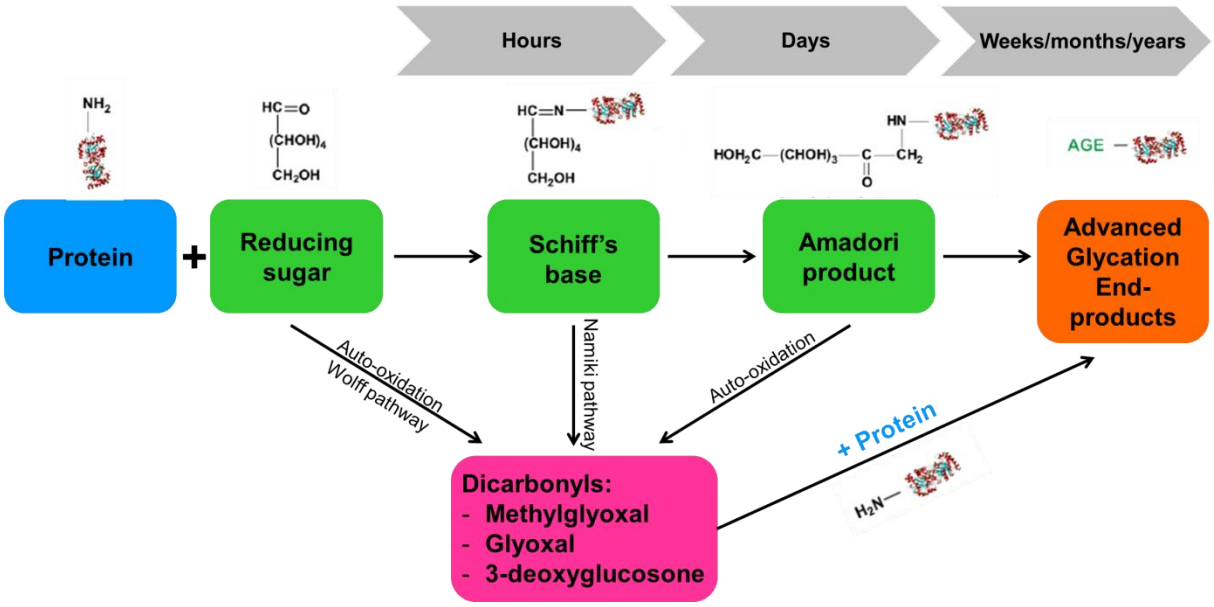

Figure 13: Glycation of proteins through the Maillard reaction.

Since the discovery of glucose-glycated hemoglobin, a biomarker currently used in diabetes, protein glycation by glucose has been intensively investigated. However, glucose is the least reactive of all sugars and dicarbonyl compound; MG and GO, are much more reactive than glucose towards protein glycation. Rate constants for glycation of proteins by MG are 10 000 to 50 000 fold higher than for glucose glycation (Thornalley 2005, Rabbani and Thornalley 2012). GO is 4 fold less reactive than MG for protein glycation. Given that MG is found in all cells and is the most reactive glycation agent *in vivo*, it rapidly attracted the attention of the scientific community (Thornalley 1996). The main targets of MG glycation process are macromolecules with free amino groups including proteins, nucleotides and some phospholipids. Steady-state levels of glycation adducts are 0.1-1% of lysine and arginine residues in proteins, 1 in 10^5 nucleotides in DNA and 0.1% of basic phospholipids (Thornalley et al. 2003). Accumulation of these modified molecules as

well as their glycating agents leads to a new type of cellular stress: the carbonyl stress, firstly described as carbonylic stress (Baynes 1991).

3.2.1. Protein glycation

Both N-terminal amino group and side chain of arginine/lysine residues and thiol group of cysteine residues are the main targets of glycation in proteins. In contrast with arginine and lysine residues, cysteine glycation leads to reversible and unstable hemithioacetals adducts (Lo et al. 1994). Lysine and arginine residues are the main MG glycation targets in proteins and their modifications are named MAGEs (MG-AGEs) and are described in Figure 14 (Lo et al. 1994, Dobler et al. 2006, Queisser et al. 2010). The reaction between methylglyoxal and lysine residues forms N^{ε}-(carboxyethyl)lysine (CEL), a MAGE found in human lens proteins with increased concentrations over ageing (Ahmed et al. 1997). However, the MG-preferred targets are arginine residues (Lo et al. 1994, Oya et al. 1999). Quantitatively the most important MAGEs are the hydroimidazolones (MG-H). Hydroimidazolone adducts exist as 3 structural isomers, MG-H1, 2 and 3 (Ahmed et al. 2002, Ahmed and Thornalley 2002). MG-H adducts account for more than 90% of adducts on proteins and have relatively moderate half-lives, 2-6 weeks (Ahmed et al. 2003, Ahmed et al. 2005, Ahmed et al. 2005). Another MAGE, tetrahydropyrimidine (THP) is also derived from the reaction of MG with arginine residues (Oya et al. 1999). Bovine serum albumin (BSA) and other proteins modified by MG display fluorescent properties (Lo et al. 1994, Riley and Harding 1995, Oya et al. 1999). The MAGE bearing this property was identified as argpyrimidine (N^{δ}-(5-hydroxy-4,6-dimethylpyrimidine-2-yl)-L-ornithine) (Shipanova et al. 1997, Oya et al. 1999). Historically, the first AGEs discovered were Nε-carboxymethyl-lysine (CML) and pentoside (Figure 14), both glyoxal-derived adducts (Ahmed et al. 1986, Takanashi et al. 1992). MG is also responsible for protein cross-linking. With lysine residues, methylglyoxal-lysine dimers (MOLD) are found in an age dependent concentration in lens proteins and in diabetic patients (Nagaraj et al. 1996, Frye et al. 1998). A lysine-arginine methylglyoxal-derived cross-link (MODIC) has been also described (Lederer and Klaiber 1999).

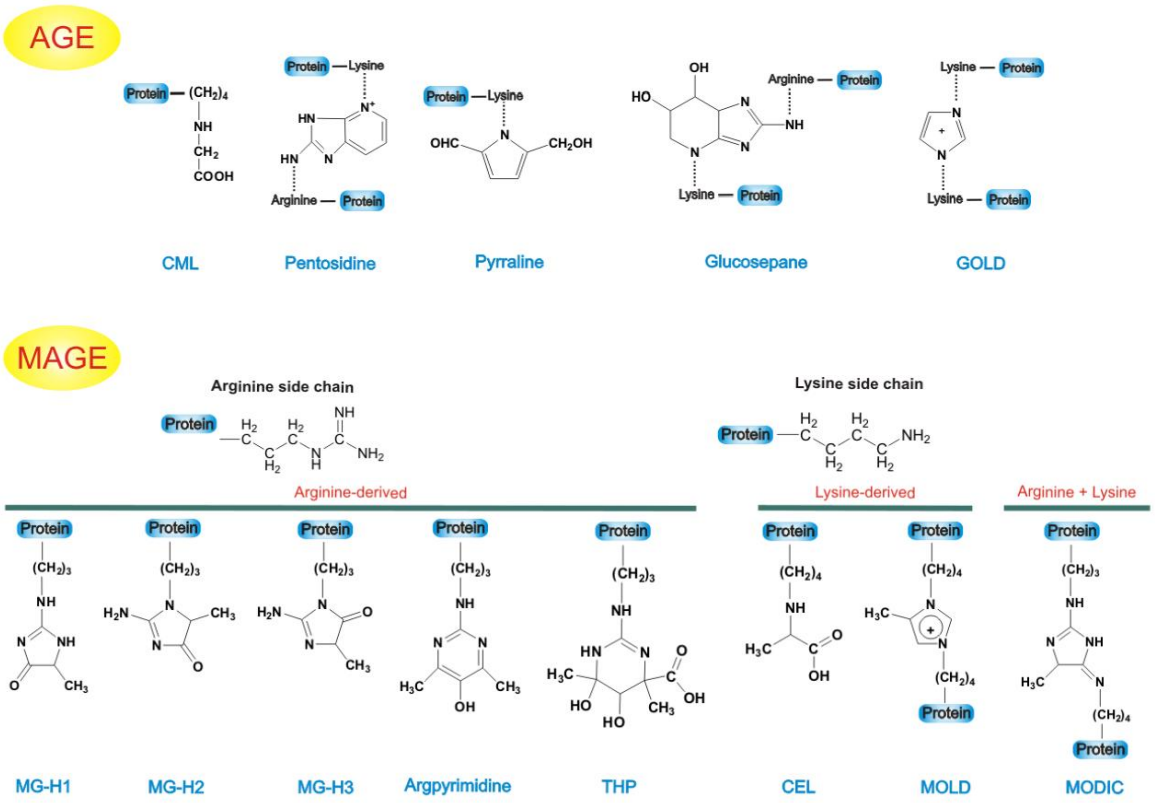

Figure 14: Chemical structures of the main AGEs and MAGEs on proteins.

Proteins are made of amino acids linked by peptide bonds in a linear chain with secondary and tertiary levels of structure. Post-translational modifications, phosphorylation, acetylation, glycosylation, alkylation, among others, play a major role in proteins structure, function, half-life and in protein-protein interaction. Glycation modifications may regulate protein structure and functions which ultimately may cause cellular and tissue alteration observed in several pathological conditions and ageing. The modification of proteins by MG is particularly relevant because functionally important residues in proteins are targeted. Indeed, arginine, lysine and cysteine residues are usually present in the active sites of enzymes. As an example, almost all glycolytic enzymes contain arginine residues in their active site (Riordan et al. 1977). Analysis of residues involved in catalysis at 178 enzyme active sites indicated that 11% of residues were arginines, despite these latter only represented 4.9% of the total residues (Bartlett et al. 2002). More extensively, the examination of Swissprot database sequences and Protein Data Bank information has indicated that arginine is the most abundant and frequent amino acid residue within both the protein receptor binding domains and the protein nucleotide binding sites and the third most

frequent residue in enzyme active sites (Gallet et al. 2000, Bartlett et al. 2002, Lejeune et al. 2005, Chetyrkin et al. 2011). Altogether, these observations suggest that arginine glycation could have severe functional consequences. Accordingly, MG modifications on arginine residues of human serum albumin (HSA) seriously impaired its esterase activity. The five, out of 24, arginine residues in HSA with high susceptibility to MG modification are in the receptor binding domain (Ahmed et al. 2005). Chaplen and colleagues estimate that 5-10% of cellular proteins may be modified to physiologically significant levels (Chaplen et al. 1998). Furthermore, between 0.1% and 3% of arginine residues on cellular proteins are known to be modified by MG, and these modifications typically increase 2 to 5 fold in diabetes (Thornalley et al. 2003, Rabbani and Thornalley 2011). Besides serum albumin, the functions of several enzymes such as cysteine proteases, Cu, Zn-superoxide dismutase (Kang 2003), GAPDH, glutathione reductase, LDH (Morgan et al. 2002), enolase 2 (Gomes et al. 2008) are also inhibited by MG-modifications. In contrast, MG modification can increase Hsp27 and α-crystallins chaperone activity (Nagaraj et al. 2003, Oya-Ito et al. 2006) as well as hemoglobin and myoglobin esterase activity (Sen et al. 2007). MG-modified proteins and their subsequent functional impairment are summarized in Table 2.

The turnover of MG-modified proteins by cellular proteasomal and lysosomal proteolysis generates free glycation adducts which are released from tissues in the circulation and excreted in urine (Thornalley et al. 2003).

Table 2: Components of the dicarbonyl proteome. Adapted from (Rabbani and Thornalley 2012).

Protein	Species	Functional impairment	References
20S proteasome subunits	Human	Decreased proteasome activity	(Queisser et al. 2010)
Collagen type IV	Human	Decreased integrin binding	(Dobler et al. 2006)
Cu,Zn-superoxide dismutase	Human	Decreased enzymatic activity	(Kang 2003)
Enolase 2	Yeast	Decreased enzymatic activity	(Gomes et al. 2008)
GAPDH	Mouse	Decreased enzymatic activity	(Morgan et al. 2002)
Glutathione reductase	Mouse	Decreased enzymatic activity	(Morgan et al. 2002)
Hemoglobin	Human	Increased oxygen binding; increased esterase activity	(Ahmed et al. 2005, Gao and Wang 2006, Sen et al. 2007)
HIF1α co-activator protein p300	Human	Decreased HIF1α and responsive to hypoxia	(Thangarajah et al. 2009)
Hsp27	Human	Increased anti-apoptotic activity	(Sakamoto et al. 2002, Oya-Ito et al. 2006, van Heijst et al. 2006, Oya-Ito et al. 2011)
Lactate dehydrogenase	Mouse	Decreased enzymatic activity	(Morgan et al. 2002)
Mitochondrial respiratory chain proteins	Rat	Increased ROS formation	(Rosca et al. 2005)
mSin3a co-repressor	Mouse	Increased angiopoietin-2 transcription	(Yao et al. 2007)
Myoglobin	Human	Increased esterase activity	(Sen et al. 2007)
Serum albumin	Human	Inhibition of esterase activity and decreased drug binding	(Ahmed et al. 2005)
α-Crystallin	Human	Increased chaperone activity	(Nagaraj et al. 2003, Gangadhariah et al. 2010)

3.2.2. Nucleotide glycation

As shown in Figure 15, MG reacts with nucleic acids to form nucleotide AGEs, with deoxyguanosine (dG) being the most reactive nucleotide (Shapiro et al. 1969, Thornalley 2008). The major nucleotide AGEs are the imidazopurinone derivatives: dG-G (3-(2'-deoxyribosyl)-6,7-dihydro-6,7-dihydroxyimidazo[2,3-b]purin-9(8)one), constituted from the reaction of dG with GO, and dG-MG (3-(2'-deoxyribosyl)-6,7-dihydro-6,7-dihydroxy-6-methylimidazo-[2,3-b]purine-9(8)-one), derived from the reaction of dG with MG (Thornalley et al. 2010). GO and MG also produces 2 other adducts identified as CMdG (*N*2-carboxymethyl-deoxyguanosine) and CEdG (*N*2-(1-carboxyethyl)-deoxyguanosine), respectively (Papoulis et al. 1995, Thornalley 2003). Through DNA glycation, MG is considered as mutagenic and genotoxic by causing loss of genomic integrity associated with crosslinking, strand breaks and mutations (Brambilla et al. 1985, Migliore et al. 1990, Rahman et al. 1990, Pischetsrieder et al. 1999, Murata-Kamiya and Kamiya 2001).

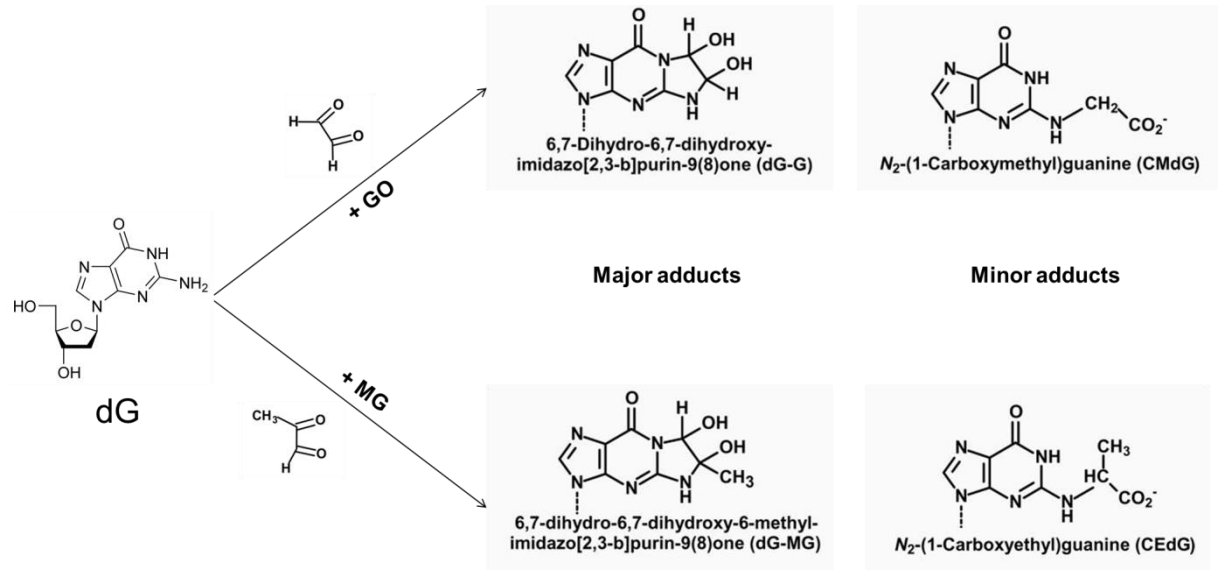

Figure 15: MG and GO-adducts on deoxyguanosine (dG). Adapted from (Thornalley 2008).

3.2.3. Lipid glycation

Basic phospholipids such as phosphatidylethanolamine and phosphatidylserine are also targets of MG glycation forming lipid-linked AGEs, notably carboxymethylethanolamine (Bucala et al. 1993, Requena et al. 1997). This reaction is followed by the oxidation of unsaturated fatty acid side chains, with 4-hydroxyhexenal and 4-hydroxynonenal as major products (Bucala et al. 1993, Al-Abed et al. 1996). Glycated phospholipids were especially detected in liver of diabetic rats and in human plasma of diabetic patients (Bucala et al. 1993, Pamplona et al. 1995). Phospholipid AGEs are removed by lipid turnover (Requena et al. 1997).

3.3. Enzymatic defense against MG and carbonyl stress

MG formation is unavoidable in living systems and is even increased in pathological conditions such as diabetes and cancer. Once produced, MG inevitably reacts and modifies macromolecules thus perturbing basal physiological maintenance. Accumulation of glycated proteins is associated with enzyme inactivation, protein denaturation and degradation. Nucleotide glycation is associated with mutagenesis and apoptosis and lipid glycation with cellular membrane disruption. However, dicarbonyl damage to the genome and proteome is caused by less than one percent of the MG produced in the body. Over 99% of MG is enzymatically metabolized in less reactive compounds by the glyoxalase (Glo) system and other more minor defense systems (Rabbani and Thornalley 2012).

3.3.1. The glyoxalase system

In 1913, two research groups independently discovered a new enzyme, glyoxalase (initially termed ketonaldehydemutase), catalyzing the conversion of MG into lactic acid (for review (Sousa Silva et al. 2013)). Thenceforth, research focused on its putative role in glycolysis. In 1928, Neuberg and Kobel proposed a model for glycolysis consisting of the splitting of glucose into two trioses resulting in MG formation and its conversion into lactate through Glo (for review (Sousa Silva et al. 2013)). In 1933, several observations dismissed a glycolytic role for Glo: (1) the elucidation of the complete glycolysis pathway and (2) the need of reduced glutathione (GSH) as a co-factor for Glo enzyme while GSH did not interfere with glycolysis (Jowett and Quastel 1933). Later, in 1951, Racker (Racker 1951) found

that the end-product of the glyoxalase system was D-lactate and not L-lactate, which is the end-product of glycolysis and proved that two enzymes, glyoxalase 1 and 2 (Glo1 and Glo2) are required to produce lactate from MG. This definitely ruled out MG and Glo enzymes from glycolysis and interest in the glyoxalase system severely diminished.

Nevertheless, the widespread distribution of glyoxalase enzymes in all organism suggested a fundamental and conserved role of these proteins (Hopkins and Morgan 1945). In the 1960s, from their research on cancer cells, Szent-Györgyi and Egyud proposed a role for Glo1 in the regulation of cell division (Egyud and Szent-Gyorgyi 1966, Egyud and Szent-Gyorgyi 1966, Szent-Gyorgyi and Egyud 1966, Szent-Gyorgyi et al. 1967). However, until today, their hypothesis was not clearly proven since a mechanistic link between Glo1 and the regulation of the cell cycle has not been found yet. On the basis of the observation that MG and other dicarbonyls are highly reactive and that glutathione-dependent enzymes serve detoxification roles, Mannervik linked Glo enzymes to the elimination of toxic dicarbonyls (for review (Sousa Silva et al. 2013)).

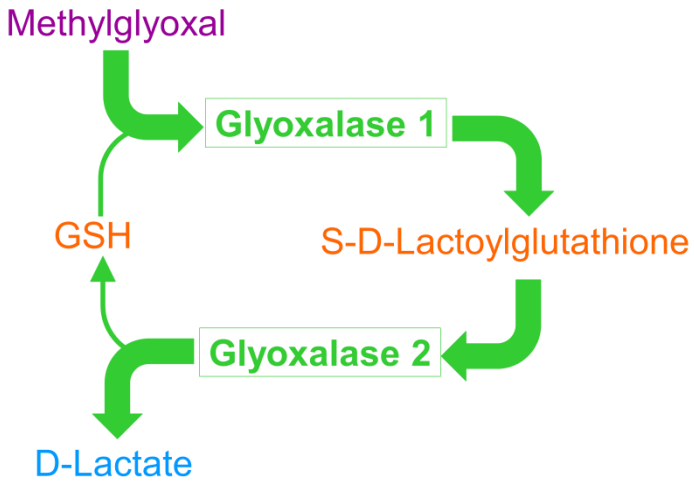

Figure 16: The glyoxalase system. MG reacts non-enzymatically with reduced GSH to form the hemithioacetal intermediate. Subsequently, Glo1 catalyzes the isomerization of this hemithioacetal to S-D-lactoylglutathione. This latter is hydrolyzed by Glo2 into D-lactate, hereby regenerating reduced GSH. Adapted from (Thornalley and Rabbani 2011).

The glyoxalase system is now well defined (Figure 16). It consists of two cytosolic enzymes, Glo1 (E.C. 4.4.1.5) and Glo2 (E.C. 3.1.2.6) and the co-factor GSH. MG reacts non-enzymatically with reduced GSH, thereby forming the MG-

glutathione hemithioacetal. Subsequently, Glo1, also termed lactoylglutathione methylglyoxallyase, catalyzes the isomerization of this hemithioacetal to S-D-lactoylglutathione, which, in turn, is hydrolyzed to D-lactate, hereby regenerating reduced GSH. The latter reaction is catalyzed by Glo2 (Thornalley 1990). D-lactate can cross cell membrane by diffusion or via specific lactate transporter (Thornalley 1993). In bacteria, it can also be metabolized into pyruvate by the D-lactate dehydrogenase (D-LDH). The committed step in this pathway is the reaction catalyzed by Glo1 since, under physiological conditions, it is considered irreversible (Sellin and Mannervik 1983). The efficiency of MG detoxification is primarily determined by the spontaneous formation of the hemithioacetal which depends of the level of GSH. MG is generally considered as the major physiological substrate of the glyoxalase system. Indeed, MG accumulates markedly when Glo1 is inhibited by cell permeable Glo1 inhibitors and by depletion of GSH (Thornalley 1993, Thornalley et al. 1996, Abordo et al. 1999). Additionally, Glo1 overexpression prevents the accumulation of MG in cells and thereby suppresses MAGEs formation (Shinohara et al. 1998). Others α-oxoaldehydes such as GO, phenylglyoxal and hydroxyl-pyruvaldehyde, are also substrates of Glo1 (Racker 1952, Vander Jagt et al. 1972).

Glo1 has been described in various organisms, from prokaryotes to humans. The human Glo1 gene is located on chromosome 6 and its locus is linked to the Human Leukocyte Antigen- antigen D Related (HLA-DR) (Kompf and Bissbort 1976, Mayr et al. 1976). Human Glo1 is a homodimeric metalloenzyme, using Zn^{2+} as a cofactor (Figure 17). The 2 active sites are located at the dimer interface and residues from both subunits contribute to the thiol binding pocket. The 2 zinc cations are located in each active site (Aronsson et al. 1978, Sellin et al. 1983, Cameron et al. 1997). Monomeric human Glo1 is a protein of 184 amino acids with a molecular mass of approximately 21 kDa. In bacteria, Glo1 is also found as a dimeric proteins but uses Ni^{2+} as a cofactor in contrast to human Glo1 (Clugston et al. 1998) while in yeast, Glo1 is present as a monomer and contains two active sites (Frickel et al. 2001). Human Glo1 has 51% homology at the nucleotide level and 42% homology at the amino acid level with bacterial Glo1 (Ranganathan et al. 1993). Glo1 is present at a concentration of approximately 0.2 µg/mg of proteins in most human tissues (Larsen et al. 1985). It is well established that Glo1 sequence contains several phosphorylation sites and that nitric oxide can modify by S-nitrosylation cysteine

residues (Van Herreweghe et al. 2002, de Hemptinne et al. 2009). However, the real biological function of these post-translational modifications and the regulation of Glo1 enzymatic activity remain largely unclear. It is noteworthy that Glo1 gene deletion is embryonically lethal (Rabbani and Thornalley 2014).

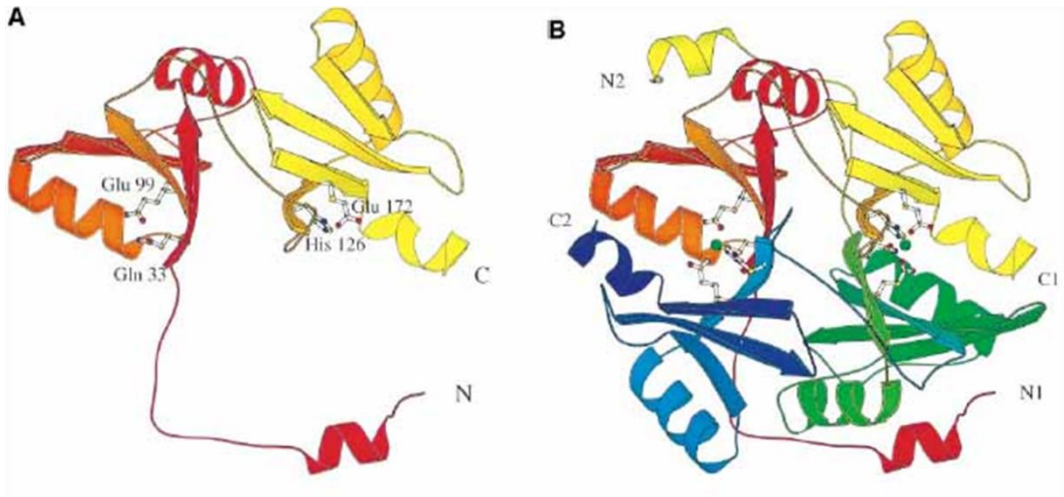

Figure 17: Schematic representation of Glo1. A. Monomeric form of Glo1. **B.** Representation of the dimeric form. The first monomer has been color ramped according to residue number from red (N-terminus) to yellow (C-terminus). The second monomer is represented in colors passing from yellow (N-terminus) to blue (N-terminus). The zinc and its coordinating residues are shown in a ball and stick representation with the zinc colored green. The active site is situated in a barrel which is formed only on dimerization. Adapted from (Cameron et al. 1997).

Glo2 is considered as the rate limiting enzyme of the glyoxalase system (Hooper et al. 1987). Human Glo2 (Figure 18) is a monomeric thiolesterase containing a binuclear metal-binding site (Zinc or Iron) essential for substrate binding and catalysis (Cameron et al. 1999). The human gene for Glo2, also called hydroxyacylglutathione hydrolase (HAGH) is located on chromosome 16 (Honey and Shows 1981). Like Glo1, Glo2 has been described in various organisms, from prokaryotes over plants to mammals. However, Glo2 has been observed not only in the cytosol, but also in the matrix and intermembrane space of mitochondria (Talesa et al. 1988). In mammals, cytosolic and mitochondrial Glo2 are coded by the same gene and result of an alternative translation initiation of the gene transcripts (Cordell et al. 2004). In *S. cerevisiae*, two different genes encode the mitochondrial (Glo4) and the cytosolic (Glo2) forms (Bito et al. 1997). The role of Glo2 in the mitochondria is not clear. Scire and collaborators (Scire et al. 2000) proposed that it could be a source of GSH in this organelle. In addition to S-D-lactoylglutathione, another

possible role is to hydrolyze other GSH thioesters formed in mitochondria (Thornalley 1990, Thornalley 1993, Vander Jagt 1993). Glo2 appears to be regulated by p63 and p73, two members of the p53 family that have fundamental roles in development (Xu and Chen 2006). Glo2 could act as a pro-survival factor and plays a critical role in the normal development and in the pathogenesis of various human diseases (e.g. cancer and diabetes).

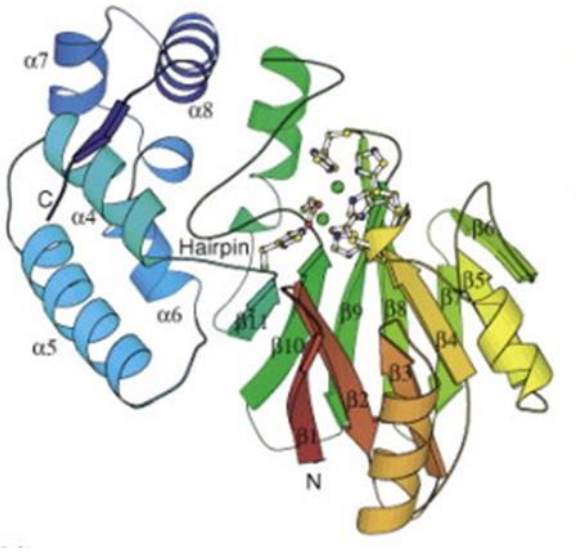

Figure 18: Overall structure of Glo2. The molecule has been color ramped according to residue number starting with red at the N terminus and finishing with blue at the C terminus. The metal ions and the coordinating residues are represented by balls and sticks. Adapted from (Cameron et al. 1999).

In *Escherichia coli*, the existence of another Glo enzyme, glyoxalase 3 (Glo3), has been described (Misra et al. 1995). Glo3 catalyzes the irreversible conversion of MG to D-lactate independently of the others glyoxalases, S-D-lactoylglutathione formation and GSH as cofactor. Glo3 homologues have been discovered in mouse and in *C. elegans*. A novel Glo enzyme able to convert MG into lactate without GSH has been identified in human cells. This enzyme is the protein deglycase DJ-1, also termed PARK7 (Parkinson disease protein 7), a molecular chaperone associated with the early onset of Parkinson's disease (Tao and Tong 2003, Lee et al. 2012). A recent study showed that human DJ-1 repairs MG- and GO-glycated proteins by acting on early glycation intermediates and releases repaired amino acids and lactate or glycolate, respectively (Figure 19). By deglycating cysteine, arginine and lysine

residues, DJ-1 reactivates serum albumin, GAPDH, aldolase and aspartate aminotransferase (Richarme et al. 2015).

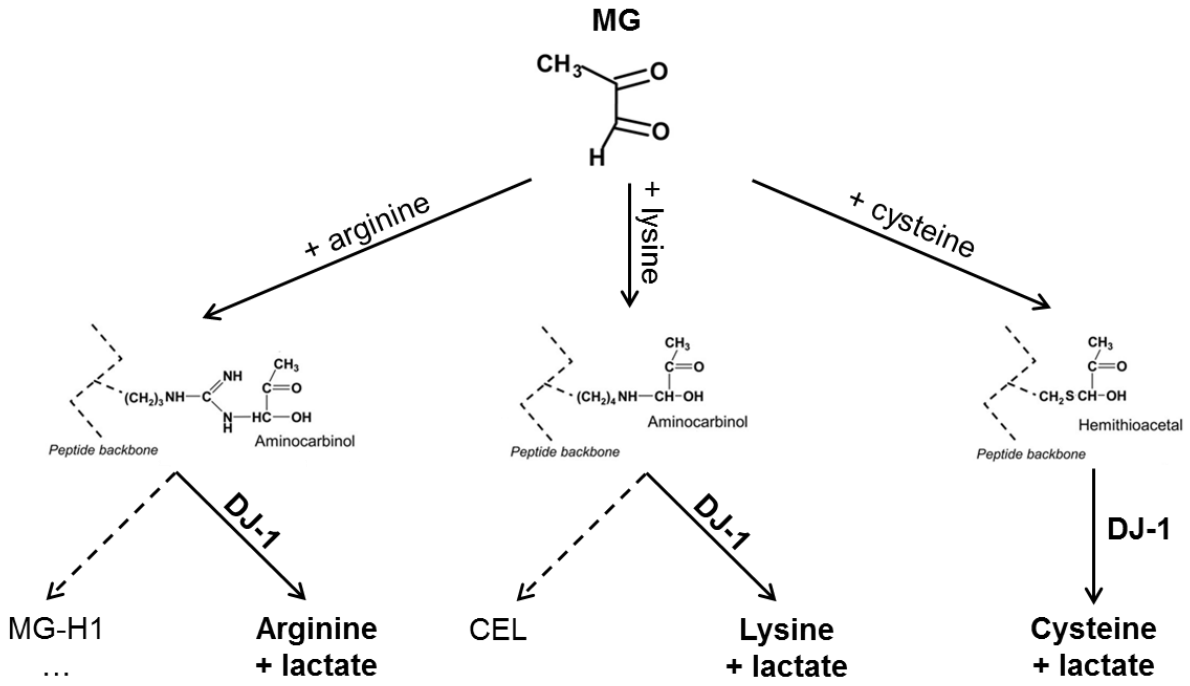

Figure 19: DJ-1 deglycation of MG-glycated intermediates. MG forms covalent adducts with cysteines, arginines, and lysines (hemithioacetals with cysteines and aminocarbinols with arginines and lysines). Aminocarbinols intermediates are transformed into AGEs (MG-H1 from arginine residues and CEL from lysine residues). DJ-1 transforms hemithioacetal into cysteine and lactate, and aminocarbinols into arginine/lysine and lactate. This latter prevents the formation of AGEs. Adapted from (Richarme et al. 2015).

3.3.2. Other detoxification systems

The glyoxalase system is a key enzymatic system of the defense mechanism against glycation. However, GO and MG are also metabolized by aldose reductases (aldoketo reductases) and aldehyde dehydrogenases (ALDHs). With glyoxalase enzymes, these enzymes are under stress-responsive control by the transcription factor nuclear factor erythroid 2-related factor 2 (Nrf2), through regulatory antioxidant response element (AREs) (Thimmulappa et al. 2002, Xue et al. 2012). Aldose reductase with sorbitol dehydrogenase participates to the polyol pathway converting glucose into fructose. However, MG is a better substrate than glucose for aldose reductase (Lindstad and McKinley-McKee 1993). This latter catalyzes the reduction of MG to propanediol through NADPH-dependent reactions. MG or the

hemithioacetal forms with GSH are reduced in acetol (or hydroxyacetone, 95%) or lactaldehyde (5%), respectively and then, both are reduced to propanediol (Vander Jagt et al. 1992, Thornalley 1994).

Betaine aldehyde dehydrogenase, a NAD-dependent ALDH, oxidizes several aldehydes, among which MG, but its efficiency toward MG is considerably low (Izaguirre et al. 1998). 2-oxoaldehyde dehydrogenase catalyzes the NADP-dependent oxidation of MG to pyruvate, essentially in the liver (Monder 1967, Oimomi et al. 1989).

3.4. Carbonyl stress and pathologies

Different cellular functions may be altered upon glycation. By inducing miscleavage and misfolding, glycation may impair the final processing of many proteins, resulting in their degradation or aggregation. Glycation can also alter the structure and function of essential macromolecules for cell homeostasis. Therefore, the level of AGEs should be maintained at very low levels in living cells. Accumulation of AGEs, increased level of MG and perturbation of the main detoxification enzyme, Glo1, have been associated with ageing and several diseases (Figure 20).

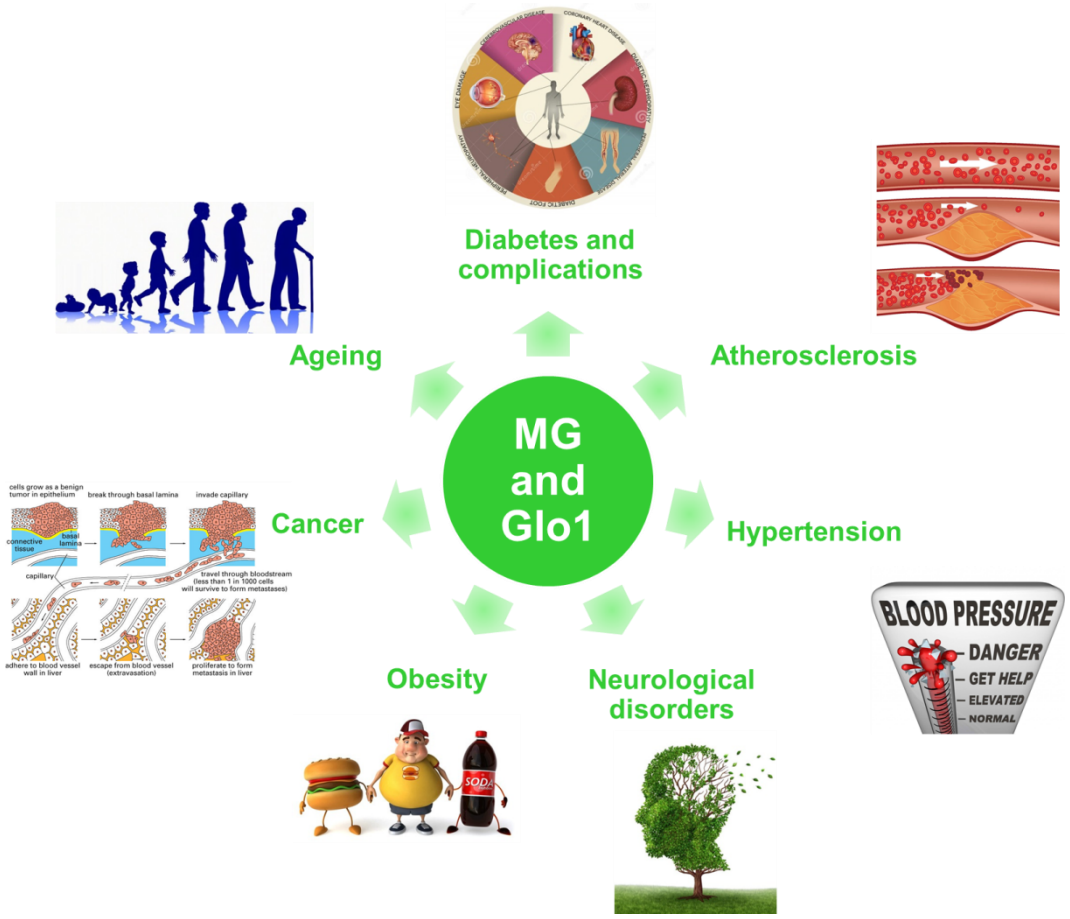

Figure 20: MG and Glo1 are associated with ageing and the pathogenesis of several diseases. Adapted from (Maessen et al. 2015).

3.4.1. MG an Glo1 in ageing

Human ageing is multifactorial and results from a complex combination of environmental, genetic, epigenetic and stochastic factors. As mentioned above, glycation of DNA is associated with an increased mutation frequency and DNA strand breaks that could be related to ageing through the induction of apoptosis and senescence. In 1960, John Kirk evaluated Glo1 activity in human arterial tissues of individuals with various ages. He observed a decrease of Glo1 activity with age which may contribute to the increased risk of cardiovascular disease with ageing (Kirk 1960). In the 80-90s, studies reported a reduction of Glo1 and Glo2 activities in human red blood cells (McLellan and Thornalley 1989), human lens (Haik et al. 1994), human brain (Kuhla et al. 2006) and in mice tissues (Sharma-Luthra and Kale 1994) with age. Others groups demonstrated an increase of GO and MG and their derived-AGEs, CML and CEL, in ageing human lens and skin/articular collagen

(Figure 21) (Dunn et al. 1989, Dunn et al. 1991, Ahmed et al. 1997, Frye et al. 1998, Verzijl et al. 2000). The accumulation of MG-H1 adducts in ageing human lens was further confirmed (Ahmed et al. 2003). Extensive accumulation of AGEs in cartilage collagen with age leads to stiffer and less resistant cartilage and therefore contributes to osteoarthritis (Verzijl et al. 2000, Verzijl et al. 2002). Lens proteins as well as skin and articular collagen are good candidates to evaluate protein damage in ageing due to their limited proteasomal degradation and long half-lives (15 to >100 years), respectively (Verzijl et al. 2000). Moreover, β-enolase observed in skeletal muscle (Snow et al. 2007) and glutamate dehydrogenase encountered in hepatic mitochondria (Hamelin et al. 2007) showed a significant increase of AGE modifications in aged rats. Caloric restriction of rats during 20 months decreased levels of AGEs in skin collagen (Cefalu et al. 1995). The CEL and CML adducts content increased with age in *Drosophila melanogaster*. The accumulation of damaged proteins could be linked to age-related loss of proteasomal activity (Carrard et al. 2002, Viteri et al. 2004).

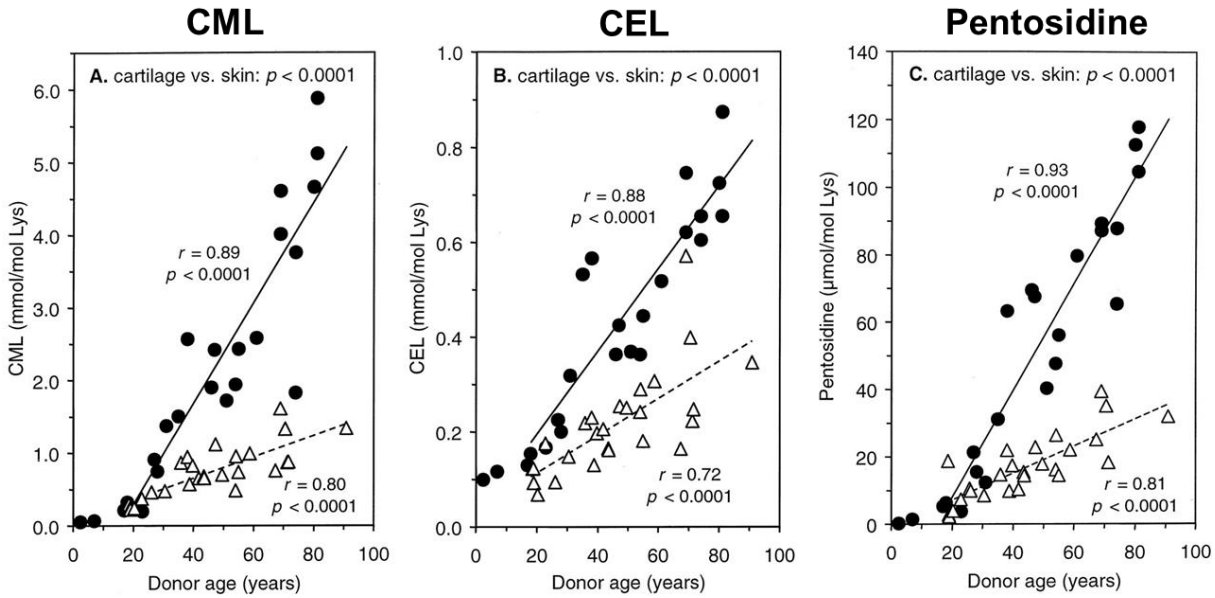

Figure 21: AGEs accumulate linearly with chronological age in both cartilage and skin collagen. Age-dependent increase concentration of CML, CEL, and pentosidine in human articular cartilage collagen (●) and skin collagen (△) are shown. The accumulation rate is higher in cartilage collagen. Adapted from (Verzijl et al. 2000).

The decreased Glo1 activity is associated with impaired wound healing (Fleming et al. 2013). In addition, this reduction of Glo1 enzymatic activity promotes accumulation of both MG modifications of mitochondrial proteins and mitochondrial ROS production leading to the decreased lifespan of *Caenorhabditis elegans* (Morcos et al. 2008). Interestingly, Glo1 overexpression in this nematode increased the mean and maximum lifespan of 30% (Morcos et al. 2008). Therefore, Glo1 is considered as an influential lifespan gene or "vitagene". Glo1 activity is directly proportional to the concentration of GSH. The concentration of GSH in human lenses declines with age (Kamei 1993). In *Drosophila*, the restoration of Glo1 activity by increasing tissue concentrations of GSH extended lifespan up to 50% (Orr et al. 2005). Therefore, the protective role of GSH in ageing is not only linked to its function as an antioxidant but also to its role as a cofactor of the glyoxalase system.

3.4.2. MG and Glo1 in neurological disorders

MG and its main detoxifying enzyme, Glo1, have also been linked to some pathologies of the central nervous system, most notably in Alzheimer's and Parkinson's diseases as well as in schizophrenia and anxiety disorders. In Alzheimer's disease, Glo1 expression is increased in early stages, but then decreases below normal levels at later stages, correlating with a marked increase in the accumulation of AGEs (Luth et al. 2005, Kuhla et al. 2007). Both extracellular plaques of amyloid β-peptide and intracellular neurofibrillary tangles of tau protein are highly modified by AGEs (Vitek et al. 1994, Yan et al. 1994). It has been suggested that protein glycation could stabilize the amyloid deposits and accounts for both their high insolubility and protease resistance (Smith et al. 1994). MG, through AGEs formation, induced RAGE up-regulation as well as GSK3β and p38 activation leading to tau hyperphosphorylation and neurofibrillary tangles. Aminoguanidine (MG scavenger) reversed the MG-induced tau hyperphosphorylation (Li et al. 2012). Increased MG-H1 free adducts was detected in cerebrospinal fluid of patients with Alzheimer's disease and was linked to cognitive impairment (Ahmed et al. 2005). MG promotes neuron apoptosis through the induction of oxidative stress and the activation of the pro-apoptotic protein Bax (Tajes et al. 2014).

Increased protein glycation plays also a role in the development of Parkinson's disease (Auburger and Kurz 2011, Kurz et al. 2011, Hipkiss 2014). Recently,

Parkinsonism-associated protein DJ-1/Park7 was identified as a major protein deglycase that repairs MG-glycated proteins (Figure 19) (Richarme et al. 2015). DJ-1 is a multifunctional protein involved in oxidative stress response and acting as a chaperone (Shendelman et al. 2004), a peroxidase (Andres-Mateos et al. 2007), a glyoxalase (Lee et al. 2012), a stabilizer of Nrf2 (Clements et al. 2006), an apoptotic inhibitor (Junn et al. 2005) and a translational regulator (van der Brug et al. 2008). Richarme and collaborators demonstrated that DJ-1 deglycates cysteine, arginine and lysine residues of several proteins *in vitro* and thus reactivates these proteins (Richarme et al. 2015).

There is also, but to a lower extent, evidence that MG and Glo1 play a role in both schizophrenia and anxiety. Carbonyl stress has been reported in schizophrenia patients (Arai et al. 2010). In contrast, increased levels of Glo1 and, therefore, lower levels of MG in the brain have been associated to anxiety disorder (Hovatta et al. 2005, Kromer et al. 2005, Distler et al. 2012).

3.4.3. MG and Glo1 in diabetes, vascular complications and related disorders

Besides ageing and neurological disorders, carbonyl stress has been mainly studied in the context of diabetes. In 2013, 382 million people have been estimated suffering of diabetes; this number is expected to rise to 592 million by 2035 (Guariguata et al. 2014). Diabetes mellitus, commonly referred as diabetes, is a group of metabolic diseases in which there are high blood sugar levels over a prolonged period of time. Two different types of diabetes exist. Type 1 diabetes results from a pancreas failure to produce insulin, while type 2 diabetes results from an insulin resistance in which body cells fail to respond to insulin stimulation. Diabetes can cause many complications notably vascular complications such as nephropathy, retinopathy and neuropathy. One of the great challenges for clinicians is the early detection of these vascular diseases associated with diabetes. Hyperglycemia has been established as a major risk factor for diabetic vascular complications (Group 1993). Therefore, increased MG and AGEs levels could explain, at least in part, the development of these complications in diabetic patients and could be used as reliable biomarkers for vascular diseases.

In 1988, Thornalley reported that human red blood cells, cultured in high glucose containing medium (mimicking hyperglycemia) increased their level of MG,

S-D-lactoylglutathione and D-lactate, while glyoxalases activities were unchanged (Thornalley 1988). Similar studies with both bovine and human aortal endothelial cells as well as human microvascular endothelial cell line (HMEC) confirmed the increased MG formation when cultured in hyperglycemic-like medium (Shinohara et al. 1998, Dobler et al. 2006, Yao and Brownlee 2010). Overexpression of Glo1 in endothelial cells cultured in high glucose medium decreased AGEs formation (Shinohara et al. 1998) and decreased tubules formation, a model for decreased angiogenesis in diabetes (Ahmed et al. 2008). Several studies demonstrated that the concentration of MG is increased in plasma and red blood cells of diabetic patients (Thornalley et al. 1989, McLellan et al. 1994, Beisswenger et al. 1999, Nicolay et al. 2006). Indeed, the plasma concentration of MG in healthy human is ~100-150nM and increases by 5-6 fold and 2-3 fold in patients with type 1 and type 2 diabetes, respectively (Rabbani and Thornalley 2011). Increased MG formation could be due to an increased glucose uptake by GLUT1 glucose transporter in hyperglycemia conditions (Haik et al. 1994, Dobler et al. 2006), or decreased enzymatic activities of GAPDH and/or Glo1 (Du et al. 2003, Yego and Mohr 2010). There is evidence of downregulation of Glo1 expression via RAGE pro-inflammatory signaling. Among AGEs, MG-H1 adducts have the highest affinity for RAGE (Xue et al. 2014). The binding of MG-H1-modified proteins or free MG-H1 to RAGE leads to the activation of signaling pathways and the downregulation of Glo1. The signaling mechanism that mediates this effect is still unclear but could involve NF-κB (nuclear factor-κB) activation. Hyperglycemia-induced ROS production increases RAGE expression and NF-κB activation. These effects are mediated by MG and prevented by Glo1 overexpression (Yao and Brownlee 2010). Altogether, this suggests that RAGE-dependent Glo1 downregulation, followed by increased MG-modified proteins, ultimately lead to further ligation and activation of RAGE. Therefore, it induces a continued and self-perpetual inflammatory response which contributes to diabetes and its vascular complications. Functional genomic studies with Glo1 deficient or overexpressing transgenic mice support increased MG as a factor linked to the development of diabetic vascular complications (Berner et al. 2012, Bierhaus et al. 2012, Giacco et al. 2014). Glo1 downregulation and the subsequent increase of MG level were also observed in ageing and atherosclerosis (Morcos et al. 2008, Hanssen et al. 2014). Conversely, Atkins and Thornalley found an 50-60% increased Glo1 activity and 20-30% increased Glo2 activity in erythrocytes of streptozotocin (STZ)-

induced diabetic mice while MG blood concentration increased by 2-fold (Atkins and Thornalley 1989). Importantly, diabetic patients with microvascular complications had a higher Glo1 activity in erythrocytes compared to uncomplicated patients (Thornalley et al. 1989, McLellan et al. 1994). Increased levels of MG-metabolizing enzymes were also found in mononuclear and polymorphonuclear cells from insulin-dependent diabetic patients with vascular complications (Ratliff et al. 1996). In STZ-induced diabetic rats, diminished Glo1 and Glo2 activities were found in the liver and increased activities in skeletal muscle (Uchino et al. 2004). Proteomic analysis revealed increased Glo1 protein in glomeruli of diabetic mice compared to controls (Barati et al. 2007). Glo1 gene has been reported as a genetic factor linked to body mass index and has been added to the human obesity genome (Wilson et al. 1991, Rankinen et al. 2006). Ranganathan and co-workers (Ranganathan et al. 1999) found an insulin response element on the Glo1 gene promoter, linking Glo1 expression with insulin dysfunction in diabetes. Regulation of Glo1 expression and activity is probably a tiny process. Down regulation of Glo1 may increase MG concentration/glycation and, in response, cells increase their Glo1 activity. It has been demonstrated that Nrf2 activators increase the levels of Glo1 expression and decrease cellular and extracellular concentrations of MG and MG-derived protein adducts, therefore, reducing mutagenesis and cell detachment (Xue et al. 2012). Isothiocyanates, including sulforaphane, which can be found in cruciferous vegetables, are known to activate Nrf2.

Increased amounts, up to 4 fold, of AGE-modified forms of LDL (Low-Density Lipoprotein) have been detected in the plasma of diabetic patients compared to healthy people (Schleicher et al. 1981, Bucala et al. 1993). The blood accumulation of modified LDLs has been associated with atherosclerosis development in diabetic patients, notably due to their impaired recognition by LDL receptor and altered renal clearance (Witztum et al. 1982, Bucala et al. 1994). More recently, the MG-modification of Arg18 residue in the N-terminal domain of ApoB100 of LDL was shown to cause both structural distortion and disruption of the antiparallel β-sheet. These MG-H1 modifications led to smaller and denser LDL with increased retention in arterial wall and atherogenic properties. Diabetic patients treated with metformin, a hypoglycemic agent, had decreased plasma MG levels (Beisswenger et al. 1999)

and MG-modified LDL. Therefore, metformin could protect diabetic patients from cardiovascular complications (Rabbani et al. 2010, Rabbani et al. 2011).

In diabetes, MG-modified proteins accumulation, mainly due to alteration in both chaperone-mediated autophagy in kidney (Sooparb et al. 2004) and proteasomal activity (Queisser et al. 2010), leads to functional perturbation and vascular complications. In bovine aortal endothelial cells cultured in high glucose medium, AGE-modified proteins content was increased up to 14-fold and was prevented by Glo1 overexpression (Shinohara et al. 1998). Ahmed and collaborators reported that CEL and MG-H1 residue contents increased by 3-fold in plasma proteins in patients with type 1 diabetes. These free adduct concentration increased up to 10-fold in plasma and a 15-fold increase of urinary excretion of MG-H1 was demonstrated (Ahmed et al. 2005).

In diabetic rats, the percentage of vascular type IV collagen modified by MG is increased by 2-fold, from 5 to 12%, compared to healthy rats (Dobler et al. 2006). Type IV collagen, an important component of the basement membrane, interacts with integrins of endothelial cells to anchor and sustain the vascular endothelium. Endothelial cell adhesion is notably mediated by the binding of integrins to the GFOGER and RGD sequence found in collagens (Ruoslahti 1996, Pedchenko et al. 2004). Hotspots of MG-H1 modifications are localized at 3 different arginine residues, Arg-390, Arg-889 and Arg-1452, part of the GFOGER and RGD sequences. Therefore, as expected, these MG-adducts impaired the interaction with integrins and led to endothelial cell detachment, anoikis and impaired angiogenesis (Figure 22) (Dobler et al. 2006). The number of detached circulating endothelial cells is increased in plasma of diabetic patients and is associated with cardiovascular disease (McClung et al. 2005). Pedchenko and collaborators demonstrated that perturbation of integrin-mediated cell-matrix interactions, via MG-modifications of renal extracellular matrix, contributes to the development of diabetic nephropathy. Interestingly, pyridoxamine, a promising treatment for diabetic nephropathy (Metz et al. 2003) and a MG scavenger (Voziyan et al. 2002), protects cell adhesion and integrin binding from inhibition by MG (Pedchenko et al. 2005). Another study has linked MG-glycation of fibronectin to apoptosis of retinal capillary pericytes and its implication in diabetic retinopathy (Liu et al. 2004).

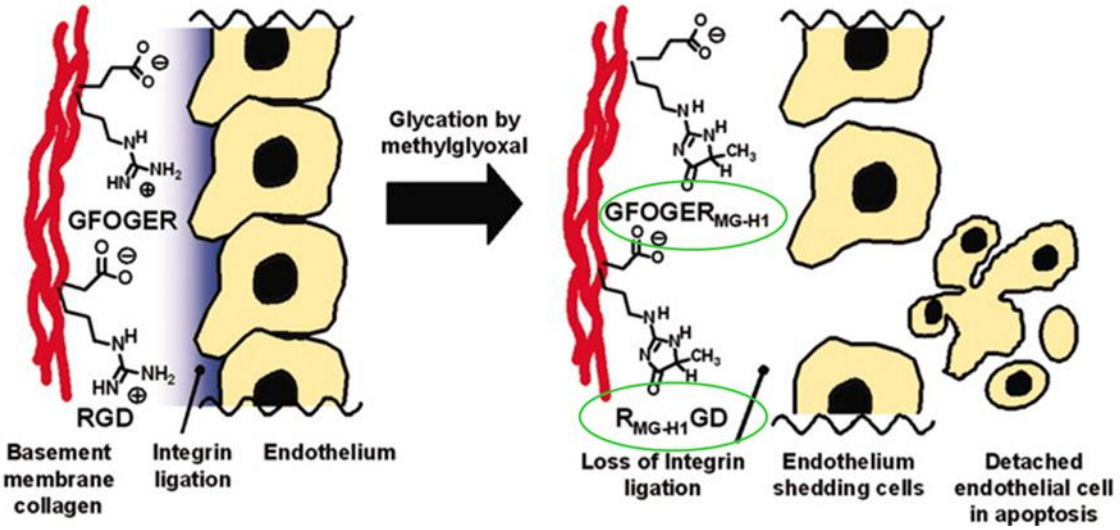

Figure 22: MG-H1 modifications on type IV collagen leads to endothelial cell detachment, anoikis and impaired angiogenesis. GFOGER and RGD motifs in type IV collagen present in the basal membrane interact with integrins of endothelial cells to anchor and sustain the vascular endothelium. MG-glycation of the arginine residues present in these motifs impairs the binding with integrins. The detachment of endothelial cells from the basement membrane induces apoptosis. Adapted from (Dobler et al. 2006).

A proteomic and functional study demonstrated that mitochondrial protein glycation leads to increased ROS formation in diabetic nephropathy (Rosca et al. 2005). The use of renal cortical mitochondria isolated from STZ-induced diabetic rats allowed the identification of 2 MG-H1-modified proteins from the respiratory complex III: ubiquinol-cytochrome c reductase, core protein I and cytochrome c1. As this complex is the major site for superoxide production in health and disease (Chen et al. 2003), its decreased activity leads to increased ROS production and oxidative damage in the kidneys of diabetic patients. Aminoguanidine treatment, a potent MG scavenger inhibiting AGEs formation (Lo et al. 1994), has been shown to improve mitochondrial respiration and complex III activity. As mentioned above, Morcos and colleagues identified MG modifications of mitochondrial proteins and mitochondrial ROS production leading to the decreased lifespan of *C. elegans* (Morcos et al. 2008).

Others proteins have also been shown as potential targets of MG glycation. In 2006, Jia and collaborators identified *in vitro* MG-modifications on insulin β-chain altering its function (Jia et al. 2006). The modification of co-repressor mSin3A by MG in renal endothelial cells leads to increased angiopoietin-2 as well as pro-inflammatory-mediated signaling pathways implicated in nephropathy pathogenesis

(Yao et al. 2007). Bierhaus and colleagues found that glycation of the nociceptor-specific sodium channel $Na_v1.8$ by MG is associated with enhanced sensory neuron excitability and hyperalgesia in diabetic neuropathy (Bierhaus et al. 2012). Interestingly, aminoguanidine has been shown to reduce MG-induced hyperalgesia in diabetes suggesting that this MG scavenger could be used as a new therapeutic strategy against painful diabetic neuropathy.

In 2006, Schalkwijk and collaborators (Schalkwijk et al. 2006) established that under hyperglycemic conditions, argpyrimidine adducts were significantly increased in endothelial cells. Using western blot and mass spectrometry analysis, they identified heat shock protein 27 (Hsp27) as the major argpyrimidine-modified protein in endothelial cells. This study confirmed results obtained previously in rat glomerular mesangial cells (Padival et al. 2003). Hsp27 is an important protein chaperone and plays a role in apoptosis and in actin polymerization. The modification by MG of Hsp27 promotes its chaperone activity and could protect cells from hyperglycemic and oxidative damage in diabetes. The MG-glycation of α-crystallin, another protein chaperone, also enhanced its chaperone activity and protected the lens from deleterious protein modifications associated with ageing (Nagaraj et al. 2003). Therefore, the post-translational MG-modification of these 2 proteins could be a protective mechanism against environmental and metabolic stresses. However, modified Hsp27 was also associated with cataract development. In this context, MG-modifications of Hsp27 increased its anti-apoptotic potential by inhibition of caspases activity (Oya-Ito et al. 2006). Hsp27 has also been shown to be targeted by MG in human cancer cells as discussed below. The modification of Hsp27 by MG protects cells from apoptosis (Sakamoto et al. 2002, van Heijst et al. 2006, Bair et al. 2010, Oya-Ito et al. 2011). We can conclude that, depending of the context, MG-modifications on the same protein can have different effects on cells.

3.4.4. MG and Glo1 in cancer

In the 60-70s, MG was considered as an anti-tumor agent. An arrest of tumor growth and a reduction of tumor size were observed when MG was injected intraperitoneally or intravenously in mice bearing experimental tumors (Apple and Greenberg 1967, Jerzykowski et al. 1970, Conroy 1978). The problem of this strategy was the high toxicity of MG for the normal cells and the need of selective anti-tumor

therapy. Later, *in vitro* studies reported that treatment of human cancer cell lines with MG induced cell-cycle arrest and apoptosis (Kang et al. 1996, Milanesa et al. 2000).

In order to survive, highly glycolytic cancer cells require a high rate and functional detoxification system of MG. Ten years after the discovery of the Warburg effect, glyoxalase activities in malignant and non-malignant tissues from rats were reported (for review (Thornalley and Rabbani 2011). In 1956, McKinney and Rundles demonstrated that glyoxalase activity is higher in leukemic human leukocytes compared to normal leukocytes *in vitro* (McKinney and Rundles 1956). Several transcriptomic, proteomic and/or immunohistochemical studies (Table 3), reported an increase of Glo1 expression/activity in cancer cells suggesting an important role of this protein during carcinogenesis. In 2010, Santarius and collaborators reported that increased Glo1 expression in human cancer cells is related to its gene amplification (Santarius et al. 2010). However, a genomic study identified Glo1 as a tumor suppressor gene which is located in frequently deleted genomic zones in both hepatocellular and breast carcinoma. They produced a short hairpin RNA (shRNA) library targeting the mouse orthologues of genes deleted in hepatocellular carcinoma and screened for shRNAs which promote tumorigenesis in a mouse model of hepatocellular carcinoma. Significantly, they identified and functionally validated 13 tumor suppressor genes, among which Glo1 (Zender et al. 2008).

Table 3: Glo1 expression and activity in human cancers.

Tumor origin	Glo1 status	References
Breast	Increased Glo1 **expression** and **activity** in tumors	(Rulli et al. 2001)
	Increased Glo1 **expression** in HER2+ cancer	(Zhang et al. 2005)
	Increased Glo1 **expression** associated with tumor grade	(Fonseca-Sanchez et al. 2012)
Pancreas	Increased Glo1 **expression** in liver metastasis	(Nakamura et al. 2004)
	Increased Glo1 **expression** in tumors	(Wang et al. 2012)
Prostate	Increased Glo1 **activity** in tumors	(Davidson et al. 1999, Davidson et al. 2002)
	Increased Glo1 **expression** associated with cancer progression	(Romanuik et al. 2009)
	Increased Glo1 **expression** in tumors	(Samadi et al. 2001)
Gastric	Increased Glo1 **expression** associated with poor prognosis	(Cheng et al. 2012)
	Increased Glo1 **expression** in tumors	(Hosoda et al. 2015)
Lung	Increased Glo1 **activity** in cancer cell lines	(Sakamoto et al. 2001)
	Glo1 **activity** similar in tumoral and non-tumoral tissues	(Di Ilio et al. 1987)
Skin	Increased Glo1 **expression associated with** tumor stage	(Bair et al. 2010)
Ovarian	Increased Glo1 **expression** in invasive tumors	(Jones et al. 2002)
	Increased Glo1 **expression** in pre-malignant lesions	(Smith-Beckerman et al. 2005)
Bladder	Increased Glo1 **expression** and **activity** in superficial tumors and not in invasive tumors	(Mearini et al. 2002)
Colon	Increased Glo1 **expression** and **activity** in tumors	(Ranganathan and Tew 1993)
Liver	Increased Glo1 **expression** in tumors	(Hu et al. 2014)
	Increased Glo1 **expression** in tumors (Glo1 genetic amplification)	(Zhang et al. 2014)
Blood (Leukemia)	Increased Glo1 **expression** in Acute Myeloid Leukemia compared to Acute Lymphoid Leukemia	(Cui et al. 2004)

Since late 60's, Glo1 inhibitors, such as S-p-bromobenzylglutathione, are tested as anticancer agents (Vince and Wadd 1969, Vince et al. 1971). The first Glo1 inhibitors were GSH conjugates and acted as Glo1 substrate analogues. They had poor cellular permeability and were unstable to cleavage by γ-glutamyl transferase in the extracellular environment. In order to improve these two latter features, a diesterification of GSH conjugate inhibitors has been performed. When these GSH conjugate diesters are delivered to the tumor, ester groups are removed by non-specific esterases and Glo1 inhibitor is revealed. S-p-bromobenzylglutathione cyclopentyl diester (BBGC) has been shown to have potent anti-tumor activities *in vitro* and *in vivo* by increasing MG levels and inducing apoptosis (Lo and Thornalley 1992, Thornalley et al. 1996). Delivery of the prodrug inhibitors was potentially impaired by plasma esterases which release Glo1 inhibitors before tissue delivery. Therefore, improvements of the chemical structure of these Glo1 inhibitors have been performed (Murthy et al. 1994, Kavarana et al. 1999, Sharkey et al. 2000). Some current clinical and investigational drugs have been shown to inhibit Glo1 such as methotrexate (Bartyik et al. 2004) and curcumin (Santel et al. 2008). Interestingly, BBGC selectively induced apoptosis in human lung cancer cells that overexpressed Glo1 (Sakamoto et al. 2001). Highly glycolytic tumor cells produce high level of MG and, consequently, need high level of Glo1 to detoxify MG. As expected, inhibition of Glo1 activity by BBGC induced high/toxic amount of MG and led to cell death. Moreover, intraperitoneal injection of BBGC in mice bearing subcutaneous lung or prostate tumors reduced significantly tumor growth with little toxicity to the mice (Sakamoto et al. 2001). In this study, the observed apoptosis was mediated through JNK and p38 phosphorylation as well as caspase-3 and -9 cleavage and activation. However, MG can induce apoptosis in cancer cells through various mechanisms: (1) generation of ROS and GSH depletion (Amicarelli et al. 2003), (2) inhibition of cellular respiration (Milanesa et al. 2000, Davidson et al. 2002, Ghosh et al. 2011), (3) DNA modification and DNA-protein cross-link resulting in DNA instability (Thornalley et al. 2010), (4) cell cycle progression inhibition (Kang et al. 1996, Milanesa et al. 2000), (5) negative regulation of anti-apoptotic proteins as well as positive regulation of pro-apoptotic proteins (Antognelli et al. 2013) and (6) impaired mitochondrial permeability via the glycation of mitochondrial proteins and release of cytochrome c (Speer et al. 2003).

Glo1 overexpression has been associated with multidrug resistance (MDR) in cancer chemotherapy (Sakamoto et al. 2000). Glo1 activity was increased in several antitumor agent resistant leukemia and other cancer types cells, compared with their parental cells. Sakamoto and colleagues generated a variant (UK711) of human monocytic leukemia U937 cells which was resistant to apoptosis induced by several chemotherapeutic agents such as Etoposide, Adriamycin and Mitomycin C. Using a complementary DNA subtractive hybridization of these 2 leukemia cell lines, they found a Glo1 overexpression in the apoptotic-resistant UK711. In human T-cell leukemia Jurkat cells, Glo1 overexpression confers resistance to Etoposide and Adriamycin antitumor agents. Moreover, co-treatment with BBGC sensitized drug-resistant leukemia UK711 cells to Etoposide (Sakamoto et al. 2000). Santarius and collaborators have confirmed that cancer cells with high level of Glo1 were resistant to current chemotherapeutic agents but were sensitive to Glo1 inhibition by BBGC or Glo1 silencing. In contrast, they showed that tumor cells with low Glo1 are insensible to anti-Glo1 treatment (Santarius et al. 2010). As mentioned above, cancer cells express high level of Glo1 in order to survive in highly glycolytic and high MG level conditions. Therefore, Glo1 inhibition induces higher MG level and its cytotoxicity properties which increase the efficacy of antitumor agents. These results suggest that high Glo1 expression and high MG levels are required in order to observe a cytotoxic response to Glo1 inhibition combined with chemotherapeutic agents. Taken together, these studies indicate that Glo1 could represent an interesting marker for drug resistance.

The presence of MG-adducts in malignant lesions has been only poorly explored to date. The pioneer study, published 10 years ago, demonstrated an accumulation of argpyrimidine adducts in human larynx and breast carcinoma cells (van Heijst et al. 2005). Until now, Hsp27 is the only MG-modified protein identified in cancer cells. Hsp27 is highly expressed in cancer cells and its expression is associated with increased tumorigenicity, metastatic potential and resistance to chemotherapy. This latter is a powerful anti-apoptotic protein counteracting apoptosis at different steps (for review (Wang et al. 2014). Sakamoto and colleagues found argpyrimidine adducts of Hsp27 in cancer cells (Sakamoto et al. 2002). The arginine 188 at the C-terminus was identified as the residue of MG-modification. MG-glycation leads to oligomerization and multimers formation of Hsp27 which are required for a

correct chaperone function of Hsp27 (Rogalla et al. 1999). Furthermore, MG-modification of Hsp27 prevents cytochrome c-mediated caspase-3 and -9 activation. Therefore, MG avoids cancer cells from undergoing apoptosis by enhancing Hsp27 anti-apoptotic activities. Interestingly, inhibition of MG-modification of Hsp27 by treatment with MG scavenger sensitizes cancer cell to Camptothecin and Etoposide antitumor agents (Sakamoto et al. 2002). Later, an inverse correlation between argpyrimidine-modified Hsp27 and active caspase-3 was demonstrated in squamous cell from lung carcinoma. Cancer cells with high expression of MG-modified Hsp27 are resistant against Cisplatin-induced caspase-3 activation compared to cells with low MG-Hsp27 cells in which cisplatin induced a strong activation of caspase 3 (van Heijst et al. 2006). Therefore, besides Glo1, MG-AGEs could also be implicated in MDR. More recently, a proteomic analysis identified Hsp27 as the major argpyrimidine-modified protein in human melanoma cells (Bair et al. 2010). MG-Hsp27 was also observed in gastrointestinal carcinoma cell lines as well as in colon and rectum from cancer patients, but not in healthy subjects. Additionally, the transfer of MG-Hsp27 using a cationic lipid is more effective in preventing H_2O_2 induced apoptosis than naïve Hsp27 in rat intestinal epithelial cells. MG-modified Hsp27 effectively inhibited caspase activation, ROS production and apoptosis mediated by hydrogen peroxide treatment. Mass spectrometry analysis of MG-glycated human recombinant Hsp27 identified 6 modified residues: arginines 5, 96, 127, 136 and 188 and lysine 123 (Oya-Ito et al. 2011). Altogether, these results demonstrated that high expression of MG-glycated Hsp27, associated with apoptosis inhibition and increased chaperone activity, could represent a mechanism responsible of tumor growth.

After their observation that CML, a glyoxal-derived adduct, is strongly present in lung cancer tissues, Van Heijst and colleagues raised an interesting hypothesis (van Heijst et al. 2006). By binding to RAGE, CML modified proteins may be involved in tumor progression through the activation of NF-kB (Kislinger et al. 1999) as well as the upregulation of VEGF (Okamoto et al. 2002) and of vascular cell adhesion molecule 1 (VCAM-1) (Schmidt et al. 1995). Interestingly, RAGE expression was found to be strongly associated with the invasive and metastatic activity of gastric and pancreatic carcinomas (Takada et al. 2001, Kuniyasu et al. 2002). We can also

speculate that MG-AGEs, by binding to RAGE, could favor tumor progression and metastasis development.

To summarize, a timeline with the most important findings concerning MG and Glo1 is shown in Figure 23.

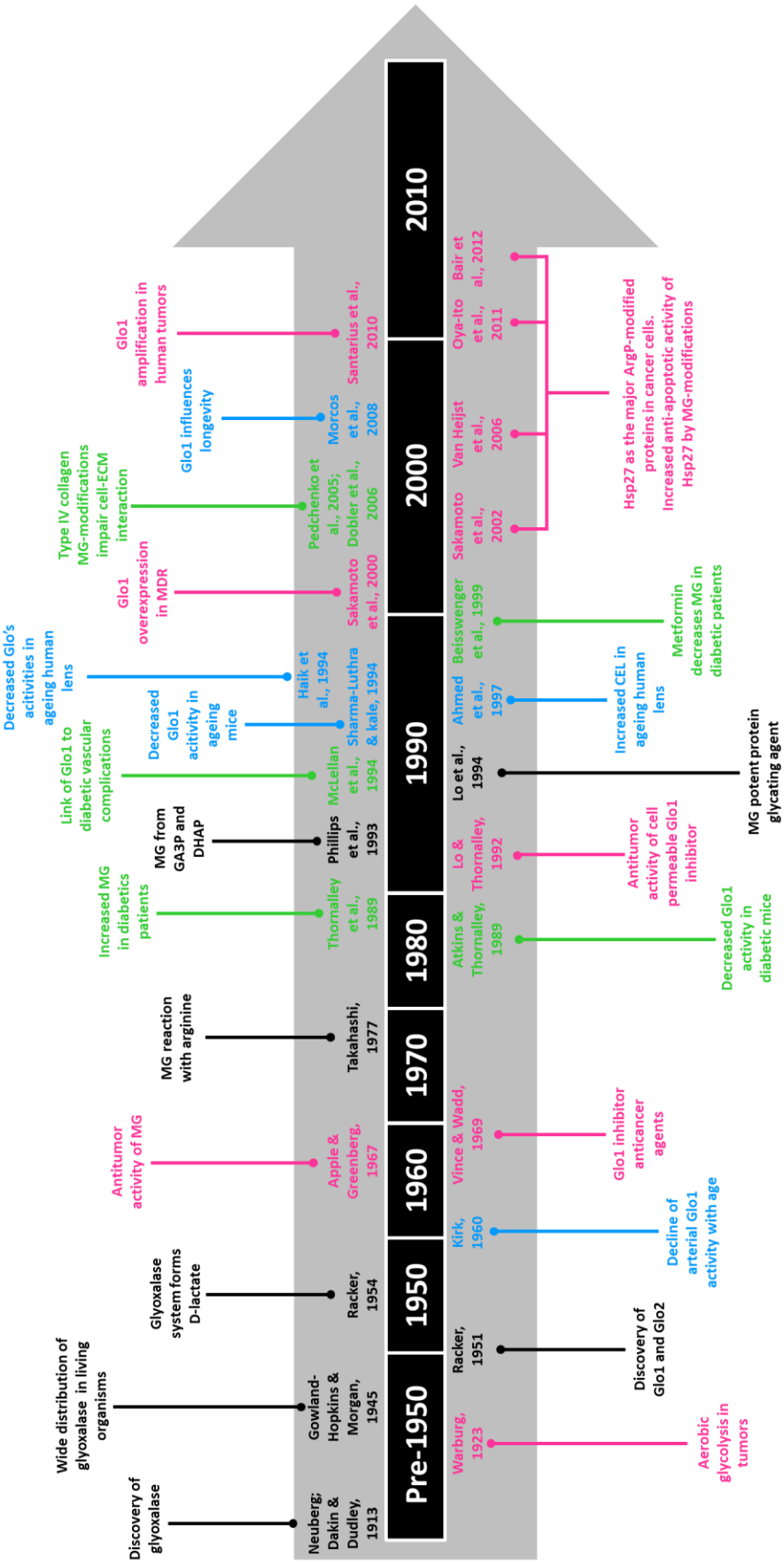

Figure 23: Timeline of some important findings concerning MG and Glo1. The general outcomes are written in black. The reports related to diabetes, cancer and ageing are described in green, pink and blue, respectively. Adapted from (Rabbani and Thornalley 2011, Thornalley and Rabbani 2011, Xue et al. 2011).

3.5. MG scavengers

It is clear now that carbonyl stress represents a good candidate for anti-cancer therapy. As mentioned above, Glo1 inhibitors by increasing MG accumulation are able to induce cancer cell death and help to sensitize resistant cancer cells to chemotherapeutic agents. However, MG favors tumor progression by helping cancer cell escape from apoptosis. Therefore, drugs decreasing MG level and adducts formation are now developed for cancer therapy but also for the treatment of other pathologies such as diabetes and neurological disorders. Carbonyl stress may be impaired by preventing dicarbonyl formation, scavenging dicarbonyls and enhancing detoxifying enzymes such as Glo1. Investigational MG scavenging molecules are aminoguanidine, N-phenacylthiazolium bromide, alagebrium, carnosine, pyridoxamine and metformin.

Aminoguanidine, a nucleophilic hydrazine compound, lowers the formation of AGEs by its scavenging capacity for MG through reaction with its guanidine group (Brownlee et al. 1986, Lo et al. 1994). In experimental conditions, aminoguanidine prevents diabetic complications such as nephropathy (Soulis-Liparota et al. 1991, Soulis et al. 1996), retinopathy (Hammes et al. 1991) and neuropathy (Kihara et al. 1991).

N-phenacylthiazolium bromide and **alagebrium**, considered as AGE cross-link breakers, impair vascular diabetic complications in preclinical studies by inhibiting AGEs formation (Ferguson et al. 1999, Cooper et al. 2000, Vasan et al. 2003, Sell and Monnier 2012, Engelen et al. 2013).

Carnosine is a pluripotent dipeptide (β-alanyl-L-histidine) produced by brain, kidney and skeletal muscle in mammals. Functionally, carnosine can scavenge reactive oxygen species (Boldyrev et al. 2004), reactive nitrogen species (Fontana et al. 2002) and reactive dicarbonyl (Hipkiss and Chana 1998) and acts as a metal ion chelator (Trombley et al. 2000). By scavenging MG, carnosine delays cellular senescence (McFarland and Holliday 1994). Paradoxically, the dipeptide inhibits the proliferation of cultured cancer cells (Holliday and McFarland 1996, Iovine et al. 2012, Shen et al. 2014). The anti-neoplastic effect of carnosine was also described *in vivo* (Renner et al. 2010, Horii et al. 2012). Carnosine has been also explored for its therapeutic potential towards neurological disorders (Bellia et al. 2011) and

complications associated with type 2 diabetes (Kamei et al. 2008, Pfister et al. 2011, Riedl et al. 2011). The underlying mechanism of the beneficial effects of carnosine is not clear but it has been suggested that inhibition of AGEs formation may be part of it (Hipkiss 2005). Unfortunately, the metabolic instability of carnosine in human serum due to the presence of carnosinase is an obstacle to its therapeutic use in patients. The development of more stable carnosine derivatives is needed.

The natural vitamin B6 analogue, **pyridoxamine**, is another MG scavenger and increases also Glo1 activity (Nagaraj et al. 2002). Treatment of diabetic experimental animals with pyridoxamine improves significantly renal function (Degenhardt et al. 2002, Alderson et al. 2003, Tanimoto et al. 2007, Waanders et al. 2008, Zhu et al. 2012). Because pyridoxamine demonstrated beneficial effects without major adverse effects, this compound is currently studied as a potential treatment for type 2 diabetes patients (Williams et al. 2007).

Metformin is currently the first-line treatment option for patients with type 2 diabetes. The blood glucose-lowering activity of metformin is linked to suppression of hepatic gluconeogenesis and increased cellular uptake of glucose, for review (Viollet et al. 2012). In addition to its glucose-lowering action, this drug can also trap MG (Ruggiero-Lopez et al. 1999). This reaction between the guanidino group of metformin and the dicarbonyl group of MG is similar to the one with aminoguanidine, another guanidine compound (Lo et al. 1994). Indeed, it has been shown that metformin treatment is able to reduce plasma MG levels in type 2 diabetic patients (Beisswenger et al. 1999). Beisswenger and collaborators postulated that MG decrease is either due to the scavenging capacity of metformin or to the increased production of GSH and enhanced glyoxalase detoxification system. Interestingly, metformin decreased specifically MG levels and not the others dicarbonyls such as 3-DG. Several studies demonstrated a beneficial effect of metformin on vascular complications in type 2 diabetes patients (De Jager et al. 2005, Takiyama et al. 2011, Kender et al. 2014). Although the link with its MG-scavenging function is not established, increasing evidence showed a potential efficacy of metformin as an anticancer drug. Indeed, treatment with metformin decreased proliferation in various cancer cell lines by inducing cell cycle arrest and apoptosis (Ben Sahra et al. 2008, Gotlieb et al. 2008, Wang et al. 2008, Zhuang and Miskimins 2008, Alimova et al. 2009). These results have been confirmed in several animal cancer models

(Schneider et al. 2001, Buzzai et al. 2007, Hirsch et al. 2009, Kisfalvi et al. 2009, Liu et al. 2009)

The vitamin B1 derivative, **benfotiamine**, commonly used as a treatment for diabetic neuropathy, is not a direct scavenger of MG; but, by activating transketolase and the pentose phosphate pathway, it decreases MG formation (Hammes et al. 2003).

Until now, most MG scavengers have failed to achieve translation to clinical efficacy due to toxicity and short half-life (Thornalley 2003), instability (Thornalley and Minhas 1999) and dose-activity profile that is difficult to translate clinically (ca. 4 g/kg) (Nagaraj et al. 2002). The discovery of Glo1 inducers which increase Nrf2 binding to Glo1 promoter offers an alternative to MG scavengers that is more effective and safe. Natural isothiocyanates, which could be found in cruciferous vegetables, activate Nrf2. These Nrf2 activators increase Glo1 expression and decrease cellular MG level and MG-derived protein adducts (Xue et al. 2012). Glo1 inhibitors such as BBGC could be used for cancer treatment in MDR context for example or against bacteria in case of microbial infections. Finally, BBGC had potent anti-malarial activity against the red blood stage of *Plasmodium falciparum* (Thornalley et al. 1994).

II. Objectives of the study

II. Objectives of the study

Tumor cells use glycolysis rather than mitochondrial respiration to produce their energy (Warburg effect). Methylglyoxal (MG), a highly reactive glycolysis by-product, is thus accumulated in tumor cells where it glycates lipids, proteins and nucleic acids, thereby inducing a carbonyl stress. All mammalian cells developed a detoxifying system composed of 2 enzymes, glyoxalase 1 and 2 (Glo1 and 2) transforming MG into D-lactate. The contribution of MG in diabetes and its complications has been extensively studied since the 80s. However, the role of carbonyl stress in the context of cancer is still at its early days. To date, the only target of MG identified in cancer cells is heat shock protein 27 (Hsp27), a regulator of apoptosis.

Since 2013, a new research thematic has been launched in our Laboratory to study the potential role of MG and Glo1 in cancer development and progression. The project conducted in the context of this thesis comprised three main objectives:

The first objective was to evaluate carbonyl stress in breast cancer. To achieve this first goal, we notably developed the immunohistochemical staining of argpyrimidine MG-adducts and Glo1 using specific antibodies as well as Glo1 enzymatic activity assay.

The second objective was to identify new MG-modified proteins in breast cancer cells. In collaboration with the Laboratory of Pr. Edwin De Pauw (ULg), we performed mass spectrometry analysis to identify the modified residues within protein sequence of new MG targets.

The third objective was to determine the consequences of high carbonyl stress on cancer progression and metastasis development. Besides exogenous MG treatment, we choose the strategy to inhibit Glo1 in breast cancer cells in order to induce high endogenous MG level. These Glo1-deficient cancer cells were used for *in vitro* and *in vivo* experiments to help characterize their phenotype. The link between the biological effects mediated by Glo1-silencing and MG stress was further established using anti-glycating agents such as carnosine and aminoguanidine.

III. Results

III. Results

1. Triple negative tumors accumulate significantly less methylglyoxal specific adducts than other human breast cancer subtypes

1.1. Introduction

Breast cancer represents the most frequent cancer in women and regroups different lesions characterized by biological and molecular features. Breast tumors are divided into 4 molecular subtypes on the basis of estrogen/progesterone receptors and HER2 expression: luminal A (or HER2 negative), luminal B (or triple positive), HER2 positive and basal (or triple negative). Around 15-20% of diagnosed breast cancers are triple negative (Penault-Llorca and Viale 2012). These tumors are generally considered as aggressive tumors due to their high proliferation rate, high histologic grade and hormone-independent growth (Foulkes et al. 2010). Currently no specific treatment except surgery and chemo/radiotherapy is available for these patients. Therefore, patients with triple negative tumors have a poor prognosis.

In proliferating cells, glucose metabolism and growth control are strictly linked. Tumor cells use glycolysis rather than mitochondrial respiration to produce their energy, even in normoxic conditions (Vander Heiden et al. 2009). This adaptation is known as the Warburg effect. Methylglyoxal (MG), a highly reactive glycolysis by-product, is thus accumulated in tumor cells where it glycates lipids, proteins and nucleic acids, generating advanced glycation end products (AGEs). The reaction of MG with arginine residues on proteins generates MG-adducts including argpyrimidine. All mammalian cells possess a detoxifying system composed of 2 enzymes, glyoxalase 1 (Glo1) and 2 (Glo2) transforming MG into D-lactate (Racker 1951). The imbalance between MG detoxification and AGEs production generates a carbonyl stress that leads to major cellular damage.

The possible role of MG in breast cancer development and progression has not been yet extensively explored. Van Heijst and collaborators detected argpyrimidine adducts in several human tumor types including adenocarcinoma of the breast and squamous cell carcinoma of the larynx using MG-adducts immunohistochemical analysis (van Heijst et al. 2005). It has been demonstrated that Glo1 detoxification enzyme is overexpressed in many human cancers (Ranganathan and Tew 1993, Davidson et al. 1999, Bair et al. 2010). In 2001, Rulli and collaborators showed an increased Glo1 expression and activity in human

breast cancer tissues compared to normal counterparts (Rulli et al. 2001). More recently, *Glo1* gene amplification was evidenced in several human breast cancer cell lines (Santarius et al. 2010) and Glo1 expression has been positively correlated with high tumor grade in breast cancer (Fonseca-Sanchez et al. 2012).

The objective of this study was to evaluated carbonyl stress in human breast cancer tissues and cell lines.

1.2. Results

We first evaluated the presence of argpyrimidine adducts in 7 breast cancer tissues and in the corresponding non-tumoral counterparts using a specific antibody against argpyrimidine adducts by western blot. Tumoral lesions consistently accumulated more argpyrimidine MG-adducts compared to non-tumoral matched breast tissue (Figure 24).

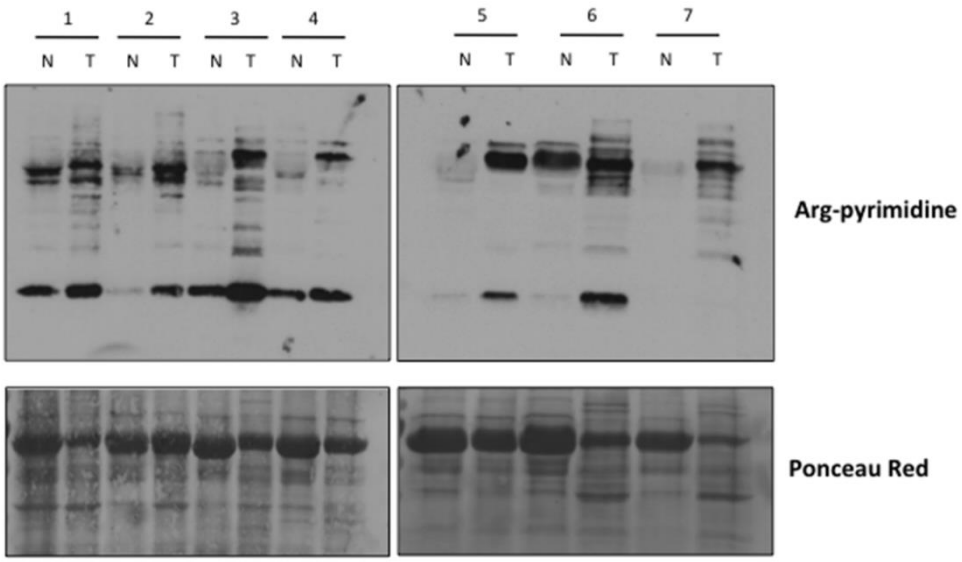

Figure 24: Increased argpyrimidine adducts in human breast cancer tissues compared with the non-tumoral counterparts. Using western blot analysis, argpyrimidine residues were evaluated in 7 human breast cancer tissues (T) and in their non-tumoral counterparts (N). Ponceau Red is shown as an indicator of equal protein loading.

Using immunohistochemistry, we next evaluated argpyrimidine level in 2 normal human breast tissues and in a cohort of breast cancers (n=93) divided in the 4 main subtypes (triple negative, triple positive, HER2 positive and HER2 negative). In good accordance with previous results, a moderate argpyrimidine staining was observed in normal breast tissues (Figure 25A-C). Interestingly, we found a significant association of argpyrimidine accumulation with breast cancer subtypes. We observed that the triple negative breast cancer tissues exhibited lower argpyrimidine immunostaining compared to the other subtypes (Figure 25E-I).

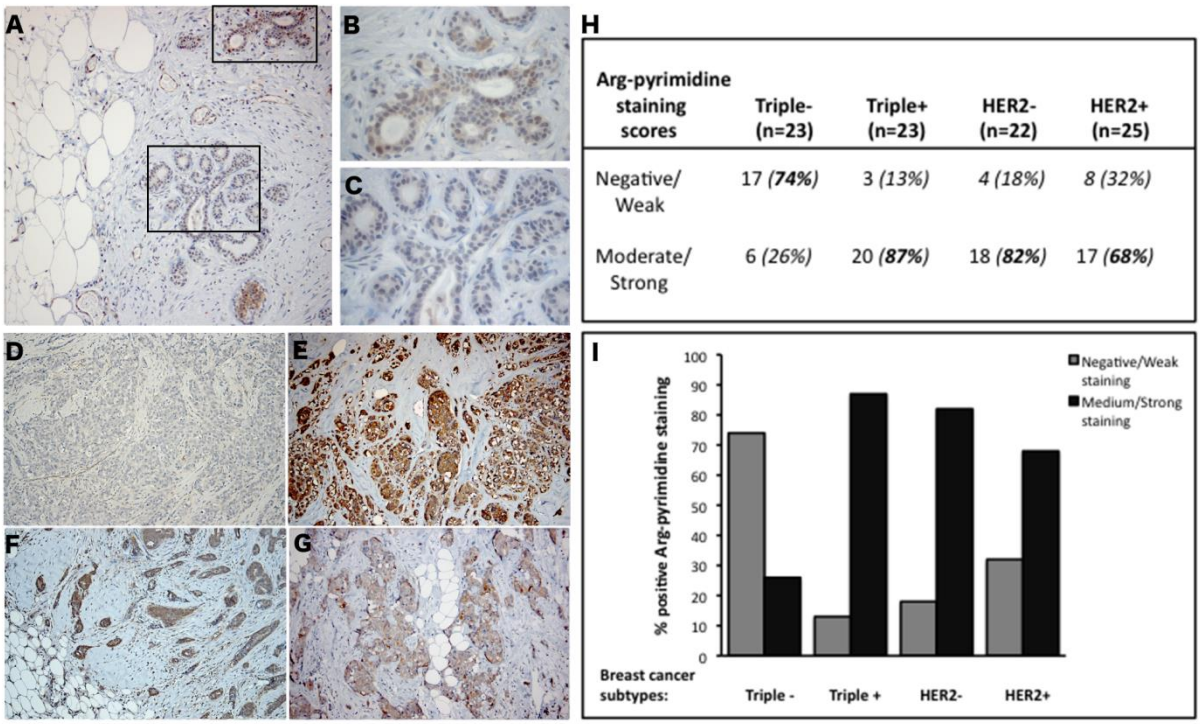

Figure 25: Triple negative breast tumors accumulated less argpyrimidine adducts in comparison with triple positive, HER2- and HER2+ tumors. A. Argpyrimidine adducts are detectable in breast tissue from reduction mammoplasty, magnification 100x. **B.** and **C.** show a higher magnification (400x) of regions boxed in panel A. Triple negative lesions (**D.**) exhibited a significantly lower accumulation of argpyrimidine residues compared to triple positive (**E.**), HER2- (**F.**) and HER2+ (**G.**) ones, magnification 100x. **H. and I.** Immunohistochemical scoring and graphical representation of argpyrimidine immunodetection, respectively.

To further explore the observed difference in the accumulation of MG-adducts in the different breast cancer subtypes, we performed Glo1 immunostaining on the same tissues using serial sections. No significant difference was found between the different groups. Indeed, Glo1 was highly expressed in most of the tissues evaluated. Therefore, we sought to examine the enzymatic activity of Glo1 rather its expression in triple positive and triple negative breast tumor samples. We demonstrated a significant increase of Glo1 activity in triple negative lesions when compared to triple positive ones, suggesting that they displayed a better MG detoxification capacity (Figure 26).

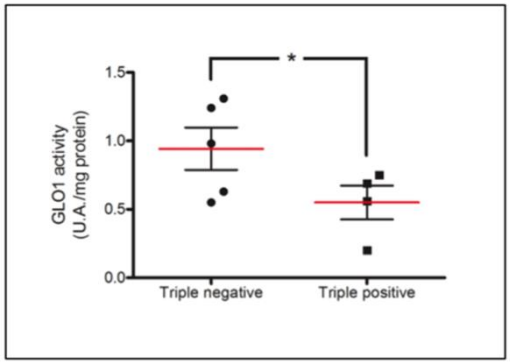

Figure 26: Increased Glo1 activity in triple negative breast cancer tissues in comparison with triple positive ones. Glo1 activity was measured in total breast tumors proteins extracts comprising 5 triple negative and 4 triple positive samples. * $p \leq 0.05$.

Next, we investigated argpyrimidine adducts in breast cancer cell lines from different molecular subtypes. Consistent with immunohistochemical results, triple negative breast cancer cell lines (MDA-MB-231 and MDA-MB-468) showed less argpyrimidine accumulation compared to HER2+ cells (SKBR3) and ER+/PR+ cells (MCF7). Interestingly, only triple negative breast cancer cells responded to MG treatment by increasing Glo1 expression and activity (Figure 27).

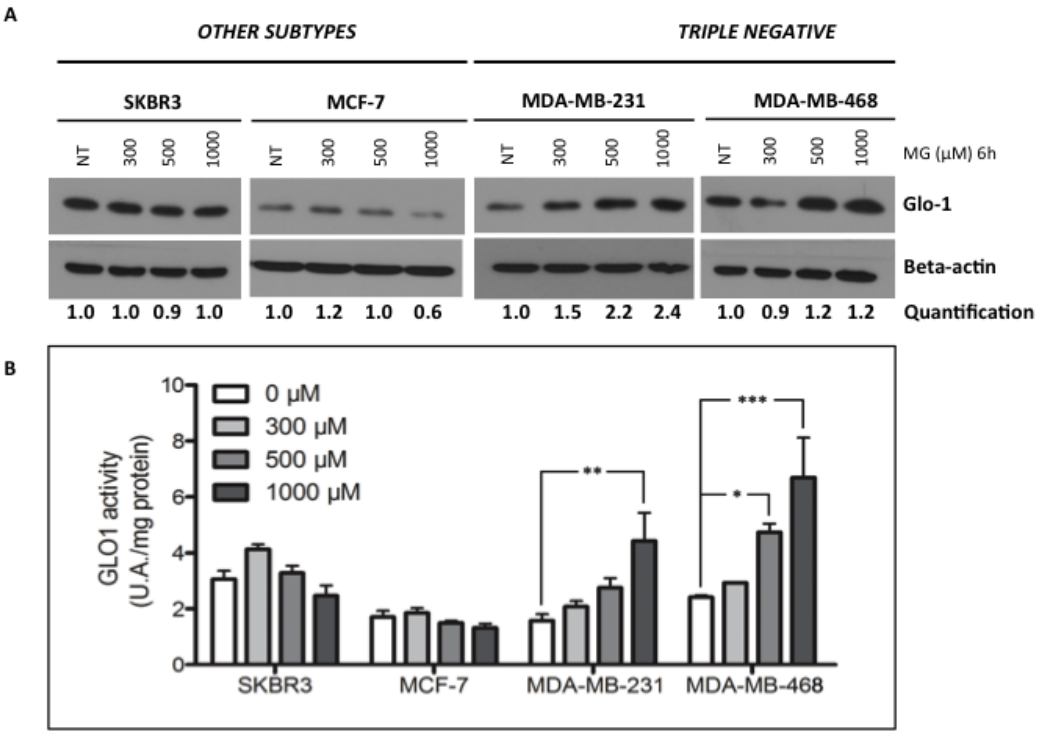

Figure 27: Glo1 expression and activity in human breast cancer cell lines upon MG treatment. Breast cancer cells were treated with increasing concentrations of MG for 6 hours. Only triple negative cells are able to respond to MG stimulation by increasing Glo1 protein level (**A.**) and activity (**B.**). Beta-actin was used for normalisation and densitometric quantification was performed. * $p \leq 0.05$, ** $p \leq 0.01$, *** $p \leq 0.001$.

1.3. Conclusions

In this first study, we demonstrated that carbonyl stress is a common feature in breast tumors compared to normal breast tissues. We showed that triple negative breast cancers accumulate less argpyrimidine MG-adducts compared to other breast tumor subtypes, probably due to a more efficient detoxification activity. Our data indicate that breast cancer cells originating from different tumor molecular subtypes react differently to MG stress. The most aggressive breast cancer cells are able to respond to MG stimulation by increasing Glo1 activity thus reducing their carbonyl stress level and escape from MG cytotoxic effects. These findings suggest that sensitizing triple negative tumor cells to carbonyl stress may represent a good therapeutic strategy for this aggressive cancer subtype.

Triple negative tumors accumulate significantly less methylglyoxal specific adducts than other human breast cancer subtypes

Chiavarina B*, **Nokin MJ***, Durieux F, Bianchi E, Turtoi A, Peulen O, Peixoto P, Irigaray P, Uchida K, Belpomme D, Delvenne P, Castronovo V and Bellahcène A

Oncotarget, 2014, 5 (14), 5472-82

Triple negative tumors accumulate significantly less methylglyoxal specific adducts than other human breast cancer subtypes

Barbara Chiavarina[1,*], Marie-Julie Nokin[1,*], Florence Durieux[1], Elettra Bianchi[2], Andrei Turtoi[1], Olivier Peulen[1], Paul Peixoto[1], Philippe Irigaray[3], Koji Uchida[4], Dominique Belpomme[3], Philippe Delvenne[2], Vincent Castronovo[1] and Akeila Bellahcène[1]

[1] Metastasis Research Laboratory, GIGA-Cancer, University of Liège, Liège, Belgium

[2] Department of Anatomy and Pathology, University of Liège, Liège, Belgium

[3] Association for Research and Treatments Against Cancer (ARTAC), Paris, France

[4] Laboratory of Food and Biodynamics, Graduate School of Bioagricultural Sciences, Nagoya University, Nagoya, Japan

[*] These Authors contributed equally to this work

***Correspondence to**: Akeila Bellahcène, **email**: a.bellahcene@ulg.ac.be*

Keywords: methylglyoxal, breast cancer, advanced glycation end-products, Arg-pyrimidine adducts, glyoxalase 1

***Received**: April 11, 2014* ***Accepted**: June 18, 2014* ***Published**: June 20, 2014*

This is an open-access article distributed under the terms of the Creative Commons Attribution License, which permits unrestricted use, distribution, and reproduction in any medium, provided the original author and source are credited.

ABSTRACT

Metabolic syndrome and type 2 diabetes are associated with increased risk of breast cancer development and progression. Methylglyoxal (MG), a glycolysis by-product, is generated through a non-enzymatic reaction from triose-phosphate intermediates. This dicarbonyl compound is highly reactive and contributes to the accumulation of advanced glycation end products. In this study, we analyzed the accumulation of Arg-pyrimidine, a MG-arginine adduct, in human breast adenocarcinoma and we observed a consistent increase of Arg-pyrimidine in cancer cells when compared with the non-tumoral counterpart. Further immunohistochemical comparative analysis of breast cancer subtypes revealed that triple negative lesions exhibited low accumulation of Arg-pyrimidine compared with other subtypes. Interestingly, the activity of glyoxalase 1 (Glo-1), an enzyme that detoxifies MG, was significantly higher in triple negative than in other subtype lesions, suggesting that these aggressive tumors are able to develop an efficient response against dicarbonyl stress. Using breast cancer cell lines, we substantiated these clinical observations by showing that, in contrast to triple positive, triple negative cells induced Glo-1 expression and activity in response to MG treatment. This is the first report that Arg-pyrimidine adduct accumulation is a consistent event in human breast cancer with a differential detection between triple negative and other breast cancer subtypes.

INTRODUCTION

Breast cancer represents the highest incidence of cancers and the second most common cause of death in women. This malignancy is characterized by a highly heterogeneous group of lesions with molecular and biochemical signatures, disease course, prognosis and treatment response. The classification based on gene expression patterns is commonly used to assess prognosis and therapy regimen. Breast malignant tumors are categorized into 4 main subtypes: luminal A (or HER2 negative tumors), luminal B (or triple positive tumors), HER2 positive, and basal-like (or triple negative tumors) [1-3]. This latter group represents around 15-20% of newly diagnosed breast cancers [4]. Typically, these lesions are characterized by high proliferation rate, high histologic grade, tumor necrosis and poor prognosis [5, 6]. Currently no treatment except chemoterapy is available for these patients.

Emerging evidence shows that cancer is a metabolic

disease and that altered cellular energy metabolism is a common feature of malignant tumors. In recent studies, a link between obesity, diabetes and breast cancer has been made through insulin/insulin-like growth factor and PI3K/Akt/mTOR signaling pathways and through obesity-induced chronic inflammation caused by adipose tissue dysfunction [7-9].

In proliferating cells, glucose metabolism and growth control are strictly linked [10, 11]. The Warburg effect according to which cells can rely on glycolysis as a major source of energy rather than oxidative phosphorylation, even in normoxic conditions, has been well described in many tumors including breast, melanoma, lung and colorectal cancer [12, 13]. Methylglyoxal (MG) is a highly reactive dicarbonyl compound and a potent glycating agent, mainly generated as a by-product of glycolysis through a spontaneous degradation of triosephosphates [14]. Accumulation of glycated proteins has been observed in several human diseases including diabetes, inflammation, aging, neurodegenerative disorders and cancer [15-25].

MG reacts with arginine, lysine and cysteine residues, nucleic acids and lipids generating advanced glycation end products (AGEs). In mammalian cells, MG is detoxified by the glyoxalase system, an enzymatic pathway consisting of two enzymes called glyoxalase 1 (Glo-1) and glyoxalase 2 (Glo-2). Glo-1 catalyzes the isomerisation of the hemithioacetal, formed spontaneously from MG and reduced glutathione (GSH) to S-D-lactoylglutathione. The second enzyme, Glo-2, converts the S-D-lactoylglutathione to D-lactate and recycles reduced glutathione [26, 27]. It has been shown that Glo-1 expression and activity is increased in many human cancer types such as colon [28], prostate [29, 30], melanoma [31], lung [32], and breast [33] and that Glo-1 overexpression is correlated with cancer progression and drug resistance [34, 35]. In a recent proteomic study, Glo-1 expression has been shown to be positively correlated with high tumor grade in breast cancer [36].

The reaction of MG with arginine residues generates stable MG-moieties called Arg-pyrimidine [37, 38]. So far only few studies analyzed the expression of Arg-pyrimidine adducts in cancer. Van Heijst and collaborators performed an Arg-pyrimidine immunohistochemical evaluation in 4 different types of human cancers, including a limited number of breast cancer lesions (n=5). Their conclusion was that Arg-pyrimidine level differs greatly between different types of tumors. To date the best-studied Arg-pyrimidine-modified protein identified in malignant tumors is the heat shock protein 27 (Hsp27). This chaperone protein facilitates the proper refolding of damaged proteins and plays a key role in cell resistance to stress. In cancer cells, MG post-translationally modified Hsp27 prevented apoptotic cell death notably through the inhibition of cytochrome C-mediated caspase activation [39-41].

In this study, we evaluated for the first time Arg-pyrimidine adducts accumulation in a large collection of breast cancer lesions categorized into the 4 main molecular subtypes using an immunohistochemistry approach. We demonstrated that triple negative breast tumors accumulate least Arg-pyrimidine adducts because of an efficient Glo-1-based detoxification system. These findings suggest that sensitizing triple negative tumors to carbonyl stress may represent a good strategy for aggressive cancer subtypes.

RESULTS

Arg-pyrimidine adducts are accumulated in human breast cancer tissues

We evaluated the presence of Arg-pyrimidine adducts in 7 breast cancer tissues and in their non-tumoral

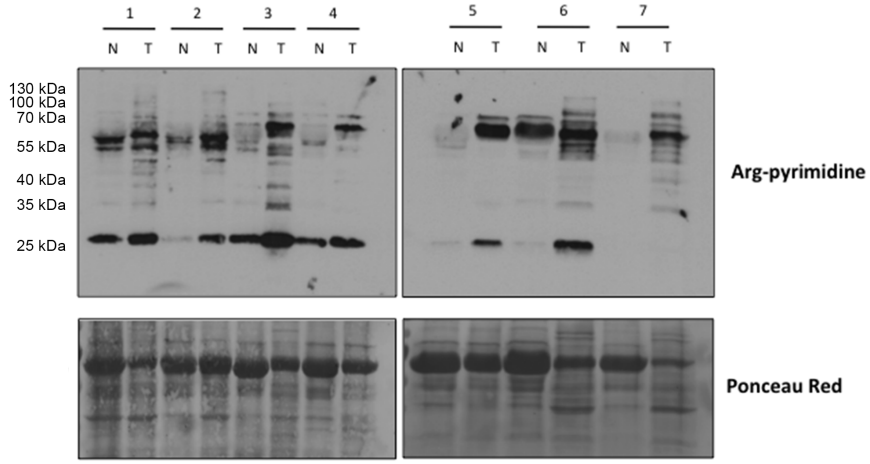

Figure 1: Increased Arg-pyrimidine residues in human breast cancer tissues compared with the non-tumoral counterparts. Arg-pyrimidine adducts were evaluated in 7 breast cancer tissues (T) and in their non-tumoral counterpart (N) using western blot analysis (20 µg of proteins were loaded). The Ponceau S-stained membrane is shown as an indicator of equal protein loading.

counterparts by Western blot analysis. The antibody was specifically directed against Arg-pyrimidine adducts. As shown in Figure 1, tumoral lesions accumulated more Arg-pyrimidine moieties in comparison with the corresponding non-tumoral counterparts. Some MG-modified proteins appeared enriched and/or uniquely observed in cancer lesions.

Triple negative breast tumors accumulate less Arg-pyrimidine adducts compared with other breast cancer subtypes

Using immunohistochemistry, we next examined Arg-pyrimidine accumulation in 2 normal human breast samples and in a collection of 93 breast tumors categorized in triple negative, triple positive, HER2 positive and HER2 negative. Arg-pyrimidine staining was mainly localized to the cytoplasm of breast epithelial cells, however in some cells a nuclear staining was also detectable. In good accordance with the Western blot analysis conducted on adjacent non tumoral breast samples, a moderate Arg-pyrimidine immunostaining was detected in normal breast tissue (Figure 2A-C). It is noteworthy that endothelial cells lining the visible blood vessels adjacent to normal mammary glands were positive (Figure 2A). Interestingly, when we evaluated Arg-pyrimidine accumulation in the different breast cancer subtypes we found that Arg-pyrimidine staining was significantly associated (chi-square test $p<0.0001$) with the cancer subtypes. Indeed, we observed that the majority of triple negative lesions (Figure 2D) exhibited low staining for MG-adducts in comparison with the other subtypes (Figure 2E-G). In fact, more than 70% of triple negative breast tumors exhibited a negative to weak staining for Arg-pyrimidine while the majority of the 3 other breast cancer subtypes evaluated showed a moderate to strong level of MG-adducts (Figure 2H). No significant staining was observed in tumor stroma in all the sections analyzed.

Triple negative breast cancer cell lines globally showed less Arg-pyrimidine adducts than other tumor subtypes

Next, we investigated Arg-pyrimidine accumulation in HER2 positive (SKBR3), estrogen/progesterone receptor-positive (MCF-7) and 4 triple negative (MDA-MB-231, MDA-MB-468, BT549, Hs579T) human breast cancer cell lines using Western blot analysis. All triple negative cell lines showed less Arg-pyrimidine accumulation compared with non-triple negative cell lines (Figure 3). This result is consistent with our immunohistochemical observations indicating that different breast cancer subtypes show distinct glycated adducts accumulation.

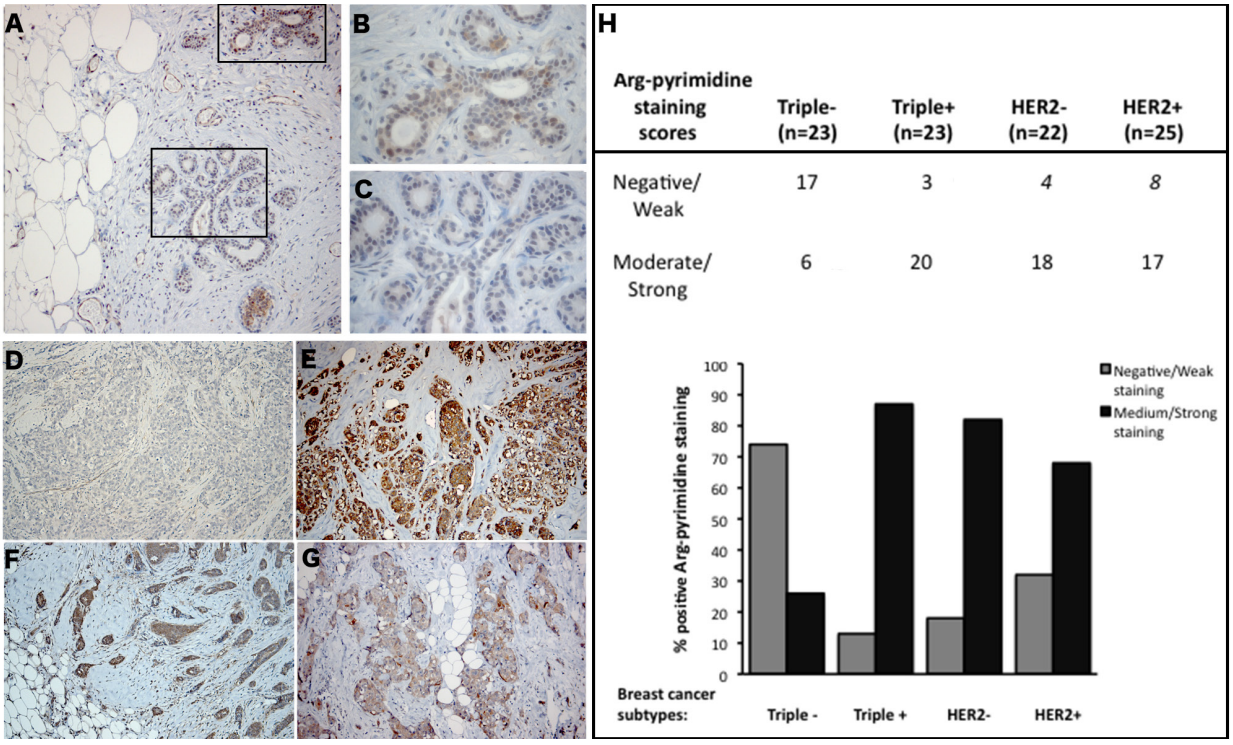

Figure 2: Triple negative breast tumors accumulated less Arg-pyrimidine adducts in comparison with triple positive, HER2- and HER2+ tumors. (A) Arg-pyrimidine adducts are detectable in breast tissue from reduction mammoplasty. The panels (B) and (C) show a higher magnification (400x) of the cellular regions boxed in panel A. Triple negative lesions (D) exhibited a significantly lower accumulation of Arg-pyrimidine residues compared to triple positive (E), HER2- (F) and HER2+ (G) subtypes, magnification 100x. Immunohistochemical quantification (H) was performed as described in Materials and Methods section.

Increased glyoxalase 1 (Glo-1) activity in triple negative tissues

To further explore the observed difference in accumulation of glycated adducts, serial sections were stained for both Arg-pyrimidine (Figure 4A, a and b) and the main MG-detoxifying enzyme, Glo-1 (Figure 4A, c and d). High Glo-1 staining was observable in both tumor subtypes regardless of the different levels of Arg-pyrimidine and no significant association (Fisher's exact test) was observed between the staining intensity and the different cancer subtypes evaluated. Indeed, most of triple negative (80%) and triple positive (90%) lesions expressed high levels of Glo-1 (Figure 4B). Therefore, we sought to examine the enzymatic activity of Glo-1 in these samples. The measurement performed on tissue extracts showed a significant increase in Glo-1 activity in triple negative tumors when compared with triple positive ones (Figure 5).

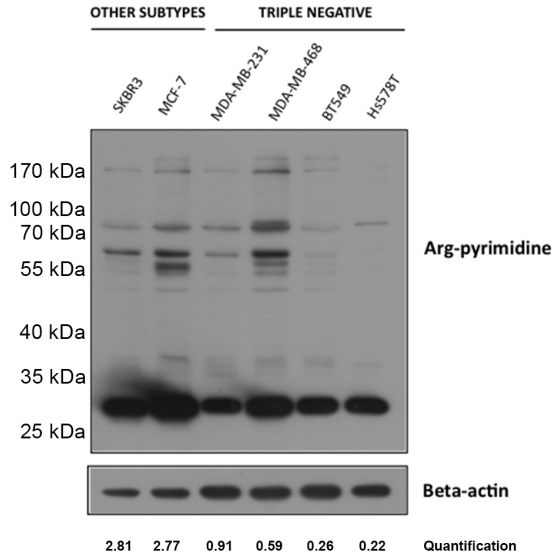

Figure 3: Low basal Arg-pyrimidine adducts accumulation in triple negative breast cancer cell lines. Arg-pyrimidine levels were evaluated using Western blot analysis on 6 breast cancer cell lines including SKBR3, MCF-7 and 4 triple negative cell lines. In comparison with MCF-7 and SKBR3, all triple negative cells expressed less Arg-pyrimidine accumulation. Beta-actin expression was used to normalize the amount of loaded proteins. Semi-quantitation of total Arg-pyrimidine adducts was done using beta-actin.

Only triple negative breast cancer cell lines respond to MG stimulation by increasing their Glo-1 expression and activity

To investigate whether triple negative breast cancer cells could respond to MG stimulation by increasing Glo-1 expression and activity, we treated breast cancer cells with MG at 300, 500 or 1000 μM during 6 hours. MG treatment neither affected the level of expression (Figure 6A) nor the activity (Figure 6B) of Glo-1 in MCF-7 and SKBR3 breast cancer cells. However, MG significantly induced a dose-dependent effect on both Glo-1 expression and activity in MDA-MB-231 and MDA-MB-468 triple negative cell lines (Figure 6A and B). Moreover, the 2-way ANOVA

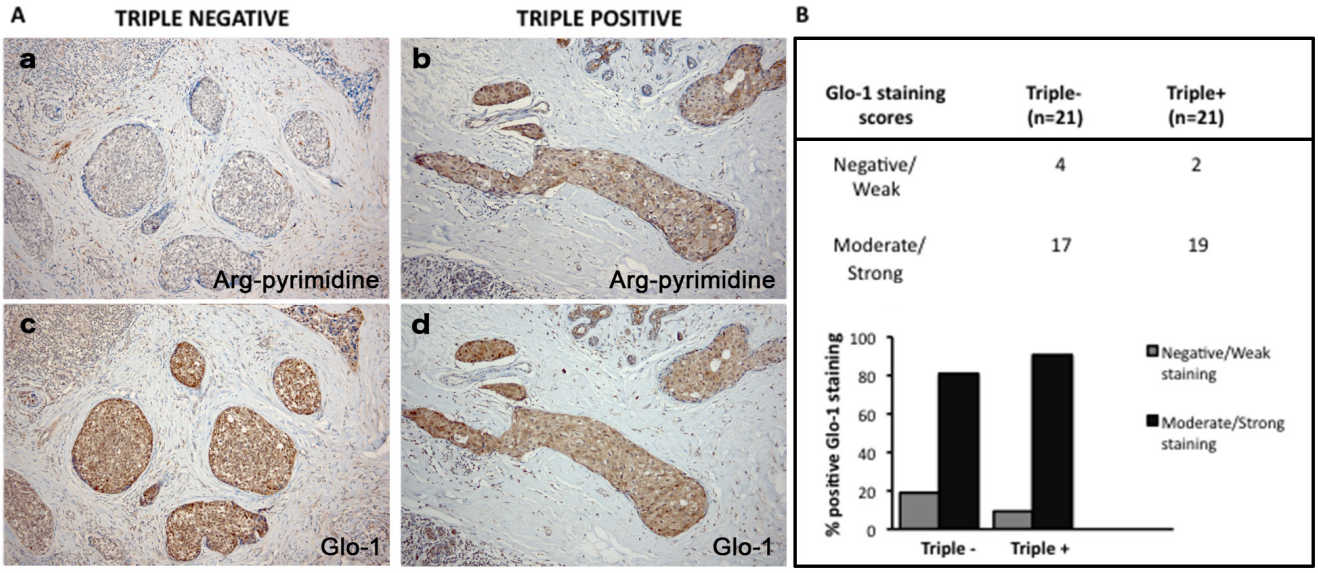

Figure 4: Representative immunohistochemical staining of Glo-1 expression in triple negative versus triple positive human breast tissues. Glo-1 expression was evaluated in triple negative (n= 21) and triple positive (n= 21) breast cancer patients and one representative case of each is shown in panel A (c, d). The staining of Glo-1 was compared with the immunostaining for Arg-pyrimidine accumulation in the same triple negative (a) and triple positive (b) human specimen. Glo-1 is highly expressed in both triple positive and triple negative tumors and there was no significant difference between the two breast cancer subtypes. Glo-1 immunohistochemical quantification is shown in panel (B). The evaluation of the staining was performed as described in Materials and Methods section. Magnification 100x.

analysis proved that the 4 cell lines evaluated responded differently to MG treatment. Indeed, the interaction between MG concentration and cell lines significantly accounted for 32.11% of the total variance ($p<0.0001$). In order to exclude the potential MG acute toxicity on cancer cells, we also measured Glo-1 activity in MDA-MB-231 and MCF-7 cells after 3 weeks of chronic treatment at lower concentrations of MG (5-50 µM) (Figure 7). As observed under acute treatment, triple negative cells showed a dose dependent induction of Glo-1 activity while MCF-7 cells maintained their basal level of Glo-1 activity in all conditions tested (Figure 7). Moreover, the 2-way ANOVA analysis indicated that the interaction between MG concentration and the 2 cell lines accounted for 20.33% of the total variance ($p<0.0015$).

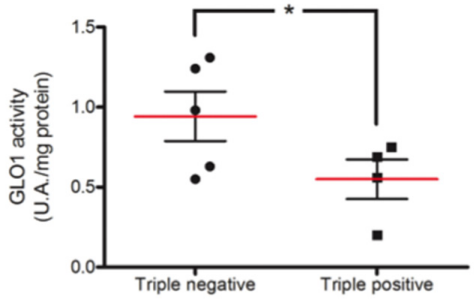

Figure 5: Increased Glo-1 activity in triple negative breast cancer tumors in comparison with triple positive ones. Glo-1 activity was measured in breast cancer tumor samples comprising 4 triple positive and 5 triple negative lesions. Glo-1 enzymatic assay was performed on tissue total protein extracts as described in Material and Methods. Statistical comparison was performed by one-tailed Student's t-test (*$p \leq 0.05$).

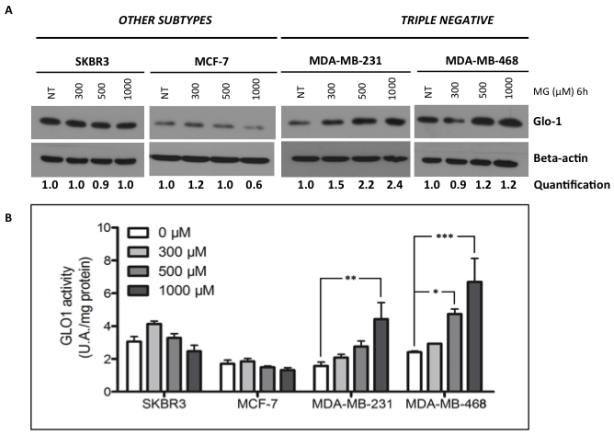

Figure 6: Glo-1 expression and activity in human breast cancer cells upon MG stimulation. Breast cancer cells were treated with MG at 300, 500 or 1000 µM for 6 hours. Only triple negative cancer cells are capable to respond to MG treatment by up-regulating both Glo-1 expression (A) and activity (B). No modulation of Glo-1 was observed in the other cell subtypes analyzed. Beta-actin expression was used to normalize the amount of loaded proteins. Semi-quantitation analysis was done using beta-actin as a loading control.Results are the average of independent experiments (n= 3). Data were statistically analyzed with two-way ANOVA followed by Bonferroni multiple comparisons (* $p \leq 0.05$, ** $p \leq 0.01$ and *** $p \leq 0.001$ vs untreated cells).

DISCUSSION

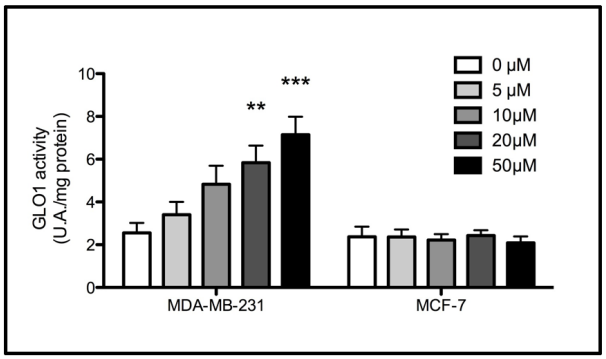

Figure 7: Increased Glo-1 activity in triple negative cells exposed to chronic treatment with MG. Glo-1 activity was measured in triple negative MDA-MB-231 and in ER/PR positive MCF-7 cells after three weeks treatment with low doses of MG. A significant increase of Glo-1 activity was observed only in triple negative cells. Results are the average of 4 independent experiments.Data were statistically analyzed with two-way ANOVA followed by Bonferroni multiple comparisons (* $p \leq 0.05$, ** $p \leq 0.01$ and *** $p \leq 0.001$ vs untreated cells).

While both cancer initiation and progression have been linked to oxidative stress [42] to date there is no clear evidence regarding the importance of the carbonyl stress in such processes. In cancer, reactive oxygen species (ROS) generate genomic damage and instability, activate mitogenic and survival mechanisms and favor cell invasion [43]. However, when the intracellular levels of oxidants reach a cytotoxic threshold, apoptotic and necrotic pathways are activated and cancer cells need to protect themselves from oxidative stress to survive [44].

Beside the well-established oxidative stress concept, endogenous dicarbonyl compounds such as MG also affect proteins, lipids and nucleic acids, leading to AGEs formation and carbonyl stress [45]. The carbonyl stress has been primarily described in diabetes where AGEs accumulation is a major event associated with diabetic complications [46]. High concentrations of MG and formation of AGEs have been reported in diabetic patients [47]. To date, known MG protein targets include albumin, hemoglobin, Sin3A, type IV collagen, alpha A-crystallin, protein p300 and 20S proteasome subunits, all associated with protein dysfunction [45].

Cancer cells predominantly produce energy by increasing their rate of glycolysis and as a consequence, triosephosphates-derived MG is increased in malignant

tumor cells. MG is a potent cytotoxic compound and exerts an anti-tumor activity in vivo [48, 49] and was first viewed as a potential therapeutic agent in cancer [50]. However, the recent identification of MG-modified proteins in cancer cells brought the new possibility where MG may have pro-tumorigenic effects. Indeed, MG induced the modification of Hsp-27 at arginine 188 (MG-Hsp27) in cancer cells and MG-Hsp27 facilitated cancer cell evasion from caspases-dependent cell apoptosis [39-41].

Several types of protein modifications by MG have been reported [37, 51], among which those directed to the guanidino group of arginine residues are well represented. In this study, we detected Arg-pyrimidine adducts using immunohistochemistry in a large series of human breast cancer lesions. Non-tumoral breast tissue presented detectable Arg-pyrimidine basal accumulation which was consistently lower than the one observed in matched tumoral samples. We report for the first time the differential accumulation of Arg-pyrimidine moieties between the different breast cancer subtypes analyzed. We observed that triple negative breast cancer tumors had fewer detectable Arg-pyrimidine adducts than the ER/PR positive, HER2 negative and HER2 positive lesions. These original findings were further reinforced by our observation that Arg-pyrimidine adducts were significantly less detectable in triple negative breast cancer cell lines when compared to cell lines from other subtypes. Interestingly, while Arg-pyrimidine immunostaining was mainly cytoplasmic some nuclei presented a positive staining suggesting the presence of nuclear MG-modified proteins in cancer cells. Using the same antibody, Nakadate and collaborators have reported the accumulation of Arg-pyrimidines in the nucleus of neural cells [52]. Ongoing experiments in our laboratory aim to identify new potential nuclear targets of MG such as transcription factors and co-regulator proteins in breast cancer cells.

Glo-1 is the main enzyme involved in the detoxification of MG. It has been reported that Glo-1 expression and activity are increased in breast tumor cells, most likely to control the high MG level spontaneously produced due to high glycolytic activity [33]. Glo-1 expression was significantly higher in Her-2 positive breast tumors when compared with Her-2 negative ones. Thus, Her-2 positive tumors associated with an aggressive phenotype and a poor prognosis overexpress Glo-1 [53]. However, Glo-1 enzymatic activity was not evaluated in these tumors. In this study, Glo-1 immunostaining performed on human triple negative and triple positive breast cancer lesions did not show any significant difference. Conversely, the measurement of Glo-1 activity performed on fresh samples showed a significant increase in Glo-1 enzymatic activity in triple negative tumors. Accordingly, we found that MDA-MB-231 and MDA-MB-468 triple negative breast cancer cells adapted their level of Glo-1 expression and activity when treated with exogenous increasing doses of MG. Considering that MCF-7 cells remained stable for Glo-1 under the same conditions, it is tempting to speculate that triple negative breast cancer cells increased their Glo-1 activity as a control defense mechanism to prevent MG accumulation. This hypothesis was further sustained by the increased dose-dependent Glo-1 activity observed in both MDA-MB-231 and MDA-MB-468 cells in response to a chronic sub-toxic MG treatment when compared to MCF-7 cells. Such adaptive response to MG has been previously reported in Carl-1 human melanoma cells and was described as a defense mechanism against MG toxicity [54].

Our study adds to the growing body of evidence suggesting a major role of non-enzymatic glycation in cancer. The increase of Glo-1 activity may represent a strategy adopted by aggressive cancer cells such as triple negative breast cancer cells as a defense mechanism against the glycation damage induced by high intracellular MG accumulation. Our data suggest that inhibition of Glo-1 activity in triple negative breast tumors could be a new potential therapeutic strategy. In support of this concept, previous studies reported that a specific Glo-1 inhibitor, S-p-bromobenzyl-glutathione cyclopentyl diester ($SpBrGSHCp_2$), demonstrates an anti-tumor effect against Glo-1-overexpressing tumors that are unresponsive to conventional therapies. This Glo-1 inhibitor has been shown to increase the sensitivity of human leukemia cells to anti-tumor agents [55]. In human lung cells with high expression and activity of Glo-1, the treatment with $SpBrGSHCp_2$ activated apoptosis through the activation of the stress-activated protein kinases JNK1 and p38 MAPK which finally led to caspase activation [32]. In human prostate cancer cells, the treatment with $SpBrGSHCp_2$ significantly affected tumor growth [14].

Oxidative stress has several pro-tumorigenic effects but it also exerts an anti-tumorigenic action as it has been linked to senescence and apoptosis. As a major actor of the carbonyl stress, MG also plays a dual role as a cytotoxic compound and as a pro-tumorigenic factor depending on the global cellular context. Moreover, one must consider that oxidative and carbonyl stresses are tightly linked together and may work in tandem to influence tumor phenotype. Indeed, the formation of both ROS and AGEs by cancer cells generates a sequence of reactions mutually enhancing each other [56].

Our study opens a new alley of investigations toward individualized cancer therapy based on the determination of metabolomic changes in tumors that might enable the targeted blockade of cancer progression.

MATERIALS AND METHODS

Clinical tumor samples

Patient tissue samples were obtained from the Pathology Department of the University Hospital of Liège in accordance with ethical guidelines of the University of Liège (Liège, Belgium). The immunohistochemical analysis was conducted on a collection of 93 breast cancer patients grouped into 4 biological subtypes (triple negative, triple positive, HER2- and HER2+) and 2 normal breast specimens obtained from reduction mammoplasties. ER, PR, and HER2 status was evaluated routinely by anatomo-pathological examination. In this series, HER2 positive tumors were all negative for ER and PR receptors and all HER2 negative tumors were positive for both hormone receptors. Patients received standard guideline-based according to standard guideline: hormonotherapy for all patients with ER-positive tumours, trastuzumab for those with HER2-positive tumours, anthracycline chemotherapy for high-risk lymph node-negative lesions, and anthracycline plus taxane chemotherapy for lymph node positive tumors. Western blot analysis was conducted on total protein extracts from 7 breast ductal adenocarcinoma (grade II and III) and their matched non-tumoral counterpart.

Cell lines

Human breast cancer cell lines BT549, Hs578T, MCF-7, MDA-MB-231, SKBR3 were obtained from the American Type Culture Collection (ATCC) and MDA-MB-468 cell line was a kind gift from Prof. Sebastiano Andò (Laboratory of General Pathology, University of Calabria, Italy). Breast cancer cell lines usually cultured in DMEM (standard glucose concentration of 4.5 g/L, Lonza) containing 10% fetal bovine serum, and 2 mM L-glutamine, were adapted to grow in DMEM medium with a glucose concentration of 1 g/L for several weeks. This glucose level is physiological and reflects the in vivo concentration in human serum. Conversely, the routine culture media concentration of 4.5 g/L corresponded to a diabetic condition.

Western blot analysis and antibodies

Cell and tissue samples were extracted in RIPA buffer (150 mM NaCl, 0.5% Na-deoxycholate, 1% Triton X-100, 0.1%SDS, 50 mM Tris-HCl pH 7.5) containing protease and phosphatase inhibitors (Roche). After incubation under rotation at 4°C for 40 minutes, lysates were then centrifugated at 14,000 g for 15 minutes at 4°C to remove insoluble debris. Protein concentrations were determined using the BCA assay (Pierce). Protein extracts were then separated by SDS-PAGE and transferred to a PVDF membrane. Next, the membranes were blocked for 1h in TBS-Tween containing 5% nonfat dried milk (Bio-Rad) and incubated with the primary antibodies overnight at 4°C. The membranes were probed with anti-Arg-pyrimidine (mAb6B) monoclonal antibody (1:10,000). The specificity of this antibody has been previously confirmed by competitive ELISA and it has been shown to not react with other MG-arginine adducts such as 5-hydro-5-methylimidazolone and tetrahydropyrimidine [57]. Anti-Human Glyoxalase I monoclonal antibody (1:1,000 dilution, cat#02-14, BioMac Leipzig) and anti-beta-actin (1:5,000 dilution, cat# A5441, Sigma) were used. Horseradish peroxidase-conjugated secondary antibodies [anti-mouse, 1:6,000 dilution (Dako) or anti-rabbit 1:3,000 (Invitrogen)] were used to visualize bound primary antibodies, with the ECL Western blotting substrate (Pierce). Where indicated, ImageJ software 1.46r (imagej.nih.gov) was used for semi-quantitation using beta-actin as a loading control.

Immunohistochemistry on breast tissues

Formalin-fixed paraffin-embedded sections were deparaffinized in xylene and rehydrated. To block endogenous peroxidase activity, the tissues were treated with 3% hydrogen peroxide in methanol for 30 minutes and washed in PBS for 20 minutes. Antigen retrieval was performed in 10 mM sodium citrate, pH 6.0 for 40 minutes at 95°C. Sections were then incubated with 1.5% normal horse serum (cat#S-2000, Vector Laboratories) for 30 minutes to block the nonspecific serum-binding sites. Then, sections were incubated with anti-Arg-pyrimidine (1:2,000 dilution) or anti-human Glyoxalase I (1:100 dilution) antibody overnight at 4°C. Antibody binding was detected using an anti-mouse biotinylated secondary (cat#BA-2000, Vector Laboratories) for 30 minutes followed by incubation with the avidin-biotin-peroxidase complex (Vectastain ABC Kit, Vector Laboratories). Immunoreactivity was revealed using 3,3′ diaminobenzidine tetrahydrochloride (DAB). The slides were counterstained with hematoxylin, dehydrated and mounted.

Evaluation of immunohistochemical staining

The immunohistochemically stained sections were reviewed by two examiners including an anatomopathologist (E.B). Scoring of the staining was done according to the intensity of the staining (0, 1+, 2+, 3+) and the percentage of positive cancer cells (0-25%, 25-50%, 50-75%, 75-100%). The results obtained with the 2 scales were multiplied together as we previously described [58], yielding a single scale with steps of 0, 1+,

2+, 3+, 4+, 6+ and 9+ where 0, 1+ and 2+ were considered to be negative or weak staining and 3+, 4+, 6+ and 9+ were considered to be medium or strong staining.

Glyoxalase I assay

The activity of Glo-1 was measured in breast cancer cell lines and in human breast cancer tissues after protein extraction in RIPA buffer, by measuring the initial rate of S-D-lactoylglutathione formation from the hemimercaptal obtained by preincubation of an equimolar (1 mM) mixture of MG (cat#M0252, Sigma) and GSH (cat#G4251, Sigma) in 50 mM sodium phosphate buffer, pH 6.8, at 25°C for 15 minutes. S-D-lactoylglutathione formation was followed spectrophotometrically by the increase in absorbance at 240 nm at 25 °C. One enzyme unit was defined as the amount of enzyme that catalyzes the formation of 1 µmol of S-D-lactoylglutathione per minute at the saturating substrate concentration.

Chronic treatment with MG. Breast cancer cells MDA-MB-231 and MCF-7 were treated with MG at different concentrations (5, 10, 20, 50 µM) for three weeks. The first week, a daily treatment was performed and for the remaining 2 weeks the treatment was repeated twice a week. Glo-1 activity was measured as described above on cell lysates after protein extraction in RIPA buffer.

Statistical analysis

The data were statistically analyzed using either one-tailed Student t-test or with two-way ANOVA followed by Bonferroni multiple comparisons. One-tailed t-test was selected because the H1 hypothesis was "triple negative Glo-1 activity is below or equal to triple positive". Number of cases for Arg-pyrimidine or Glo-1 staining in each cancer subtypes was analyzed in a contingency table using chi-square test and Fisher's exact test, respectively. P values less than 0.05 were considered statistically significant.

ACKNOWLEDGEMENTS

BC is a Télévie Post-Doctoral Fellow, MJN is a Télévie Fellow, AT is a Post-Doctoral Research Fellow and AB is a Senior Research Associate, all from the National Fund for Scientific Research (FNRS, Belgium). This work was also supported by the Centre Anti-Cancéreux, University of Liège, Belgium. The authors are thankful to Prof. Talesa's laboratory (University of Perugia, Italy) and Pr. M-C De Pauw (University of Liège) for technical support for the measure of Glyoxalase 1 enzymatic activity and Mrs. N. Maloujahmoum for expert technical assistance with the cell culture. We also thank the Biothèque of the University of Liège - CHU Liège for providing human tumor samples.

Author contributions

BC and MJN contributed equally to this work; BC, MJN, FD performed the experiments; EB performed the immunohistochemistry quantification; OP performed all the statistical analysis; KU provided the anti-Arg-pyrimidine antibody; DB and PD contributed to data analysis and discussion of the results; KU, AT, PI, PP gave technical support and conceptual advices; AT sampled and provided fresh tissue for analysis; BC and AB wrote the paper; VC and AB supervised the work and analyzed the data. All authors analyzed the data and discussed the results.

No conflicts of interest were declared.

REFERENCES

1. Perou CM, Sorlie T, Eisen MB, van de Rijn M, Jeffrey SS, Rees CA, Pollack JR, Ross DT, Johnsen H, Akslen LA, Fluge O, Pergamenschikov A, Williams C, Zhu SX, Lonning PE, Borresen-Dale AL, et al. Molecular portraits of human breast tumours. Nature. 2000; 406(6797):747-752.
2. Sorlie T, Perou CM, Tibshirani R, Aas T, Geisler S, Johnsen H, Hastie T, Eisen MB, van de Rijn M, Jeffrey SS, Thorsen T, Quist H, Matese JC, Brown PO, Botstein D, Lonning PE, et al. Gene expression patterns of breast carcinomas distinguish tumor subclasses with clinical implications. Proceedings of the National Academy of Sciences of the United States of America. 2001; 98(19):10869-10874.
3. Goldhirsch A, Wood WC, Coates AS, Gelber RD, Thurlimann B, Senn HJ and Panel m. Strategies for subtypes--dealing with the diversity of breast cancer: highlights of the St. Gallen International Expert Consensus on the Primary Therapy of Early Breast Cancer 2011. Annals of oncology : official journal of the European Society for Medical Oncology / ESMO. 2011; 22(8):1736-1747.
4. Penault-Llorca F and Viale G. Pathological and molecular diagnosis of triple-negative breast cancer: a clinical perspective. Annals of oncology : official journal of the European Society for Medical Oncology / ESMO. 2012; 23 Suppl 6:vi19-22.
5. Foulkes WD, Smith IE and Reis-Filho JS. Triple-negative breast cancer. The New England journal of medicine. 2010; 363(20):1938-1948.
6. Kim S, Kim do H, Jung WH and Koo JS. Metabolic phenotypes in triple-negative breast cancer. Tumour biology : the journal of the International Society for Oncodevelopmental Biology and Medicine. 2013; 34(3):1699-1712.
7. Jiang W, Zhu Z and Thompson HJ. Dietary energy restriction modulates the activity of AMP-activated

protein kinase, Akt, and mammalian target of rapamycin in mammary carcinomas, mammary gland, and liver. Cancer research. 2008; 68(13):5492-5499.

8. Hursting SD, Lashinger LM, Wheatley KW, Rogers CJ, Colbert LH, Nunez NP and Perkins SN. Reducing the weight of cancer: mechanistic targets for breaking the obesity-carcinogenesis link. Best practice & research Clinical endocrinology & metabolism. 2008; 22(4):659-669.
9. Sundaram S, Johnson AR and Makowski L. Obesity, metabolism and the microenvironment: Links to cancer. Journal of carcinogenesis. 2013; 12:19.
10. Ward PS and Thompson CB. Metabolic reprogramming: a cancer hallmark even warburg did not anticipate. Cancer cell. 2012; 21(3):297-308.
11. Vander Heiden MG, Cantley LC and Thompson CB. Understanding the Warburg effect: the metabolic requirements of cell proliferation. Science. 2009; 324(5930):1029-1033.
12. Warburg O. On respiratory impairment in cancer cells. Science. 1956; 124(3215):269-270.
13. Bensinger SJ and Christofk HR. New aspects of the Warburg effect in cancer cell biology. Seminars in cell & developmental biology. 2012; 23(4):352-361.
14. Thornalley PJ. Protein and nucleotide damage by glyoxal and methylglyoxal in physiological systems--role in ageing and disease. Drug metabolism and drug interactions. 2008; 23(1-2):125-150.
15. Brownlee M. Biochemistry and molecular cell biology of diabetic complications. Nature. 2001; 414(6865):813-820.
16. Goldin A, Beckman JA, Schmidt AM and Creager MA. Advanced glycation end products: sparking the development of diabetic vascular injury. Circulation. 2006; 114(6):597-605.
17. Yan SF, Ramasamy R, Naka Y and Schmidt AM. Glycation, inflammation, and RAGE: a scaffold for the macrovascular complications of diabetes and beyond. Circulation research. 2003; 93(12):1159-1169.
18. Yan SF, Ramasamy R and Schmidt AM. Mechanisms of disease: advanced glycation end-products and their receptor in inflammation and diabetes complications. Nature clinical practice Endocrinology & metabolism. 2008; 4(5):285-293.
19. Oudes AJ, Herr CM, Olsen Y and Fleming JE. Age-dependent accumulation of advanced glycation end-products in adult Drosophila melanogaster. Mechanisms of ageing and development. 1998; 100(3):221-229.
20. Morcos M, Du X, Pfisterer F, Hutter H, Sayed AA, Thornalley P, Ahmed N, Baynes J, Thorpe S, Kukudov G, Schlotterer A, Bozorgmehr F, El Baki RA, Stern D, Moehrlen F, Ibrahim Y, et al. Glyoxalase-1 prevents mitochondrial protein modification and enhances lifespan in Caenorhabditis elegans. Aging cell. 2008; 7(2):260-269.
21. Yan SD, Yan SF, Chen X, Fu J, Chen M, Kuppusamy P, Smith MA, Perry G, Godman GC, Nawroth P and et al. Non-enzymatically glycated tau in Alzheimer's disease induces neuronal oxidant stress resulting in cytokine gene expression and release of amyloid beta-peptide. Nature medicine. 1995; 1(7):693-699.
22. Kuhla B, Boeck K, Schmidt A, Ogunlade V, Arendt T, Munch G and Luth HJ. Age- and stage-dependent glyoxalase I expression and its activity in normal and Alzheimer's disease brains. Neurobiology of aging. 2007; 28(1):29-41.
23. Kalaria RN. Neurodegenerative disease: Diabetes, microvascular pathology and Alzheimer disease. Nature reviews Neurology. 2009; 5(6):305-306.
24. van Heijst JW, Niessen HW, Hoekman K and Schalkwijk CG. Advanced glycation end products in human cancer tissues: detection of Nepsilon-(carboxymethyl)lysine and argpyrimidine. Annals of the New York Academy of Sciences. 2005; 1043:725-733.
25. Grote VA, Nieters A, Kaaks R, Tjonneland A, Roswall N, Overvad K, Nielsen MR, Clavel-Chapelon F, Boutron-Ruault MC, Racine A, Teucher B, Lukanova A, Boeing H, Drogan D, Trichopoulou A, Trichopoulos D, et al. The associations of advanced glycation end products and its soluble receptor with pancreatic cancer risk: a case-control study within the prospective EPIC Cohort. Cancer epidemiology, biomarkers & prevention : a publication of the American Association for Cancer Research, cosponsored by the American Society of Preventive Oncology. 2012; 21(4):619-628.
26. Xue M, Rabbani N and Thornalley PJ. Glyoxalase in ageing. Seminars in cell & developmental biology. 2011; 22(3):293-301.
27. Rabbani N and Thornalley PJ. Glyoxalase in diabetes, obesity and related disorders. Seminars in cell & developmental biology. 2011; 22(3):309-317.
28. Ranganathan S and Tew KD. Analysis of glyoxalase-I from normal and tumor tissue from human colon. Biochimica et biophysica acta. 1993; 1182(3):311-316.
29. Davidson SD, Cherry JP, Choudhury MS, Tazaki H, Mallouh C and Konno S. Glyoxalase I activity in human prostate cancer: a potential marker and importance in chemotherapy. The Journal of urology. 1999; 161(2):690-691.
30. Romanuik TL, Ueda T, Le N, Haile S, Yong TM, Thomson T, Vessella RL and Sadar MD. Novel biomarkers for prostate cancer including noncoding transcripts. The American journal of pathology. 2009; 175(6):2264-2276.
31. Bair WB, 3rd, Cabello CM, Uchida K, Bause AS and Wondrak GT. GLO1 overexpression in human malignant melanoma. Melanoma research. 2010; 20(2):85-96.
32. Sakamoto H, Mashima T, Sato S, Hashimoto Y, Yamori T and Tsuruo T. Selective activation of apoptosis program by S-p-bromobenzylglutathione cyclopentyl diester in glyoxalase I-overexpressing human lung cancer cells. Clinical cancer research : an official journal of the American

Association for Cancer Research. 2001; 7(8):2513-2518.

33. Rulli A, Carli L, Romani R, Baroni T, Giovannini E, Rosi G and Talesa V. Expression of glyoxalase I and II in normal and breast cancer tissues. Breast cancer research and treatment. 2001; 66(1):67-72.

34. Sakamoto H, Mashima T, Kizaki A, Dan S, Hashimoto Y, Naito M and Tsuruo T. Glyoxalase I is involved in resistance of human leukemia cells to antitumor agent-induced apoptosis. Blood. 2000; 95(10):3214-3218.

35. Thornalley PJ and Rabbani N. Glyoxalase in tumourigenesis and multidrug resistance. Seminars in cell & developmental biology. 2011; 22(3):318-325.

36. Fonseca-Sanchez MA, Rodriguez Cuevas S, Mendoza-Hernandez G, Bautista-Pina V, Arechaga Ocampo E, Hidalgo Miranda A, Quintanar Jurado V, Marchat LA, Alvarez-Sanchez E, Perez Plasencia C and Lopez-Camarillo C. Breast cancer proteomics reveals a positive correlation between glyoxalase 1 expression and high tumor grade. International journal of oncology. 2012; 41(2):670-680.

37. Shipanova IN, Glomb MA and Nagaraj RH. Protein modification by methylglyoxal: chemical nature and synthetic mechanism of a major fluorescent adduct. Archives of biochemistry and biophysics. 1997; 344(1):29-36.

38. Westwood ME and Thornalley PJ. Molecular characteristics of methylglyoxal-modified bovine and human serum albumins. Comparison with glucose-derived advanced glycation endproduct-modified serum albumins. Journal of protein chemistry. 1995; 14(5):359-372.

39. Sakamoto H, Mashima T, Yamamoto K and Tsuruo T. Modulation of heat-shock protein 27 (Hsp27) anti-apoptotic activity by methylglyoxal modification. The Journal of biological chemistry. 2002; 277(48):45770-45775.

40. Oya-Ito T, Naito Y, Takagi T, Handa O, Matsui H, Yamada M, Shima K and Yoshikawa T. Heat-shock protein 27 (Hsp27) as a target of methylglyoxal in gastrointestinal cancer. Biochimica et biophysica acta. 2011; 1812(7):769-781.

41. van Heijst JW, Niessen HW, Musters RJ, van Hinsbergh VW, Hoekman K and Schalkwijk CG. Argpyrimidine-modified Heat shock protein 27 in human non-small cell lung cancer: a possible mechanism for evasion of apoptosis. Cancer letters. 2006; 241(2):309-319.

42. Sosa V, Moline T, Somoza R, Paciucci R, Kondoh H and ME LL. Oxidative stress and cancer: an overview. Ageing research reviews. 2013; 12(1):376-390.

43. Visconti R and Grieco D. New insights on oxidative stress in cancer. Current opinion in drug discovery & development. 2009; 12(2):240-245.

44. Pani G, Galeotti T and Chiarugi P. Metastasis: cancer cell's escape from oxidative stress. Cancer metastasis reviews. 2010; 29(2):351-378.

45. Rabbani N and Thornalley PJ. Methylglyoxal, glyoxalase 1 and the dicarbonyl proteome. Amino acids. 2012; 42(4):1133-1142.

46. Giacco F, Du X, D'Agati VD, Milne R, Sui G, Geoffrion M and Brownlee M. Knockdown of glyoxalase 1 mimics diabetic nephropathy in nondiabetic mice. Diabetes. 2014; 63(1):291-299.

47. Thornalley PJ, Hooper NI, Jennings PE, Florkowski CM, Jones AF, Lunec J and Barnett AH. The human red blood cell glyoxalase system in diabetes mellitus. Diabetes research and clinical practice. 1989; 7(2):115-120.

48. Szent-Gyorgyi A. Bioelectronics. Intermolecular electron transfer may play a major role in biological regulation, defense, and cancer. Science. 1968; 161(3845):988-990.

49. Antognelli C, Mezzasoma L, Fettucciari K and Talesa VN. A novel mechanism of methylglyoxal cytotoxicity in prostate cancer cells. The international journal of biochemistry & cell biology. 2013; 45(4):836-844.

50. Kang Y, Edwards LG and Thornalley PJ. Effect of methylglyoxal on human leukaemia 60 cell growth: modification of DNA G1 growth arrest and induction of apoptosis. Leukemia research. 1996; 20(5):397-405.

51. Thornalley PJ. Pharmacology of methylglyoxal: formation, modification of proteins and nucleic acids, and enzymatic detoxification--a role in pathogenesis and antiproliferative chemotherapy. General pharmacology. 1996; 27(4):565-573.

52. Nakadate Y, Uchida K, Shikata K, Yoshimura S, Azuma M, Hirata T, Konishi H, Kiyama H and Tachibana T. The formation of argpyrimidine, a methylglyoxal-arginine adduct, in the nucleus of neural cells. Biochemical and biophysical research communications. 2009; 378(2):209-212.

53. Zhang D, Tai LK, Wong LL, Chiu LL, Sethi SK and Koay ES. Proteomic study reveals that proteins involved in metabolic and detoxification pathways are highly expressed in HER-2/neu-positive breast cancer. Molecular & cellular proteomics : MCP. 2005; 4(11):1686-1696.

54. Amicarelli F, Bucciarelli T, Poma A, Aimola P, Di Ilio C, Ragnelli AM and Miranda M. Adaptive response of human melanoma cells to methylglyoxal injury. Carcinogenesis. 1998; 19(3):519-523.

55. Thornalley PJ, Edwards LG, Kang Y, Wyatt C, Davies N, Ladan MJ and Double J. Antitumour activity of S-p-bromobenzylglutathione cyclopentyl diester in vitro and in vivo. Inhibition of glyoxalase I and induction of apoptosis. Biochemical pharmacology. 1996; 51(10):1365-1372.

56. Kalapos MP. The tandem of free radicals and methylglyoxal. Chemico-biological interactions. 2008; 171(3):251-271.

57. Oya T, Hattori N, Mizuno Y, Miyata S, Maeda S, Osawa T and Uchida K. Methylglyoxal modification of protein. Chemical and immunochemical characterization of methylglyoxal-arginine adducts. The Journal of biological chemistry. 1999; 274(26):18492-18502.

58. Waltregny D, Bellahcene A, Van Riet I, Fisher LW, Young

M, Fernandez P, Dewe W, de Leval J and Castronovo V. Prognostic value of bone sialoprotein expression in clinically localized human prostate cancer. Journal of the National Cancer Institute. 1998; 90(13):1000-1008.

2. Methylglyoxal induces Hsp90 post-translational glycation and YAP-mediated breast tumor growth and metastasis

2.1. Introduction

An other objective in our study of carbonyl stress in the context of breat cancer is to identify new MG-modified proteins. While we were looking for new MG targets, we have been interested by five studies published in the last two years making a link between glucose metabolism and Yes-associated protein (YAP), an important oncogenic protein (DeRan et al. 2014, Mulvihill et al. 2014, Enzo et al. 2015, Mo et al. 2015, Wang et al. 2015). These authors reported that reducing cellular ATP levels by glucose deprivation decreased YAP activity (DeRan et al. 2014, Mo et al. 2015, Wang et al. 2015). Energy stress activates AMPK, that in turn leads to phophorylation of YAP by the Hippo pathway main kinase LATS (Large Tumor Supressor) and thereby promoting its exclusion from the nucleus. In particular, Enzo and collaborators demonstrated that aerobic glycolysis promotes YAP activity through a mechanism involving phosphofructokinase 1 binding to TEAD (Transcriptional Enhancer Factor) transcription factors.

The Hippo pathway, also known as the Salvador-Warts-Hippo pathway, has originally been discovered in *Drosophila melanogaster*. It comprises two main kinases, Hippo and Warts, that function in series to restrict the activity of Yorkie, the transcriptional co-activator. Yorkie binds to Scalloped transcription factors and activates pro-growth genes expression. While flyes bearing inactivating mutations of Hippo and Warts display hyperproliferation and reduced apoptosis, leading to larval overgrowth and tumor development, Yorkie mutations decrease cell proliferation. The Hippo cascade leading to the incativation of the effector Yorkie is resumed in Figure 28, left panel (Zhao et al. 2010).

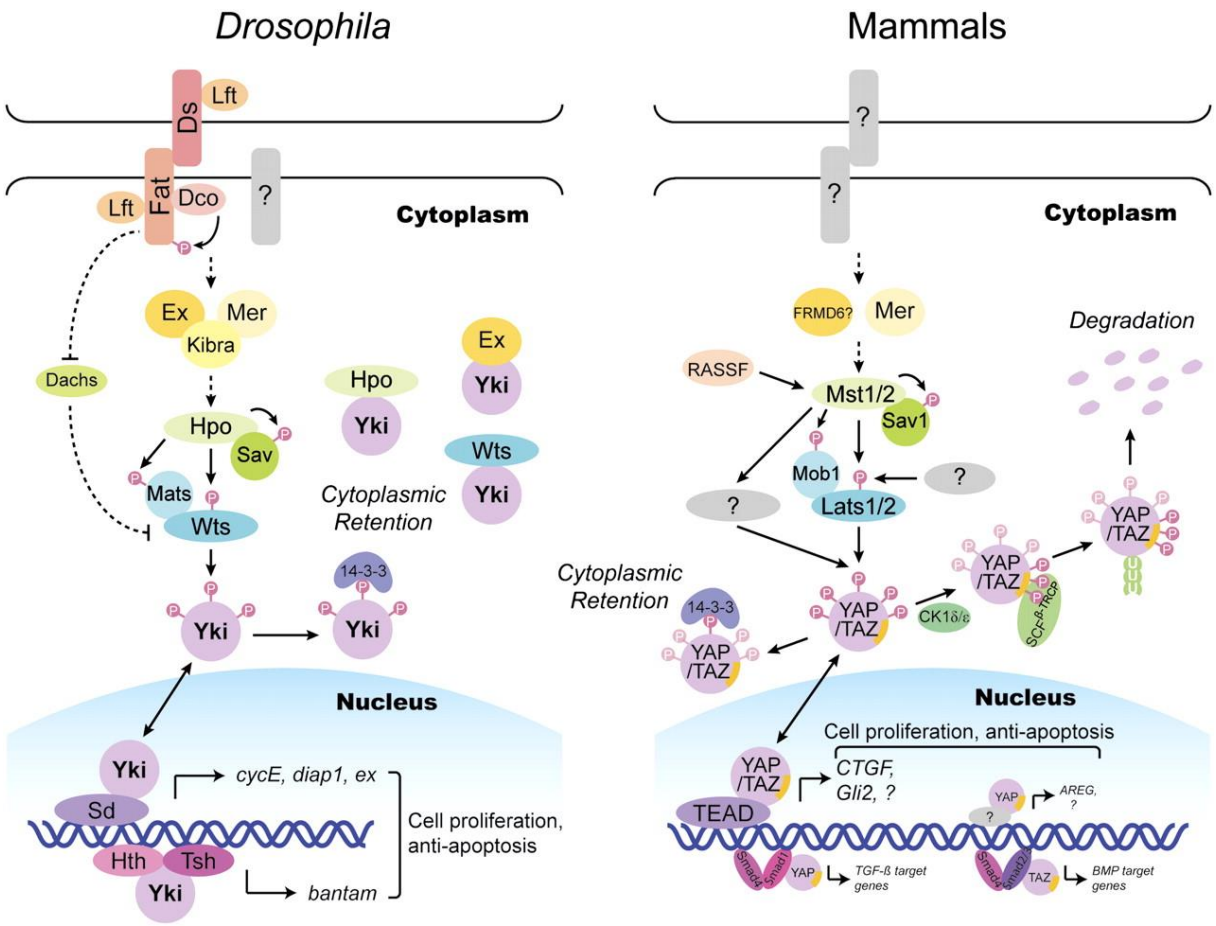

Figure 28: Models of the Hippo pathway in Drosophila and mammals. Left panel. In Drosophila, Fat protocadherin may initiate the Hippo pathway signal in response to Ds binding. Fat may also activate Ex. Mer and Ex may form a complex with Hpo and Sav. Kibra interacts with both Mer and Ex, and may also be in the complex. Hpo kinase interacts with and phosphorylates a scaffold protein, Sav. Together, they phosphorylate and activate Wts kinase. Wts phosphorylates a transcription coactivator, Yki, on three different sites. Phosphorylation of Yki S168 induces 14–3–3 binding and cytoplasmic retention. When Yki is relieved from inhibition and gets into the nucleus, it binds and activates a transcription factor, Sd, to induce proliferation and anti-apoptotic genes. **Right panel.** In mammals, functional significance of Fat and Ex homologs are not clear. After its activation, Mst1/2 (Hpo homolog) phosphorylates Sav1 (Sav homolog), Lats1/2 (Wts homolog), and Mob (Mats homolog). Lats1/2 phosphorylates YAP on five conserved HXRXXS motifs. S127 phosphorylation-dependent leads to 14–3–3 binding and cytoplasmic retention. YAP is also inhibited by S381 phosphorylation which mediates its ubiquitination and degradation. Sd homologs, TEADs, are major YAP target transcription factors. They mediate expression of CTGF, Gli2, and several target genes that stimulate proliferation and inhibit apoptosis. (Zhao et al. 2010)

All the key components of this pathway are evolutionarily conserved. In mammals, the corresponding components consist of two paralogs: Mst1 and 2 for Hippo, LATS1 and 2 for Warts and YAP and TAZ paralogs for Yorkie. YAP cannot bind directly to DNA and acts as a transcriptional co-activator. YAP forms complexes with TEAD transcription factors, homologs of Scalloped, to promote the expression of genes that induce cell growth and proliferation and inhibit apoptosis. The best described target genes are CTGF, CYR61, ANKRD1, BIRC5 and AXL. The Hippo pathway in mammals is resumed in Figure 28, right panel. YAP was originally discovered as a binding protein of non-receptor tyrosine kinase YES1 in chicken hence its name of Yes-associated protein (Sudol 1994). There are two major isoforms of YAP that are generated by alternative splicing, YAP1 and YAP2, containing one or two WW domains, respectively. WW domain mediates transcription activation and protein-protein interaction. Both isoforms contain a proline-rich region, a TEAD factor binding domain at the amino-terminal region, a SH3-binding motif and a transcriptional activation domain at the carboxy-terminal region. A PDZ-binding motif (FLTWL) is located on the very carboxy-terminal end of YAP and is critical for nuclear translocation. A schematic representation of YAP1 is shown in Figure 29. YAP lacks of a nuclear localization signal (NLS) and the machinery for its nucleo-cytoplasmic shuttling is unclear.

Figure 29: Schematic representation depicting the different domains of YAP1 protein and the phosphorylated residues. From left to right: proline-rich domain (P-rich), TEAD binding domain (TEAD BD), 14-3-3 binding domain (14-3-3 BD), 1 or 2 WW domains for YAP1 and YAP2 respectively, SH3 binding motif (SH3 BM), coiled-coil domain (C-C), transactivation domain (TAD) and PDZ binding domain (PDZ BD). P letters represent the five serines of YAP that are phosphorylated by LATS. Adapted from (Piccolo et al. 2014).

The nuclear localization of YAP is important for its transcriptional activity and is regulated by the Hippo pathway. When this pathway is activated, YAP is phospohrylated, excluded out of the nucleus and inactivated. LATS phosphorylates YAP at five serine/threonine residues defined by the consensus sequence HxRxxS. Phosphorylation of S127 promotes binding to 14-3-3 protein and cytoplasmic sequestration of YAP while phosphorylation of S381 leads to its proteasomal degradation (Figure 28, right panel). Moreover, the non-phosphorylation of S94 enables the binding of YAP to TEAD transcription factors. Other pathways and kinases such as Akt, JNK, Src can also phosphorylate YAP thus regulating its co-transcriptional activity. Several signals such as cell crowding, changes in

stiffness of the extracellular matrix, regulators of the actin cytoskeleton and G-protein coupled receptor signaling can activate the Hippo pathway to regulate YAP activity.

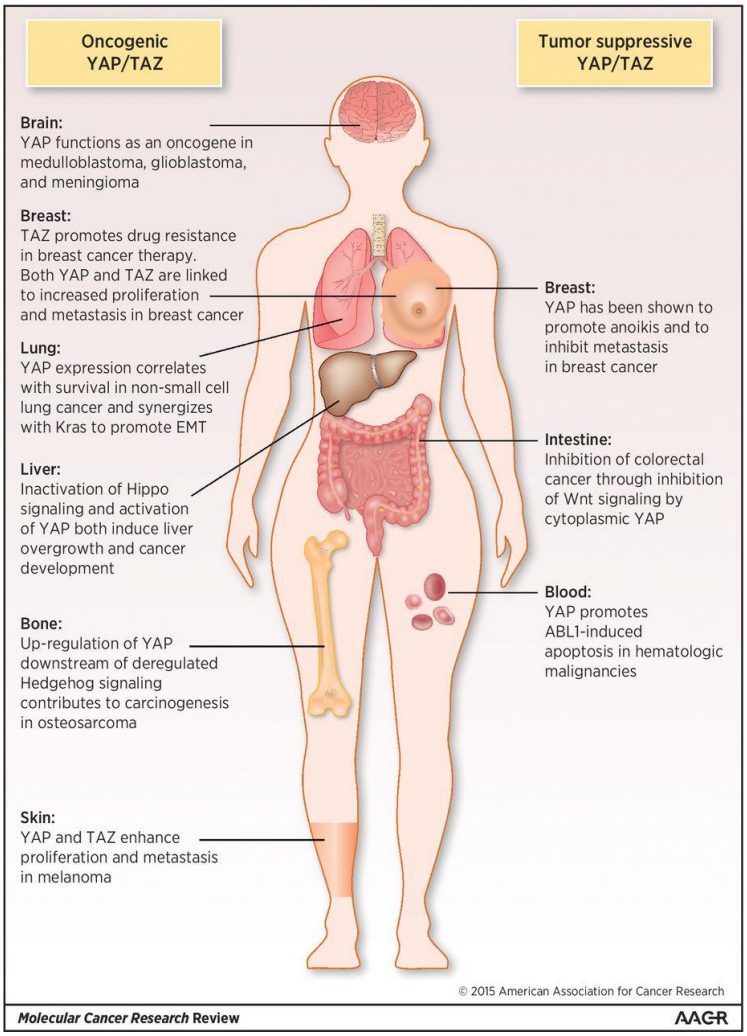

Figure 30: Oncogenic and tumor-suppressive functions of YAP and TAZ in human cancer. (Ehmer and Sage 2016)

YAP plays a very important role during embryonic development and in tissue growth control. Overexpression of YAP in the liver of transgenic mice induces a fourfold increase in liver size due to the hyperproliferation of hepatocytes (Camargo et al. 2007, Dong et al. 2007). YAP knockout embryos die shortly after gastrulation, at stage E8.5. Embryos notably display a shortened and highly disorganised body axis, abnormal neural morphogenesis, failure in chorioallantoic fusion and defects in the yolk sac vasculature (Morin-Kensicki et al. 2006). As other key regulators of development, YAP has beenassociated with cancer initiation, progression and metastasis development. Several studies have demonstrated that YAP is overexpressed in ovarian, liver, gastric, colon, lung and breast cancers. Furthermore, YAP nuclear localization has been associated with poor outcome in breast caner patients.

YAP, through the regulation of target genes, underlies some hallmarks of cancer such as uncontrolled cell proliferation, escape of cell death and induction of cancer stem cells. Despite YAP is considered as an oncogenic protein, some studies reported tumor suppressor function of YAP in breast, intestine and hematologic cancers. A summary of the oncogenic and tumor suppressive functions of YAP and its paralog TAZ is described in Figure 30 (Ehmer and Sage 2016).

Besides YAP, the other components of the Hippo pathway are more and more studied in the context of cancer. LATS1/2 is considered as a tumor suppressor gene. Hypermethylation of its promoters and mRNA downregulation have been observed in human soft tissue sarcoma, astrocytoma and breast cancer (Hisaoka et al. 2002, Takahashi et al. 2005, Jiang et al. 2006). LATS1 inhibits epithelial-to-mesenchymal transition (EMT) and proliferation of cancer cells by inactivating YAP *in vitro* (Xia et al. 2002, Hao et al. 2008, Zhang et al. 2008). In 2010, Huntoon and collaborators demonstrated that LATS1 folding and activity are regulated by the molecular chaperone, Heat shock protein 90 (Hsp90) (Huntoon et al. 2010). Hsp90 stabilizes and activates more than 400 proteins, referred to as Hsp90 clients, many of which are oncogenic transcription factors and kinases (for review, (Whitesell and Lindquist 2005, Trepel et al. 2010). Hsp90 is a highly regulated protein notably through post-translational modifications. Overexpression of Hsp90 has been found in many cancers and it is now considered as a good druggable target for cancer treatment. Several synthetic Hsp90 inhibitors are now in clinical trials for cancer patients treatment (Neckers and Workman 2012). Interestingly, Bento and collegues showed that MG downregulated Hsp90 and Hsc70 expression levels in human retinal pigment epithelial cells (Bento et al. 2010). All these findings encouraged us to explore the potential role of methylglyoxal in the regulation of the Hippo pathway.

2.2. Results

2.2.1. MG adducts and nuclear YAP are positively correlated in human breast cancer

As mentioned above, recent reports highlighted the importance of glucose metabolism for the regulation of YAP activity in cancer cells (DeRan et al. 2014, Mulvihill et al. 2014, Enzo et al. 2015). To explore possible links between YAP and carbonyl stress, we performed immunohistochemistry staining of YAP on a series of 87 breast tumors categorized as low to intermediate or high carbonyl stress tumors based on their endogenous argpyrimidine level. Remarkably, breast cancer lesions with high carbonyl stress also showed high YAP expression (Figure 31A). YAP was scored for nuclear and

cytoplasmic staining. A significant difference was found only when considering nuclear YAP staining between low/intermediate and high carbonyl stress tumors (Figure 31B and C).

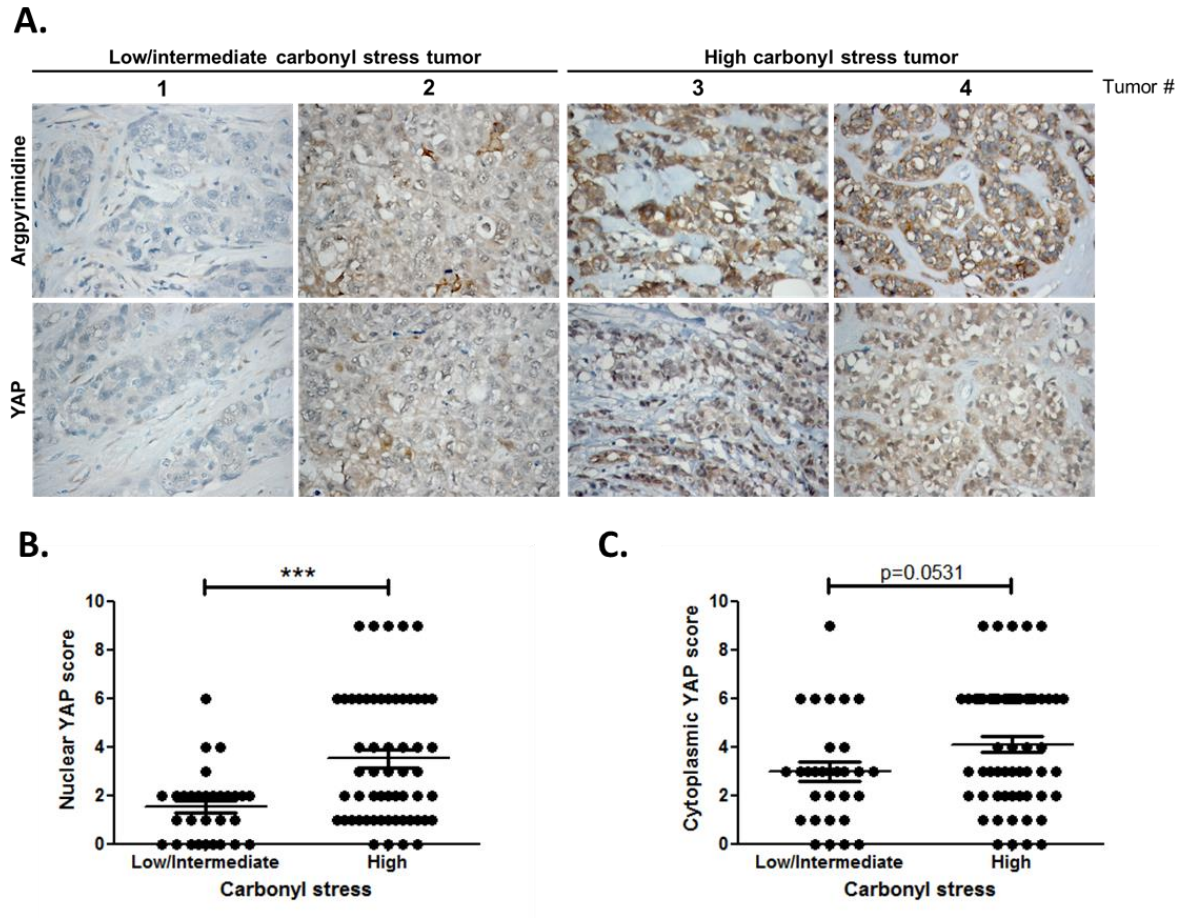

Figure 31: High carbonyl stress and nuclear YAP are positively correlated in human breast cancer. A. YAP IHC staining in representative low/intermediate and high carbonyl stress human breast tumors as assessed by their argpyrimidine level. **B.** Quantification of nuclear and **C.** cytoplasmic YAP IHC staining in a series of human breast cancer (n=87). Each dot represents one case and bars represent mean ± SEM. *** p<0.001.

2.2.2. MG induces YAP accumulation in confluent breast cancer cells

Although deficient contact inhibition is a hallmark of invasive cancer cells, the density at which cancer cells are cultured impacts on the activation of the Hippo pathway. In order to explore further the potential connection existing between MG-induced carbonyl stress and YAP, we first examined cell density dependent YAP subcellular localization in MDA-MB-231 breast cancer cell lines. YAP was mainly localized in the nucleus of low-density cultured cancer cells as detected by immunofluorescence. When breast cancer cells reached confluence, YAP was not detectable in the nucleus and became generally less visible suggesting that it underwent degradation (Figure 32A). Upon MG treatment, MDA-MB-231 cells showed a concentration dependent persistence of YAP in both the cytoplasm and the nucleus despite the cells reached confluence (Figure 32A). As a transcriptional co-activator, YAP's function is strictly constrained by its subcellular localization thus we essentially focused on YAP nuclear localization thereafter. Quantification of nuclear YAP immunostaining proved to be dose dependently higher in MG treated cells when compared to untreated cells in high density cultures (Figure 32B).

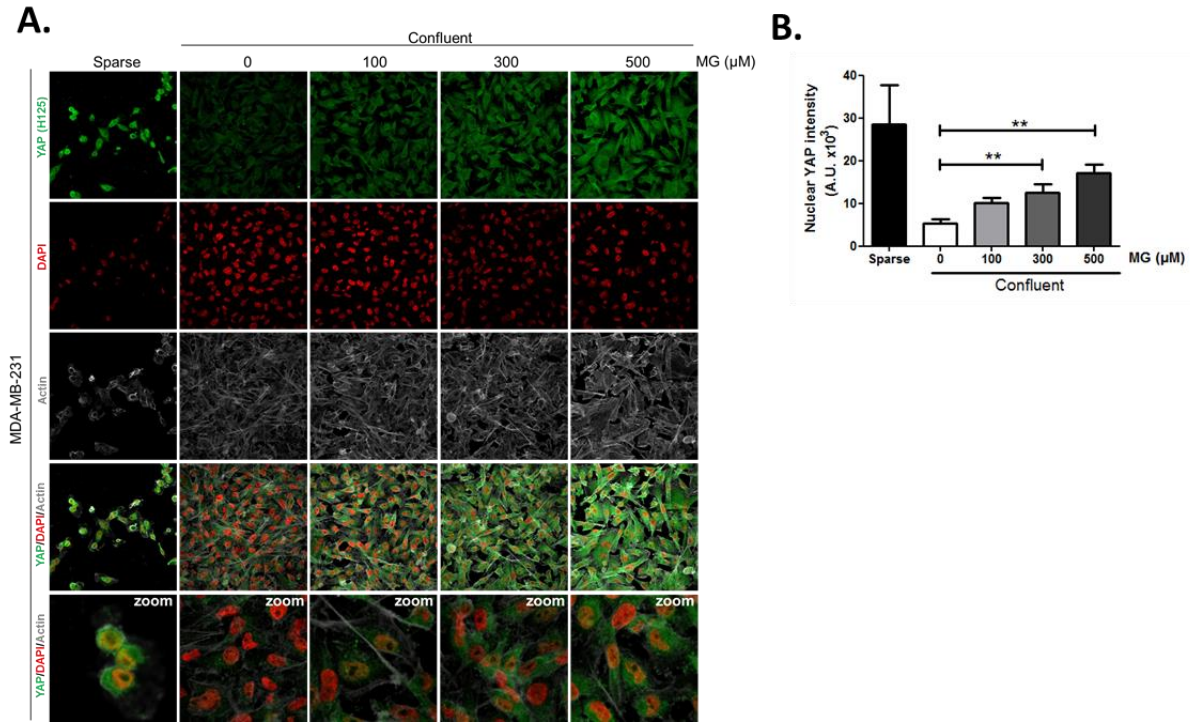

Figure 32: Methylglyoxal induces YAP persistence in confluent breast cancer cells. A. Immunofluorescence (IF) staining shows that YAP (Santa Cruz antibody, H125) is mainly localized in the nucleus at low cellular density (Sparse) and is weakly detectable a at high cellular density (Confluent) in MDA-MB-231 cells. In contrast, cells treated with increasing doses of MG until they reached confluence showed significant YAP cellular accumulation. Magnification 630x. Zoomed pictures are shown where indicated. **B.** Quantification of panel A experiment reports the intensity of YAP staining that colocalized with DAPI staining. Nuclear YAP IF staining intensity shows a significant dose-dependent increase in presence of MG. Data are shown as the mean values ± SEM of three independent experiments. ** $p<0.01$

Next, we asked whether the blockade of MG-mediated carbonyl stress using carnosine, a known MG scavenger (Hipkiss and Chana 1998), could abolish these effects. When MDA-MB-231 cells were concomitantly treated with MG and carnosine, YAP cellular accumulation in high density cultures was significantly returned to the basal level of untreated cells (Figures 33A and B) indicating that YAP persistence in confluent cells directly or indirectly resulted from MG-mediated carbonyl stress. Carnosine alone did not affect YAP significantly.

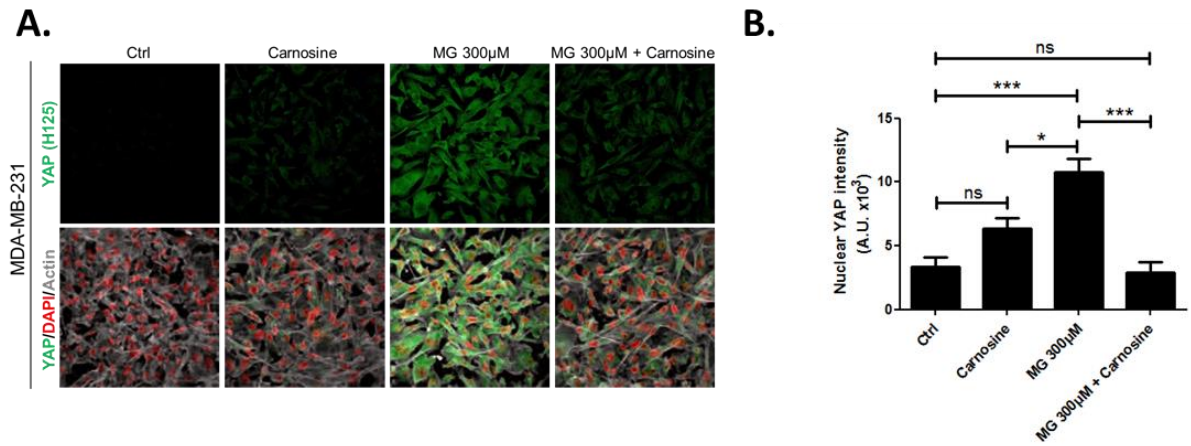

Figure 33: Carnosine reverses MG-induced YAP accumulation in MDA-MB-231 cancer cells. A. MDA-MB-231 cells cultured until they reached high density and treated concomitantly with MG (300µM) and carnosine (10mM), a MG scavenger, impeded cellular accumulation of YAP. Magnification 630x. **B.** Quantification of panel A experiment. Data are shown as the mean values ± SEM of three independent experiments.* p<0.05, ** p<0.01, *** p<0.001, ns=not significant.

2.2.3. High endogenous MG induces nuclear YAP accumulation in breast cancer cells

After we have validated exogenous MG effects, we used 2 strategies in order to assess high endogenous MG impact on YAP in breast cancer cells: (a) inhibition of Glo1, the main MG-detoxifying enzyme and (b) high glucose culture condition.

First, Glo1 inhibition was achieved by the use of specific siRNAs on one hand and the use of S-p-bromobenzylglutathione cyclopentyl diester (BBGC), an effective Glo1 inhibitor on the other hand (Tikellis et al. 2014). MBo, a specific fluorescent sensor for MG in live cells (Wang et al. 2013), demonstrated endogenous MG increase upon Glo1 expression inhibition and BBGC treatment in MDA-MB-231 cells (Figure 34A). Consistent with exogenous MG treatment experiments, both Glo1-depleted and BBGC-treated MDA-MB-231 cells (Figure 34A and B) displayed nuclear YAP persistence in high-density cultures.

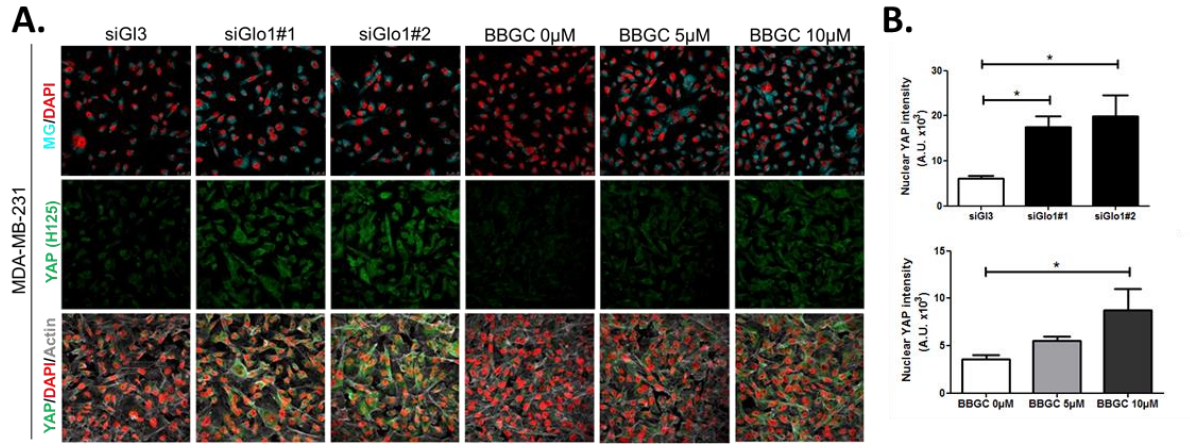

<u>Figure 34</u>: High endogenous MG induces YAP nuclear accumulation in breast cancer cells. A. Detection of MG was performed using MBo specific fluorescent probe and showed MG cellular increase in MDA-MB-231 cells that were Glo1-depleted using siRNAs (siGlo1#1 and #2) or treated with BBGC, a Glo1 inhibitor. Upon Glo1 silencing/inhibition, MDA-MB-231 cells displayed more YAP (Santa Cruz antibody, H125) than control cells (siGl3 and BBGC 0µM, respectively). Magnification 630x. **B.** Quantification of panel A experiment reports the intensity of YAP staining that colocalized with nuclear staining (DAPI). Data are shown as the mean values ± SEM of three independent experiments. * $p<0.05$

Second, we cultured MDA-MB-231 (highly glycolytic) and MCF7 (low glycolytic) cells in low and high glucose medium. Lactate measurement using ^{1}H-NMR showed that MDA-MB-231 cells significantly increased their glycolytic activity when cultured in high glucose (HG) compared to low glucose (LG) (Figure 35A). In these cells, HG culture induced elevated endogenous MG level that was assessed using both FACS detection of MBo fluorescent probe (Figure 35B) and LC-MS/MS quantification (Figure 35C). As expected, low glycolytic MCF7 cells used for comparison did not react to high glucose culture condition and kept stable lactate and stable MG levels (Figure 35A, B and C) thus pointing for the first time to MG increase as a specific response of glycolytic cancer cells to glucose stimulus. After having validated the response of breast cancer cells to high glucose, we next asked whether YAP nuclear persistence occurred under glucose-induced elevated endogenous MG levels. MDA-MB-231 cells cultured to confluence in high glucose demonstrated positive nuclear YAP staining (Figure 35D and E) when compared with cells cultured in low glucose. Under the same culture conditions, we did not observe any significant persistence of YAP in MCF7 breast cancer cells (Figure 35F and G) as expected from their stable glycolytic rate and unaffected MG level. It is noteworthy that MCF7 cells are able to induce YAP accumulation in response to an exogenous MG supply suggesting that low glycolytic cells could be stimulated in a high MG environment created by neighboring cells for example and this, independently of their own glycolytic flux. Altogether, these data demonstrate that the glycolytic switch in cancer cells is accompanied by high MG levels and YAP nuclear persistence and establish a new link between glucose utilization, MG stress and YAP regulation in cancer cells.

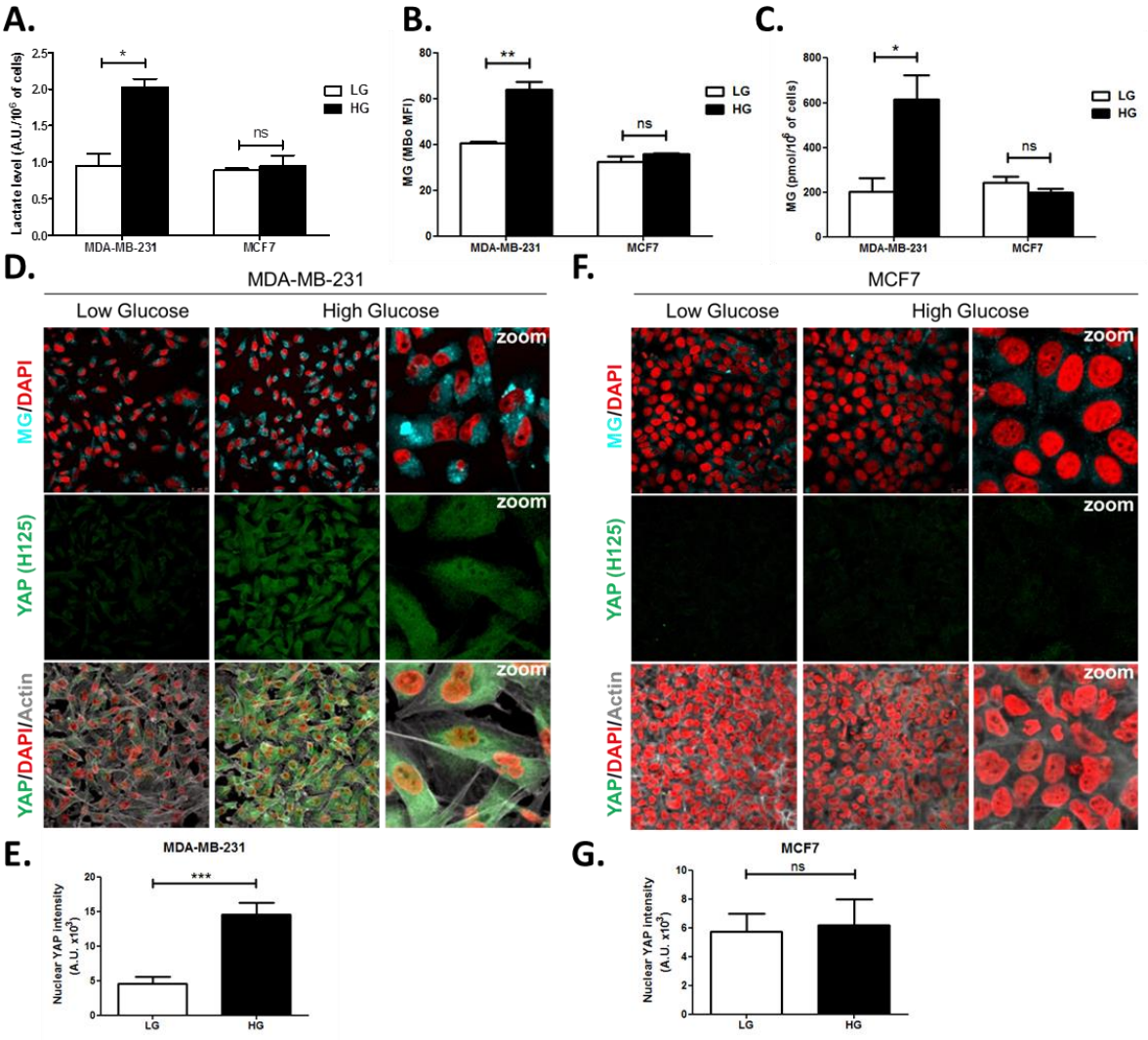

Figure 35: High endogenous MG induces YAP nuclear accumulation in breast cancer cells. A. Lactate level measured using ^{1}H-NMR increased in highly glycolytic MDA-MB-231 cells cultured in high glucose (HG) compared to low glucose (LG) while MCF7 low glycolytic cells did not. **B.** and **C.** MG quantification using both FACS MBo mean fluorescence intensity (MFI) and LC-MS/MS analysis on conditioned medium in the indicated conditions. MDA-MB-231 cells significantly increased their MG production in HG when compared to MCF7. **D.** and **F.** MG detection and YAP immunofluorescence staining (Santa Cruz antibody, H125) in the indicated breast cancer cell line cultured in low and high glucose medium. Magnification 630x. Zoomed pictures are shown for high glucose condition. **E.** and **G.** Quantification of D and F panels, respectively. Data are shown as the mean values ± SEM of three independent experiments. * p<0.05, ** p<0.01, *** p<0.001 and ns=not significant.

2.2.4. MG induces YAP co-transcriptional activity in breast cancer cells

We next explored the functional relevance of MG-mediated nuclear accumulation of YAP in breast cancer cells. For this purpose, we used two shRNAs specifically directed against Glo1 to stably induce high endogenous MG stress in MDA-MB-231 breast cancer cells. Efficient Glo1 silencing (shRNAs #1 and #2) at the mRNA and protein levels,

decreased Glo1 activity (Figures 36A, B and C) and MG increase (Figure 36D) were validated in stably depleted clones. As expected, Glo1-depleted MDA-MB-231 cells also showed YAP accumulation in high-cell density cultures when compared to control cells (Figure 36E and F).

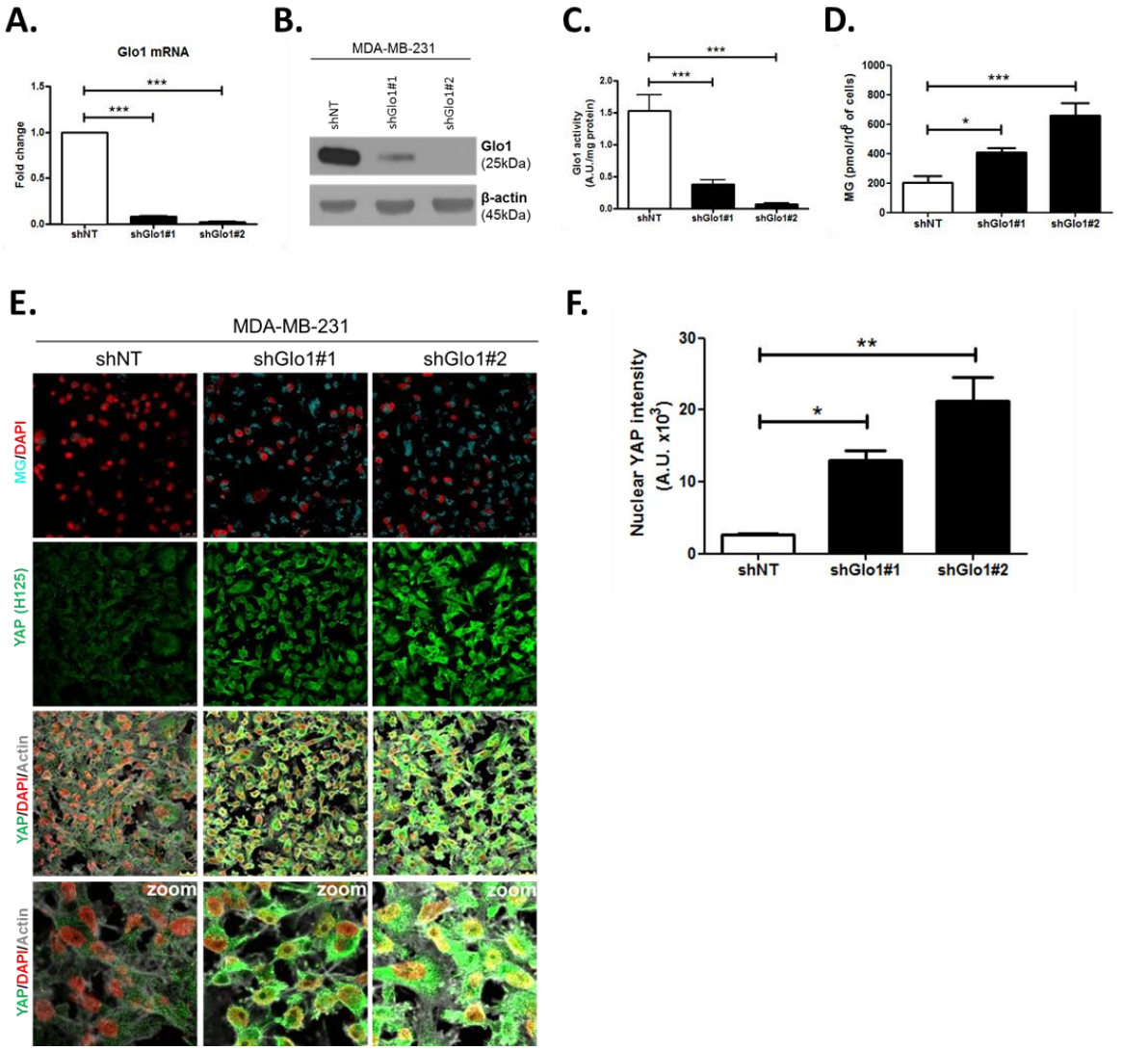

Figure 36: YAP cellular accumulation in shGlo1 MDA-MB-231 clones. A. Glo1 mRNA, **B.** protein and **C.** activity level in MDA-MB-231 shNT control and shGlo1#1 and #2. **D.** Quantification of MG levels in conditioned medium using LC-MS/MS indicated a significant increase in shGlo1#1 and #2 cells. Data are presented as mean ± SEM of three independent experiments. **E.** YAP immunofluorescence (Santa Cruz antibody, H125) in MDA-MB-231 silenced for Glo1 (shGlo1#1 and #2) cultured from low to high density. Detection of MG was performed using MBo specific fluorescent probe. Data are representative of three independent experiments. Magnification 630x. Zoomed pictures are shown when indicated. **F.** Quantification of nuclear YAP corresponding to E experiment. * p<0.05, ** p<0.01 and *** p<0.001.

Stably depleted Glo1 MDA-MB-231 cells were used to assess YAP target genes expression based on a previously established gene signature denoting YAP/TAZ activity (Zhao et al. 2008, Zhang et al. 2009, Cordenonsi et al. 2011, Dupont et al. 2011). Among the 14 targets tested and known to be regulated positively by YAP, we found that 8 genes, including CTGF gene, showed a significant increase at the mRNA level in Glo1 depleted cells when compared to control. Knock-down of YAP by siRNA transfection reversed the expression of all the evaluated genes thus establishing the link between YAP target genes expression and Glo1 status in cancer cells (Figure 37).

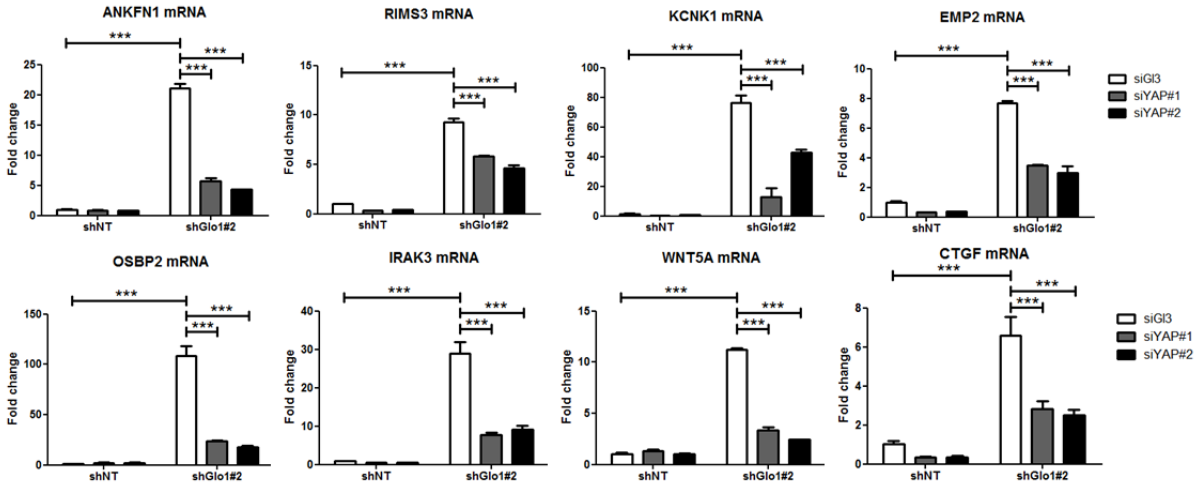

Figure 37: MG induces YAP co-transcriptional activity in breast cancer cells. Stable knockdown of Glo1 using shGlo1#2 shRNA in MDA-MB-231 results in upregulation of several YAP target genes (ANKFN1, RIMS3, KCNK1, EMP2, OSBP2, IRAK3, WTN5A and CTGF) at the mRNA level as assessed by qRT-PCR. Silencing of YAP using 2 independent siRNAs (siYAP#1 and #2, 48h post-transfection) significantly reversed YAP target genes induction in Glo1 depleted cells. Data are shown as the mean values ± SD of one representative experiment (n=4). *** p<0.001.

In order to assess more concretely the impact of MG stress on breast cancer cells through YAP activation, we next focused on CTGF gene expression, a well-described YAP transcriptional target (Zhao et al. 2008) that has been linked to YAP pro-growth and tumorigenic functions. We performed chromatin IP assays to assess the presence of YAP at CTGF promoter in both sparse and confluent MDA-MB-231 cells. In low-density cultured cells, YAP was bound to CTGF promoter while in confluent cells YAP was not detectable which is consistent with YAP absence in the nucleus of high-density cells. In contrast, YAP was found at CTGF promoter in MG-treated confluent cells at a comparable level to that in sparse cells (Figure 38A). CTGF mRNA level was not significantly affected by MG treatment in MDA-MB-231 cells. Smad2/3 collaborate with TEAD and YAP to form an active transcriptional complex at CTGF promoter in breast cancer cells (Fujii et al. 2012, Hiemer et al. 2014). MDA-MB-231 cells cultured in presence of MG and treated with TGF-β (2.5ng/ml) responded by a two-fold increase of CTGF mRNA level compared to TGF-β alone confirming the requirement of TGF-β pathway activation for MG-mediated induction of CTGF expression

(Figure 38B). Smad2 and Smad3 phosphorylation following TGF-β treatment in MDA-MB-231 cells was not affected by MG treatment indicating that CTGF up-regulation was linked to YAP accumulation in presence of active TGF-β pathway effectors. In agreement with this deduction, we showed that YAP silencing prevented MG-mediated CTGF mRNA induction in presence of TGF-β in confluent MDA-MB-231 cells (Figure 38B).

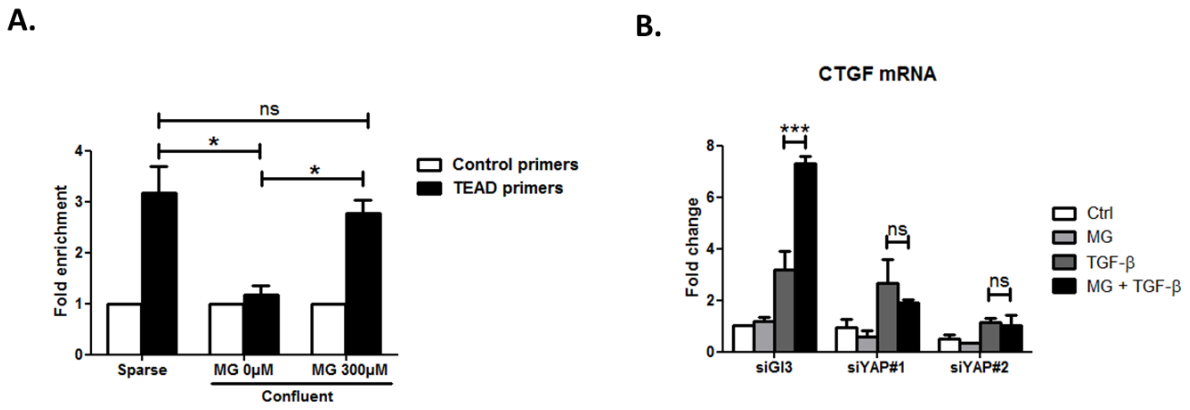

Figure 38: MG induces CTGF expression in a YAP-dependent manner in breast cancer cells. A. Chromatin immunoprecipitation of YAP at the CTGF promoter in sparse and confluent MDA-MB-231 cells treated or not with MG. TEAD PCR primers, and not control primers, target TEAD binding site on CTGF promoter. The use of TEAD primers indicated that YAP was present at the CTGF promoter in sparse cells (positive control) and in confluent MG-treated cells when compared to untreated confluent cells. **B.** CTGF mRNA level assessed by qRT-PCR in MDA-MB-231 cells treated with MG 300µM until confluence and then with TGFβ 2.5ng/ml during 2h. MG-mediated CTGF induction in presence of TGFβ is not observed upon YAP silencing (siYAP#1 and #2) when compared to control (siGl3) cells. Data are represented as the mean values ± SEM of three independent experiments. * $p<0.05$, *** $p<0.001$ and ns=not significant.

2.2.5. MG favors LATS1 kinase degradation through the proteasome in breast cancer cells

To gain insight into possible mechanisms by which MG regulates YAP activity, we first considered that YAP could be a direct target of MG glycation. However, MG-adducts immunoprecipitation in MDA-MB-231 treated with MG did not allow western blot detection of YAP. LATS1 is the main upstream Hippo pathway kinase that phosphorylates YAP thus preventing its nuclear translocation and oncogenic activity. We hypothesized that MG-mediated sustained YAP nuclear localization could be related to a relaxed LATS1 control notably due to its decreased expression. Indeed we demonstrated by western blotting that LATS1 was significantly decreased upon MG treatment in MDA-MB-231 breast cancer cells (Figure 39). A previous study has shown that LATS1 kinase degradation occurs through polyubiquitination and the 26S proteasome pathway in breast cancer cells (Chan et al. 2014). In good accordance, the treatment of breast cancer cells with MG132 proteasome inhibitor induced an increase of LATS1 and reverted MG-induced LATS1 decrease (Figure 39).

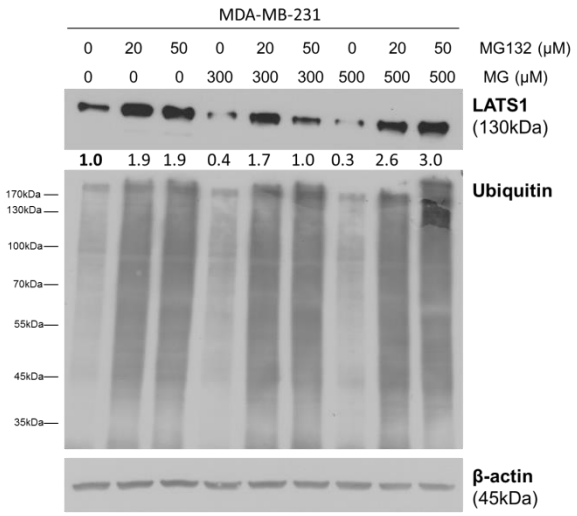

Figure 39: MG induces LATS1 kinase decrease in breast cancer cells. LATS1 expression in MDA-MB-231 cells treated with MG (300 and 500μM) during 6h in presence of increasing concentrations of MG132 proteasome inhibitor. Immunoblot data were quantified by densitometric analysis and normalized for β-actin. Data are representative of three independent experiments.

Next, we explored whether LATS1 decrease could explain, at least in part, the sustained YAP nuclear localization induced by MG. Accordingly, when we overexpressed LATS1, we were able to revert MG effects on YAP accumulation as assessed by immunofluorescence in MDA-MB-231 cells (Figure 40). Data gathered so far indicate that MG favors LATS1 decrease in breast cancer cells through the proteasome, which leads to sustained activity of YAP in the nucleus.

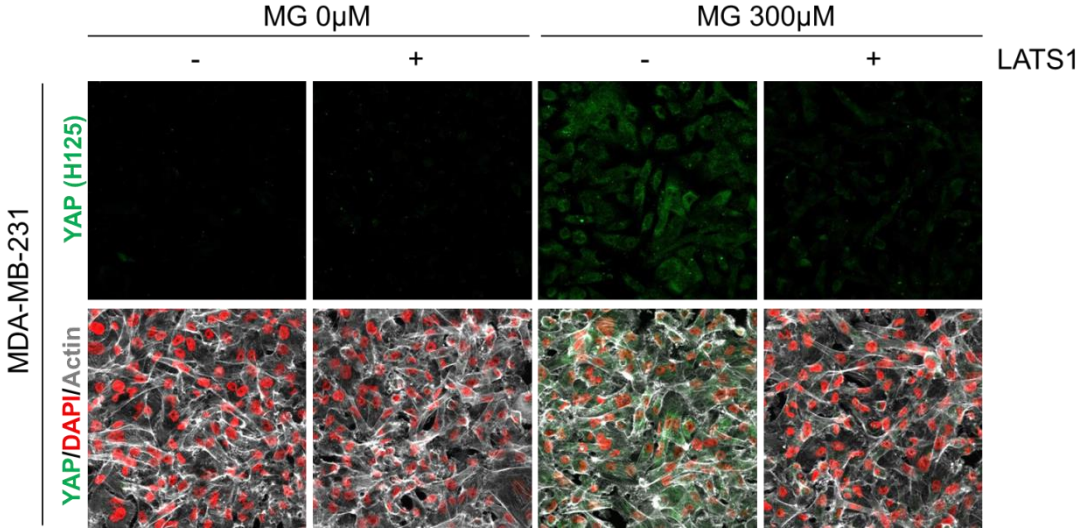

Figure 40: LATS1 overexpression reverses MG-induced YAP accumulation in breast cancer cells. YAP immunofluorescence (Santa Cruz antibody, H125) in MDA-MB-231 cells transiently transfected with LATS1 expression vector (+) or empty vector used as control (-) and then treated with MG (300μM) until confluence. Magnification 630x. Data are representative of three independent experiments.

2.2.6. MG induces post-translational glycation of Hsp90 and affects its chaperone activity on LATS1

To explore further MG mechanism of action on LATS1, we first excluded the possibility of a direct glycation of LATS1 by MG using immunoprecipitation technique with anti-argpyrimidine specific antibody. Then, we got interested in LATS1 as a client of Hsp90 chaperone protein. Indeed, LATS1 kinase expression level and activity are dependent on its stabilization by Hsp90. 17-AAG, a potent Hsp90 inhibitor, disrupts LATS1 tumor suppressor activity in human cancer cells (Huntoon et al. 2010). Hsp90 mRNA and protein levels were not modulated by MG treatment in breast cancer cells. Therefore, we sought to explore whether MG could modify Hsp90 thus indirectly impacting on LATS1 stability and degradation. The incubation of human recombinant Hsp90 with MG followed by MS analysis revealed the modification of several lysine and arginine residues notably yielding to the formation of carboxyethyllysine (CEL) and argpyrimidine/MG-H adducts, respectively. Next, we examined whether endogenous MG-modified Hsp90 could be detected in MG-treated MDA-MB-231 cells. Immunoprecipitation of MG-treated MDA-MB-231 extracts using anti-argpyrimidine MG adducts and followed by Hsp90 immunoblot analysis led to the detection of a basal level of glycated Hsp90 in MDA-MB-231 glycolytic cells that was further enhanced upon MG treatment (Figure 41A). Hsp27, which is recognized as a major MG target in cancer cells, was also efficiently detected in argpyrimidine immunoprecipitates (Figure 41A). Argpyrimidine immunoprecipitates subjected to MS analysis revealed the presence of modified Hsp90 on several residues. Glycation hot spots observed on recombinant and endogenous Hsp90 are summarized in Figure 41B. The mapping of MG modifications on Hsp90 amino-acid sequence indicated that functionally important domains involved in both substrate/co-chaperone and ATP binding showed several glycated residues suggesting that Hsp90 activity could be affected. Next, we further documented LATS1 binding to Hsp90 in the context of MG treatment. LATS1 immunoprecipitates contained detectable Hsp90 however this interaction was disrupted upon MG treatment in MDA-MB-231 cells (Figure 41C). Collectively, our findings show that MG relieves LATS1 control on YAP nuclear localization through a mechanism identifying for the first time MG-mediated post-translational glycation and inactivation of Hsp90 in cancer cells.

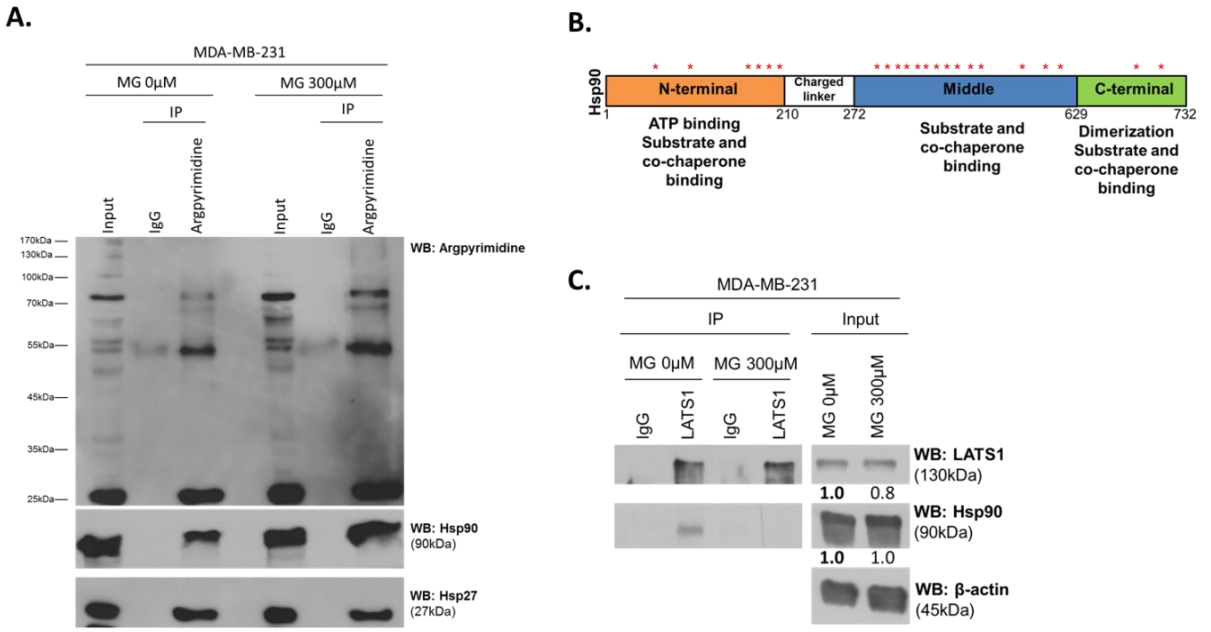

Figure 41: MG induces Hsp90 post-translational glycation in breast cancer cells. A. Immunoprecipitation of MG adducts on MG-treated MDA-MB-231 cells (300µM, 6h) using a specific anti-argpyrimidine monoclonal antibody. Mouse immunoglobulins (IgG) were used as control. Total cell lysates (Input) and immunoprecipitates (IP) were immunoblotted for argpyrimidine, Hsp90 and Hsp27. **B.** Schematic representation of Hsp90 protein domains where hot spots (*) of MG-modified residues are indicated. **C.** Co-immunoprecipitation of LATS1 and Hsp90 from MDA-MB-231 cells treated with MG 300µM during 24h reveals a decreased interaction between the 2 proteins. Data are representative of three independent experiments.

2.2.7. Glo1-depleted breast cancer cells show an increased tumorigenic and metastatic potential *in vivo*

Data gathered so far indicate that MG stress favors sustained YAP activity in breast cancer cells. Next, we explored the biological relevance of this observation for tumor growth and metastases development. Stably Glo1-depleted MDA-MB-231 cells that were grafted subcutaneously in mice showed an increased tumor weight and volume which reached significance for shGlo1#2-silenced clones (Figure 42A). Further exploration of shGlo1 experimental tumors using immunoblotting revealed the effective *in vivo* induction of argpyrimidine adducts and a strong inverse relationship between Glo1 silencing and total YAP expression (Figure 42B). In Glo1-silenced experimental tumors, we further demonstrated a specific increase of YAP in the nucleus of tumor cells using immunohistochemistry (Figures 42C). Elevated proportion of Ki67 positive cells in shGlo1 tumors sustained the observed increased tumor growth (Figure 42C).

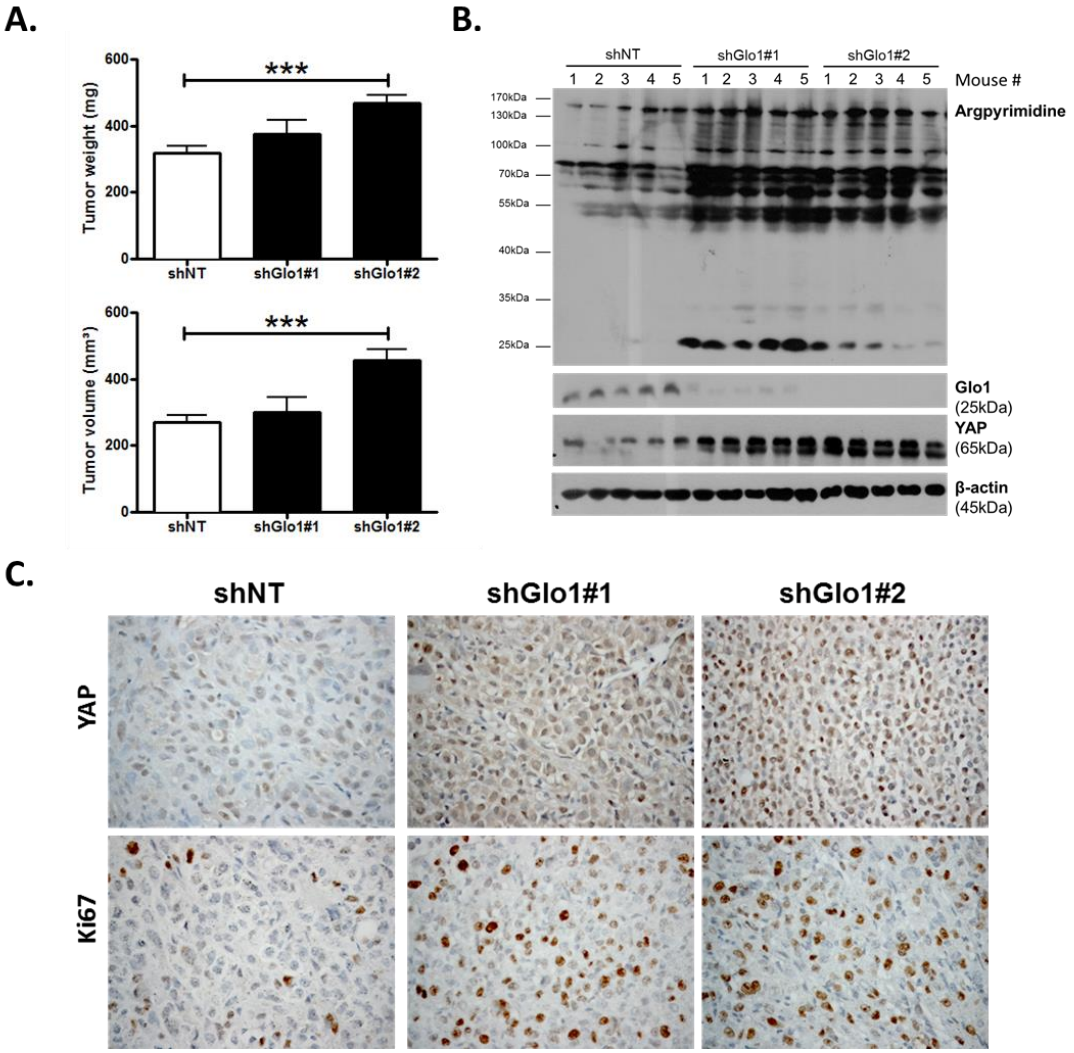

Figure 42: Glo1-depleted breast cancer cells show an increased tumorigenic potential *in vivo*. **A.** MDA-MB-231 shGlo1#1 and #2 and control shNT cells were injected subcutaneously in NOD-SCID mice (15 mice/group). After 4 weeks, primary tumors were surgically removed and weighed. Tumor weight (mg) and volume (mm³) are shown as mean ± SEM. **B.** Western blot detection of argpyrimidine, Glo1 and YAP in 5 representative experimental primary tumors. β-actin is used for normalization. **D.** Representative YAP and Ki67 IHC staining in experimental primary tumors. Magnification 400x. *** p<0.001.

In order to explore further the association between high MG, YAP activity and tumor growth, we used the *in vivo* chicken chorioallantoic membrane assay (CAM). Grafted shGlo1 cells showed increased growth as assessed by the measure of tumor volume and compared to control cells (Figure 43A and B). As shown on mice experimental tumors, we observed significant YAP nuclear localization in CAM shGlo1 tumors (Figure 43C and D). Remarkably, YAP silencing in shGlo1 cells efficiently reverted tumor growth to control levels (Figure 43A and B).

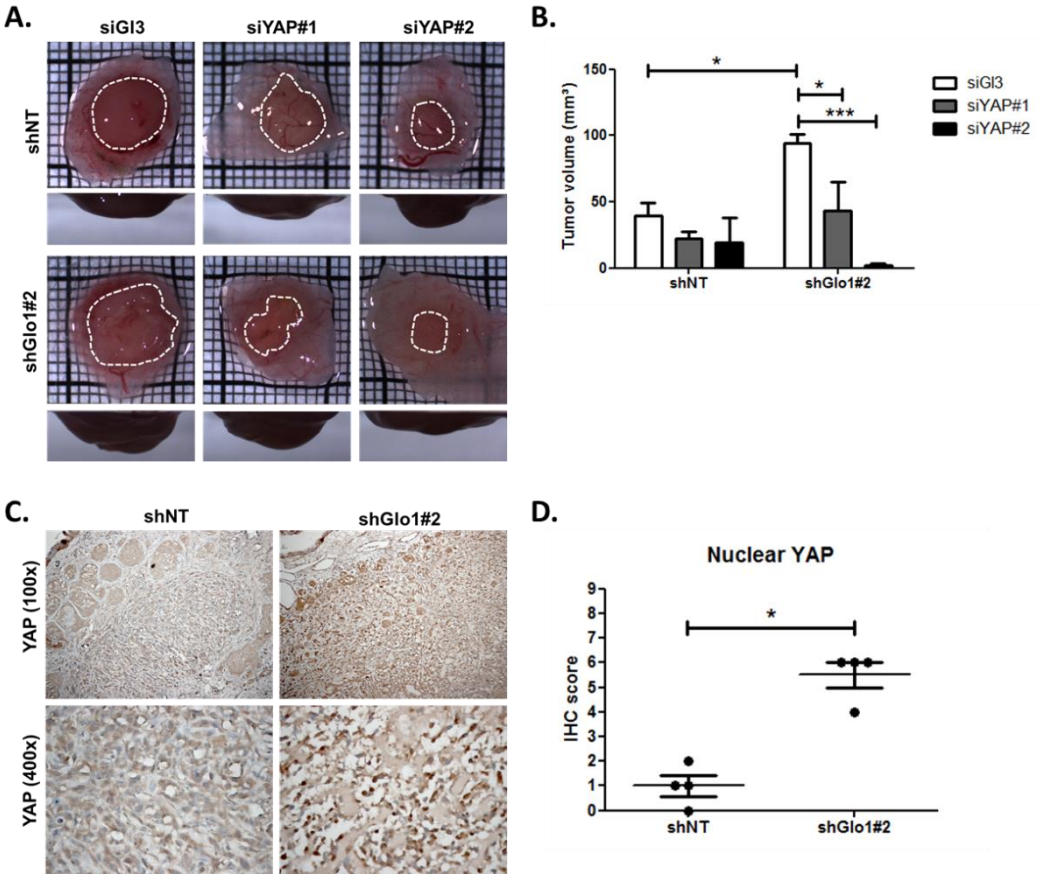

Figure 43: Glo1-depleted breast cancer cells show a YAP-dependent increased tumorigenic potential *in vivo*. A. Glo1-depleted MDA-MB-231 (shGlo1#2) and control shNT cells were transfected with YAP siRNAs (siYAP#1 and 2) and grown on the chicken chorioallantoic membrane (CAM). After 7 days, tumors were collected and measured. Top and profile views of representative experimental CAM tumors are shown. **B.** Tumor volumes are represented as mean ± SEM. **C.** Representative YAP immunostaining on Glo1-depleted CAM experimental tumors. **D.** Quantification of nuclear YAP IHC shown in panel C. Each dot represents one case and bars represent mean ± SEM. * $p<0.05$ and *** $p<0.001$.

Following the assessment of Glo1-silencing impact on tumor growth, we next evaluated the metastatic behavior of Glo1-depleted breast cancer cells. After surgical removal of the primary tumors, the mice were followed for metastases development during an additional period of 6 weeks. The follow-up of the mice showed that lung metastases were detectable already after 3 weeks in Glo1-depleted conditions but not in control condition. After 6 weeks post-tumor removal, metastasized tumors were observed in the lungs of Glo1-depleted mice (68%) when compared to control (20%). To evaluate further lung colonization, we performed human vimentin immunohistochemical detection that revealed a significant increase of both number and size of metastatic foci in Glo1-depleted condition (Figure 44A and B). We assessed efficient Glo-1 depletion in the metastatic foci on serial sections (Figure 44A). These data demonstrate that breast cancer cells undergoing a carbonyl stress show enhanced growth and metastatic capacity thus highlighting an unexpected pro-tumoral role for MG endogenous accumulation. Finally, to better assess the importance of MG stress on metastatic dissemination, shGlo1#1 mice received carnosine (10mM) in drinking water from

the day of primary tumor removal until the end of the experiment (during 6 weeks). We observed a significant decrease of lung colonization in shGlo1 mice treated with carnosine when compared with control mice (Figure 44C and D). Collectively the data indicate that MG stress pro-cancer effects unveiled here are tightly associated with YAP enhanced activity that can be efficiently blocked by carnosine scavenger.

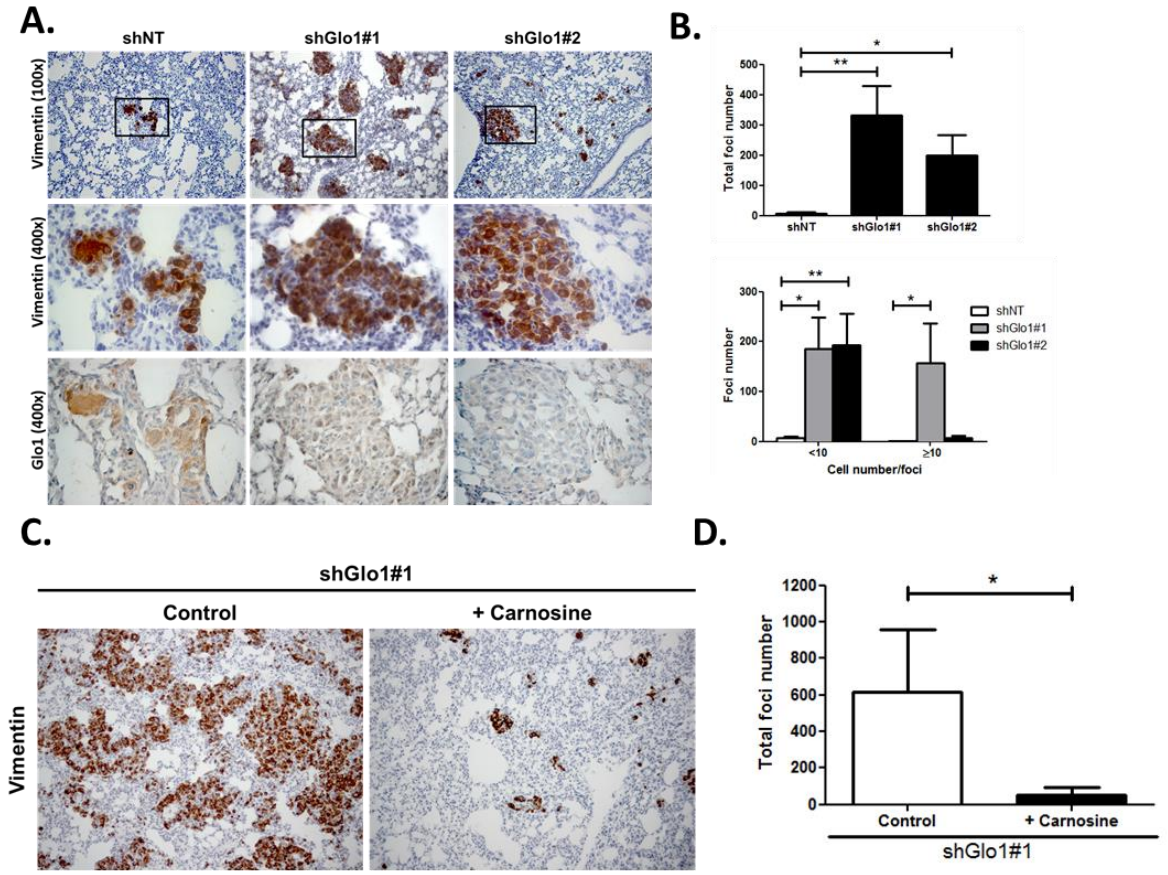

Figure 44: Glo1-depleted breast cancer cells show an increased metastatic potential in a mouse xenograft model. A. MDA-MB-231 shGlo1#1 and #2 and control shNT cells were injected subcutaneously in NOD-SCID mice (15 mice/group). After 4 weeks, primary tumors were surgically removed. Six weeks after tumor removal, mice were sacrificed and lungs were collected. Representative human vimentin IHC highlights lung metastatic tumor lesions. Adjacent serial sections were used to perform Glo1 IHC staining. Magnifications 100x and 400x. **B.** Quantification of number and size of vimentin positive foci on whole lung sections. **C.** MDA-MB-231 shGlo1#1 cells were injected subcutaneously in NOD-SCID mice (5 mice/group). After 4 weeks, primary tumors were surgically removed and mice were treated with carnosine (10mM) in drinking water. Six weeks after tumor removal, mice were sacrificed and lungs were collected. Human vimentin IHC staining of whole lung sections highlights metastatic tumor lesions. Magnification 100x. **D.** Quantification of vimentin positive foci on whole lung sections. Data are represented as mean ± SEM. * $p<0.05$ and ** $p<0.01$.

2.3. Conclusions

In this study, we demonstrated that MG-mediated carbonyl stress interferes with LATS1, a major kinase of the Hippo tumor suppressor pathway to induce sustained YAP activity. We identified Hsp90 as a novel target protein of MG. We showed for the first time that carbonyl stress can have pro-tumoral and pro-metastatic effects. Altogether, these results highlight the fact that Hsp90 and Glo1 targeted therapies should be adapted depending of the carbonyl stress status of the tumors. MG scavengers like carnosine and metformin could be good candidates in therapeutic strategies for triple negative breast cancer patients.

Methylglyoxal, a glycolysis by-product, induces Hsp90 glycation and YAP-mediated tumor growth and metastasis

Nokin MJ, Durieux F, Peixoto P, Chiavarina B, Peulen O, Blomme A, Turtoi A, Costanza B, Smargiasso N, Baiwir D, Leenders J, De Tullio P, Bianchi E, Thiry M, Uchida K, Spiegel DA, R. Cochrane JR, Hutton CA, De Pauw E, Delvenne P, Belpomme D, Castronovo V and Bellahcène A

Under review at eLife Journal (July 2016)

Methylglyoxal, a glycolysis side-product, induces Hsp90 glycation and YAP-mediated tumor growth and metastasis

Marie-Julie Nokin[1], Florence Durieux[1], Paul Peixoto[1], Barbara Chiavarina[1], Olivier Peulen[1], Arnaud Blomme[1], Andrei Turtoi[1], Brunella Costanza[1], Nicolas Smargiasso[2], Dominique Baiwir[3], Justine Leenders[4], Pascal De Tullio[4], Elettra Bianchi[5], Marc Thiry[6], Koji Uchida[7], David A. Spiegel[8], James R. Cochrane[9], Craig A. Hutton[9], Edwin De Pauw[2], Philippe Delvenne[5], Dominique Belpomme[10], Vincent Castronovo[1] and Akeila Bellahcène[1*]

[1]Metastasis Research Laboratory, GIGA-CANCER, University of Liège (ULg), Liège, Belgium; [2]Mass Spectrometry Laboratory, GIGA-Systems Biology and Chemical Biology, ULg; [3]GIGA Proteomic Facility, ULg; [4]Laboratory of Medicinal Chemistry - CIRM, ULg; [5]Department of Pathology, CHU, ULg; [6]Laboratory of Cellular and Tissular Biology, GIGA-Neurosciences, ULg; [7]Laboratory of Food and Biodynamics, Graduate School of Bioagricultural Sciences, University of Nagoya, Nagoya, Japan; [8]Department of Chemistry, Yale University, 225 Prospect Street, New Haven, Connecticut, USA; [9]School of Chemistry and Bio21 Molecular Science and Biotechnology Institute, University of Melbourne, Australia; [10]Association for Research and Treatments Against Cancer (ARTAC), Paris, France

*****Corresponding author: Akeila BELLAHCENE, University of Liège, GIGA-CANCER, Metastasis Research Laboratory, Pathology Tour, +4 level, Building 23, 4000 LIEGE, BELGIUM, Tel. +32 4 366 25 57, Fax +32 4 366 29 75, e-mail a.bellahcene@ulg.ac.be

Metabolic reprogramming toward aerobic glycolysis unavoidably induces methylglyoxal (MG) formation in cancer cells. MG mediates the glycation of proteins to form advanced glycation end products (AGEs). We have recently demonstrated that MG-induced AGEs are a common feature of breast cancer. Little is known regarding the impact of MG-mediated carbonyl stress on tumor progression. Breast tumors with MG stress presented with high nuclear YAP, a key transcriptional co-activator regulating tumor growth and invasion. Elevated MG levels resulted in sustained YAP nuclear localization/activity that could be reverted using Carnosine, a scavenger for MG. MG treatment affected Hsp90 chaperone activity and decreased its binding to LATS1, a key kinase of the Hippo pathway. Cancer cells with high MG stress showed enhanced growth and metastatic potential *in vivo*. These findings reinforce the cumulative evidence pointing to hyperglycemia as a risk factor for cancer incidence and bring renewed interest in MG scavengers for cancer treatment.

INTRODUCTION

Unlike normal cells, cancer cells mainly rely on glycolysis to generate energy needed for cellular processes even in normoxia conditions. This process referred to aerobic glycolysis or the "Warburg effect" is considered as a hallmark of cancer cells [1]. Although aerobic glycolysis is less efficient than respiration to generate ATP, we know now that it effectively supports the anabolic requirements associated with cancer cell growth and proliferation. One underestimated consequence of increased glucose uptake and glycolytic flux is the accumulation of potent toxic metabolites such as reactive carbonyl species. Among those, methylglyoxal (MG) is a highly reactive α-oxoaldehyde that is primarily formed in cells by the spontaneous degradation of triose phosphate intermediates of glycolysis, dihydroxyacetone phosphate and glyceraldehyde 3-phosphate [2]. Alpha-oxoaldehydes are up to 20,000-fold more reactive than glucose in glycation processes [3]. MG leads to chemical modification of proteins, lipids and nucleotides that result in cellular dysfunction and mutagenicity. MG interaction with amino groups of proteins notably leads to the formation of advanced glycation end products (AGEs) called

hydroimidazolones (MG-H) and argpyrimidines [4]. All mammalian cells possess a detoxifying system constituted of glyoxalase 1 and 2 (Glo1 and Glo2, respectively), which catalyze the conversion of MG to D-lactate [5]. The disturbance in the balance between endogenous reactive carbonyl species generation and the ability to counteract their harmful effects is defined as the carbonyl stress.

At the molecular level, carbonyl stress is a common feature of the metabolic dysfunction associated with diabetes and cancer. MG-related AGEs have been mostly studied and identified in the context of diabetes. For example, MG post-translational modification of vascular basement membrane type IV collagen [6] and of voltage-gated sodium channel Nav1.8 [7] have been associated with long-term diabetic complications.

Whereas the link between oxidative stress, cancer development, progression and response to therapy is clearly established, carbonyl stress and cancer connection remains largely unexplored and has never been envisaged as potentially interconnected. To the best of our knowledge, only one study has reported MG-derived AGEs detection in malignant tumors [8]. Using immunohistochemistry, we have recently reported the accumulation of argpyrimidine MG adducts in breast cancer tumors [9]. Remarkably, MG-mediated glycation of specific target proteins happens to be beneficial to cancer progression. For example, the formation of argpyrimidine on heat shock protein 27 (Hsp27) prevented cancer cell apoptosis in lung [10] and gastrointestinal [11] cancers. Moreover, inhibition of MG modification on Hsp27 caused sensitization of cancer cells to anti-tumoral drugs [12].

MG has been shown to down regulate Hsp90 and Hsc70 expression levels in human retinal pigment epithelial cells [13]. Hsp90 is a molecular chaperone that gained great interest over the last 20 years as a druggable target for cancer treatment. Hsp90 stabilizes and activates more than 400 proteins, referred to as Hsp90 ‘clients’, many of which are oncoproteins including transcription factors and kinases that are essential for cellular signal transduction pathways and adaptive responses to stress [14]. One such client protein is the large tumor suppressor 1 (LATS1) [15], a key kinase that relays anti-proliferative signals in the Hippo pathway through Yes-associated protein (YAP) phosphorylation and inactivation [16]. Consistent with its fundamental role in the control of organ growth and size in vertebrates, the dysfunction of the Hippo signalization triggers tumorigenesis in human [17]. As a co-activator of TEAD family of transcription factors [18], YAP has been notably shown to enhance cancer progression through transcriptional activation of proliferation promoting genes such as c-myc and CTGF [19]. Recent studies established a link between glucose deprivation stress, aerobic glycolysis and YAP activation in cancer [20, 21, 22]. Thus reinforcing the increasing evidence indicating that metabolic pathways play causative roles in conferring an aggressive phenotype upon cancer cells. Because spontaneous MG accumulation results from the glycolytic flux, we hypothesized that MG stress might couple glycolysis to YAP activity. In this study, we show that MG induces YAP nuclear persistence and activity in breast cancer cells and we validate a molecular mechanism implicating MG-mediated HSP90 inactivation and subsequent LATS1 kinase decrease. Our study establishes for the first time the functional significance of endogenous MG stress and reveals its unexpected connection with cancer cells propensity to grow and metastasize.

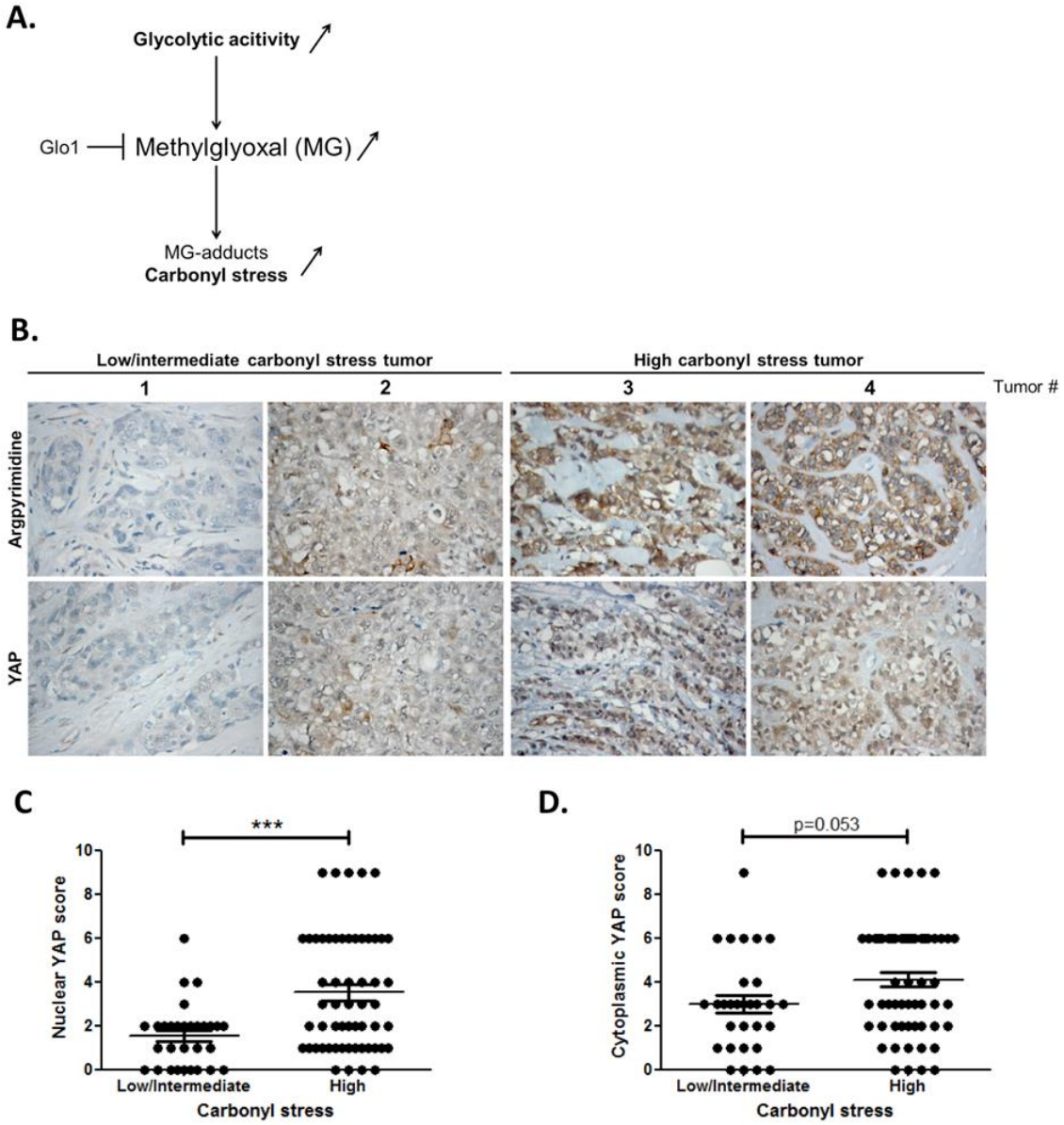

Figure 1: High carbonyl stress and nuclear YAP are positively correlated in human breast cancer. A. In cancer cells, a high glycolytic metabolism and/or a decrease of the MG-detoxifying activity of Glyoxalase 1 (Glo1) lead to high MG level thus establishing a carbonyl stress. **B.** YAP IHC staining in representative low/intermediate and high carbonyl stress human breast tumors as assessed by their argpyrimidine level. **C.** Quantification of nuclear and **D.** cytoplasmic YAP IHC staining in a series of human breast cancer (n=87). Each dot represents one case and bars represent mean ± SEM. Data were analyzed using Mann Whitney U test and *** represents p<0.001.

RESULTS

Methylglyoxal adducts and nuclear YAP are positively correlated in human breast cancer. At the molecular level, a predictable consequence of the glycolytic switch in cancer cells is the induction of carbonyl stress (Figure 1A). We have previously reported MG-mediated carbonyl stress, assessed by argpyrimidine adducts detection, in a series of breast cancer lesions [9]. Recent reports highlighted the importance of glucose metabolism for the regulation of YAP activity in cancer cells [20, 21, 22]. To explore possible links between YAP activity and carbonyl stress, we performed immunohistochemistry staining of YAP on a series of 87 breast tumors categorized as high and low to intermediate carbonyl stress tumors based on their endogenous argpyrimidine level. Remarkably, breast cancer lesions with high carbonyl stress also showed high

YAP expression (Figure 1B). YAP was scored for nuclear and cytoplasmic staining. Statistical analysis revealed a significant difference between nuclear YAP staining in low/intermediate and high carbonyl stress tumors (Figure 1C). We demonstrated a positive correlation (R_{sp}=0.318, p=0.028) between carbonyl stress intensity and nuclear YAP detection. Cytoplasmic YAP staining showed no significant difference between high and low/intermediate carbonyl stress

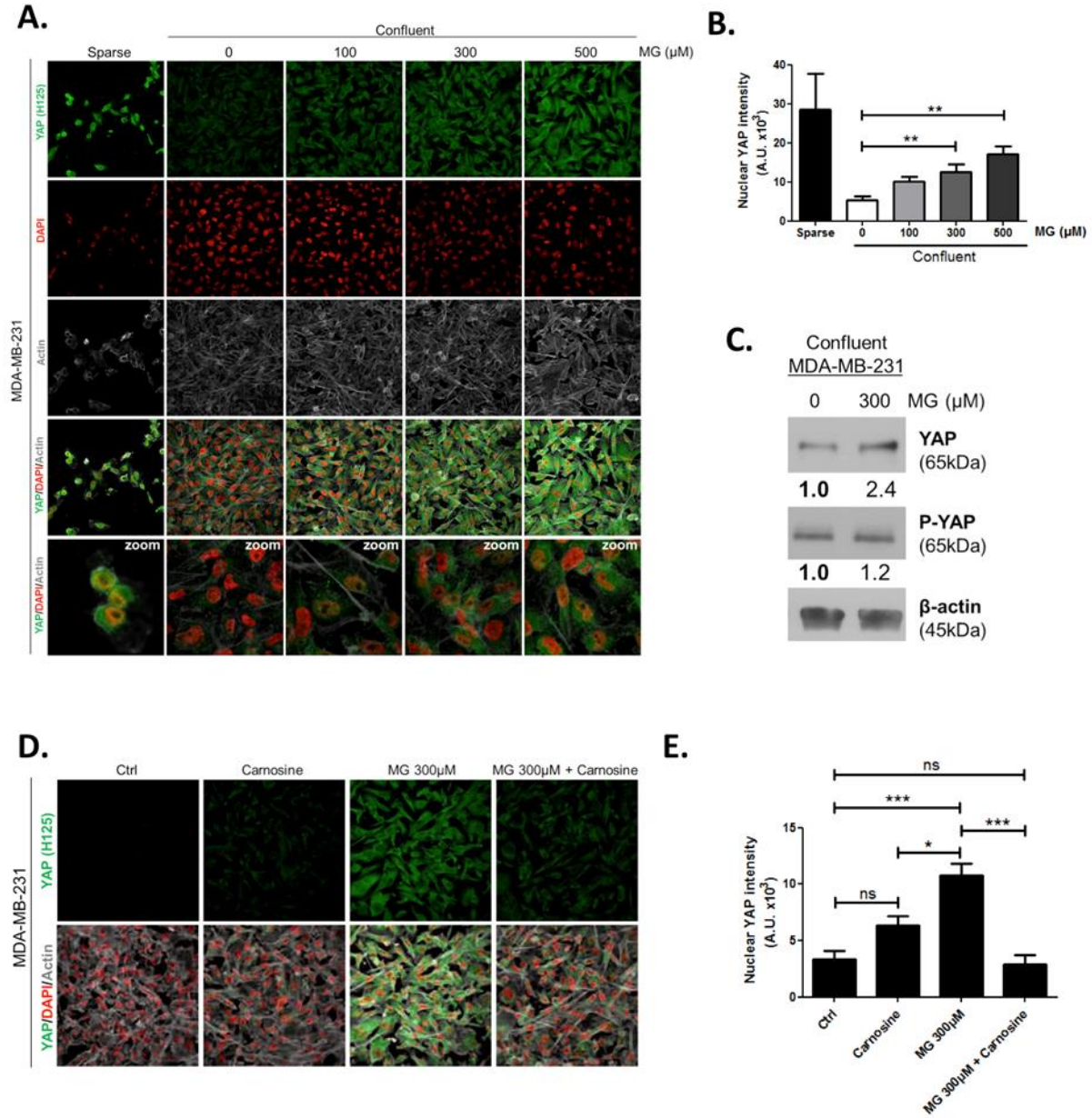

Figure 2: Methylglyoxal induces YAP persistence in confluent breast cancer cells. A. Immunofluorescence (IF) staining shows that YAP (Santa Cruz antibody, H125) is mainly localized in the nucleus at low cellular density (Sparse) and is weakly detectable at high cellular density (Confluent) in MDA-MB-231 cells. In contrast, cells treated with increasing doses of MG until they reach confluence showed significant YAP cellular accumulation. Zoomed pictures are shown where indicated. Magnification 630x. Data are representative of three independent experiments. **B.** Quantification of panel A experiment reports the intensity of YAP staining that colocalized with DAPI staining as described in Materials and Methods section. Nuclear YAP IF staining intensity shows a significant dose-dependent increase in presence of MG. Data were analyzed using one-way ANOVA followed by Dunnett post-test and shown as the mean values ± SEM of three independent experiments. **C.** YAP and P-YAP (ser127) expression in MDA-MB-231 cells treated with MG (300µM) until they reach confluence using western blot. Immunoblot data were quantified by densitometric analysis and normalized for β-actin. Numbers represent fold increase relative to the condition shown with bold number. **D.** MDA-MB-231 cells cultured until they reached high density and treated concomitantly with MG (300µM) and carnosine (10mM), a MG scavenger, impeded cellular accumulation of YAP. Magnification 630x. Data are representative of three independent experiments. **E.** Quantification of panel D experiment. Data were analyzed using one-way ANOVA followed by Bonferroni post-test and are shown as the mean values ± SEM of three independent experiments. * p<0.05, ** p<0.01, *** p<0.001, ns=not significant.

breast tumors (Figure 1D).

Methylglyoxal induces YAP persistence in confluent breast cancer cells. Deficient contact inhibition is a hallmark of invasive cancer cells, yet unexpectedly the density at which cancer cells are cultured impacts on the Hippo pathway in commonly studied cancer cell lines. In order to explore further the potential connection existing between MG-induced carbonyl stress and YAP, we first examined cell density dependent YAP subcellular localization in MDA-MB-231, MDA-MB-468 and MCF7 breast cancer cell lines. YAP was mainly localized in the nucleus of low-density cultured cancer cells as detected by immunofluorescence. When breast cancer cells reached confluence, YAP was not detectable in the nucleus and became generally less visible suggesting that it underwent degradation (Figure 2A and Supplementary Figures S1A, B, D and E). Upon MG treatment, MDA-MB-231 cells showed a concentration dependent persistence of YAP in both the cytoplasm and the nucleus despite the cells reached confluence (Figure 2A). As a transcriptional co-activator, YAP's function is strictly constrained by its subcellular localization thus we will essentially focus on YAP nuclear localization thereafter. Quantification supported that nuclear YAP immunodetection was dose dependently higher in MG treated cells when compared to untreated cells in high density cultures (Figure 2B). Nuclear YAP accumulation was also found to be significant in MDA-MB-468 and MCF7 breast cancer cells upon 300 and 500µM MG treatments (Supplementary Figures S1A, B, D, and E). Analysis of YAP expression using western blot further demonstrated an increase of total YAP in MG-treated cells. No significant change in cytoplasmic P-YAP level was observed thus indicating a nuclear YAP accumulation upon MG treatment (Figure 2C and Supplementary Figure S1C and F). We obtained similar results in all three cell lines using a second antibody specifically directed against YAP (Supplementary Figure S2A, B and C). YAP mRNA levels were not significantly changed upon MG treatment in the three breast cancer cell lines (Figure S1G).

Data gathered so far indicates that MG favors YAP persistence in cancer cells. Next, we asked whether the blockade of MG-mediated carbonyl stress using carnosine, a known MG scavenger [23], could abolish these effects. When MDA-MB-231 cells were concomitantly treated with MG and carnosine, YAP cellular accumulation in high density cultures was significantly returned to untreated cells basal level (Figures 2D and E) indicating that YAP persistence in confluent cells directly or indirectly resulted from MG-mediated carbonyl stress. Carnosine alone did not affect significantly cellular YAP immunodetection. After we have validated exogenous MG effects, we decided to use 2 strategies in order to assess high endogenous MG impact on YAP in breast cancer cells: (a) inhibition of Glo1, the main MG-detoxifying enzyme and (b) high glucose culture condition.

High endogenous methylglyoxal induces nuclear YAP accumulation in breast cancer cells. First, Glo1 inhibition was achieved by the use of siRNAs on one hand and the use of S-p-bromobenzylglutathione cyclopentyl diester (BBGC), an effective Glo1 inhibitor on the other hand [24]. MBo, a specific fluorescent sensor for MG in live cells [25], demonstrated endogenous MG increase upon Glo1 expression inhibition and BBGC treatment in MDA-MB-231 cells (Figure 3A). Consistent with exogenous MG treatment experiments, both Glo1-depleted and BBGC-treated MDA-MB-231

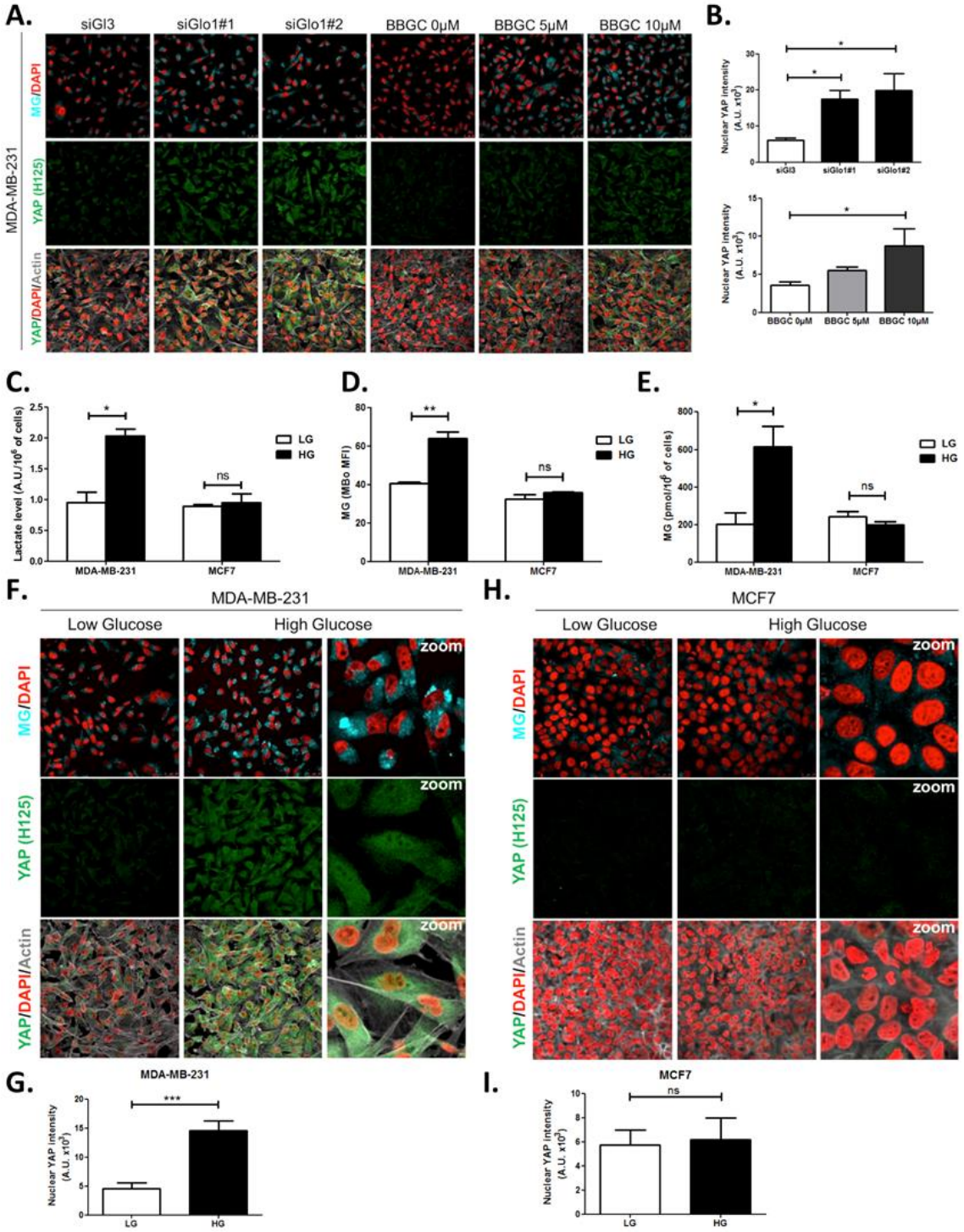

Figure 3: High endogenous MG induces YAP nuclear accumulation in breast cancer cells. A. Detection of MG was performed using MBo specific fluorescent probe, as described in Materials and Methods section, and showed MG cellular increase in MDA-MB-231 cells that were Glo1-depleted using siRNAs (siGlo1#1 and #2) or treated with BBGC Glo1 activity inhibitor. Upon Glo1 silencing/inhibition, MDA-MB-231 cells displayed more YAP (Santa Cruz antibody, H125) than control cells (siGl3 and BBGC 0µM, respectively). Magnification 630x. Data are representative of three independent experiments. **B.** Quantification of panel A experiment reports the intensity of YAP staining that colocalized with DAPI staining as described in Materials and Methods section for Glo1 silencing and BBGC conditions. Data were analyzed using one-way ANOVA followed by Dunnett post-test and shown as the mean values ± SEM of three independent experiments. **C.** Lactate level measured using ^{1}H-NMR increased in highly glycolytic MDA-MB-231 cells cultured in high glucose (HG) compared to low glucose (LG) while MCF7 low glycolytic cells did not. **D.** and **E.** MG quantification using both FACS MBo mean fluorescence intensity (MFI) and LC-MS/MS analysis on conditioned medium in the indicated conditions as described under Material and Methods section. MDA-MB-231 cells significantly increased their MG production in HG when compared to MCF7. **F** and **H.** MG detection and YAP immunofluorescence staining (Santa Cruz antibody, H125) in the indicated breast cancer cell line cultured in low and high glucose medium. Magnification 630x. Zoomed pictures are shown for high glucose condition. Data are representative of three independent experiments. **G** and **I.** Quantification of F and H panels, respectively. Data shown in C., D., E., G. and I. were analyzed using unpaired Student's t test for each cell line independently and shown as the mean values ± SEM of three independent experiments. * p<0.05, ** p<0.01, *** p<0.001 and ns=not significant.

cells (Figure 3A and B) displayed nuclear YAP persistence in high-density cultures. Similar results were obtained under both conditions in MDA-MB-468 cells (Supplementary Figure S3A and B). Efficient Glo1 silencing in breast cancer cells was assessed by Glo1 immunoblotting (Supplementary Figures S3C and D). Altogether, these results showed that MG stress maintained detectable YAP nuclear levels in confluent breast cancer cells. Second, we cultured MDA-MB-231 (highly glycolytic) and MCF7 (low glycolytic) cells in low and high glucose medium. Lactate measurement using ^{1}H-NMR showed that MDA-MB-231 cells significantly increased their glycolytic activity when cultured in high glucose (HG) compared to low glucose (LG) (Figure 3C). In these cells, HG culture induced elevated endogenous MG level that was assessed using both FACS detection of MBo fluorescent probe (Figure 3D) and LC-MS/MS quantification (Figure 3E). Similar results were observed using another highly glycolytic breast cancer cell line, MDA-MB-468 (Supplementary Figures S3, E to G). As expected, low glycolytic MCF7 cells used for comparison did not react to high glucose culture condition and kept stable lactate (Figure 3C). More importantly, MCF7 cells showed stable MG levels (Figure 3D and E) thus pointing for the first time to MG increase as a specific response of glycolytic cancer cells to glucose stimulus. After having validated the response of breast cancer cells to high glucose, we next asked whether YAP nuclear persistence occurred under glucose-induced elevated endogenous MG levels. MDA-MB-231 and MDA-MB-468 cells cultured to confluence in high glucose demonstrated positive nuclear YAP staining (Figure 3F and G and Supplementary Figure S3 H and I) when compared with cells cultured in low glucose. Under the same culture conditions, we did not observe any significant persistence of YAP in MCF7 breast cancer cells (Figure 3H and I) as expected from their stable glycolytic rate and unaffected MG level. It is noteworthy that MCF7 cells are able to induce YAP accumulation in response to an exogenous MG supply (Supplementary Figure S1) suggesting that low glycolytic cells could be stimulated in a high MG environment created by neighboring cells for example and this, independently of their own glycolytic flux. The observed effects of endogenous high MG levels on YAP were significantly reversed using 2 MG scavengers, carnosine and aminoguanidine in MDA-MB-231 cells (Supplementary Figure S4). Altogether, these data demonstrate that the glycolytic switch in cancer cells is accompanied by high MG levels and YAP nuclear persistence and establish a new link between glucose utilization, MG stress and YAP regulation in cancer cells.

MG induces YAP co-transcriptional activity in breast cancer cells. We next explored the functional relevance of MG-mediated nuclear accumulation of YAP in breast cancer cells. For this purpose, we used two shRNAs specifically directed against Glo1 to stably induce high endogenous MG stress in MDA-MB-231 breast cancer cells. Efficient Glo1 silencing (shRNAs #1 and #2) at the mRNA and protein levels, decreased Glo1 activity (Supplementary Figures S5A, B and C, respectively) and MG increase (Supplementary Figure S5D) were validated in stably depleted clones. As expected, Glo1-depleted MDA-MB-231 cells showed YAP accumulation in high-cell density cultures when compared to control cells (Supplementary Figures S5E and F). Consistently, this effect was significantly reversed using carnosine and aminoguanidine MG scavengers (Supplementary (Supplementary Figure S6A and B). Stably depleted Glo1 MDA-

MB-231 cells were used to assess YAP target genes expression based on a previously established gene signature denoting YAP/TAZ activity [18, 26, 27, 28]. Among the 14 targets tested and known to be regulated positively by YAP, we found that 8 genes, including CTGF gene, showed a significant increase at the mRNA level in Glo1 depleted cells when compared to control (Figure 4A). Importantly, knock-down of YAP using siRNA transfection reversed, at least in part, the expression of all the evaluated genes thus establishing the link between YAP target genes expression and Glo1 status in cancer cells. Efficient YAP silencing in Glo1-depleted MDA-MB-231 is shown in Supplementary Figure S7A. This result led us to search for a statistical association between YAP and Glo1 expression levels using a gene expression dataset of 103 primary mammary tumors [29]. However, global YAP expression did not show any significant correlation with Glo1. We reasoned that YAP activity, rather than its total expression level, would better reflect YAP nuclear accumulation related to MG stress. Indeed, we found that the expression of YAP target genes and Glo1 showed a significant inverse correlation in breast cancer patients. Top 12 genes that displayed the highest Rp Pearson correlation coefficient are reported in Supplementary Figure S7B. These data indicate that high carbonyl stress driven by low Glo1 expression in human malignant mammary tumors is significantly associated with an elevated YAP activity.

Data gathered so far indicate that MG favors YAP activity in cancer cells. In order to assess more concretely the impact of MG stress on breast cancer cells through YAP activation, we next focused on CTGF gene expression, a well-described YAP transcriptional target [18] that has been linked to YAP pro-growth and tumorigenic functions. We performed chromatin IP assays to assess the presence of YAP at CTGF promoter in both sparse and confluent MDA-MB-231 cells. In low-density cultured cells YAP was bound to CTGF promoter while in confluent cells, YAP was not detectable which is consistent with YAP absence in the nucleus of high-density cells. In contrast, YAP was found at CTGF promoter in MG-treated confluent cells at a comparable level to that in sparse cells (Figure 4B). Immublot of YAP IP loading are shown in Supplementary Figure S7C. CTGF mRNA level was not significantly affected by MG treatment in MDA-MB-231 cells (Figure 4C). Smad2/3 collaborate with TEAD and YAP to form an active transcriptional complex at CTGF promoter in breast cancer cells [30, 31]. MDA-MB-231 cells cultured in presence of MG and treated with TGF-β (2.5ng/ml) responded by a two-fold increase of CTGF mRNA level compared to TGF-β alone confirming the requirement of TGF-β pathway activation for MG-mediated induction of CTGF expression (Figure 4C). Smad2 and Smad3 phosphorylation following TGF-β treatment in MDA-MB-231 cells was not affected by MG treatment (Supplementary Figure S8A) indicating that CTGF up-regulation was linked to YAP accumulation in presence of active TGF-β pathway effectors. In agreement with this deduction, we showed that YAP silencing prevented MG-mediated CTGF mRNA induction in presence of TGF-β in confluent MDA-MB-231 cells (Figure 4D). Efficient YAP silencing was shown at the mRNA (Supplementary Figure S8B) and protein (Supplementary Figure S8C) levels.

Association with TEAD transcription factors is essential in mediating YAP-dependent gene expression [18]. As shown in Figure 4E and Supplementary Figure S8D, YAP and TEAD1 co-localized in MG-

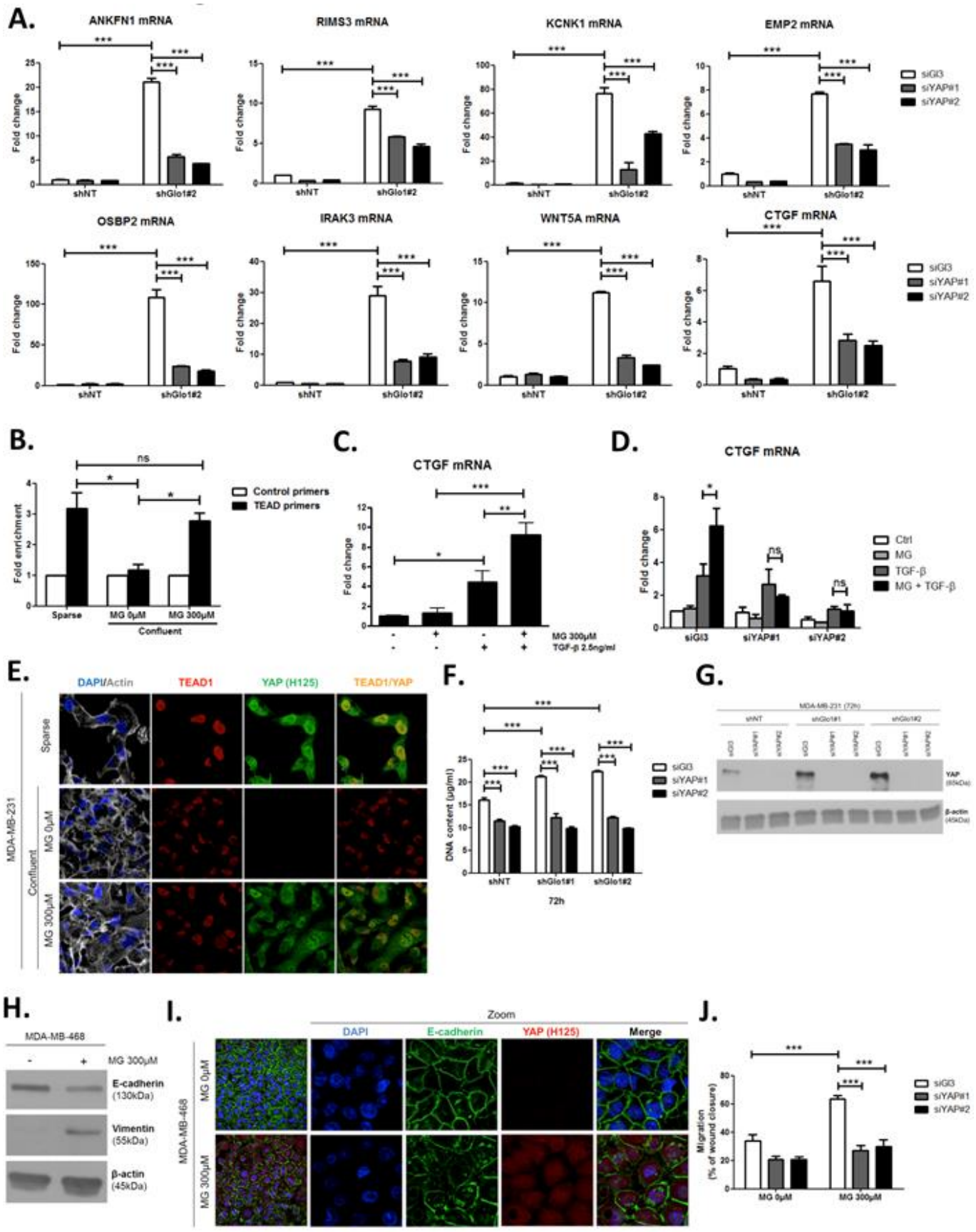
A.
ANKFN1 mRNA
RIMS3 mRNA
KCNK1 mRNA
EMP2 mRNA
OSBP2 mRNA
IRAK3 mRNA
WNT5A mRNA
CTGF mRNA
Fold change
shNT
shGlo1#2
siGl3
siYAP#1
siYAP#2
B.
Fold enrichment
Control primers
TEAD primers
Sparse
MG 0μM
MG 300μM
Confluent
C.
CTGF mRNA
MG 300μM
TGF-β 2.5ng/ml
D.
CTGF mRNA
Ctrl
MG
TGF-β
MG + TGF-β
E.
DAPI/Actin
TEAD1
YAP (H125)
TEAD1/YAP
MDA-MB-231
Sparse
Confluent
F.
DNA content (μg/ml)
72h
G.
MDA-MB-231 (72h)
YAP
β-actin
H.
MDA-MB-468
E-cadherin (130kDa)
Vimentin (55kDa)
β-actin (45kDa)
I.
Zoom
DAPI
E-cadherin
YAP (H125)
Merge
J.
Migration (% of wound closure)

Figure 4: MG induces YAP co-transcriptional activity in breast cancer cells. A. Stable knockdown of Glo1 using shGlo1#2 shRNA in MDA-MB-231 results in upregulation of several YAP target genes (ANKFN1, RIMS3, KCNK1, EMP2, OSBP2, IRAK3, WTN5A and CTGF) at the mRNA level as assessed by qRT-PCR. Silencing of YAP using 2 independent siRNAs (siYAP#1 and #2, 48h post-transfection) significantly reversed YAP target genes induction in Glo1 depleted cells. Data were analyzed using two-way ANOVA followed by Bonferroni post-test and shown as the mean values ± SD of one representative experiment (n=4). **B.** Chromatin immunoprecipitation of YAP at the CTGF promoter in sparse and confluent MDA-MB-231 cells treated or not with MG. TEAD PCR primers, and not control primers, target TEAD binding site on CTGF promoter (see sequences under Materials and Methods section). The use of TEAD primers indicated that YAP was present at the CTGF promoter in sparse cells (positive control) and in confluent MG-treated cells when compared to untreated confluent cells. Data were analyzed using one-way ANOVA followed by Newman-Keuls post-test and shown as the mean values ± SEM of three independent experiments. **C.** CTGF mRNA level assessed by qRT-PCR in MDA-MB-231 cells treated with MG 300µM until confluence and then with TGFβ 2.5ng/ml during 2h. Data were analyzed using two-way ANOVA followed by Bonferroni post-test and shown as the mean values ± SEM of five independent experiments. **D.** MG-mediated CTGF induction in presence of TGFβ is not observed upon YAP silencing (siYAP#1 and #2) when compared to control (siGl3) cells. Data were analyzed using two-way ANOVA followed by Bonferroni post-test and shown as the mean values ± SEM of three independent experiments. **E.** YAP (Santa Cruz antibody, H125) and TEAD1 IF co-localization in MDA-MB-231 cells cultured under low (Sparse) density used as positive control and in high density cultured cells (Confluent) in presence of MG. Magnification 630x. **F.** DNA quantification assay showing an increased proliferation of Glo1-silenced MDA-MB-231 (shGlo1#1 and #2) compared to control (shNT) at 72h. Silencing of YAP (siYAP#1 and #2) reversed this effect. Data were analyzed using two-way ANOVA followed by Bonferroni post-test and shown as the mean values ± SEM of four independent experiments. **G.** Validation of YAP silencing by Western blot in MDA-MB-231 shGlo1 cells after 72h related to panel F and Supplementary Figure S8E. **H.** E-cadherin and vimentin EMT markers are down-regulated and up-regulated, respectively, upon MG treatment in MDA-MB-468 breast cancer cells as shown by western blot. β-actin is used for normalization. **I.** High density MDA-MB-468 cells treated with MG demonstrated reduced and disrupted E-cadherin junctions using immunofluorescence. Magnification 630x. Zoomed pictures are shown where indicated. **J.** MDA-MB-468 cells treated with MG until confluence showed a higher migratory capacity compared to control cells as assessed by wound healing assay (16h) and not in YAP-silenced conditions. Data were analyzed using two-way ANOVA followed by Bonferroni post-test and shown as the mean values ± SEM of five independent experiments. E, H and I. are representative of three independent experiments. * $p<0.05$, ** $p<0.01$, *** $p<0.001$, ns: not significant.

treated confluent MDA-MB-231 cells, and in sparse cultured cells used as positive control, whereas this co-localization was not detected in untreated confluent cells. YAP activation stimulates cancer cell growth. We next challenged cell proliferation induced by MG stress in Glo-1 depleted MDA-MB-231 cells. The time course of Glo1-depleted cells proliferation showed a marked difference compared to control cells (Supplementary Figure S8E). At 72h, this increase in cell proliferation was significantly abrogated upon YAP silencing indicating that it is required to sustain MG-induced pro-growth effect (Figure 4F). Western blotting demonstrated both YAP increase upon Glo1 silencing and efficient YAP silencing (Figure 4G).

YAP and its paralog TAZ have been previously reported to promote EMT in human breast epithelial cells [32, 33]. To test whether MG-induced YAP activation launched EMT in breast cancer cells, immunoblotting was performed to examine the expression of well-characterized EMT markers. We observed an increase of vimentin and a decrease of E-cadherin expression, attesting of an EMT process in MDA-MB-468 cells treated with MG (Figure 4G). Confirming these results, we showed by immunofluorescence that E-cadherin network was disrupted in MG-treated cells (Figure 4H). Consistent with EMT induction, MG-treated MDA-MB-468 cells showed an enhanced migration potential that was efficiently reversed to basal level upon YAP silencing (Figure 4I and Supplementary Figure S8F).

MG favors LATS1 kinase degradation through the proteasome in breast cancer cells. To gain insight into possible mechanisms by which MG regulates YAP activity, we first considered that YAP could be a direct target of MG glycation. However, MG-adducts immunoprecipitation in MDA-MB-231 treated with MG did not allow western blot detection of YAP (data not shown). LATS1 is the main upstream Hippo pathway kinase that phosphorylates YAP thus preventing its nuclear translocation and oncogenic activity (Figure 5A). We hypothesized that MG-mediated sustained YAP nuclear localization could be related to a relaxed LATS1 control notably due to

its decreased expression. Indeed we demonstrated by western blotting that LATS1 was significantly decreased upon MG treatment (300 and 500µM) in both glycolytic MDA-MB-231 and non-glycolytic MCF7 breast cancer cells (Figure 5B). Similar results were observed in MDA-MB-468 (Supplementary Figure S9A). LATS1 mRNA levels were not affected by MG in the three breast cancer cell lines (Supplementary Figure S9B). A previous study has shown that LATS1 kinase degradation occurs through polyubiquitination and the 26S proteasome pathway in breast cancer cells[34]. In good accordance, the treatment of breast cancer cells with MG132 proteasome inhibitor induced LATS1 increase (Figure 5B and Supplementary Figure S9A). Next, we verified whether MG favored LATS1 decrease through proteasome degradation. As shown in Figure 5B and Supplementary Figure S9A, the use of MG132 proteasome inhibitor reverted MG-induced LATS1 decrease. Next, we explored whether this LATS1 decrease could explain, at least in part, the sustained YAP nuclear localization induced by MG. Accordingly, when we overexpressed LATS1, we were able to revert MG effects on YAP accumulation as assessed by immunofluorescence using 2 anti-YAP antibodies in MDA-MB-231 cells (Figure 5C and Supplementary Figure S9C), and the other breast cancer cell lines analyzed (Supplementary Figures S9D and E). LATS1 overexpression is shown using anti-Flag antibody (Supplementary Figure S9F). Data gathered so far indicate that MG decreases LATS1 expression in breast cancer cells, through the proteasome, which leads to sustained activity of YAP in the nucleus.

MG induces post-translational glycation of Hsp90 and affects its chaperone activity on LATS1. To explore further MG mechanism of action on LATS1, we first excluded the possibility of a direct glycation of LATS1 by MG using immunoprecipitation technique (data not shown). Then, we got interested in LATS1 as a client of Hsp90 chaperone protein [15]. Indeed, LATS1 kinase expression level and activity are dependent on its stabilization by Hsp90. 17-AAG, a potent Hsp90 inhibitor, disrupts LATS1 tumor suppressor activity in human cancer cells [15]. Hsp90 mRNA level was not modulated by MG treatment in breast cancer cells (Supplementary Figure S10A). Therefore, we sought to explore whether MG could modify Hsp90 thus indirectly impacting on LATS1 stability and degradation. The incubation of human recombinant Hsp90 with MG followed by MS analysis revealed the modification of several lysine and arginine residues notably yielding to the formation of carboxyethyllysine (CEL) and argpyrimidine/MG-H adducts, respectively (Supplementary Table S1). Next, we examined whether endogenous MG-modified Hsp90 could be detected in MG-treated MDA-MB-231 cells. Immunoprecipitation of MG-treated MDA-MB-231 extracts using anti-argpyrimidine MG adducts and followed by Hsp90 immunoblot analysis allowed us to detect a basal level of glycated Hsp90 in MDA-MB-231 glycolytic cells that was further enhanced upon MG treatment (Figure 5D). Hsp27, which is recognized as a major MG target in cancer cells, was also efficiently detected in argpyrimidine immunoprecipitates (Figure 5D). Consistently, the reverse IP experiment using an anti-Hsp90 antibody allowed the detection of both argpyrimidine and hydroimidazolone MG-adducts of the expected molecular weight in MG treated cells (Figure 5E). Argpyrimidine immunoprecipitates subjected to MS analysis revealed the presence of modified Hsp90 on several residues (Supplementary Table S2). Glycation hot

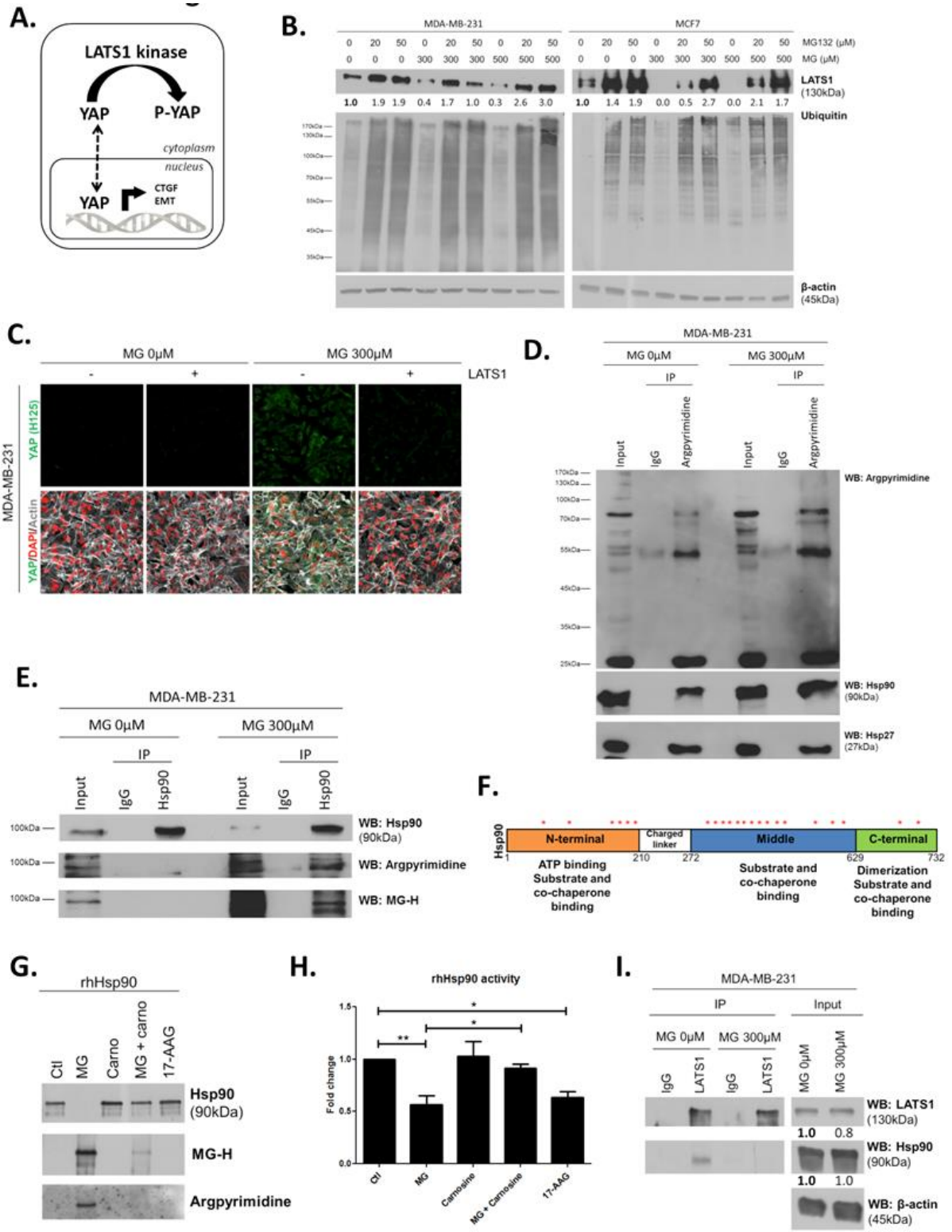

Figure 5: MG induces LATS1 kinase decrease and Hsp90 post-translational glycation in breast cancer cells. A. Schematic representation of the Hippo pathway focused on LATS1 kinase control of nuclear-cytoplasmic shuttling of YAP co-transcription factor. **B.** LATS1 expression in MDA-MB-231 and MCF7 cells treated with MG (300 and 500μM) in presence of increasing concentrations of MG132 proteasome inhibitor during 6h using western blot. **C.** YAP immunofluorescence (Santa Cruz antibody, H125) in MDA-MB-231 cells transiently transfected with LATS1 expression vector (+) or empty vector used as control (-) and then treated with MG (300μM) until confluence. **D.** Immunoprecipitation of MG adducts on MG-treated MDA-MB-231 cells (300μM, 6h) using a specific anti-argpyrimidine monoclonal antibody. Mouse immunoglobulins (IgG) were used as control. Total cell lysates (Input) and immunoprecipitates (IP) were immunoblotted for argpyrimidine, Hsp90 and Hsp27. **E.** Under the same conditions as in D, MDA-MB-231 cell lysates were immunoprecipitated using anti-Hsp90. Inputs and IPs were immunoblotted using Hsp90 antibody and two specific antibodies directed against MG-adducts (argpyrimidine and hydroimidazolone MG-H). **F.** Schematic representation of Hsp90 protein domains where hot spots (*) of endogenously and/or exogenously MG-modified residues are indicated. See also detailed amino acid sequence in Supplementary Figure S8. **G.** Western blot analysis using the indicated antibodies on recombinant human Hsp90 (rhHsp90) incubated in presence of MG ± carnosine (10mM) or 17-AAG Hsp90 inhibitor (1μM) during 24h. **H.** Hsp90 ATPase activity was decreased after incubation with MG or 17-AAG. This effect is efficiently blocked in presence of carnosine MG scavenger. Data were analyzed using two-way ANOVA followed by Bonferroni post-test and shown as the mean values ± SEM of five independent experiments. * $p<0.05$ and ** $p<0.01$. **I.** Co-immunoprecipitation of LATS1 and Hsp90 from MDA-MB-231 cells treated with MG 300μM during 24h reveals a decreased interaction between the 2 proteins. Immunoblot data were quantified by densotimetric analysis and normalized for β-actin. Numbers represent fold increase relative to the condition shown with bold number. All data are representative of three independent experiments.

endogenous Hsp90 are summarized in Figure 5F and detailed amino acid sequence is provided in Supplementary Figure S10B. The mapping of MG modifications on Hsp90 amino-acid sequence indicated that functionally important domains involved in both substrate/co-chaperone and ATP binding showed several glycated residues (Figure 5F) suggesting that Hsp90 activity could be affected. Recombinant human Hsp90 (rhHsp90) was effectively modified by MG and was protected by carnosine MG-scavenger as assessed using both anti-argpyrimidine and anti-hydroimidazolone antibodies in western blot experiments (Figure 5G). Using an *in vitro* enzymatic assay, MG decreased rhHsp90 activity to an extent that was comparable to that seen with 17-AAG, an inhibitor of Hsp90 (Figure 5H). Incubation of rhHsp90 with MG in presence of carnosine efficiently reversed this effect indicating for the first time that direct MG glycation of Hsp90 affects its ATPase activity (Figure 5H). Furthermore, both MG and 17-AAG decreased LATS1 expression in the 3 breast cancer cell lines under study (Supplementary Figure S10C). Next, we further documented LATS1 binding to Hsp90 in the context of MG treatment. LATS1 immunoprecipitates contained detectable Hsp90 however this interaction was disrupted upon MG treatment in MDA-MB-231 cells (Figure 5I). Collectively, our findings show that MG relieves LATS1 control on YAP nuclear localization through a mechanism identifying for the first time MG-mediated post-translational glycation and inactivation of Hsp90 in cancer cells.

Glo1-depleted breast cancer cells show an increased tumorigenic and metastatic potential in a mouse xenograft model. Data gathered so far indicate that MG stress favors sustained YAP pro-proliferative and pro-migratory activity in breast cancer cells. Next, we explored the biological relevance of this observation for tumor growth and metastases development. Stably Glo1-depleted MDA-MB-231 cells that were grafted subcutaneously in mice showed an increased tumor weight and volume that reached significance for shGlo1#2-silenced clones (Figure 6A). Further exploration of shGlo1 experimental tumors using immunoblotting revealed the effective *in vivo* induction of argpyrimidine adducts and a strong inverse relationship between Glo1 silencing and total YAP expression (Figure 6B and C). In Glo1-silenced experimental tumors, we further demonstrated a specific increase of YAP in the nucleus of tumor cells using immunohistochemistry (Figures 6D and E). Elevated proportion of Ki67 positive cells in shGlo1 tumors sustained the observed increased tumor growth, as shown and scored in Figure 6D and E, respectively. In order to explore further the association between high MG, YAP activity and tumor growth, we used the *in vivo* chicken chorioallantoic membrane assay (CAM). Grafted Glo1-depleted cells on the CAM showed increased growth as assessed by the measure of tumor volume and compared to control cells (Figures 6F and G). Remarkably, YAP knockdown with 2 independent siRNAs further demonstrated the causative role of YAP in MG-induced tumor growth. Indeed, YAP silencing in shGlo1 cells efficiently reverted tumor growth to control levels (Figures 6F and G). As shown on mice experimental tumors, we observed significant YAP nuclear localization in CAM shGlo1 tumors (Figures 6H and I). YAP silencing was maintained for the entire duration of the CAM assay experiment (Supplementary Figure S11).

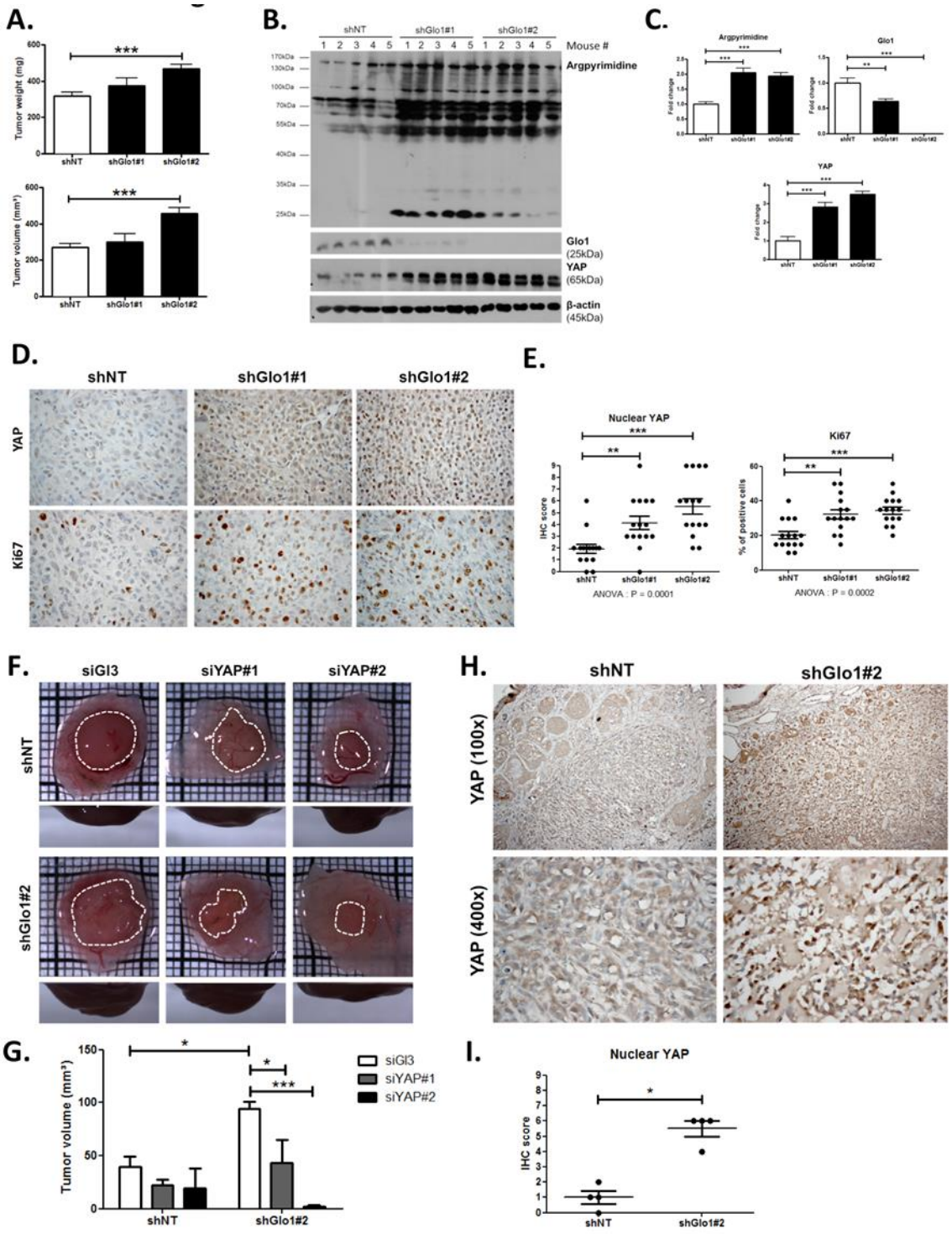

Figure 6: Glo1-depleted breast cancer cells show an increased tumorigenic potential *in vivo*. A. MDA-MB-231 shGlo1#1 and #2 and control shNT cells were injected subcutaneously in NOD-SCID mice (15 mice/group). After 4 weeks, primary tumors were surgically removed and weighed. Tumor weight (mg) and volume (mm³) were analyzed using one-way ANOVA followed by Dunnett post-test and shown as the mean values ± SEM. **B.** Western blot detection of argpyrimidine, Glo1 and YAP in 5 representative experimental primary tumors. β-actin is used for normalization. **C.** Quantification of the western blot shown in panel B. Data were analyzed using one-way ANOVA followed by Dunnett post-test and shown as the mean values ± SEM. **D.** Representative YAP and Ki67 IHC staining in experimental primary tumors. **E.** Quantification of IHC shown in panel D. Each dot represents one case and bars represent mean ± SEM. Data were analyzed using one-way ANOVA Kruskal-Wallis test followed by Dunn post-test (YAP) and one-way ANOVA followed by Dunnett post-test (Ki67). **F.** Glo1-depleted MDA-MB-231 (shGlo1#2) and control shNT cells were transfected with YAP siRNAs (siYAP#1 and 2) and grown on the chicken chorioallantoic membrane (CAM). After 7 days, tumors were collected and measured. Top and profile views of representative experimental CAM tumors are shown. **G.** Tumor volumes (4 tumors/condition) were analyzed using two-way ANOVA followed by Bonferroni post-test and shown as the mean values ± SEM. **H.** Representative YAP immunostaining on Glo1-depleted CAM experimental tumors. **I.** Quantification of nuclear YAP IHC shown in panel F. Each dot represents one case and bars represent mean ± SEM. Data were analyzed using Mann Withney t test. * p<0.05, ** p<0.01 and *** p<0.001.

Following the assessment of Glo1-silencing impact on tumor growth, we next evaluated the metastatic behavior of Glo1-depleted breast cancer cells. After surgical removal of the primary tumors, the mice were followed for metastases development during an additional period of 6 weeks. The follow-up of the mice showed that lung metastases were detectable already after 3 weeks in Glo1-depleted conditions but not in control condition. After 6 weeks post-tumor removal, metastasized tumors were observed in the lungs of Glo1-depleted mice (68%) when compared to control (20%). To evaluate further lung colonization, we performed human vimentin immunohistochemical detection that revealed a significant increase of both number and size of metastatic foci in Glo1-depleted condition (Figure 7A), as quantified in Figure 7B. Using serial sections, we assessed efficient Glo-1 depletion on the same metastatic foci (Figure 7A). These data demonstrate that breast cancer cells undergoing a carbonyl stress show enhanced growth and metastatic capacity thus highlighting an unexpected pro-tumoral role for MG endogenous accumulation. Finally, to better assess the importance of MG stress on metastatic dissemination, shGlo1#1 mice received carnosine (10mM) in drinking water from the day of primary tumor removal until the end of the

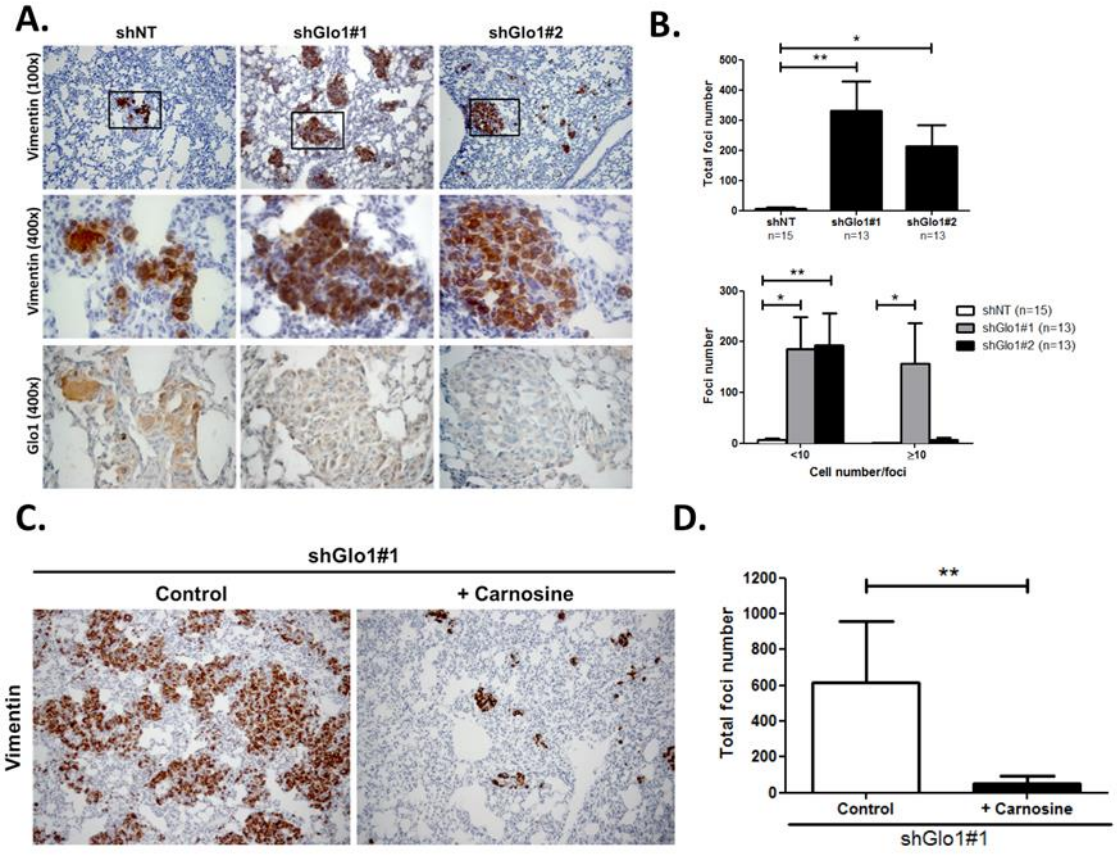

Figure 7: Glo1-depleted breast cancer cells show an increased metastatic potential in a mouse xenograft model. A. MDA-MB-231 shGlo1#1 and #2 and control shNT cells were injected subcutaneously in NOD-SCID mice. After 4 weeks, primary tumors were surgically removed. Six weeks after tumor removal, mice were sacrificed and lungs were collected. We had to ethically sacrifice 2 mice in both shGlo1#1 and shGlo1#2 groups before the end of the experiment. Representative human vimentin IHC highlights lung metastatic tumor lesions. Adjacent serial sections were used to perform Glo1 IHC staining. **B.** Quantification of number and size of vimentin positive foci on whole lung sections. Data were analyzed using two-way ANOVA followed by Newman Keuls or Bonferroni post-test and shown as the mean values ± SEM. The number of mice per group is indicated on the graph. **C.** MDA-MB-231 shGlo1#1 cells were injected subcutaneously in NOD-SCID mice (5 mice/group). After 4 weeks, primary tumors were surgically removed and mice were treated with carnosine (10mM) in drinking water. Six weeks after tumor removal, mice were sacrificed and lungs were collected. Human vimentin IHC staining of whole lung sections highlights metastatic tumor lesions. Magnification 100x. **D.** Quantification of vimentin positive foci on whole lung sections. Data were analyzed using unpaired Student's t test and shown as the mean values ± SEM. * $p<0.05$ and ** $p<0.01$.

experiment (during 6 weeks). We observed a significant decrease of lung colonization in shGlo1 mice treated with carnosine when compared with control mice (Figure 7C and D). Collectively, our data indicate that the pro-cancer effects of carbonyl stress unveiled here are tightly associated with YAP enhanced activity and can be efficiently blocked using a MG scavenger.

DISCUSSION

Cancer cell metabolism is characterized by an enhanced uptake and utilization of glucose through aerobic glycolysis. This overactive metabolism switch leads unavoidably to the formation of potent glycating agents such as MG. However, the concept of a causal relationship between non-enzymatic glycation and cancer progression is still in its early days. Here, we demonstrate that MG-mediated carbonyl stress interferes with LATS1, a major kinase of the Hippo tumor suppressor pathway to induce sustained YAP activity. The hypermethylation of the promoter region of LATS1 gene (50% of breast tumors) is associated with an aggressive breast cancer phenotype and poor survival[35]. We show in this study that LATS1 proteasomal degradation is favored in presence of MG thus bringing to light a new concept according to which MG stress could directly and/or indirectly participate to the control of tumor suppressor genes in cancer cells without affecting their transcriptional rate.

YAP is regulated by diverse mechanisms including microenvironmental factors (cell crowding and ECM stiffness) and extracellular signaling (G-coupled receptors) (for review [19]). Our study meets a new trend of thoughts proposing that energy metabolism is an additional upstream signal that regulates YAP oncogenic activity. Three independent studies recently established a link between the Hippo-YAP pathway and cellular energy stress using a glucose deprivation strategy [20, 36, 37]. These studies are in agreement that under low glucose condition an AMPK-LATS1 axis inhibits YAP activity. Enzo and collaborators [21] have recently demonstrated that aerobic glycolysis impacts on YAP/TAZ transcriptional activity through a mechanism involving phosphofructokinase 1 binding to TEAD transcription factors. A recent metabolic profiling study using breast cancer progression cellular models reported the induction of several glycolytic enzymes upon constitutive activation of TAZ/YAP factors [22]. Therefore, it is tempting to speculate that MG could regulate key glycolytic enzymes expression in a YAP-dependent manner thus creating a mutual regulatory loop where glycolysis-induced MG stress favors YAP activity, which in turn activates glycolysis. Considering that glucose metabolism inevitably leads to MG formation, one might speculate that any signaling pathway favoring the Warburg effect, e.g the Wnt signaling [38], will ultimately feed MG carbonyl stress in cancer cells.

We show for the first time that Hsp90 is post-translationally glycated by MG. Although several post-translational modifications have been previously reported to affect Hsp90 stability and chaperone function, our study importantly uncovers that a natural metabolite derived from glycolysis is involved in regulating Hsp90 in cancer cells. Decreasing Hsp90 client binding has been considered as an attractive anti-cancer therapy because of its role in stabilizing the active form of a wide range of client oncoproteins and several synthetic Hsp90 inhibitors are now in clinical trials [39]. Nevertheless, cumulative evidence tends to prove that Hsp90-directed therapy also induces pro-

cancer effects. For example, Hsp90 inhibition promotes prostate cancer growth through Src kinase activation [40] and favors breast cancer bone metastases formation [41]. It is generally estimated that over sixty percent of all cancers are glycolytic. This study showing that an endogenous glycolysis metabolite interferes with Hsp90 activity even more crucially raises significant concerns about the use of Hsp90 inhibitors as cancer treatment. The above-mentioned tumor-promoting effects related to Hsp90 inhibition could be potentially recapitulated under MG-mediated carbonyl stress condition in cancer cells. Consistent with this hypothesis and our data, LATS1 signalization in the Hippo pathway is rendered ineffective in ovarian cancer xenograft tumors from mice treated with an Hsp90 inhibitor [15].

MG is a potent cytotoxic compound and was first viewed as a potential therapeutic agent in cancer [42]. However, the recent identification of MG-modified proteins with pro-tumorigenic potential indicated that MG could also support tumor progression. Three independent groups have shown that Hsp27 heath shock protein is switched from a pro-apoptotic to an anti-apoptotic factor upon MG glycation and facilitates cancer cell evasion from caspase dependent cell apoptosis [10, 11, 12]. These data and ours point to an important regulatory role of MG stress on Hsps which have been particularly shown to be overexpressed in a wide range of tumors and are associated with a poor prognosis and resistance to therapy[43].

Glo1 appears to be a dual mediator for growth regulation in cancer as it has been described both as an oncogene and a tumor suppressor. On one hand, the search for copy number changes on a large set of cancer cell lines revealed that Glo1 is amplified in many types of human cancer with breast tumors (22%) and sarcomas (17%) showing the highest rates [44]. Most of the recent studies aimed at the inhibition of Glo1 to induce a toxic MG accumulation effectively showed a decreased tumor growth. These studies generally depicted Glo1 as an amplified and/or overexpressed oncogene and as a bad prognosis marker in different types of malignant tumors [45, 46, 47, 48, 49]. On the other hand, a study aimed at functionally identifying tumor suppressor genes in liver cancer identified and validated Glo1 as a tumor suppressor gene which knockdown using shRNAs increased tumor growth in a mouse model[50]. Using stably depleted Glo1 xenografts *in vivo*, we have also demonstrated the pro-tumorigenic and pro-metastatic role of endogenous MG accumulation in breast cancer cells. These results are consistent with (a) enhanced nuclear YAP and increased Ki67-positive proliferating cells *in vivo*, (b) increased YAP oncogenic activity including the induction of growth factors expression such as CTGF and the initiation of EMT process observed *in vitro* and (c) the positive correlation between high MG-adducts detection and nuclear YAP in human primary mammary tumors thus supporting the clinical relevance of our findings.

Therefore, it can be expected that different cancer types, with different backgrounds and for instance different MG detoxification rates would react differently to MG stress. Remarkably, cell lines with Glo1 amplification[44] or high Glo1 expression[51] are reported to be much more sensitive to Glo1 inhibitors such as BBGC than those without. Thus suggesting that a high Glo1 activity, putatively associated with high MG production, is necessary for their survival. In our hands, Glo1 knockdown or inhibition using BBGC did not induce any significant cell apoptosis and hence conferred pro-

growth and pro-metastatic advantages to breast cancer cells. These apparently controversial results could be potentially ascribed to differences in the cell lines and animal models used. No doubt that the validation of Glo1 as a target for cancer therapy will need a better characterization of those breast tumors that are more likely to be sensitive.

Many chemotherapeutic drugs used to treat cancer have been shown to exert their biologic activity through induction of oxidative stress. However, compelling experimental and clinical evidence indicates that this latter is diverted by cancer cells to promote their growth and resistance to apoptosis. Such promoting effect of carbonyl stress in cancer is inferred for the first time from our data and certainly awaits more comprehensive studies before confirmation. In a non-tumoral context, MG dual effect has been shown recently for neurons where MG is favorable to neurons development and activity while high MG levels are toxic [52].

Elevated blood concentrations of MG have been reported in type 2 diabetic patients [53] and plasma MG-derived hydroimidazolone was higher in type 1 diabetics as compared with non diabetics [54]. Future studies will have to assess the potential use of circulating MG and/or specific MG adducts as cancer biomarkers. Recent studies indicated that cancer in diabetic patients presents with a higher incidence and a poorer prognosis than in non-diabetic persons [55, 56]. Our study hereby provides with a potential molecular mechanism for cancer-diabetes connection. A better understanding of MG pro-cancer effects could lead to the development of preventive and therapeutic strategies based on the scavenging of MG. Interestingly, both MG scavengers metformin and carnosine have been shown to exert anti-tumoral effects [57, 58] and metformin proved efficient to reduce systemic MG levels in diabetic patients [59]. DeRan and collaborators [20] reported that metformin, and its more potent analog phenformin, inhibited YAP activity through AMPK signaling. Metformin is better known as a mitochondrial complex I inhibitor and a potent AMPK inducer and it is somehow overlooked for its MG scavenging capacities. Accordingly, it is not excluded that metformin could have also exerted, at least in part, its inhibitory activity on YAP function through its MG scavenging properties. In support of this hypothesis, we have shown that high MG stress-tumor xenografts showed a significantly lower propensity to metastasize in animals supplemented with carnosine in their drinking water. The crucial role of glucose metabolism in aggressive tumors has logically directed cancer therapy research towards the use of anti-diabetic drugs as effective anti-cancer agents and metformin is actually tested in several anti-cancer clinical trials[60].

Studies using mass spectrometry and antibodies directed against MG specific AGEs are currently underway in our laboratory in order to identify other targets of MG that will hopefully contribute to bring to light the critical position of MG-mediated carbonyl stress in cancer.

MATERIALS AND METHODS

Cell culture and reagents. Human breast cancer cell lines MDA-MB-231 and MCF7 were obtained from the American Type Culture Collection (ATCC). Human breast cancer cell line MDA-MB-468 was kindly provided by Dr. C. Gilles (Laboratory of Tumor and Development Biology, University of Liège, Belgium). Cells were either cultured in high glucose DMEM (standard glucose concentration of 4.5g/L, Lonza) or in DMEM medium with a

glucose concentration of 1g/L (low glucose medium) both containing 10% fetal bovine serum (FBS, ThermoFisher Scientific) and 2mM L-glutamine (Lonza). One g/L glucose level is physiological and reflects the *in vivo* concentrations in human serum. Conversely, the routine culture media concentration of 4.5g/L (high glucose medium) corresponded to a diabetic condition. In our experimental model, sparse cells are defined as low glucose cultured cells seeded at low density (for example, for a 6-wells plate: MDA-MB-231, MCF7 and MDA-MB-468 were seeded at $2x10^5$ cells/well). Confluent cells were obtained by seeding the same number of cells as indicated above and cultured for 3 days until they reached confluence. During these 3 days, cells were treated where indicated with methylglyoxal (MG, cat#M0252, Sigma-Aldrich) at micromolar concentrations every day. We excluded the presence of significant formaldehyde contamination (<3%) in MG (lot: BCBF6939V) by NMR analysis. The natural anti-glycation dipeptide L-carnosine (C9625), the MG scavenger aminoguanidine (396494), the proteasome inhibitor MG132 (C2211) and the Hsp90 inhibitor 17-AAG (A8476) were obtained from Sigma-Aldrich. TGF-β was obtained from Roche. Human recombinant Hsp90α (rhHsp90) was obtained from Enzo Life Sciences. S-p-bromobenzylglutathione cyclopentyl diester (BBGC), a cell-permeable inhibitor of Glo1, was synthesized as previously described[61]. Anti-argpyrimidine antibody (mAb6B) specificity has been previously confirmed by competitive ELISA and it has been shown to not react with other MG-arginine adducts such as 5-hydro-5-methylimidazolone and tetrahydropyrimidine[62].

Clinical tumor samples. Human breast tumor tissues (n=87) were obtained from the Pathology Department of the University Hospital of Liège in agreement with ethical guidelines of the University of Liège (Belgium).

Immunohistochemistry (IHC). Formalin-fixed paraffin embedded sections were dewaxed and rehydrated. Sections were treated with 3% hydrogen peroxide in methanol for 30min to block endogenous peroxidase activity. Antigen retrieval was performed in 10mM sodium citrate buffer pH6 at 95°C for 40min. To block non-specific binding sites, tissues were incubated with 1.5% normal serum (Vector Laboratories) for 30min. Next, they were incubated with mouse anti-Argpyrimidine (mAb6B, 1:2000), rabbit anti-YAP (Santa Cruz, H125, 1:100), mouse anti-Ki67 (Dako, 1:100), mouse anti-Glo1 (BioMac, 1:100) and mouse anti-vimentin (Ventana, Roche, 1:4) antibodies overnight at 4°C followed by incubation with an anti-mouse or anti-rabbit biotinylated secondary antibody (Vector Laboratories) for 30min at room temperature (RT). Sections were then stained with avidin-biotin-peroxidase complex (Vectastain ABC Kit, Vector Laboratories) for 30min followed by staining with 3,3' diaminobenzidine tetrachloride (DAB). Slides were finally counterstained with hematoxylin, dehydrated and mounted with DPX (Sigma-Aldrich). Tissue sections incubated without primary antibody showed no detectable immunoreactivity.

Evaluation of immunohistochemical staining. The immunostaining was reviewed and scored by two examiners including an anatomopathologist (E.B). As we previously described [63], scoring of the staining was done according to the intensity of the staining (0, 1+, 2+, 3+) and the percentage of positive cancer cells within the tumor (0-25%, 25-50%, 50-75%, 75-100%). The results obtained with the 2 scales were multiplied together, yielding a single score with steps of 0, 1+, 2+, 3+,

4+, 6+ and 9+. For argpyrimidine staining, scores of 0 to 2+ were considered as low to intermediate staining (low/intermediate carbonyl stress) and scores from 3+ to 9+ were considered as high staining (high carbonyl stress). Expression status of YAP in tumor cells was assessed using the same scoring as described above according to YAP cellular compartment (nucleus and cytoplasmic). Ki67 immunostaining was evaluated as the percentage of nucleus positive cells present in experimental tumor tissue sections. Human vimentin detection was used to quantify (a) the total number of positive foci and (b) the number of cells per foci categorized as follows: <10 and ≥10 vimentin positive cells. Metastatic foci number and size were counted in one whole lung section per mice.

Immunofluorescence (IF) and evaluation of nuclear YAP staining. MDA-MB-231, MDA-MB-468 and MCF7 cells were plated on coverslips in 24-well plates. Sparse cells were seeded at $4x10^4$ cells/well. Confluent cells were obtained by seeding the same number of cells as indicated above and treated for 3 days with MG until they reached confluence. For YAP and/or TEAD1 staining, cells were fixed with 3% paraformaldehyde (PAF) for 20min and then permeabilized with 1% Triton X-100. After blocking (3% BSA for 30min), slides were incubated with rabbit anti-YAP (Santa Cruz, H125 or Cell Signaling, 4912, 1:100) and/or mouse anti-TEAD1/TEF1 (BD Biosciences, 1:100) antibodies diluted in 1% BSA overnight at 4°C. After washing with PBS, slides were incubated with anti-rabbit IgG AlexaFluor488 or anti-mouse IgG AlexaFluor633 conjugated secondary antibodies (Life Technologies, 1:1000) for 1h at RT. AlexaFluor568 Phalloidin (Invitrogen) was used to stain actin filaments. For E-cadherin and YAP co-staining, cells were fixed in cold methanol for 10min at -20°C. After rehydratation in PBS, slides were blocked in 3% BSA for 30min and stained with mouse E-cadherin antibody (BD Biosciences, 1:200) and/or YAP antibody (Santa Cruz, H125, 1:100) diluted in 1% BSA for 1h at RT. After a washing step, slides were incubated with anti-mouse IgG AlexaFluor488 and/or anti-rabbit IgG AlexaFluor546 (Invitrogen). Nuclei were stained using DAPI (EMD Chemicals). Coverslips were mounted on glass slides using Mowiol (Sigma-Aldrich) and observed using confocal microscope (Leica SP5). All microscope settings were kept the same for sparse and confluent cells imaging. To quantify the intensity of YAP nuclear staining, at least 5 pictures/condition (magnification 630x) were used. Using ImageJ software [64] the intensity of YAP staining that colocalized with DAPI staining was measured. A mean of YAP staining intensity per nucleus was obtained. All the data are presented as the mean ± SEM of three independent experiments.

Western Blot. Cells were extracted in SDS 1% buffer containing protease and phosphatase inhibitors (Roche). Tissues samples were extracted in RIPA buffer (150mM NaCl, 0.5% Na^+-deoxycholate, 1% Triton X-100, 0.1% SDS, 50mM Tris-HCl pH7.5 and protease/phosphatase inhibitors). After incubation under rotation at 4°C during 30 min, tissues lysates were centrifuged at 14000g for 15 min at 4°C. Protein concentrations were determined using the bicinchoninic acid assay (Pierce). Twenty or 30µg of proteins were separated by 7.5% to 12.5% SDS-PAGE and transferred to PVDF or nitrocellulose membranes. After blocking in TBS-Tween 0.1% containing 5% nonfat dried milk (Bio-Rad), membranes were incubated with primary antibodies overnight at 4°C. Antibodies are listed in Supplementary Table S3. Then, the membranes were exposed to appropriate secondary

antibody at RT for 1 hour. The immunoreactive bands were visualized using ECL Western Blotting substrate (Pierce). Immunoblots were quantified by densitometric analysis and normalized for β-actin using ImageJ software. A representative western blot of three independent biological replicates is shown.

siRNA transfection. YAP and Glo1 small interfering RNAs (siRNA) and siGl3 irrelevant used as control were synthesized by Eurogentec. Sequences are detailed in Supplementary Table S4. Calcium phosphate-mediated transfections were performed using 20nM of each siRNA.

RNA isolation and quantitative reverse transcription-PCR (qRT-PCR). RNA extraction was performed according to the manufacturer's protocol (NucleoSpin RNA, Macherey-Nagel). Reverse transcription was done using the Transcription First Strand cDNA Synthesis Kit (Roche). Hundred ng of cDNA were mixed with primers, probe (Universal ProbeLibrary System, Roche) and 2x FastStart Universal Probe Master Mix (Roche) or Fast Start SYBR Green Master Mix (Roche). Q-PCR were performed using the 7300 Real Time PCR System and the corresponding manufacturer's software (Applied Biosystems). Relative gene expression was normalized to 18S rRNA. Primers were synthesized by IDT and their sequences are detailed in Supplementary Table S5. Three technical replicates of each samples have been performed and data are presented as mean ± SEM or ± SD (as indicated in figure legends) of minimum 3 biological replicates.

Cellular MG quantification. MBo (Methyl diaminobenzene-BODIPY) was used to detect endogenous MG in different conditions. The cells were treated with 5µM MBo in complete medium as previously described [25] . After 1h, the cells were washed with PBS and incubated in low or high glucose medium for 6 (FACS) and 24h (confocal microscopy). Cells were either trypsinized and analyzed by flow cytometry (BD Biosciences FACSCanto), or fixed with PAF and prepared for confocal microscope visualization as described above.

Nuclear Magnetic Resonance (NMR) analysis. Five hundred microliters of conditioned culture media (24h) were supplemented with 100µl of deuterated phosphate buffer (pH7.4), 100µl of a 35mM solution of maleic acid and 10µl of TMSP. The solution was distributed into 5-mm tubes for NMR measurement. ^{1}H NMR spectra were acquired using a 1D NOESY sequence with presaturation. The Noesypresat experiment used a RD-90°-t1-90°-tm-90°-acquire sequence with a relaxation delay of 4sec, a mixing time tm of 10msec and a fixed t1 delay of 4µsec. Water suppression pulse was placed during the relaxation delay (RD). The number of transient is 32 (64K data points) and a number of 4 dummy scans is chosen. Acquisition time is fixed to 3.2769001sec. Lactate dosages were achieved by integrations of the lactate signal at 1.34ppm using maleic acid as internal standard. Deuterium oxide (99.96% D) and trimethylsilyl-3-propionic acid-*d*4 (TMSP) were purchased from Eurisotop (St-Aubin, France), phosphate buffer powder 0.1M and maleic acid were purchased from Sigma-Aldrich. The NMR spectra were recorded at 298K on a Bruker Avance spectrometer operating at 500.13MHz for proton and equipped with a TCI cryoprobe. Deuterated water was used as the internal lock. The data have been processed with Bruker TOSPIN 3.0 software with standard parameter set. Phase and baseline correction were performed manually over the entire range of the spectra and the δ scale was

calibrated to 0ppm using the internal standard TMSP.

Methylglyoxal measurement in cell culture medium. MG level was determined in 48h-conditioned culture media of breast cancer cells (85-90% confluence). The culture media were collected, centrifugated at 1000rpm for 5min and immediately stored at -20°C. Attached cells were trypsinized and counted to normalize the MG dosage. Samples preparation and LC-MS/MS analysis were performed as previously described [65] with some adaptations. Briefly, 20µl aliquot of culture medium was treated with ice-cold 20% TCA/0.9% saline (Sigma-Aldrich) and 5µl of 5-MQX (Sigma-Aldrich) internal standard were added. Samples were incubated on ice for 10 min and after centrifugation at 10,000g for 10min at 4°C, 35µl of supernatant were collected and used for the analysis. Then, 5µl of sodium azide (Sigma-Aldrich) were added to the 35µl of samples and mixed. The derivatization step was performed by adding 1,2-diaminobenzene (Acros Organics, ThermoFisher Scientific) to the samples and incubating for 4h in the dark at RT. A calibration curve with 2-MQX was prepared in the range of 0-16pmoles with 2pmoles of internal standard. HPLC analyses of 2-MQX and 5-MQX were performed on an Acquity UPLC I-Class system (Waters, Milford, USA) with a Xevo TQ-S mass spectrometry detector (Waters, Milford, USA). The column was a BEH C18, 1.7µm particle size, 2.1x50mm (Waters, Milford, USA) at 40°C. The mobile phases were 0.1% formic acid (v/v) in water as solvent A and 0.1% formic acid (v/v) in acetonitrile as solvent B. The initial conditions, 5% of solvent B, were maintained for 1min followed by a linear gradient of 4min to 100% of solvent B, the column was then washed for 1min with 100% solvent B and then re-equilibrated for 4min with 5% of solvent B. The injection volume was 9µl. 2-MQX and 5-MQX were detected by electro-spray positive-ion selected reaction monitoring (SRM). Five MRM mass transitions were recorded for analyte and internal standard. MRM mass transition and collision energy (in brackets) were as follows: 2-MQX – 145.20 > 65.20 (22.0), 145.20 > 77.10 (22.0), 145.20 > 92.20 (20.0), 145.20 > 104.30 (20.0), 145.20 > 118.20 (20.0) and 5-MQX - 145.20 > 65.03 (30.0), 145.20 > 91.20 (22.0), 145.20 > 102.50 (25.0) (not used), 145.20 > 104.20 (12.0) (not used), 145.20 > 118.20 (20.0), 145.20 > 128.10 (22.0). Quantification was based on transition 145.20 > 118.20 for 2-MQX and 145.20 > 91.20 for the internal standard. For secure identification of 2-MQX, ion ratios were checked to be within 10% of that of 2-MQX standard. Limits of detection (LOD) and of quantification (LOQ) were established as previously reported [66]. LOD and LOQ were respectively 0.589 and 1.262pmoles.

shRNA transfection. Lentiviral vectors (rLV) were generated with the help of the GIGA Viral Vectors platform (University of Liège). Briefly, Lenti-X 293T cells (Clontech) were co-transfected with a pSPAX2 (a gift of Dr D. Trono, Addgene plasmid #12260) and a VSV-G encoding vector [67] along with a shRNA transfer lentiviral plasmid (Glo1 shRNAs plasmids : Sigma-Aldrich, TRCN0000118627 (#1) and TRCN0000118631 (#2) or non-target (NT, anti-eGFP) shRNA plasmid (Sigma-Aldrich, SHC005)). Forty-eight, 72 and 96h post transfection, viral supernatants were collected, filtrated and concentrated 100x by ultracentrifugation. The lentiviral vectors were then titrated with qPCR Lentivirus Titration Kit (ABM). MDA-MB-231 cells were stably transduced with shGlo1#1, shGlo1#2 and shNT and selected with puromycin (0.5µg/ml, Sigma-Aldrich).

Glo1 activity assay. The activity of Glo1 was performed as previously described [9]. Briefly, proteins were extracted with RIPA buffer, quantified and mixed with a pre-incubated (15min at 25°C) equimolar (1mM) mixture of MG and GSH (Sigma-Aldrich) in 50mM sodium phosphate buffer, pH6.8. S-D-lactoylglutathione formation was followed spectrophotometrically by the increase of absorbance at 240nm at 25°C. Glo1 activity data are expressed as arbitrary units (A.U.) of enzyme per mg of proteins. Three technical replicates of each samples have been performed and data are presented as mean ± SEM of 5 biological replicates.

Chromatin Immunoprecipitation (ChIP). Formaldehyde was added directly to cell culture media to a final concentration of 1% at RT. Ten minutes later, glycine was added to a final concentration of 0.125M for 5min at RT. The cells were then washed with ice-cold PBS, scraped, and collected in cold PBS followed by extraction in cell lysis buffer (20mM Tris/HCl pH8, 85mM KCl, 0.5% NP-40, protease inhibitor). Nuclei were pelleted by centrifugation at 2600g for 5min at 4°C, suspended in nuclei lysis buffer (50mM Tris/HCl pH8, 10mM EDTA, 1% SDS, protease inhibitor) and sonicated with Bioruptor (Diagenode). Samples were centrifuged at 14000g for 15min at 4°C. Supernatant were diluted in ChIP dilution buffer (0.01% SDS, 1.1% Triton X-100, 1.1mM EDTA, 20mM Tris/HCl pH8, 167mM NaCl, protease inhibitor) to obtain a SDS final concentration of 0.2% and incubated with anti-YAP antibody (Santa Cruz, H125) or rabbit control IgG (Zymed Laboratories) overnight at 4°C. Protein G magnetic beads were blocked with BSA 0.1mg/ml and salmon sperm DNA 0.1mg/ml overnight at 4°C and then washed with ChIP dilution buffer. Beads were added to the lysate and incubated under rotation at 4°C. Four hours later, the beads were washed with low (0.1% SDS, 1% Triton X-100, 2mM EDTA, 20mM Tris/HCl pH8, 150mM NaCl), high (0.1% SDS, 1% Triton X-100, 2mM EDTA, 20mM Tris/HCl pH8, 450mM NaCl) salt wash buffer and LiCl wash buffer (0.5M LiCl, 1% NP-40, 1% deoxycholate, 20mM Tris/HCl pH8). Next, the beads were incubated in elution buffer (50mM $NaHCO_3$, 1% SDS) during 20min under agitation. NaCl was added to a final concentration of 0.2M and samples were heated at 67°C overnight to reverse crosslinking. DNA was purified by phenol/chloroform extraction. The ChIP-enriched DNA was subjected to qPCR using connective tissue growth factor (CTGF) promoter TEAD binding site-specific primers sense, 5′-ATATGAATCAGGAGTGGTGCG-3′ and antisense, 5′-CAACTCACACCGGATTGATCC-3′[31]. Primers (sens, 5'-AGACAAACCAAATCCAATCCACA-3', antisens, 5'-CTGTGTTGGGTAGGTAGGGG-3') targeting a more distal region on CTGF promoter were used as negative control. All qPCR data are normalized to Input and IgG controls and are presented as mean ± SEM of 3 biological replicates.

Wound closure migration assay. MDA-MB-468 cells were transfected with 2 siRNAs against YAP and were grown to high density with MG 300µM treatment. Multiple uniform streaks were made on the monolayer culture with 10µl pipette tips. The cells were then washed to remove detached cells. Immediately after wounding and 16h later, each wound was photographed under a phase-contrast microscope. The distance between the wound edges was measured. Mean wound width was determined and a wound closure percentage was calculated for each condition. Sixteen wounds were measured per condition and the

experiment was repeated twice. Data are expressed as the mean ± SEM.

Cell growth assay. Equal numbers of cells were seeded, transfected with 2 siRNAs targeting YAP and treated with MG until confluence. Cell number was indirectly assessed using Hoechst incorporation at the indicated time period and cell growth was expressed based on cellular DNA content (µg/ml). Three technical replicates of each samples have been performed and data are presented as mean ± SEM of 4 biological replicates.

Mass spectrometry – MG adducts localization. As previously described [6, 68, 69], 5µg of human recombinant Hsp90α (rhHsp90, Enzo Life Sciences, ADI-SPP-76D) were minimally modified with MG 500µM in PBS 100mM pH7.4 at 37°C during 24h. Proteins were reduced and alkylated, placed in 50mM ammonium bicarbonate (buffer exchange was performed using an Amicon-3k from Millipore) and then digested using a protease mixture. Peptides (15pmoles injected) were separated by reverse phase chromatography (UPLC® Waters nanoAcquity) in one dimension on a BEH C18 analytical column (25cm length, 75µM ID) with an increasing ratio of acetonitrile/water (5%-40% in 85min) at a 250nL/min flow rate. The chromatography system was coupled to a hybrid Quadrupole-Orbitrap Mass Spectrometer (Q Exactive, Thermo Fisher Scientific), operated in data-dependent acquisition mode. Survey scans were acquired at 70,000 resolving power (full width at half maximum, FWHM). Mass range was set from 400 to 1750m/z in MS mode, and 1E6 ions were accumulated for the survey scans. After each survey scan, the 10 most intense ions were selected to do MS/MS experiments. Higher energy Collision Dissociation (HCD) fragmentation was performed at NCE 25 after isolation of ions within 2amu isolation windows. A dynamic exclusion of 10sec was enabled. Database searches were performed using Proteome Discoverer 1.4 (Thermo Scientific) in a Swissprot database (2014-05, 20339 human sequences) restricted to human taxonomy. MS and MS/MS tolerances were respectively set at 5ppm and 20mmu. Argpyrimidine (+ 80.026Da, R), hydroimidazolone (+ 54.010Da, R), dihydroxyimidazolidine (+ 72.021Da, R) and carboxyethyllysine (+ 72.021Da, K) were set as variable modifications while carbamidomethylation (+57.021Da, C) was set as fixed modification.

Mass spectrometry – MG adducts detection on endogenous Hsp90. Based on the experiments conducted using rhHsp90, a targeted method was set up to reach enough sensitivity to detect endogenous Hsp90 adducts in MDA-MB-231 MG-treated cells. Modified rhHsp90 as described above was first digested using Lys-C protease (in Tris-HCl 25mM, pH8.5, 1mM EDTA overnight at 37°C; first step at 1/40 sample/protease and then addition of 1/50 sample/protease in 50% acetonitrile for 4h). Resulting peptides were separated by reverse phase chromatography (UPLC® Waters M Class) in one dimension on a HSS T3 C18 analytical column (25cm length, 75µM ID) with an increasing ratio of acetonitrile/water (2%-40% in 32min) at a 600nL/min flow rate. The system was coupled to the mass spectrometer described above. A shortlist of 54 peptides were manually selected and used in further targeted experiments. Two “Parallel Reaction Monitoring” or PRM (i.e. targeted full MS/MS) methods were set up in order to obtain at least 12 data points in chromatographic peaks and they were run consecutively for each sample. Data were then analyzed using Skyline 3.1 and were manually validated. For these experiments, protein extract from MDA-

MB-231 treated or not with MG 300µM during 6h were immunoprecipitated with argpyrimidine antibody. These samples were prepared in a slightly different way than rhHsp90: whole samples were reduced, alkylated and then purified using the 2D Clean-up kit (GE Healthcare). The samples were then resuspended in the proteolysis buffer and the digestion was performed assuming an amount of 5µg to be digested. The following steps were the same as for the recombinant protein.

Immunoprecipitation and co-immunoprecipitation. MDA-MB-231 were treated with MG 300µM during 6h. Then, argpyrimidine (mAb6B) and Hsp90 (anti-Hsp90 antibody, ab13492, Abcam) and mouse IgG (Zymed Laboratories) immunoprecipitations were performed using the "Crosslink IP" kit (#26147, ThermoFischer Sicentific) according to manufacturer instructions. For LATS1/Hsp90 co-immunoprecipitation, MDA-MB-231 were treated with MG 300µM during 24h. Proteins were extracted in Tris-HCl pH8 20mM, NaCl 137mM, NP-40 1%, EDTA 2mM and protease inhibitors. After incubation under rotation at 4°C during 30 min, cell lysates were centrifuged at 14000g for 15 min at 4°C. Five hundred µg of proteins were incubated with 2µg of LATS1 (Bethyl) or rabbit IgG (Zymed Laboratories) antibodies overnight and then 2h with Protein G magnetic beads at 4°C. After several washes, proteins were eluted and analyzed by western blot. A representative western blot of three independent biological replicates is shown.

Plasmids. pcDNA3.1-LATS-3xFlag and pcDNA3.1-3xFlag (empty vector) were kindly provided by Prof. Xiaolong Yang, Department of Pathology and Molecular Medicine, Queen's University, Kingston, Ontario K7L 3N6, Canada[70]. Cell transfection was performed using Lipofectamine (ThermoFisher Scientific) according to manufacturer's instructions.

Hsp90 ATPase activity. Hsp90 ATPase activity assay was performed as previously described[71] using Transcreener ADP^2 FI assay (BellBrook Labs). Briefly, 1µM of rhHsp90 was preincubated with MG 500µM ± carnosine 10mM or 17-AAG 1µM during 24h at 37°C in Hepes pH7.4 50mM, KCl 20mM, EGTA 2mM, $MgCl_2$ 4mM and Brij-35 0.01%. ATP was added at a final concentration of 100µM and incubated 3h at 37°C. The reaction was stopped and ADP was detected by adding ADP^2 Antibody-IRDye QC-1 at a final concentration of 93.7µg/ml and ADP Alexa594 Tracer at a final concentration of 4nM. This mix was incubated 1h at RT in a 96 well black half area plates (Greiner, #675076). Readings were performed on a Filter Max F5 plate reader (Molecular Devices). Three technical replicates of each samples have been performed and data are presented as mean ± SEM of 5 biological replicates.

***In vivo* mice experiments.** All animal experimental procedures were performed according to the Federation of European Laboratory Animal Sciences Associations (FELASA) and were reviewed and approved by the Institutional Animal Care and Ethics Committee of the University of Liege (Belgium). Animals were housed in the GIGA-accredited animal facility of the University of Liege. For human xenografts, MDA-MB-231 shNT, shGlo1#1 and shGlo1#2 cells were suspended in 10% FBS supplemented medium and Matrigel (BD Biosciences) (50% v/v). Cell suspensions (10^6cells/100µl) were inoculated subcutaneously in one flank of five week old female NOD-SCID mice (n=15 per condition). After 4 weeks, tumors were surgically removed, weighted and measured with a caliper. Tumor volume (V) was assessed using the

formula $V = \frac{4}{3} \times \pi \times \frac{H}{2} \times \frac{L}{2} \times \frac{W}{2}$ where H, L and W denote height, length and width, respectively. One piece was collected and embedded in paraffin for IHC and the rest was frozen in liquid nitrogen for total protein extraction. The animals were sutured, allowed to recover and further monitored for six weeks for metastases development. Due to animal ethics protocol, we had to sacrifice 2 mice in both shGlo1#1 and shGlo1#2 groups before the end of the experiment. A parallel experiment was conducted on shGlo1#1 mice (n=10) where they received carnosine (10mM) in drinking water refreshed every 3 days from the day of primary tumor removal until the end of the experiment (for 6 weeks). Drinking volume was monitored and found to be similar between treated and non-treated mice. The mice were sacrificed and lung metastases were collected and processed as described for the primary tumors.

Chicken chorioallantoic membrane (CAM) tumor assay. MDA-MB-231 shGlo1 were transfected with 2 different siRNAs directed against YAP (siYAP#1 and #2). On chicken embryonic day 11, 100µl of a suspension of $2x10^6$ of MDA-MB-231 cells in culture medium mixed (1:1) with Matrigel (BD Biosciences) were deposited in the center of a plastic ring on the chicken embryo chorioallantoic membrane (n=5). Tumors were harvested on embryonic day 18, and were fixed in 4% paraformaldehyde solution (30 minutes) for IHC analysis. Tumor volume was measured using a caliper and assessed using the formula described above. Parallel cultures of transfected cells were used to assess by western blot that YAP silencing was maintained for the entire duration of the CAM assay experiment.

Correlation analysis using YAP activity signature. The signature of YAP modulated genes was described in previous studies [18, 26, 27, 28] and their mRNA levels were correlated to Glo1 gene expression using publicly available GDS4057 dataset of 103 breast cancer patients [29].

Statistical analysis. Both technical and biological replicates were performed where indicated in figure legends. Technical replicates are considered as taking one sample and analysing it several times in the same experiment. Biological replicates represent the analysis of samples from independent experiments. All results were reported as means with standard deviation (SD) or Standard Error Mean (SEM) as indicated in figure legends. Two group comparisons were performed using unpaired Student's t-test with or without Welsch's correction according to homoscedasticity. When an experiment required comparisons between more than 2 groups, statistical analysis was performed using one-way or two-way ANOVA depending on the number of grouping factors. Dunnet's test was applied for simple comparisons while Student-Newman-Keul's (one-way ANOVA) or Bonferroni's (two-way ANOVA) tests were used for multiple comparisons. In the case of discrete variables (scores) or non-normally distributed variables the comparison between groups was performed by Mann-Whitney's U test or a Kruskal-Wallis ANOVA followed by a Dunn's test according to the number of groups. Correlation between scores was assessed by the Spearman's rank correlation coefficient (R_{sp}) and correlation between continuous variables was assessed by a Pearson correlation coefficient (R_p). Outliers were detected using whisker box plots. In all cases, a bilateral $p<0.05$ was considered as statistically significant with a 95% confidence interval. All experiments

were performed as several independent biological replicates.

ACKNOWLEDGMENTS

MJN, FD and BCo are Télévie Fellows, BCh, ABl and AT are Télévie Post-Doctoral Fellows, PDT and ABe are Senior Research Associates, all from the National Fund for Scientific Research (FNRS, Belgium). This work was also supported by the Centre Anti-Cancéreux, University of Liège, Belgium. The authors are thankful to Mrs. N. Maloujahmoum and Mr. V. Hennequière for expert technical assistance. We acknowledge the technology platforms of the GIGA at University of Liège: proteomic, animal, imaging and flow cytometry, viral vector and immunohistology facilities. We thank the Tissue Bank of the University of Liège/University Hospital of Liège for providing human tumor samples.

REFERENCES

1. Ward PS, Thompson CB. Metabolic reprogramming: a cancer hallmark even warburg did not anticipate. *Cancer cell* **21**, 297-308 (2012).

2. Richard JP. Mechanism for the formation of methylglyoxal from triosephosphates. *Biochemical Society transactions* **21**, 549-553 (1993).

3. Turk Z. Glycotoxines, carbonyl stress and relevance to diabetes and its complications. *Physiological research / Academia Scientiarum Bohemoslovaca* **59**, 147-156 (2010).

4. Thornalley PJ. Pharmacology of methylglyoxal: formation, modification of proteins and nucleic acids, and enzymatic detoxification--a role in pathogenesis and antiproliferative chemotherapy. *General pharmacology* **27**, 565-573 (1996).

5. Thornalley PJ. Dicarbonyl intermediates in the maillard reaction. *Annals of the New York Academy of Sciences* **1043**, 111-117 (2005).

6. Dobler D, Ahmed N, Song L, Eboigbodin KE, Thornalley PJ. Increased dicarbonyl metabolism in endothelial cells in hyperglycemia induces anoikis and impairs angiogenesis by RGD and GFOGER motif modification. *Diabetes* **55**, 1961-1969 (2006).

7. Bierhaus A*, et al.* Methylglyoxal modification of Nav1.8 facilitates nociceptive neuron firing and causes hyperalgesia in diabetic neuropathy. *Nature medicine* **18**, 926-933 (2012).

8. van Heijst JW, Niessen HW, Hoekman K, Schalkwijk CG. Advanced glycation end products in human cancer tissues: detection of Nepsilon-(carboxymethyl)lysine and argpyrimidine. *Annals of the New York Academy of Sciences* **1043**, 725-733 (2005).

9. Chiavarina B*, et al.* Triple negative tumors accumulate significantly less methylglyoxal specific adducts than other human breast cancer subtypes. *Oncotarget* **5**, 5472-5482 (2014).

10. van Heijst JW, Niessen HW, Musters RJ, van Hinsbergh VW, Hoekman K, Schalkwijk CG. Argpyrimidine-modified Heat shock protein 27 in human non-small cell lung cancer: a possible mechanism for evasion of apoptosis. *Cancer letters* **241**, 309-319 (2006).

11. Oya-Ito T*, et al.* Heat-shock protein 27 (Hsp27) as a target of methylglyoxal in gastrointestinal cancer. *Biochimica et biophysica acta* **1812**, 769-781 (2011).

12. Sakamoto H, Mashima T, Yamamoto K, Tsuruo T. Modulation of heat-shock protein 27 (Hsp27) anti-apoptotic activity by methylglyoxal modification. *The Journal of biological chemistry* **277**, 45770-45775 (2002).

13. Bento CF, Marques F, Fernandes R, Pereira P. Methylglyoxal alters the function and stability of critical components of the protein quality control. *PloS one* **5**, e13007 (2010).

14. Trepel J, Mollapour M, Giaccone G, Neckers L. Targeting the dynamic HSP90 complex in cancer. *Nature reviews Cancer* **10**, 537-549 (2010).

15. Huntoon CJ*, et al.* Heat shock protein 90 inhibition depletes LATS1 and LATS2, two regulators of the mammalian hippo tumor suppressor pathway. *Cancer research* **70**, 8642-8650 (2010).

16. Pan D. The hippo signaling pathway in development and cancer. *Developmental cell* **19**, 491-505 (2010).

17. Harvey KF, Zhang X, Thomas DM. The Hippo pathway and human cancer. *Nature reviews Cancer* **13**, 246-257 (2013).

18. Zhao B*, et al.* TEAD mediates YAP-dependent gene induction and growth control. *Genes & development* **22**, 1962-1971 (2008).

19. Moroishi T, Hansen CG, Guan KL. The emerging roles of YAP and TAZ in cancer. *Nature reviews Cancer* **15**, 73-79 (2015).

20. DeRan M*, et al.* Energy stress regulates hippo-YAP signaling involving AMPK-mediated regulation of angiomotin-like 1 protein. *Cell reports* **9**, 495-503 (2014).

21. Enzo E*, et al.* Aerobic glycolysis tunes YAP/TAZ transcriptional activity. *The EMBO journal*, (2015).

22. Mulvihill MM, *et al.* Metabolic profiling reveals PAFAH1B3 as a critical driver of breast cancer pathogenicity. *Chemistry & biology* **21**, 831-840 (2014).

23. Hipkiss AR, Chana H. Carnosine protects proteins against methylglyoxal-mediated modifications. *Biochemical and biophysical research communications* **248**, 28-32 (1998).

24. Tikellis C, *et al.* Dicarbonyl stress in the absence of hyperglycemia increases endothelial inflammation and atherogenesis similar to that observed in diabetes. *Diabetes* **63**, 3915-3925 (2014).

25. Wang T, Douglass EF, Jr., Fitzgerald KJ, Spiegel DA. A "turn-on" fluorescent sensor for methylglyoxal. *Journal of the American Chemical Society* **135**, 12429-12433 (2013).

26. Cordenonsi M, *et al.* The Hippo Transducer TAZ Confers Cancer Stem Cell-Related Traits on Breast Cancer Cells. *Cell* **147**, 759-772 (2011).

27. Dupont S, *et al.* Role of YAP/TAZ in mechanotransduction. *Nature* **474**, 179-183 (2011).

28. Zhang H, *et al.* TEAD transcription factors mediate the function of TAZ in cell growth and epithelial-mesenchymal transition. *The Journal of biological chemistry* **284**, 13355-13362 (2009).

29. Iwamoto T, *et al.* Gene pathways associated with prognosis and chemotherapy sensitivity in molecular subtypes of breast cancer. *Journal of the National Cancer Institute* **103**, 264-272 (2011).

30. Hiemer SE, Szymaniak AD, Varelas X. The transcriptional regulators TAZ and YAP direct transforming growth factor beta-induced tumorigenic phenotypes in breast cancer cells. *The Journal of biological chemistry* **289**, 13461-13474 (2014).

31. Fujii M, *et al.* TGF-beta synergizes with defects in the Hippo pathway to stimulate human malignant mesothelioma growth. *The Journal of experimental medicine* **209**, 479-494 (2012).

32. Lei QY, *et al.* TAZ promotes cell proliferation and epithelial-mesenchymal transition and is inhibited by the hippo pathway. *Molecular and cellular biology* **28**, 2426-2436 (2008).

33. Overholtzer M, *et al.* Transforming properties of YAP, a candidate oncogene on the chromosome 11q22 amplicon. *Proceedings of the National Academy of Sciences of the United States of America* **103**, 12405-12410 (2006).

34. Chan LH, Wang W, Yeung W, Deng Y, Yuan P, Mak KK. Hedgehog signaling induces osteosarcoma development through Yap1 and H19 overexpression. *Oncogene* **33**, 4857-4866 (2014).

35. Takahashi Y, *et al.* Down-regulation of LATS1 and LATS2 mRNA expression by promoter hypermethylation and its association with biologically aggressive phenotype in human breast cancers. *Clinical cancer research : an official journal of the American Association for Cancer Research* **11**, 1380-1385 (2005).

36. Mo JS, *et al.* Cellular energy stress induces AMPK-mediated regulation of YAP and the Hippo pathway. *Nature cell biology* **17**, 500-510 (2015).

37. Wang W, *et al.* AMPK modulates Hippo pathway activity to regulate energy homeostasis. *Nature cell biology* **17**, 490-499 (2015).

38. Pate KT, *et al.* Wnt signaling directs a metabolic program of glycolysis and angiogenesis in colon cancer. *The EMBO journal* **33**, 1454-1473 (2014).

39. Neckers L, Workman P. Hsp90 molecular chaperone inhibitors: are we there yet? *Clinical cancer research : an official journal of the American Association for Cancer Research* **18**, 64-76 (2012).

40. Yano A, *et al.* Inhibition of Hsp90 activates osteoclast c-Src signaling and promotes growth of prostate carcinoma cells in bone. *Proceedings of the National Academy of Sciences of the United States of America* **105**, 15541-15546 (2008).

41. Price JT, *et al.* The heat shock protein 90 inhibitor, 17-allylamino-17-demethoxygeldanamycin, enhances osteoclast formation and potentiates bone metastasis of a human breast cancer cell line. *Cancer research* **65**, 4929-4938 (2005).

42. Kang Y, Edwards LG, Thornalley PJ. Effect of methylglyoxal on human leukaemia 60 cell growth: modification of DNA G1 growth arrest and induction of apoptosis. *Leukemia research* **20**, 397-405 (1996).

43. Calderwood SK, Khaleque MA, Sawyer DB, Ciocca DR. Heat shock proteins in cancer: chaperones of tumorigenesis. *Trends in biochemical sciences* **31**, 164-172 (2006).

44. Santarius T, *et al.* GLO1-A novel amplified gene in human cancer. *Genes, chromosomes & cancer* **49**, 711-725 (2010).

45. Zhang S, *et al.* Glo1 genetic amplification as a potential therapeutic target in hepatocellular carcinoma. *International journal of clinical and experimental pathology* **7**, 2079-2090 (2014).

46. Cheng WL, *et al.* Glyoxalase-I is a novel prognosis factor associated with gastric cancer progression. *PloS one* **7**, e34352 (2012).

47. Hosoda F, *et al.* Integrated genomic and functional analyses reveal glyoxalase I as a novel metabolic oncogene in human gastric cancer. *Oncogene* **34**, 1196-1206 (2015).

48. Antognelli C, Mezzasoma L, Fettucciari K, Mearini E, Talesa VN. Role of glyoxalase I in the proliferation and apoptosis control of human LNCaP and PC3 prostate cancer cells. *The Prostate* **73**, 121-132 (2013).

49. Fonseca-Sanchez MA*, et al.* Breast cancer proteomics reveals a positive correlation between glyoxalase 1 expression and high tumor grade. *International journal of oncology* **41**, 670-680 (2012).

50. Zender L*, et al.* An oncogenomics-based in vivo RNAi screen identifies tumor suppressors in liver cancer. *Cell* **135**, 852-864 (2008).

51. Sakamoto H, Mashima T, Sato S, Hashimoto Y, Yamori T, Tsuruo T. Selective activation of apoptosis program by S-p-bromobenzylglutathione cyclopentyl diester in glyoxalase I-overexpressing human lung cancer cells. *Clinical cancer research : an official journal of the American Association for Cancer Research* **7**, 2513-2518 (2001).

52. Radu BM, Dumitrescu DI, Mustaciosu CC, Radu M. Dual effect of methylglyoxal on the intracellular Ca2+ signaling and neurite outgrowth in mouse sensory neurons. *Cellular and molecular neurobiology* **32**, 1047-1057 (2012).

53. Nakayama K*, et al.* Plasma alpha-oxoaldehyde levels in diabetic and nondiabetic chronic kidney disease patients. *American journal of nephrology* **28**, 871-878 (2008).

54. Han Y*, et al.* Plasma advanced glycation endproduct, methylglyoxal-derived hydroimidazolone is elevated in young, complication-free patients with Type 1 diabetes. *Clinical biochemistry* **42**, 562-569 (2009).

55. Ryu TY, Park J, Scherer PE. Hyperglycemia as a risk factor for cancer progression. *Diabetes & metabolism journal* **38**, 330-336 (2014).

56. Xu CX, Zhu HH, Zhu YM. Diabetes and cancer: Associations, mechanisms, and implications for medical practice. *World journal of diabetes* **5**, 372-380 (2014).

57. Shen Y*, et al.* Carnosine inhibits the proliferation of human gastric cancer SGC-7901 cells through both of the mitochondrial respiration and glycolysis pathways. *PloS one* **9**, e104632 (2014).

58. Giovannucci E*, et al.* Diabetes and cancer: a consensus report. *Diabetes care* **33**, 1674-1685 (2010).

59. Beisswenger PJ, Howell SK, Touchette AD, Lal S, Szwergold BS. Metformin reduces systemic methylglyoxal levels in type 2 diabetes. *Diabetes* **48**, 198-202 (1999).

60. Quinn BJ, Kitagawa H, Memmott RM, Gills JJ, Dennis PA. Repositioning metformin for cancer prevention and treatment. *Trends in endocrinology and metabolism: TEM* **24**, 469-480 (2013).

61. Thornalley PJ*, et al.* Antitumour activity of S-p-bromobenzylglutathione cyclopentyl diester in vitro and in vivo. Inhibition of glyoxalase I and induction of apoptosis. *Biochemical pharmacology* **51**, 1365-1372 (1996).

62. Oya T*, et al.* Methylglyoxal modification of protein. Chemical and immunochemical characterization of methylglyoxal-arginine adducts. *The Journal of biological chemistry* **274**, 18492-18502 (1999).

63. Waltregny D*, et al.* Prognostic value of bone sialoprotein expression in clinically localized human prostate cancer. *Journal of the National Cancer Institute* **90**, 1000-1008 (1998).

64. Schneider CA, Rasband WS, Eliceiri KW. NIH Image to ImageJ: 25 years of image analysis. *Nature methods* **9**, 671-675 (2012).

65. Rabbani N, Thornalley PJ. Measurement of methylglyoxal by stable isotopic dilution analysis LC-MS/MS with corroborative prediction in physiological samples. *Nature protocols* **9**, 1969-1979 (2014).

66. Kruve A*, et al.* Tutorial review on validation of liquid chromatography-mass spectrometry methods: Part I. *Analytica chimica acta* **870**, 29-44 (2015).

67. Emi N, Friedmann T, Yee JK. Pseudotype formation of murine leukemia virus with the G protein of vesicular stomatitis virus. *Journal of virology* **65**, 1202-1207 (1991).

68. Ahmed N, Thornalley PJ. Peptide mapping of human serum albumin modified minimally by methylglyoxal in vitro and in vivo. *Annals of the New York Academy of Sciences* **1043**, 260-266 (2005).

69. Lund T*, et al.* Fibrin(ogen) may be an important target for methylglyoxal-derived AGE modification in elastic arteries of humans. *Diabetes & vascular disease research : official journal of the International Society of Diabetes and Vascular Disease* **8**, 284-294 (2011).

70. Hao Y, Chun A, Cheung K, Rashidi B, Yang X. Tumor suppressor LATS1 is a negative regulator of oncogene YAP. *The Journal of biological chemistry* **283**, 5496-5509 (2008).

71. Rowlands M*, et al.* Detection of the ATPase activity of the molecular chaperones Hsp90 and Hsp72 using the TranscreenerTM ADP assay kit. *Journal of biomolecular screening* **15**, 279-286 (2010).

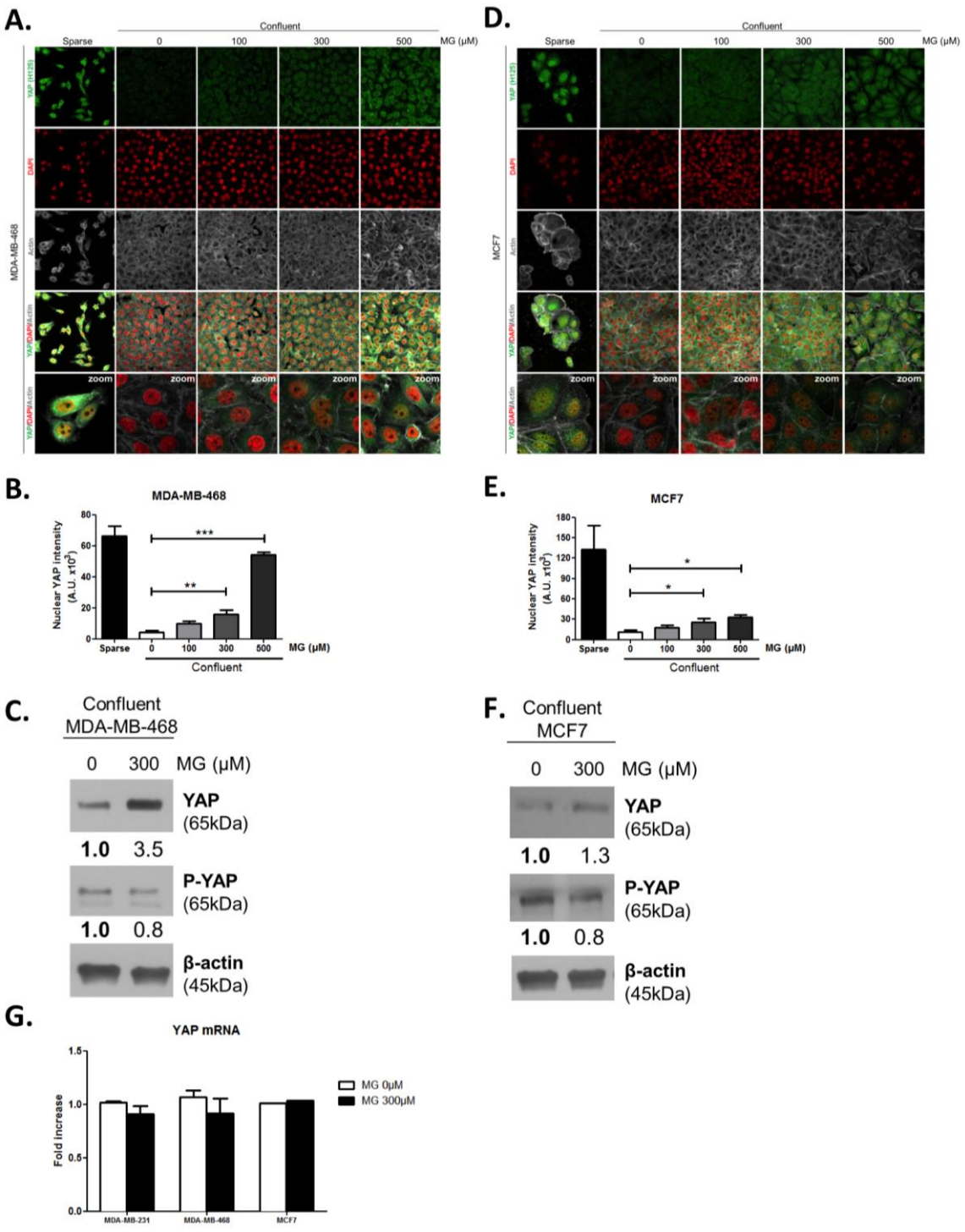

Supplementary Figure S1 (related to Figure 2): Methylglyoxal induces YAP accumulation in confluent breast cancer cells. A. and D. Immunofluorescence staining shows that YAP (Santa Cruz antibody, H125) is mainly localized in the nucleus at low cellular density (Sparse) and is weakly detectable at high cellular density (Confluent) in MDA-MB-468 and MCF7 cells. In contrast, cells treated with increasing doses of MG until they reach confluence showed YAP cellular accumulation. Magnification 630x. Zoomed pictures are shown where indicated. Data are representative of three independent experiments. **B and E.** Quantification of panel A and C experiments reports the intensity of YAP staining that colocalized with DAPI staining as described in Materials and Methods section. Nuclear YAP IF staining intensity shows a significant dose-dependent increase in presence of MG. Data were analyzed using one-way ANOVA followed by Dunnett post-test and shown as the mean values ± SEM of three independent experiments. **C and F.** YAP and P-YAP (ser127) expression in MDA-MB-468 and MCF7 cells treated with MG (300μM) until they reach confluence using western blot. Immunoblot data were quantified by densitometric analysis and normalized for β-actin. Data are representative of three independent experiments. **E.** qRT-PCR analysis of YAP gene in the indicated breast cancer cells treated with MG. Data were analyzed using unpaired Student's t test for each cell line and shown as the mean values ± SEM of three independent experiments. * $p<0.05$, ** $p<0.01$ and *** $p<0.001$.

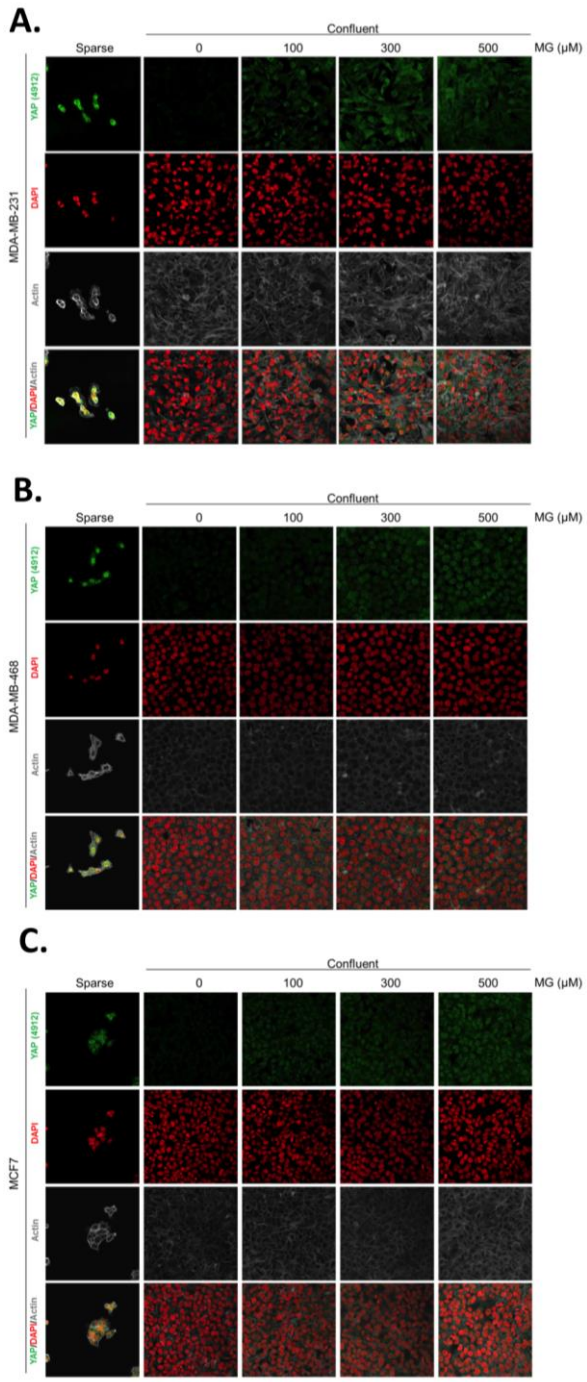

<u>Supplementary Figure S2 (related to Figure 2 and S1)</u>: Methylglyoxal induces YAP accumulation in confluent breast cancer cells. A., B. and C. Immunofluorescence (IF) staining shows that YAP (Cell Signaling antibody, 4912) is mainly localized in the nucleus at low cellular density (Sparse) and is weakly detectable at high cellular density (Confluent) in MDA-MB-231, MDA-MB-468 and MCF7 cells. In contrast, cells treated with increasing doses of MG until they reach confluence showed significant YAP cellular accumulation. Magnification 630x. Data are representative of three independent experiments.

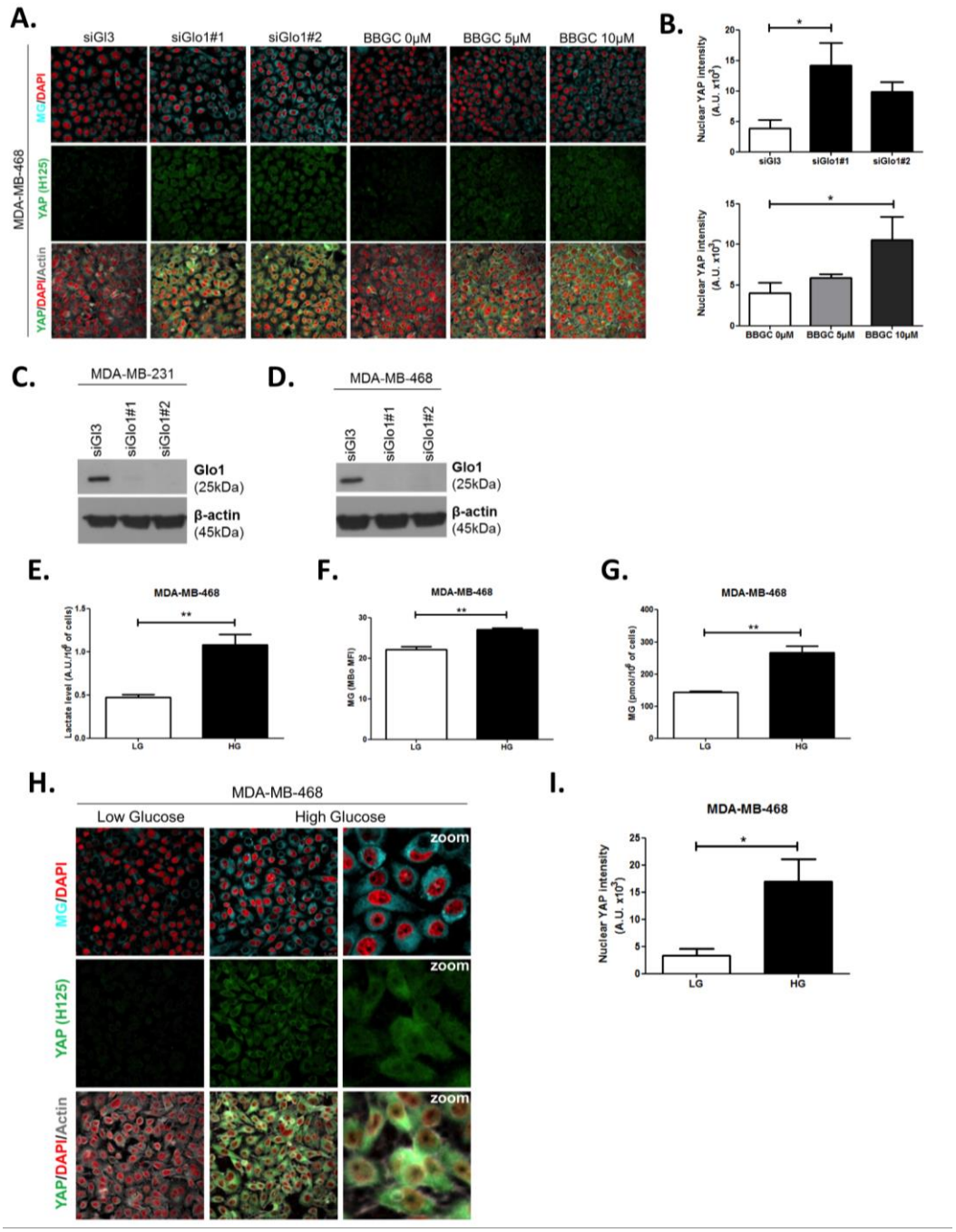

Supplementary Figure S3 (related to Figure 3): High endogenous MG induces YAP localization in breast cancer cells. **A.** Detection of MG was performed using MBo specific fluorescent probe, as described in Materials and Methods section, and showed MG cellular increase in MDA-MB-468 cells that were Glo1-depleted using siRNAs (siGlo1#1 and #2) or treated with BBGC Glo1 activity inhibitor. Upon Glo1 silencing/inhibition, MDA-MB-468 cells displayed more YAP (Santa Cruz antibody, H125) than control cells (siGl3 and BBGC 0µM, respectively). Magnification 630x. Data are representative of three independent experiments. **B.** Quantification of panel A experiment reports the intensity of YAP staining that colocalized with DAPI staining as described in Materials and Methods section for Glo1 silencing and BBGC conditions. Data were analyzed using one-way ANOVA followed by Dunnett post-test and shown as the mean values ± SEM of three independent experiments. **C and D.** Western blot validation of Glo1 silencing in MDA-MB-231 and MDA-MB-468 cells, respectively. Immunoblot data were normalized for β-actin and are representative of three independent experiments. **E.** Lactate level measured using ^{1}H-NMR increased in highly glycolytic MDA-MB-468 cells cultured in high glucose (HG) compared to low glucose (LG). **F. and G.** MG quantification using both FACS MBo mean fluorescence intensity (MFI) and LC-MS/MS analysis on conditioned medium in the indicated conditions as described under Material and Methods section. MDA-MB-468 cells significantly increased their MG production when cultured in HG. **E., F. and G.** Data were analyzed using unpaired Student's t test and shown as the mean values ± SEM of three independent experiments. **H.** MG detection and YAP immunofluorescence staining (Santa Cruz antibody, H125) in MDA-MB-468 cells cultured in low and high glucose medium. Magnification 630x. Zoomed pictures are shown for high glucose condition. Data are representative of three independent experiments. **I.** Quantification of panel H experiments. Data were analyzed using unpaired Student's t test with Welch's correction and shown as the mean values ± SEM of three independent experiments. * $p<0.05$ and ** $p<0.01$.

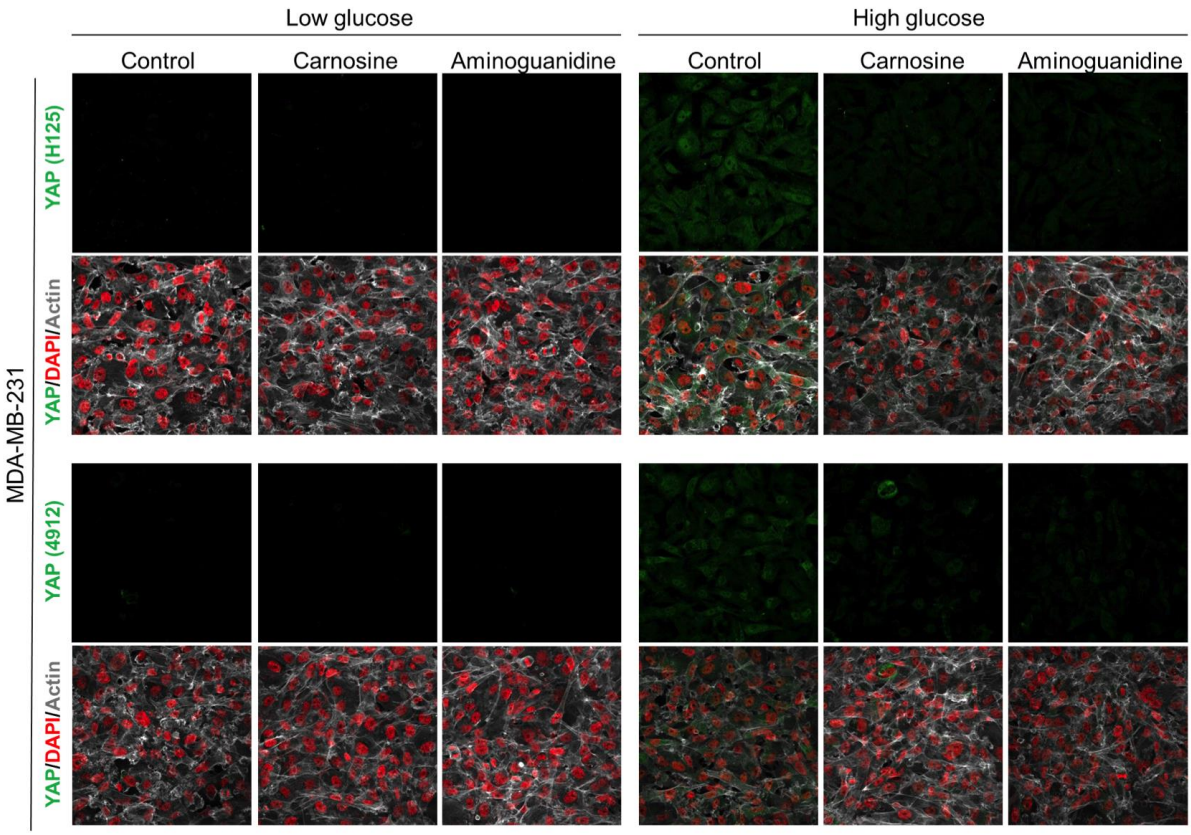

<u>Supplementary Figure S4 (related to Figure 3)</u>: Carnosine and aminoguanidine MG scavengers reverse YAP accumulation in MDA-MB-231 cultured in high glucose medium. MDA-MB-231 cells cultured in high glucose condition until they reached high density and treated with carnosine (10mM) or aminoguanidine (10mM) impeded cellular accumulation of YAP. Magnification 630x. Data are representative of 2 independent experiments.

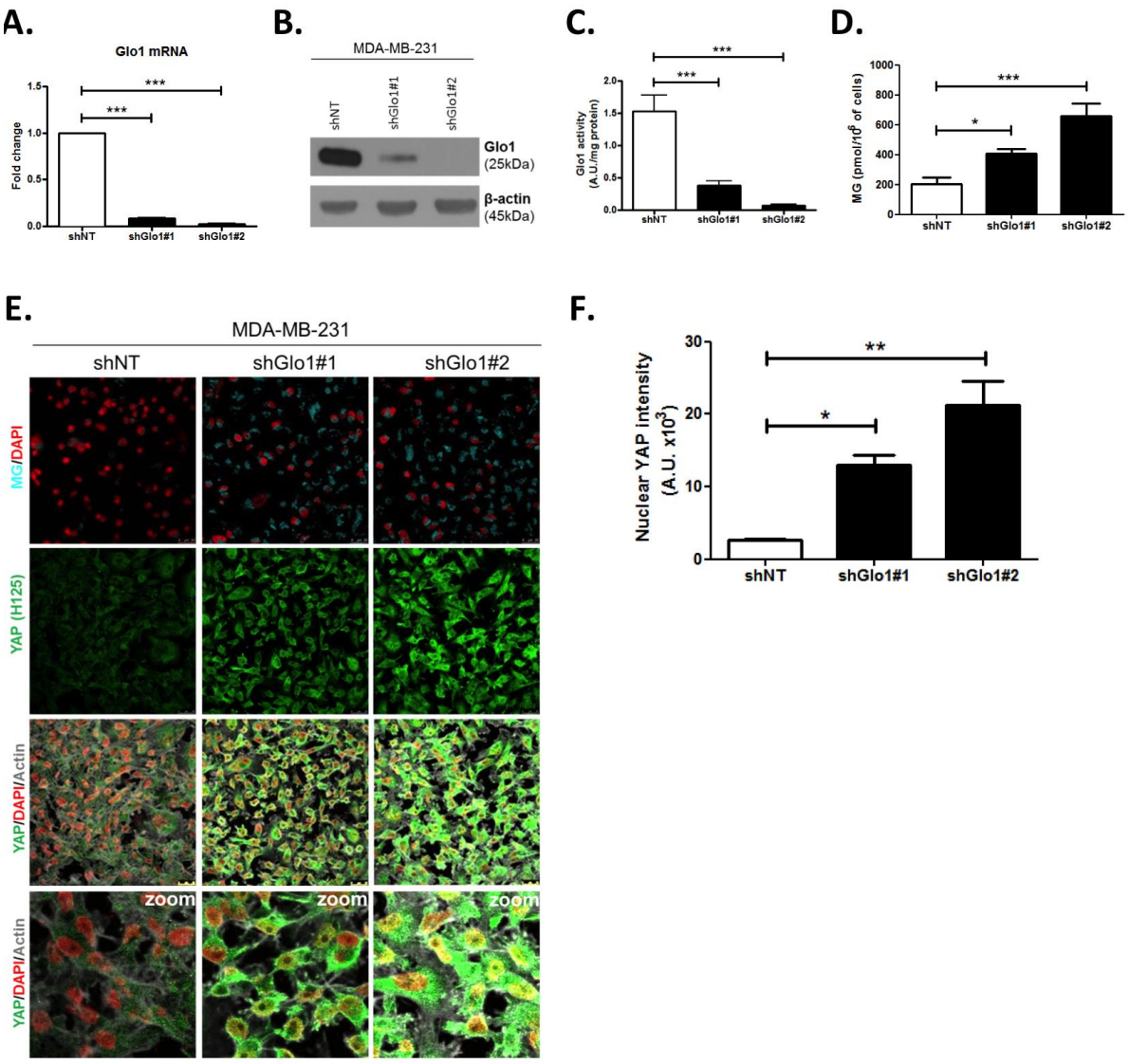

Supplementary Figure S5 (related to Figures 4, 6 and 7): YAP cellular accumulation in shGlo1 MDA-MB-231 clones. A. Glo1 mRNA, **B.** protein and **C.** activity level in MDA-MB-231 shNT control and shGlo1#1 and #2. **D.** Quantification of MG levels in conditioned medium using LC-MS/MS indicated a significant increase in shGlo1#1 and #2 cells. **E.** YAP immunofluorescence (Santa Cruz antibody, H125) in MDA-MB-231 silenced for Glo1 (shGlo1#1 and #2) cultured from low to high density. Detection of MG was performed using MBo specific fluorescent probe. Data are representative of three independent experiments. Magnification 630x. Zoomed pictures are shown when indicated. **F.** Quantification of nuclear YAP corresponding to E experiment. All data were analyzed using one-way ANOVA followed by Dunnett post-test and shown as the mean values ± SEM of at least three independent experiments. * $p<0.05$, ** $p<0.01$ and *** $p<0.001$.

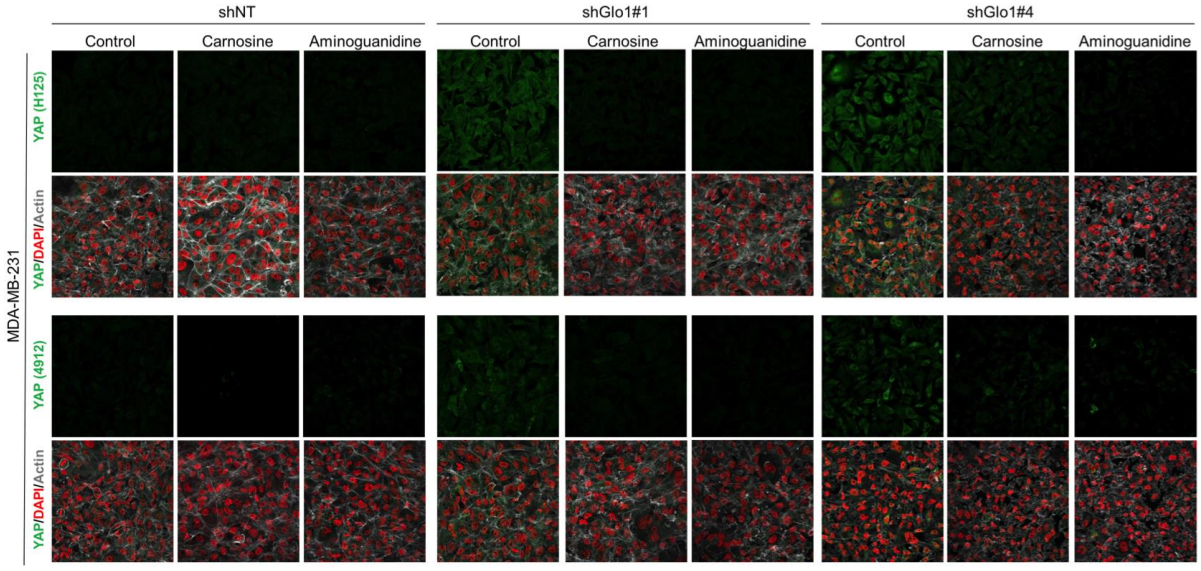

Supplementary Figure S6 (related to Figure S5): Carnosine and aminoguanidine MG scavengers reverse YAP accumulation in Glo1-depleted MDA-MB-231. MDA-MB-231 silenced for Glo1 (shGlo1#1 and #4) cells cultured until they reached high density and treated with carnosine (10mM) or aminoguanidine (10mM) impeded cellular accumulation of YAP. Magnification 630x. Data are representative of 2 independent experiments.

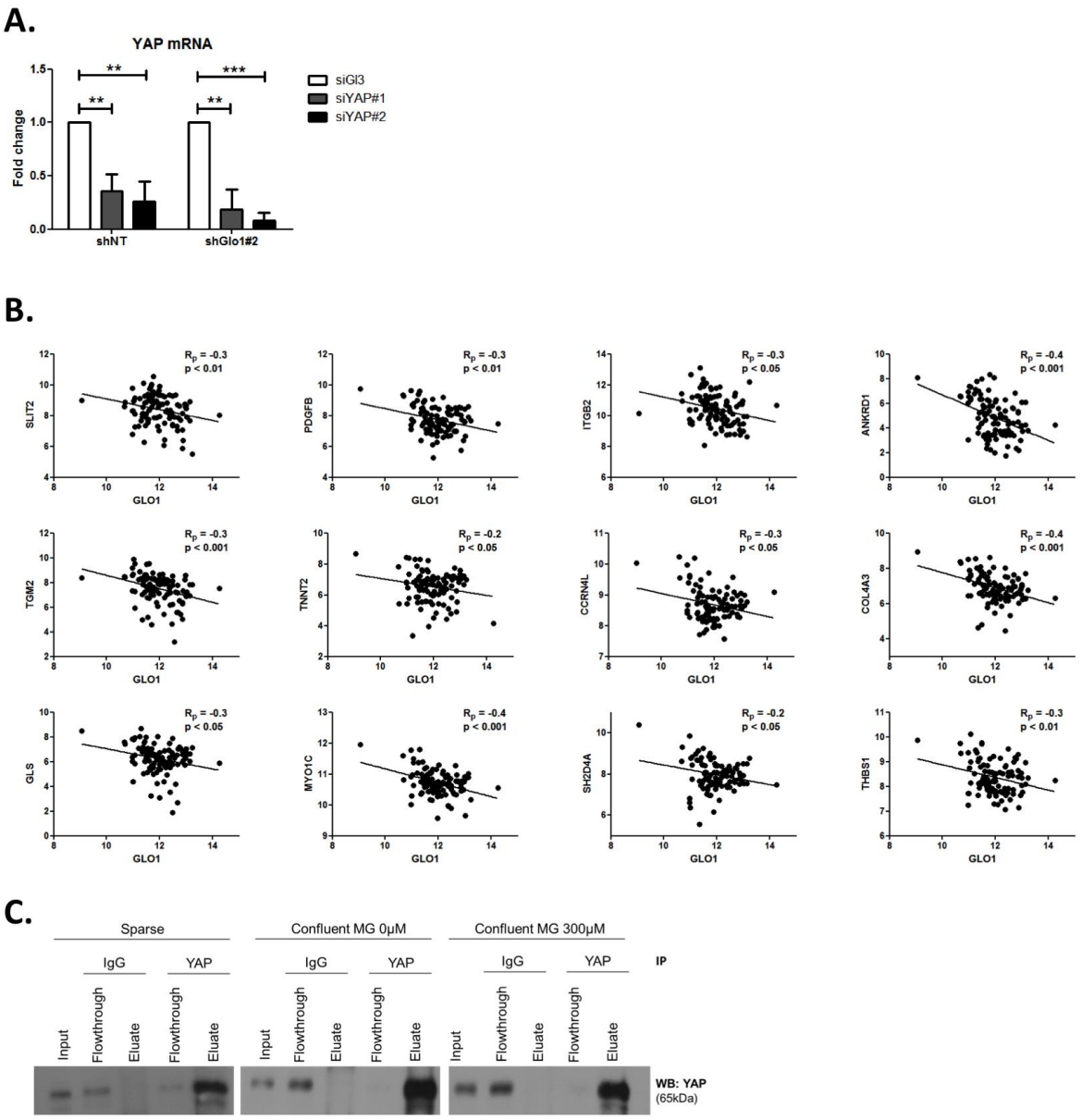

Supplementary Figure S7 (related to Figure 4): Inverse correlation between Glo1 and YAP target genes expression. A. Validation of YAP silencing (siYAP#1 and #2) in shGlo1 MDA-MB-231 cells 48h post-transfection by qRT-PCR. Data were analyzed using two-way ANOVA followed by Bonferroni post-test and shown as the mean values ± SD of one representative experiment (n=4). ** p<0.01 and *** p<0.001 **B.** Inverse correlation between the expression of Glo1 and 12 representative YAP target genes in breast cancer patients (n=103). R_p: Pearson correlation coefficient. **C.** Western blot detection of YAP in MDA-MB-231 cells under the indication conditions. Immunoblot is representative of three independent experiments.

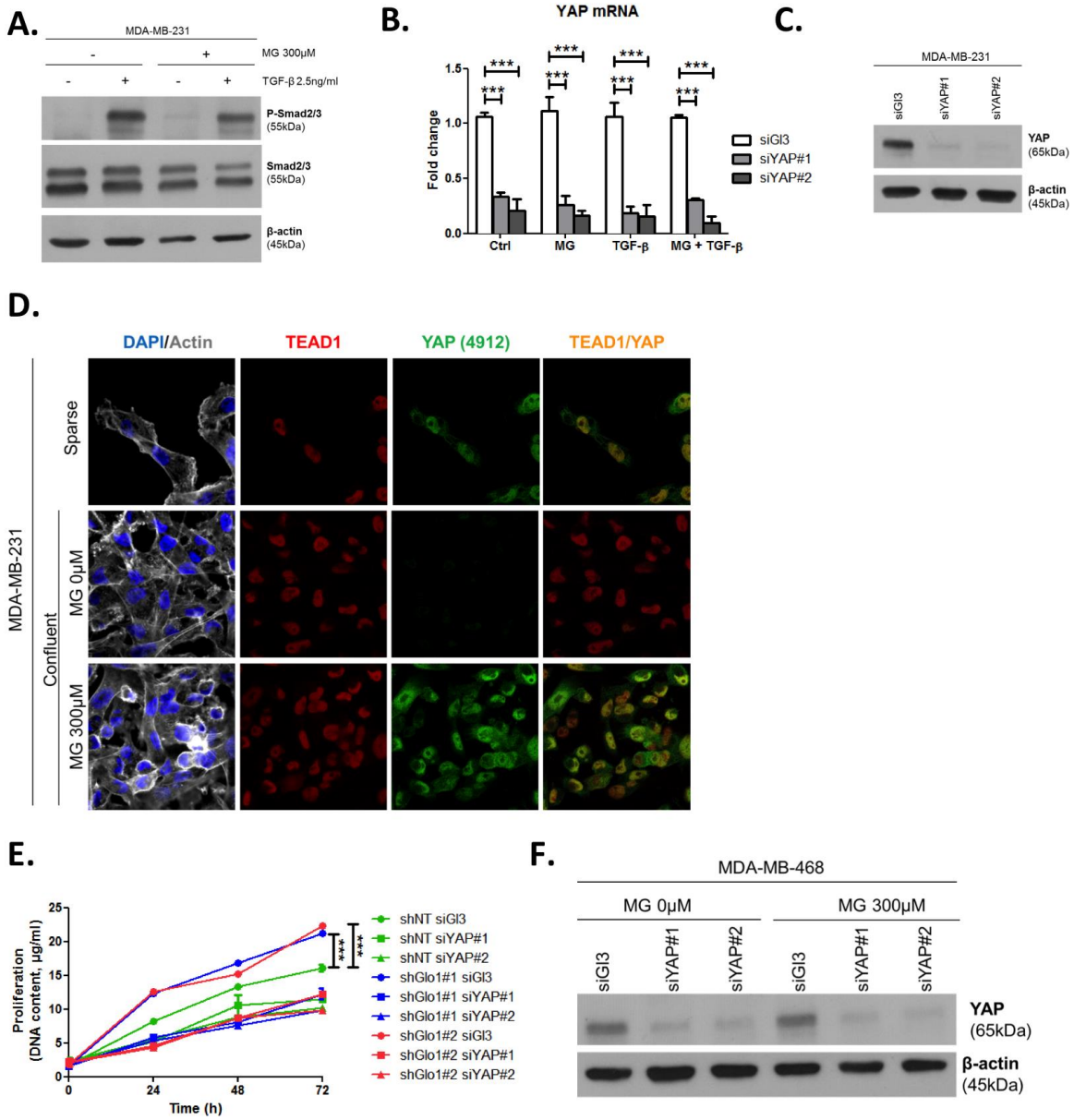

Supplementary Figure S8 (related to Figure 4): MG induces YAP co-transcriptional activity in breast cancer cells. A. Western blot of Phospho-Smad2/3 and Smad2/3 in MDA-MB-231 treated with MG until confluence and then with TGF-β during 2h. β-actin is used for normalization. **B. and C.** YAP mRNA and protein level assessed by qRT-PCR and Western blot, respectively, in MDA-MB-231 cells silenced for YAP (siYAP#1 and #2) and treated in the same conditions as in Figure 4D. Data were analyzed using two-way ANOVA followed by Bonferroni post-test and shown as the mean values ± SEM of three independent experiments. **D.** YAP (Cell Signaling, 4912) and TEAD1 IF co-localization in MDA-MB-231 cells cultured under low (Sparse) density used as positive control and in high density cultured cells (Confluent) in presence of MG. Magnification 630x. Data are representative of two independent experiments. **E.** Proliferation assay on Glo1-depleted MDA-MB-231 (shGlo1#1 and #2) silenced or not for YAP (siYAP#1 and #2) at different time points. Data (72h) were analyzed using two-way ANOVA followed by Bonferroni post-test and shown as the mean values ± SEM of three independent experiments. **F.** Validation of YAP silencing by Western blot in MDA-MB-231 shGlo1 cells after 72h related to panel D and Figure 4F. **G.** Validation of YAP silencing in MDA-MB-468 in the same conditions than Figure 4I. All immunoblots are representative of three independent experiments. *** $p<0.001$.

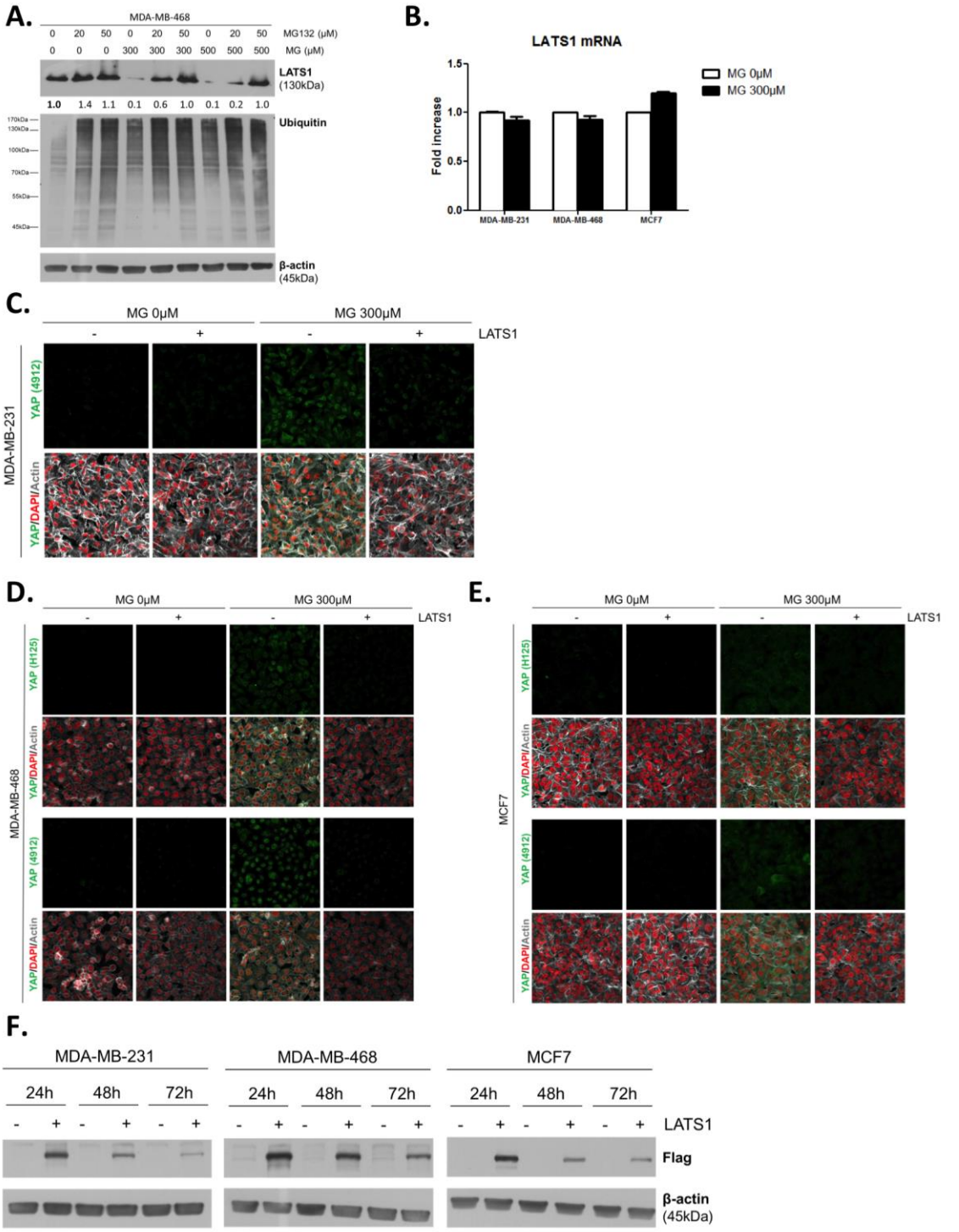

Supplementary Figure S9 (related to Figure 5): MG leads to YAP cellular accumulation through LATS1 expression decrease. A. LATS1 expression in MDA-MB-468 and MCF7 cells treated with MG (300 and 500μM) in presence or not of MG132 proteasome inhibitor at the indicated concentrations during 6h by western blot. Immunoblot loading was normalized for β-actin. **B.** MG treatment from low to high density did not affect LATS1 mRNA levels as assessed by qRT-PCR in the indicated cell lines. Data were analyzed using unpaired Student's t test and shown as the mean values ± SEM of three independent experiments. **C.** YAP immunofluorescence (Cell Signaling antibody, 4912) in MDA-MB-231 cells transiently transfected with LATS1 (+) or empty vector (-) and then treated with MG (300μM) until confluence. **D. and E.** YAP immunofluorescence detection (Santa Cruz antibody, H125 and Cell Signaling antibody, 4912) in MDA-MB-468 and MCF7 cells, respectively, transiently transfected with LATS1 (+) or empty vector (-) and then treated with MG (300μM) until confluence. **F.** Validation of LATS1 overexpression in breast cancer cells by western blot using Flag antibody. β-actin is used for normalization. Magnification 630x. All Data are representative of three independent experiments.

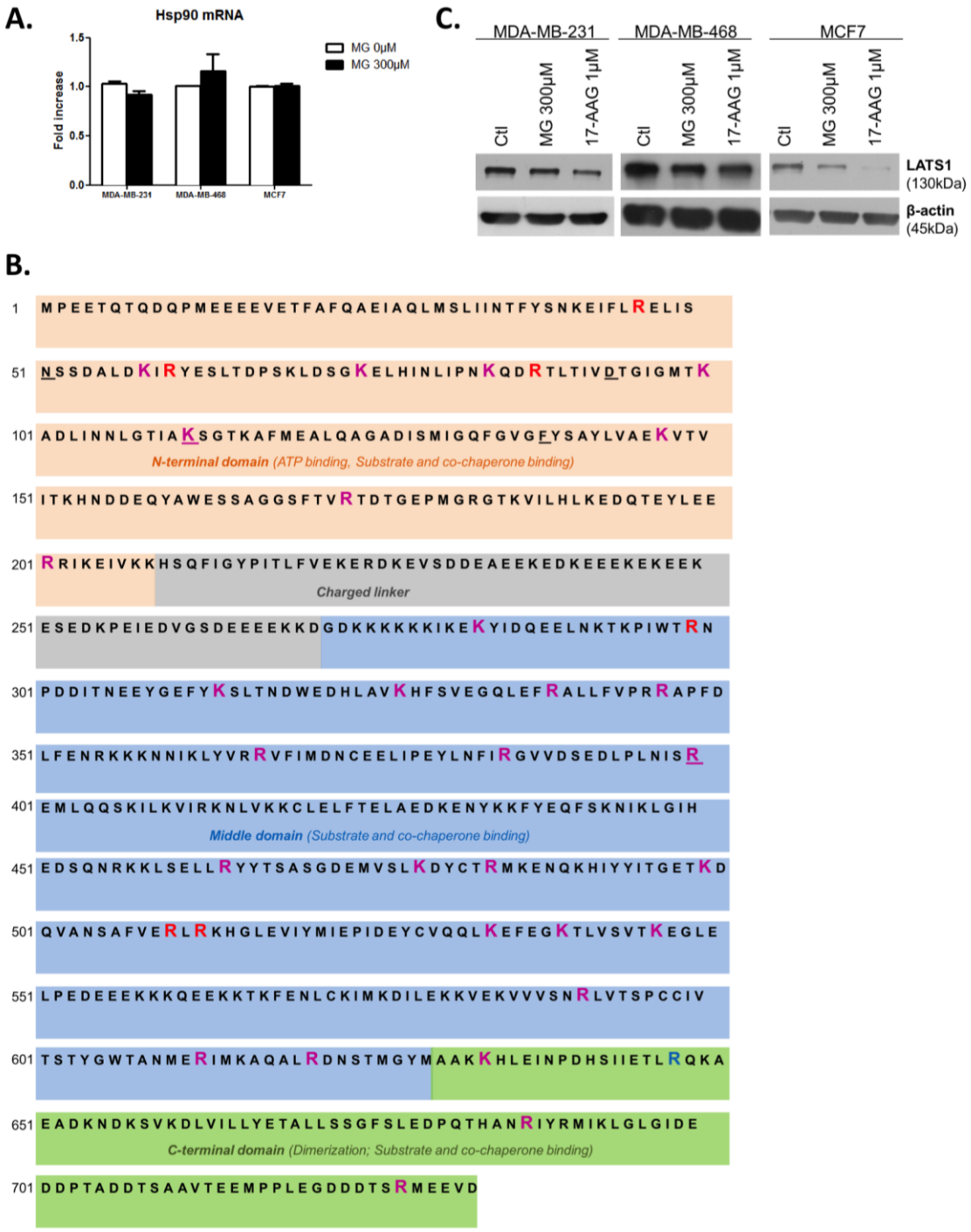

Supplementary Figure S10 (related to Figure 5): MG induces Hsp90 post-translational glycation. A. MG treatment from low to high density did not affect Hsp90 mRNA levels as assessed by qRT-PCR in the indicated cell lines. Data were analyzed using unpaired Student's t test and shown as the mean values ± SEM of three independent experiments. **B.** MG-modifications represented on Hsp90α amino acid sequence. Underlined amino acids represent ATP binding site. Magenta and blue amino acids represent MG-modifications observed on recombinant and endogenous Hsp90, respectively. Red amino acids represent MG-modifications found in both conditions. **C.** LATS1 expression is decreased in breast cancer cells treated with MG (300µM) or 17-AAG (1µM) during 24h. β-actin is used for normalization. Western blot are representative of three independent experiments.

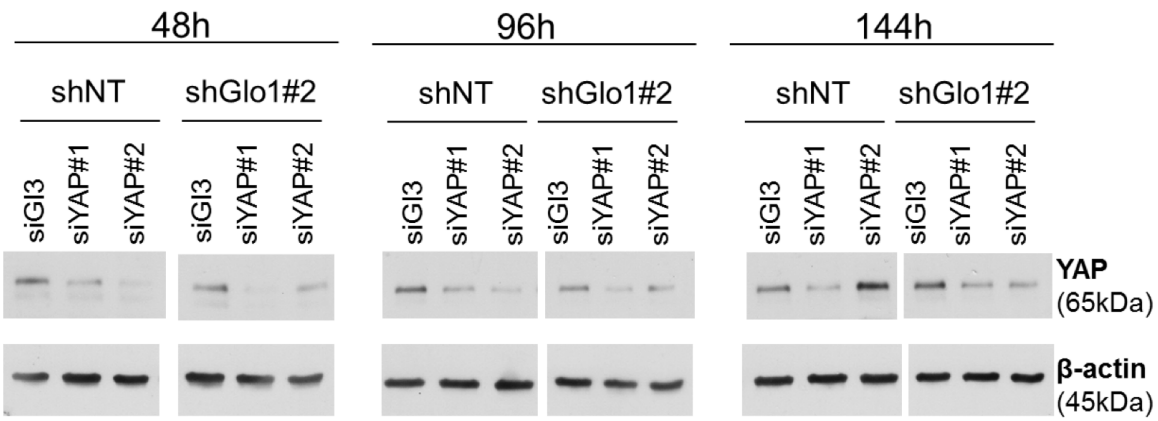

Supplementary Figure S11 (related to Figure 6): Glo1-depleted breast cancer cells show an increased tumorigenic potential *in vivo*. Validation of YAP silencing in Glo1-depleted MDA-MB-231 cells at different time points during tumor development on chicken chorioallantoic membrane described in Figures 6F-I.

Supplementary Table S1 (related to Figure 5): MG modifications on human recombinant Hsp90. Peptides identified by mass spectrometry of MG-Hsp90 enzymatic digests. Modification sites are underlined. CEL: Carboxyethyllysine.

Start	End	Peptide sequence	Modifications
38	47	YSNKEIFL**R**E	Dihydroxyimidazolidine
47	61	ELISNSSDALD**K**I**R**Y	Hydroimidazolone, Dihydroxyimidazolidine, Argpyrimidine, CEL
48	61	LISNSSDALDKI**R**Y	Hydroimidazolone, Dihydroxyimidazolidine
49	61	ISNSSDALDKI**R**Y	Dihydroxyimidazolidine
52	61	SSDALDKI**R**Y	Hydroimidazolone
59	76	I**R**YESLTDPSKLDSGKEL	Dihydroxyimidazolidine
63	76	ESLTDPSKLDSG**K**EL	CEL
71	89	DSGKELHINLIPNKQD**R**TL	Dihydroxyimidazolidine
75	89	ELHINLIPNKQD**R**TL	Hydroimidazolone
76	89	LHINLIPN**K**QD**R**TL	Dihydroxyimidazolidine, CEL
78	89	INLIPNKQD**R**TL	Dihydroxyimidazolidine
84	98	**K**QDRTLTIVDTGIGM	CEL
84	100	KQD**R**TLTIVDTGIGMTK	Dihydroxyimidazolidine
99	112	T**K**ADLINNLGTIAK	CEL
101	116	ADLINNLGTIA**K**SGTK	CEL
143	153	LVAE**K**VTVITK	CEL
163	182	ESSAGGSFTV**R**TDTGEPMGR	Dihydroxyimidazolidine
171	182	TV**R**TDTGEPMGR	Hydroimidazolone
186	202	VILHLKEDQTEYLEE**R**R	Hydroimidazolone, Dihydroxyimidazolidine
189	202	HLKEDQTEYLEE**R**R	Dihydroxyimidazolidine
280	292	IKE**K**YIDQEELNK	CEL
298	313	T**R**NPDDITNEEYGEFY	Dihydroxyimidazolidine
314	329	**K**SLTNDWEDHLAV**K**HF	CEL
330	340	SVEGQLEF**R**AL	Dihydroxyimidazolidine
338	345	**R**ALLFVPR	Dihydroxyimidazolidine
346	352	**R**APFDLF	Hydroimidazolone
367	380	**R**VFIMDNCEELIPE	Dihydroxyimidazolidine
383	396	NFI**R**GVVDSEDLPL	Dihydroxyimidazolidine
385	401	IRGVVDSEDIPLNLS**R**E	Dihydroxyimidazolidine
459	466	LSELL**R**YY	Hydroimidazolone, Dihydroxyimidazolidine
465	483	YYTSASGDEMVSL**K**DYCTR	CEL
467	489	TSASGDEMVSL**K**DYCT**R**MKENQK	Hydroimidazolone, Dihydroxyimidazolidine, CEL
474	483	MVSL**K**DYCTR	CEL
493	511	YITGET**K**DQVANSAFVE**R**L	CEL, Dihydroxyimidazolidine
500	512	DQVANSAFVE**R**LR	Argpyrimidine, Hydroimidazolone, Dihydroxyimidazolidine
511	520	LR**K**HGLEVIY	CEL
529	541	CVQQL**K**EFEG**K**TL	CEL
535	546	EFEG**K**TLVSVTK	CEL
538	564	G**K**TLVSVT**K**EGLELPEDEEEKKKQEEK	CEL
586	597	VVVSN**R**LVTSPC	Dihydroxyimidazolidine
605	614	GWTANME**R**IM	Hydroimidazolone, Dihydroxyimidazolidine
613	627	IMKAQAL**R**DNSTMGY	Dihydroxyimidazolidine
616	628	AQAL**R**DNSTMGYM	Dihydroxyimidazolidine
632	647	**K**HLEINPDHSIIETLR	CEL
673	689	SSGFSLEDPQTHAN**R**IY	Dihydroxyimidazolidine
677	689	SLEDPQTHAN**R**IY	Argpyrimidine, Dihydroxyimidazolidine
694	732	LGLGIDEDDPTADDTSAAVTEEMPPLEGDDDTS**R**MEEVD	Dihydroxyimidazolidine
715	732	EMPPLEGDDDTS**R**MEEVD	Hydroimidazolone, Dihydroxyimidazolidine

Supplementary Table S2 (related to Figure 5): MG modifications on endogenous Hsp90. Peptides identified by mass spectrometry of argpyrimidine immunoprecipitate from MDA-MB-231 treated with MG (300µM) during 6h. Modification sites are underlined.

Start	End	Peptide sequence	Modifications
42	58	EIFL**R**ELISNSSDALDK	Hydroimidazolone, Dihydroxyimidazolidine
59	69	I**R**YESLTDPSK	Hydroimidazolone, Dihydroxyimidazolidine
85	100	QD**R**TLTIVDTGIGMTK	Hydroimidazolone, Dihydroxyimidazolidine
295	314	PIWT**R**NPDDITNEEYGEFYK	Hydroimidazolone, Dihydroxyimidazolidine
500	513	DQVANSAFVE**R**L**R**K	Hydroimidazolone
633	649	HLEINPDHSIIETL**R**QK	Hydroimidazolone, Dihydroxyimidazolidine

Supplementary Table S3: Antibodies and dilution used for Western Blot experiments.

Protein targeted	Source	Reference	Dilution (WB)
Argpyrimidine	Oya et al. JBC 1999	mAb6B	1/6000
β-actin	Sigma-Aldrich (St Louis, MO, USA)	A5441	1/5000
E-cadherin	BD Biosciences (Franklin Lakes, NJ, USA)	610181	1/1000
Flag	Sigma-Aldrich (St Louis, MO, USA)	F3165	1/1000
Glyoxalase 1	BioMAC (Leipzig, Germany)	#02-14	1/1000
Hsp27	Cell Signaling (Danvers, MA, USA)	#2402	1/1000
Hsp90	Cell Signaling (Danvers, MA, USA)	#4877	1/1000
LATS1	Bethyl (Montgomery, TX, USA)	A300-477A	1/1000
MG-H (3D11)	Cell Biolabs (San Diego, CA, USA)	STA-011	1/2000
Phospho-Smad2 (Ser465/467)/Smad3 (Ser423/425)	Cell Signaling (Danvers, MA, USA)	#8828	1/500
P-YAP (Ser127)	Cell Signaling (Danvers, MA, USA)	#13008	1/1000
SMAD2/3	Cell Signaling (Danvers, MA, USA)	#8685	1/1000
Vimentin	Sigma-Aldrich (St Louis, MO, USA)	v6389	1/1000
YAP	Santa Cruz (Santa Cruz, CA, USA)	sc-15407	1/1000

Supplementary Table S4: siRNA sequences.

Name	Sequence
siYAP#1	5’-AAAUAAAGCCAUUUCUGGUUUGCUCCU-3’
	5’-AGGAGCAAACCAGAAAUGGCUUUAUUU-3’
siYAP#2	5’-ACUGGCAAAUUAUAGGCACUCCUUCCA-3’
	5’-UGGAAGGAGUGCCUAUAAUUUGCCAGU-3’
siGlo1#1	5’-CUUGGCUUAUGAGGAUAAA-3’
	5’-UUUAUCCUCAUAAGCCAAG-3’
siGlo1#2	5’-GAUGGCUACUGGAUUGAAA-3’
	5’-UUUCAAUCCAGUAGCCAUC-3’
siGl3	5’-CUUACGCUGAGUACUUCGA-3’
	5’-UCGAAGUACUCAGCGUAAG-3’

Supplementary Table S5: Primer sequences used for quantitative reverse transcription-PCR (qRT-PCR).

Name	Fw/Rv	Sequence	Probe (UPL, Roche)
CTGF	Fw	5'-CCTGCAGGCTAGAGAAGCAG-3'	85
	Rv	5'-TGGAGATTTTGGGAGTACGG-3'	
YAP	Fw	5'-ATCCCAGCACAGCAAATTCT-3'	47
	Rv	5'-TGGATTTTGAGTCCCACCAT-3'	
LATS1	Fw	5'-GGCACAAACACCATTAGAAACA-3'	31
	Rv	5'-AGAAGCTTCAGGACTGAGTTTAGC-3'	
Hsp90	Fw	5'-GTCCTGTGCGGTCACTTAGC-3'	25
	Rv	5'-AAAGGCGAACGTCTCAACC-3'	
ANKFN1	Fw	5'-CCAGTGTGTTGAGGTGCATT-3'	64
	Rv	5'-GCCCGAGAAAGTCCACACT-3'	
RIMS3	Fw	5'-GTCTCCCCAGACGATCACC-3'	37
	Rv	5'-AGCAGGCTCTGCTCTTTGAC-3'	
KCNK1	Fw	5'-CTGACAAGGGCACGGTGT-3'	22
	Rv	5'-GTCCTTCTTCGGCAGCAC-3'	
EMP2	Fw	5'-CCGCAATCATGACACACAG-3'	42
	Rv	5'-GAAGCAGGGAGAGAGGTTTG-3'	
OSBP2	Fw	5'-CGTCGTCCCCAGAGTCAT-3'	1
	Rv	5'-CCTCAAGGCCAGCTCAGA-3'	
IRAK3	Fw	5'-GCTGCTTGAAAGTCTCTCTGC-3'	26
	Rv	5'-AGAGCTCTGCGCTGTTGTG-3'	
WTN5A	Fw	5'-CCCCCTTATAAATGCAACTGTTC-3'	48
	Rv	5'-ATTGTACTGCAGGTGTACCTTAAAAC-3'	
18S	Fw	5'-CTTCCACAGGAGGCCTACAC-3'	46
	Rv	5'-CGCAAAATATGCTGGAACTTT-3'	
Glo1	Fw	5'-TGGCTTATGAGGATAAAAATGACA-3'	**SYBR Green**
	Rv	5'-CAGCTCAAGTGTAGCTTTTCTGG-3'	

3. Methylglyoxal increases the metastatic potential of human breast cancer cells

3.1. Introduction

In the previous study, we observed an increase of tumor growth and metastases formation in lung after injection of Glo1-silenced MDA-MB-231 cancer cells in mice. When the same cells were grafted on the chicken chorioallantoic membrane (CAM assay), they grew as tumors presenting a significantly bigger volume than Glo1 expressing control cells. The silencing of YAP in shGlo1 cells efficiently reverted tumor growth to control levels suggesting that nuclear accumulation of YAP in Glo1-depleted cells contributed, at least in part, to increased tumor growth and metastatic potential *in vivo*.

Our results indicate that Glo1 acts as a tumor suppressor in breast cancer. A study aimed at functionally identifying tumor suppressor genes in liver cancer identified Glo1 as a tumor suppressor gene, which knockdown using shRNAs increased tumor growth in a mouse model (Zender et al. 2008). However, most of the recent studies aimed at the inhibition of Glo1 to induce a cytotoxic MG accumulation effectively showed a decreased tumor growth. These studies generally depicted Glo1 as an amplified and/or overexpressed oncogene and as a bad prognosis marker in different types of malignant tumors (Sakamoto et al. 2001, Cheng et al. 2012, Fonseca-Sanchez et al. 2012, Antognelli et al. 2013, Zhang et al. 2014, Hosoda et al. 2015). The search for copy number changes on a large set of cancer cell lines confirmed that Glo1 is amplified in many types of human cancer (Santarius et al. 2010). We undertook this study in order to better understand the dual role attributed to Glo1 in cancer.

3.2. Results

3.2.1. RNA sequencing analysis on Glo1-depleted MDA-MB-231 breast cancer cells highlighted a pro-metastatic signature

In order to better characterize the effects mediated by a high carbonyl stress on cancer cells, we performed a RNA sequencing analysis on Glo1-silenced MDA-MB-231 breast cancer cells. Alignment of transcripts to the genome indicated that 11653, 11910 and 11813 genes were expressed in the control (shNT) and Glo1-depleted MDA-MB-231 cells shGlo1#1 and #2, respectively. For differential gene

expression, absolute fold change >2 and q-value < 0.05 filters were applied. We found 655 and 584 genes significantly upregulated in shGlo1#1 and #2, respectively, when compared to control cells. In addition, 481 and 426 genes were significantly downregulated in shGlo1#1 and #2, respectively. Among these genes, 328 genes were common between the three conditions (Figure 45A). The ten most up- and down-regulated genes are listed in Tables 4 and 5, respectively. The expression of 2 genes used as calibrators was not significantly affected (GAPDH: 0.9 and 1.1 and ACTB: 0.8 and 0.9 for shGlo1#1 and #2, respectively). As expected, Glo1 level was decreased by 4.9 and 22.6 fold in shGlo1#1 and #2 cells compared with control cells.

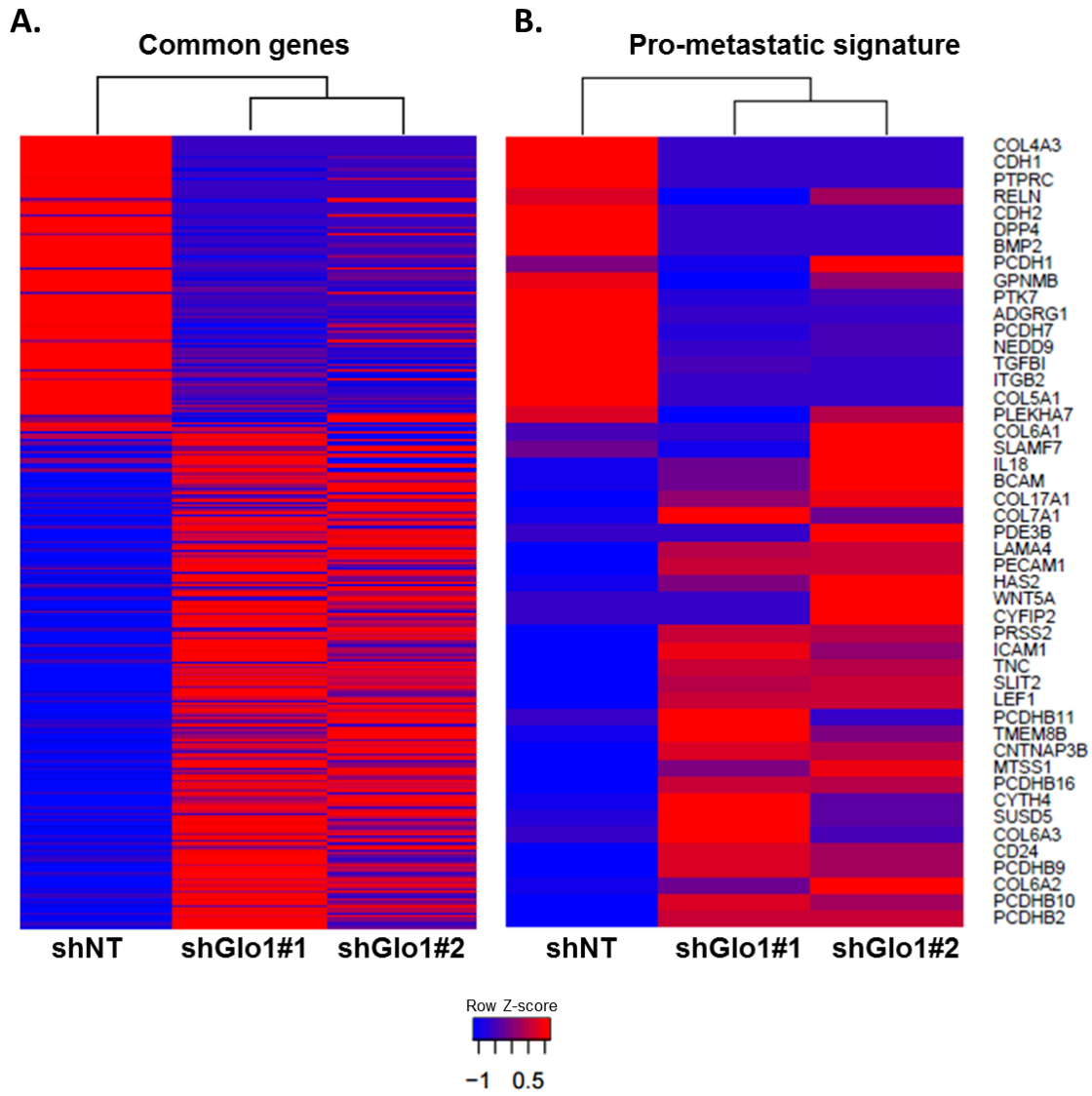

Figure 45: Gene expression analysis by RNA-seq in Glo1-depleted MDA-MB-231 breast cancer cells. A. Heat map displaying 328 differentially expressed common genes between Glo1-depleted (shGlo1#1 and #2) and control (shNT) MDA-MB-231 cells. RNA-seq was performed on three different RNA isolations for each conditions. **B.** Heat map displaying 47 differentially expressed common genes from the pro-metastatic signature between Glo1-depleted (shGlo1#1 and #2) and control (shNT) MDA-MB-231 cells. RNA-seq were performed on three different RNA isolations for each conditions. *Z*-scores are represented through the color scale where blue is used for low expression and red for high expression.

Table 4: TOP 10 of significantly *up-regulated* common genes in Glo1-silenced MDA-MB-231 cells compared to control cells (shNT).

	Gene	Name	Fold change	q-value
shGlo1#1	HLA-DRA	Major histocompatibility complex, class II, DR alpha	37.8	0.011
	ARHGEF6	Rac/Cdc42 guanine nucleotide exchange factor 6	18,1	< 0.001
	CACNG7	Calcium voltage-gated channel auxiliary subunit gamma 7	16.8	< 0.001
	CIITA	Class II, major histocompatibility complex, transactivator	15.6	< 0.001
	PCDHB2	Protocadherin beta 2	12.6	< 0.001
	COL6A2	Collagen type VI alpha 2	12.6	< 0.001
	SLC16A2	Solute carrier family 16 member 2	12.2	0.001
	OAS1	2'-5'-oligoadenylate synthetase 1	11.9	< 0.001
	COL6A3	Collagen type VI alpha 3	11.6	< 0.001
	IGSF3	Immunoglobulin superfamily member 3	9.8	< 0.001
shGlo1#2	HSPA12A	Heat shock protein family A (Hsp70) member 12A	37.3	< 0.001
	IGSF3	Immunoglobulin superfamily member 3	33.1	< 0.001
	COL6A2	Collagen type VI alpha 2	28.6	< 0.001
	MAGEC2	MAGE family member C2	22.9	< 0.001
	CYFIP2	Cytoplasmic FMR1 interacting protein 2	22.3	< 0.001
	GALNT18	Polypeptide N-acetyl-galactosaminyltransferase 18	18.5	< 0.001
	LRRN1	Leucine rich repeat neuronal 1	16.0	< 0.001
	NAP1L3	Nucleosome assembly protein 1 like 3	15.7	< 0.001
	CCNA1	Cyclin A1	14.2	< 0.001
	PCDHB2	Protocadherin beta 2	13.4	< 0.001

Table 5: TOP 10 of significantly *down-regulated* common genes in Glo1-silenced MDA-MB-231 cells compared to control cells (shNT).

	Gene	Name	Fold change	q-value
shGlo1#1	MAGEB1/4	MAGE family member B1/B4	1398.8	< 0.001
	PSG7	Pregnancy specific beta-1-glycoprotein 7	63.6	< 0.001
	CXCR4	C-X-C motif chemokine receptor 4	60.1	< 0.001
	PSG10P	Pregnancy specific beta-1-glycoprotein 10, pseudogene	30.3	0.010
	RELN	Reelin	20.8	< 0.001
	PSG8	Pregnancy specific beta-1-glycoprotein 8	20.5	0.038
	PSG5	Pregnancy specific beta-1-glycoprotein 5	18.9	< 0.001
	COL4A3	Collagen type IV alpha 3 chain	17.3	< 0.001
	PSG9	Pregnancy specific beta-1-glycoprotein 9	16.8	< 0.001
	CDH1	E-cadherin	14.5	< 0.001
shGlo1#2	MAGEB1/4	MAGE family member B1/B4	1370.0	< 0.001
	PSG7	Pregnancy specific beta-1-glycoprotein 7	58.1	< 0.001
	CDH1	E-cadherin	54.9	< 0.001
	PSG5	Pregnancy specific beta-1-glycoprotein 5	44.0	< 0.001
	PSG1	Pregnancy specific beta-1-glycoprotein 1	32.9	< 0.001
	PSG8	Pregnancy specific beta-1-glycoprotein 8	21.1	0.006
	PSG9	Pregnancy specific beta-1-glycoprotein 9	20.1	< 0.001
	SLC6A20	Solute carrier family 6 member 20	18.5	< 0.001
	LUM	Lumican	18.1	< 0.001
	PSG11	Pregnancy specific beta-1-glycoprotein 11	14.5	0.006

Gene ontology analyses were performed using the ToppFun Suite software. The 5 most significantly affected biological processes for each Glo1-depleted clone are listed in Table 6. Interestingly, these analyses revealed that important biological processes related to cancer progression such as cell adhesion, migration and extracellular matrix organization are affected by Glo1-silencing. Thus the molecular changes occurring in Glo1-depleted breast cancer cell are in good accordance with our previous results linking Glo1 inhibition to tumor growth and metastasis development. We found 140 and 120 significantly modulated genes linked to “migration” in shGlo1#1 and #2, respectively. We regrouped the 188 modulated genes linked to cell adhesion and migration, under the name of the pro-metastatic signature of Glo1-depleted cells. A heatmap representing the 47 common genes from the pro-metastatic signature is shown in Figure 45B.

Table 6: TOP 5 of biological processes (BP) significantly modulated in Glo1-silenced MDA-MB-231 cells compared to control cells (shNT).

	Biological process	p-value	Number of modulated genes	Total number of genes in the BP
shGlo1#1	Cell adhesion	< 0.001	89	1067
	Cell migration	< 0.001	89	1073
	Regulation of developmental process	< 0.001	133	1912
	Synapse assembly	< 0.001	21	97
	Extracellular matrix organization	< 0.001	44	385
shGlo1#2	Extracellular matrix organization	< 0.001	44	385
	Cell adhesion	< 0.001	82	1067
	Cell migration	< 0.001	71	1073
	Synapse assembly	< 0.001	16	97
	Cell motility	< 0.001	74	1170

A.

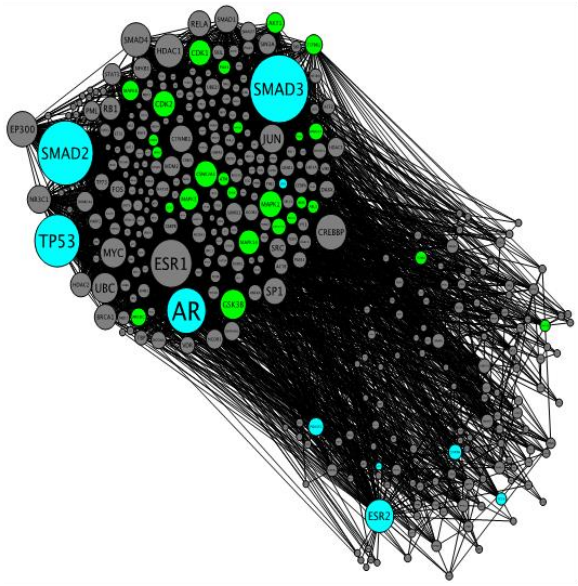

B.

Module	Pathway	Number of genes in network	Number of genes in pathway	p-value
1	**TGFβ signaling pathway**	23	80	< 0.001
2	Coregulation of androgen receptor activity	11	60	< 0.001
3	Glucocorticoid receptor regulatory network	18	77	< 0.001
4	Progesterone-mediated oocyte maturation	12	89	< 0.001
5	p53 pathway	4	57	< 0.001

C.

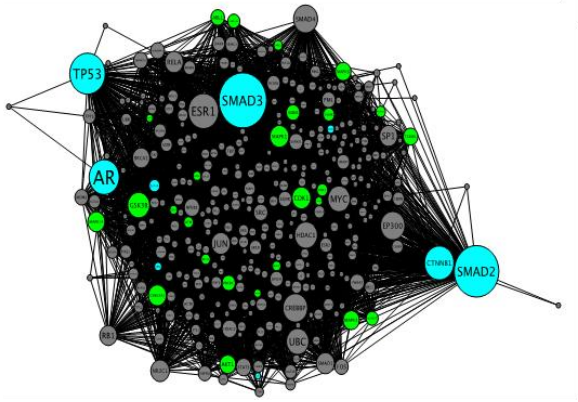

D.

Module	Pathway	Number of genes in network	Number of genes in pathway	p-value
1	**TGFβ signaling pathway**	20	80	< 0.001
2	Glucocorticoid receptor regulatory network	21	77	< 0.001
3	Signaling by ERBB2	19	155	< 0.001
4	p53 pathway	13	57	< 0.001

Figure 46: Transcriptional network associated to the pro-metastatic signature. **A** and **C.** Schematic representation of the transcriptional network significantly associated to the pro-metastatic signature in shGlo1#1 (A) and shGlo1#2 (C) compared to control MDA-MB-231 cells. The nodes represent proteins in the network. The nodes are coloured in cyan when the protein is a transcription factor, in grey when the protein has significant interactions with the identified transcription factors or in green when the protein is a kinase/phosphatase having substrates that are enriched in the network. The size of the nodes depends on how many interactions each node has within the network (node degree). **B** and **D.** List of pathway significantly and with the highest score associated to the pro-metastatic signature for shGlo1#1 (B) and #2 (D). TGFβ signalling pathway components and especially Smad3 represent the major regulator of the pro-metastatic genes in both Glo1-depleted cells.

3.2.2. Pro-metastatic signature is mediated through Transforming Growth Factor β (TGFβ) signaling pathway in Glo1-depleted cells

In order to determine which molecular pathways are involved in the pro-metastatic signature observed in Glo1-silenced MDA-MB-231 cells, we performed an *in silico* pathway analysis in collaboration with Dr. Steven van Laere (Antwerp University). A significant association with the highest score was found for both shGlo1 clones between the 188 genes of the pro-metastatic signature candidate genes and TGFβ signaling pathway (Figure 46A, B, C and D). Among the TGFβ pathway components, Smad3 appeared to be the master regulator of the pro-metastatic signature. Experiments are ongoing to confirm the implication of TGFβ signaling pathway and Smad3 in the metastatic potential of Glo1-depleted cells. Among the pro-metastatic signature, we selected 3 candidates *CD24*, *Tenascin C* and *Lumican* which are known to be linked to TGFβ (Figure 47A). Indeed, Tenascin C is a well-known pro-metastatic target gene of the TGFβ signaling pathway in cancer cells (Kalembeyi et al. 2003, Maschler et al. 2004, Minn et al. 2005, Oskarsson et al. 2011). CD24 is also linked to TGFβ in the regulation of invasiveness properties of cancer cells (Kitaura et al. 2011, Lee et al. 2012). TGFβ also regulates Lumican expression, notably, in osteosarcoma. It has been demonstrated that Lumican decrease the availability of TGFβ for cancer cells by binding it in the extracellular compartment (Nikitovic et al. 2008, Nikitovic et al. 2011). This suggests that by decreasing Lumican expression, Glo1-depleted cells favor TGFβ signaling activity. RT-qPCR analyses were performed to confirm the expression level of these up- or down-regulated genes on independent mRNA samples of Glo1-silenced MDA-MB-231 cells. As shown in Figure 47B, CD24 and Tenascin C mRNA levels were significantly increased in Glo1-depleted cells while Lumican mRNA was significantly decreased in these cells. Interestingly, the treatment of shGlo1#1 cells with the MG scavenger aminoguanidine reverted Lumican decreased expression to its basal level (Figure 47C). However, aminoguanidine had no effect on Lumican expression in shGlo1#2 (Figure 47C) while aminoguanidine decreased the global level of MG-H1 adducts in these cells (Figure 47D). We are currently validating the increased expression of other Smad3 target genes up-regulated in the RNA-seq data. We are also analyzing the expression and/or the level of phosphorylation of several components of the TGFβ pathway such as TGFβ receptors 1/2 and Smad2/3 in basal

conditions and in response to TGFβ treatment. Finally, we will consider the use of specific kinase inhibitors of p38 mitogen-activated protein kinase, Jun N-terminal kinase (JNK) and IκB kinase (IKK) to get more insights about TGFβ pathway activity in Glo1-depleted breast cancer cells.

A.

Gene	Name	Fold change shGlo1#1	Fold change shGlo1#2
CD24	Signal transducer CD24	+ 8.8	+ 7.1
TNC	Tenascin C	+ 5.4	+ 5.3
LUM	Lumican	- 5.2	- 18.1

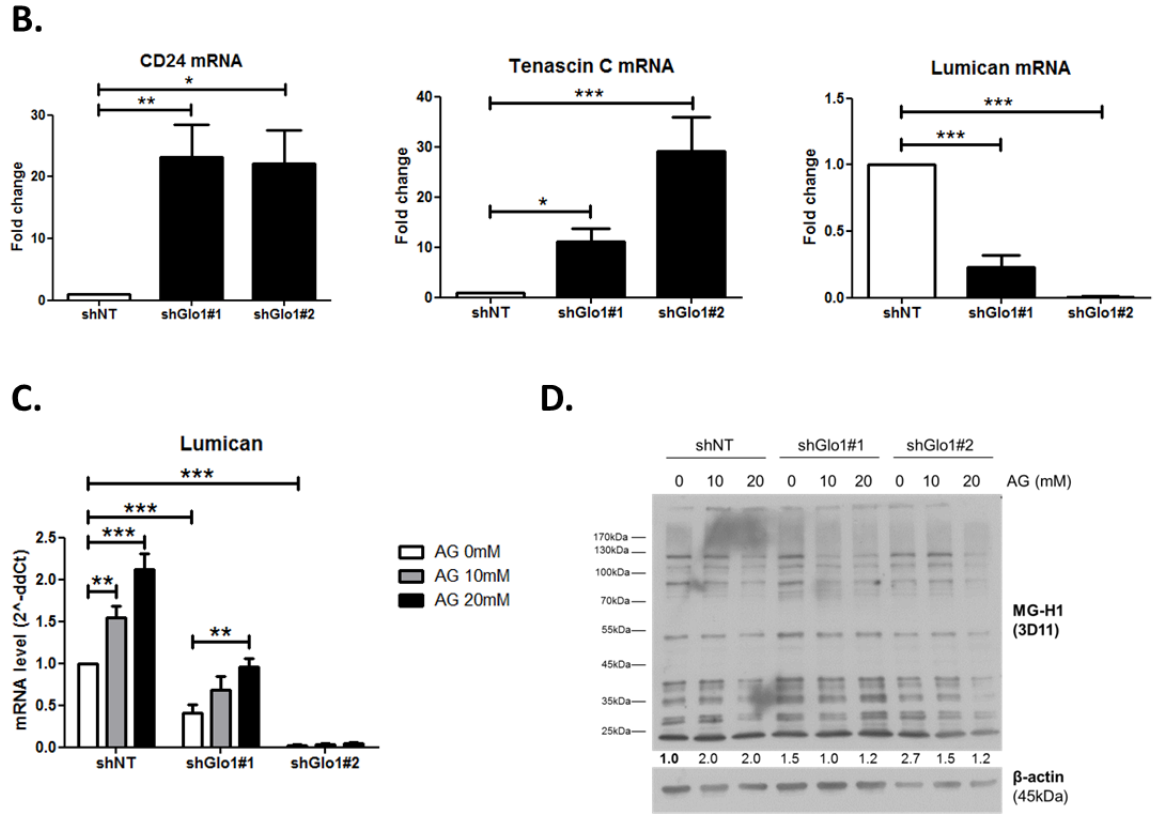

Figure 47: Validation of 3 candidate genes of the pro-metastatic signature obtained from RNA-seq analysis. A. Fold change obtained from RNA-seq analysis of 3 genes (CD24, Tenascin C and Lumican) of the pro-metastatic signature in Glo1-depleted MDA-MB-231 compared to control. **B.** qRT-PCR analysis confirmed the increase of CD24 and Tenascin C mRNA levels as well as the decrease of Lumican mRNA level in Glo1-depleted cells. RNA-seq analysis and validation were performed on distinct RNA isolations. **C.** Lumican mRNA level in Glo1-depleted MDA-MB-231 cells treated with aminoguanidine (0-10-20 mM) during 3 days. **D.** MG-H1 accumulation in MDA-MB-231 cells treated with aminoguanidine (0-10-20 mM) during 3 days using western blot. Immunoblotted data were quantified by densitometric analysis and normalized for β-actin. Data are represented as mean ± SEM of three independent experiments. * $p<0.05$, ** $p<0.01$, *** $p<0.001$.

High endogenous MG level increases migratory and invasiveness abilities of breast cancer cells *in vitro*

To explore further the functional aspects of the pro-metastatic signature in Glo1-depleted cancer cells, we performed migration, invasion and adhesion assays. Glo1 silencing significantly increased up to 2.5 fold the migratory ability of MDA-MB-231 cells (Figure 48A and B). The pre-treatment (3 days) with the MG scavenger aminoguanidine decreased the migratory capacity of Glo1-depleted cells to its basal level (Figure 48A and B). These results suggest that increased MG level induced by Glo1 silencing is responsible of the enhanced migratory ability of MDA-MB-231 cells. As shown in Figure 48C and D, Glo1-depleted cells also showed a significantly increased invasiveness in invasion assays that was efficiently blocked by aminoguanidine pre-treatment. We next analyzed the capacity of Glo1-silenced MDA-MB-231 cells to adhere on collagen, an important component of the extracellular matrix. After 1h, the attachment of shGlo1 cells was significantly reduced compared to control cells (Figure 48E and F). Altogether our data indicate that Glo1 depletion in breast cancer cells resulted in increased migration and invasion and reduced adhesion responses that are compatible with the acquisition of a pro-metastatic phenotype.

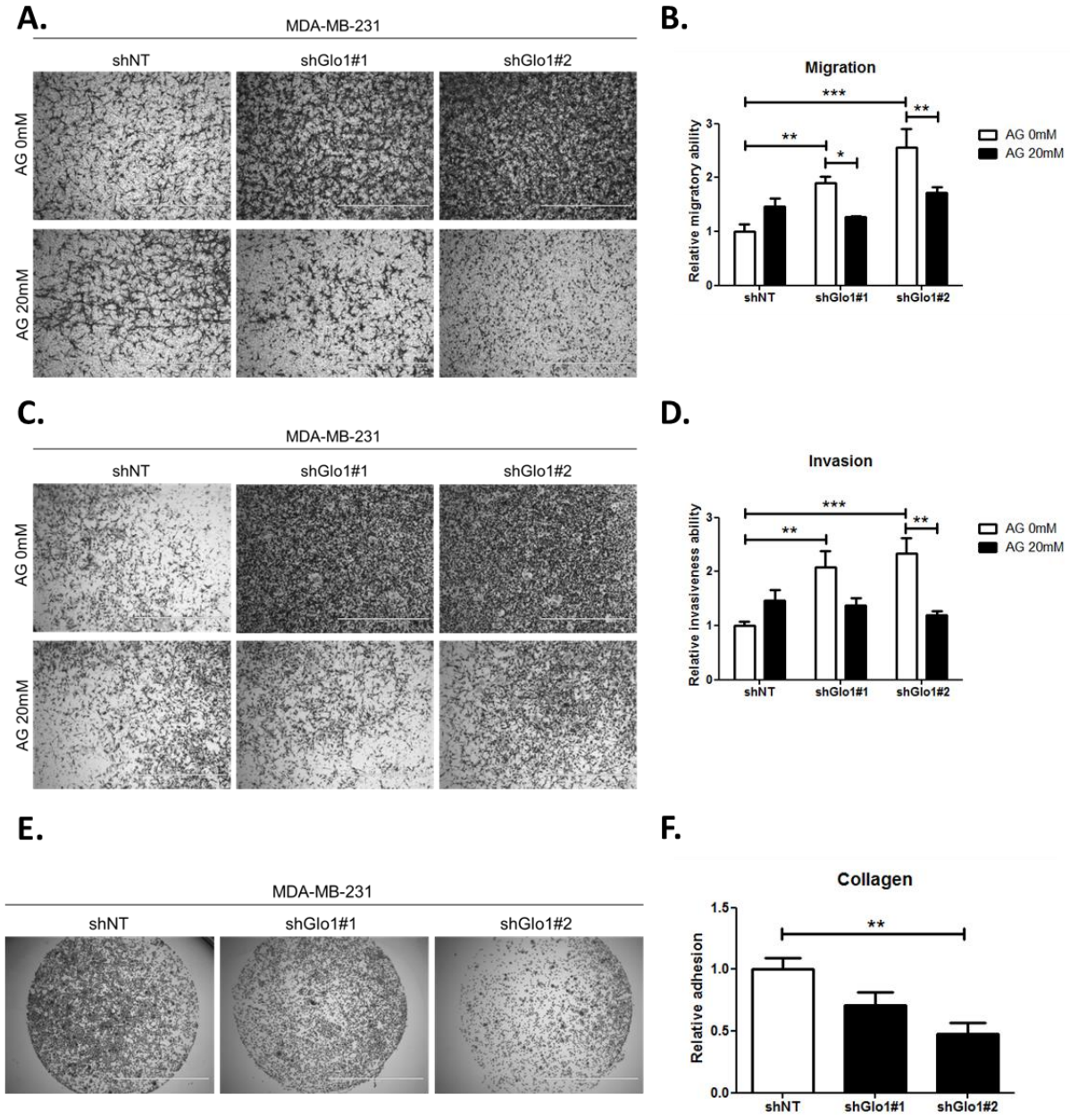

Figure 48: High endogenous MG level increases migratory and invasiveness abilities of breast cancer cells *in vitro*. A. Increased number of migrating cells after 16h of migration toward serum in Go1-depleted MDA-MB-231 cells. Aminoguanidine treatment (20mM) 3 days before migration assay reversed migratory capacity enhancement in shGlo1 cells. White bar represent 1mm. **B.** Quantification of panel A according to the area covered by cells. **C**. Increased number of invading cells after 24h of invasion through matrigel coated insert in Go1-depleted MDA-MB-231 cells. Aminoguanidine treatment (20mM) 3 days before invasion assay reversed invasiveness capacity enhancement in shGlo1 cells. White bar represent 1mm. **D.** Quantification of panel B according to the area covered by cells. **E.** Decreased number of attached cells to collagen after 1h in Glo1-silenced conditions compared to control. White bar represent 2mm. **F.** Quantification of panel E. Data are represented as mean ± SEM of three independant experiments. * p<0.05, ** p<0.01, *** p<0.001.

3.3. Conclusions and perspectives

Our preliminary data suggest that carbonyl stress modulates expression of genes implicated in migration and adhesion processes in cancer cells through the regulation of TGFβ signaling pathway. As mentioned above, ongoing experiments will help to confirm the implication of this pathway in the pro-metastatic phenotype of Glo1-depleted cancer cells. We will also test inhibitors of the TGFβ signaling pathway on the expression/phosphorylation of TGFβ pathway components as well as their effects on the enhanced migratory and invasiveness capacities of Glo1-silenced cells.

As we demonstrated that Glo1 depletion enhances the migratory and invasiveness abilities and decreases adhesion to extracellular matrix component, *in vivo* experiments are ongoing to confirm these *in vitro* results. After injection in the tail vein of Glo1-depleted MDA-MB-231 cells in mice, the development of lung metastasis will be followed by bioluminescence imaging and assessed by vimentin immunostaining of lung sections. These experiments should confirm results obtained in the second part where after primary tumor removal, Glo1-depleted cells formed more lung metastatic foci in mice.

The main cause of death in breast cancer patients is the development of secondary tumors at distant organ sites. Nowadays, it is not possible to precisely predict the risk of metastasis development in breast cancer patients. Therefore, more than 80% of these patients receive adjuvant chemotherapy while only 40% of the patients will relapse and ultimately die of metastatic breast cancer (Weigelt et al. 2005). Many women who would be cured by surgery and radiotherapy will be “over-treated” and suffer the toxic side effects of chemotherapy unnecessarily. New prognostic markers are needed to identify patients who are at the highest risk for developing metastases. We plan to perform the immunostaining of MG adducts and Glo1 in breast cancer tissues from patient with or without metastases. The measure of circulating MG levels will be also tested as a readout of MG stress in breast cancer patients. These experiments will allow us to demonstrate the potential correlation between carbonyl stress and metastasis development and eventually organ specific metastases. Once validated, the evaluation of carbonyl stress, either by MG dosage in blood or MG-adducts specific detection in primary tumors, could represent a

promising way to identify cancer patients at high risk of metastatic disease and that will benefit from adjuvant treatment.

Methylglyoxal, a glycolysis by-product, increases the metastatic potential of human breast cancer cells

Nokin MJ, Gabriel M, Monseur C, Durieux F, Chiavarina B, Henry A, Peulen O, Turtoi A, Lambert C, Colige A, Castronovo V and Bellahcène A

Manuscript in preparation

Methylglyoxal, a glycolysis side-product, increases the metastatic potential of human breast cancer cells

Marie-Julie Nokin[1], Maude Gabriel[1], Christine Monseur[1], Florence Durieux[1], Barbara Chiavarina[1], Aurélie Henry[1], Olivier Peulen[1], Andrei Turtoi[1], Charles Lambert[2], Alain Colige[2], Vincent Castronovo[1] and Akeila Bellahcène[1*]

[1]*Metastasis Research Laboratory, GIGA-CANCER, University of Liège (ULg), Liège, Belgium*; [2]*Laboratory of Connective Tissues Biology, GIGA-Cancer, University of Liège (ULg), Liège, Belgium*

*****Corresponding author: Akeila BELLAHCENE, University of Liège, GIGA-CANCER, Metastasis Research Laboratory, Pathology Tour, +4 level, Building 23, 4000 LIEGE, BELGIUM, Tel. +32 4 366 25 57, Fax +32 4 366 29 75, e-mail a.bellahcene@ulg.ac.be

Tumor cells use glycolysis rather than mitochondria respiration to produce their energy (Warburg effect). Methylglyoxal (MG), a highly reactive glycolysis by-product, is thus accumulated in tumor cells where it glycates lipids, proteins and nucleic acids, thereby inducing a carbonyl stress. All mammalian cells developed a detoxifying system, composed of 2 enzymes, glyoxalase 1 and 2 (Glo1-2), transforming MG into D-lactate. In this study, we aim to investigate the molecular mechanisms underlying the acquisition of a metastatic phenotype by breast cancer cells under high MG endogenous stress. For this purpose, we performed RNA sequencing on Glo1-silenced MDA-MB-231 cells and we found an increased expression of pro-metastatic genes and a decreased expression of anti-metastatic genes. We have validated these RNA-seq results at the mRNA levels. Further analysis also identified TGFβ signaling pathway regulation in Glo1-depleted cells. Next, we tested the migratory and invasiveness capacity of shGlo1 clones *in vitro*. We observed a significant increase of migrating and invading cells in shGlo1 condition compared with control, which was reverted by treatment with aminoguanidine, a potent MG scavenger. Altogether, our data suggest a new role for MG as a promoter of the metastatic cascade.

INTRODUCTION

Tumor cells are characterized by a metabolic shift from mitochondrial respiration to aerobic glycolysis. This metabolic pattern is called the Warburg effect. Methylglyoxal (MG), a highly reactive glycolysis by-product, is thus accumulated in tumor cells. This α-oxoaldehyde is formed after the fifth step of glycolysis by the spontaneous dephosphorylation and degradation of dihydroxyacetone phosphate and glyceraldehyde-3-phosphate [1]. MG is a dicarbonyl compound that glycates lipids, proteins and nucleic acids. The reaction between MG and the amino group of proteins leads to the formation of advanced glycation end-products (AGEs) such as hydroimidazolones (MG-H) and argpyrimidines [2]. All mammalian cells developed a detoxifying system composed of 2 enzymes, glyoxalase 1 and 2 (Glo1 and Glo2) able to transform MG into D-lactate [3]. A deregulation between MG production and its degradation by the glyoxalase system induces carbonyl stress.

Carbonyl stress has been mainly studied in the context of diabetes and its vascular complications. In cancer, the link between MG, Glo1 and cancer remains largely unexplored. Two studies reported MG-AGEs accumulation in human tumor samples [4,5]. In our recent study, we observed an increase of tumor growth and metastases formation in lung after injection of Glo1-silenced MDA-MB-231 breast cancer cells in mice. We attributed

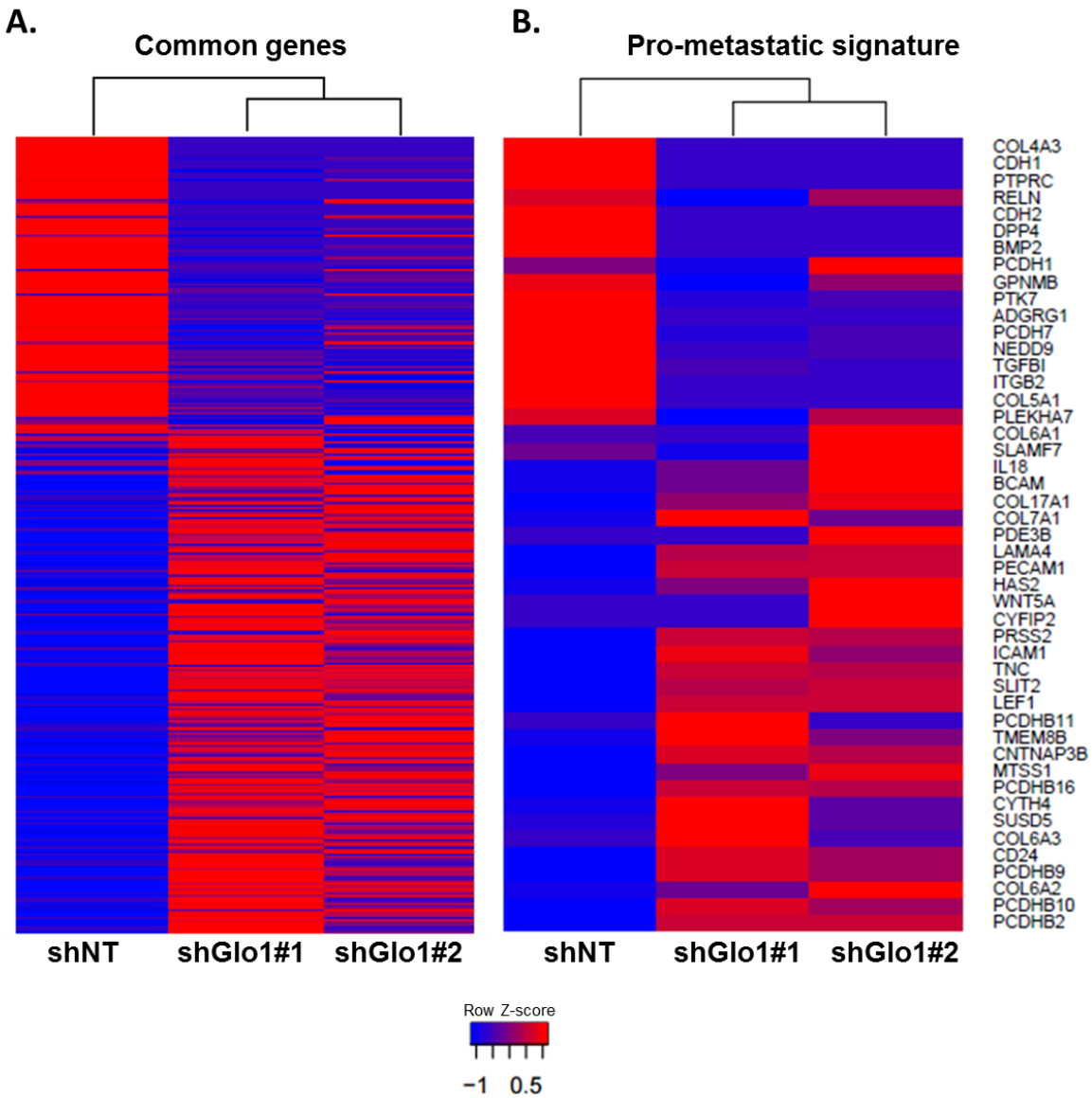

Figure 1: Gene expression analysis by RNA-seq in Glo1-depleted MDA-MB-231 breast cancer cells. A. Heat map displaying 328 differentially expressed common genes between Glo1-depleted (shGlo1#1 and #2) and control (shNT) MDA-MB-231 cells. RNA-seq were performed on three different RNA isolations for each conditions. **B.** Heat map displaying 47 differentially expressed common genes from the pro-metastatic signature between Glo1-depleted (shGlo1#1 and #2) and control (shNT) MDA-MB-231 cells. RNA-seq were performed on three different RNA isolations for each conditions. *Z*-scores are represented through the color scale where blue is used for low expression and red for high expression.

this increased tumor growth and metastatic potential *in vivo* to the nuclear accumulation of Yes-associated protein (YAP) in Glo1-depleted cells. Our results indicate that Glo1 acts as a tumor suppressor in breast cancer. A study aimed at functionally identifying tumor suppressor genes in liver cancer identified Glo1 as a tumor suppressor gene, which knockdown using shRNAs increased tumor growth in a mouse model [6]. However, most of the recent studies aimed at the inhibition of Glo1 to induce a cytotoxic MG accumulation effectively reported a decreased tumor growth. These studies generally depicted Glo1 as an amplified and/or overexpressed oncogene and as a bad prognosis marker in different types of malignant tumors [7-12]. The search for copy number changes on a large set of cancer cell lines confirmed that Glo1 is amplified in many types of human cancer [13]. We undertook this study in order to characterize the metastatic phenotype of Glo1-depleted cells and to contribute to a better understanding of the dual role attributed to Glo1 in cancer.

Table 1: **TOP 10 of significantly *up-regulated* common genes in Glo1-silenced MDA-MB-231 cells compared to control cells (shNT).**

	Gene	Name	Fold change	q-value
shGlo1#1	HLA-DRA	Major histocompatibility complex, class II, DR alpha	37.8	0.011
	ARHGEF6	Rac/Cdc42 guanine nucleotide exchange factor 6	18,1	< 0.001
	CACNG7	Calcium voltage-gated channel auxiliary subunit gamma 7	16.8	< 0.001
	CIITA	Class II, major histocompatibility complex, transactivator	15.6	< 0.001
	PCDHB2	Protocadherin beta 2	12.6	< 0.001
	COL6A2	Collagen type VI alpha 2	12.6	< 0.001
	SLC16A2	Solute carrier family 16 member 2	12.2	0.001
	OAS1	2'-5'-oligoadenylate synthetase 1	11.9	< 0.001
	COL6A3	Collagen type VI alpha 3	11.6	< 0.001
	IGSF3	Immunoglobulin superfamily member 3	9.8	< 0.001
shGlo1#2	HSPA12A	Heat shock protein family A (Hsp70) member 12A	37.3	< 0.001
	IGSF3	Immunoglobulin superfamily member 3	33.1	< 0.001
	COL6A2	Collagen type VI alpha 2	28.6	< 0.001
	MAGEC2	MAGE family member C2	22.9	< 0.001
	CYFIP2	Cytoplasmic FMR1 interacting protein 2	22.3	< 0.001
	GALNT18	Polypeptide N-acetyl-galactosaminyltransferase 18	18.5	< 0.001
	LRRN1	Leucine rich repeat neuronal 1	16.0	< 0.001
	NAP1L3	Nucleosome assembly protein 1 like 3	15.7	< 0.001
	CCNA1	Cyclin A1	14.2	< 0.001
	PCDHB2	Protocadherin beta 2	13.4	< 0.001

Table 2: **TOP 10 of significantly *down-regulated* common genes in Glo1-silenced MDA-MB-231 cells compared to control cells (shNT).**

	Gene	Name	Fold change	q-value
shGlo1#1	MAGEB1/4	MAGE family member B1/B4	1398.8	< 0.001
	PSG7	Pregnancy specific beta-1-glycoprotein 7	63.6	< 0.001
	CXCR4	C-X-C motif chemokine receptor 4	60.1	< 0.001
	PSG10P	Pregnancy specific beta-1-glycoprotein 10, pseudogene	30.3	0.010
	RELN	Reelin	20.8	< 0.001
	PSG8	Pregnancy specific beta-1-glycoprotein 8	20.5	0.038
	PSG5	Pregnancy specific beta-1-glycoprotein 5	18.9	< 0.001
	COL4A3	Collagen type IV alpha 3 chain	17.3	< 0.001
	PSG9	Pregnancy specific beta-1-glycoprotein 9	16.8	< 0.001
	CDH1	E-cadherin	14.5	< 0.001
shGlo1#2	MAGEB1/4	MAGE family member B1/B4	1370.0	< 0.001
	PSG7	Pregnancy specific beta-1-glycoprotein 7	58.1	< 0.001
	CDH1	E-cadherin	54.9	< 0.001
	PSG5	Pregnancy specific beta-1-glycoprotein 5	44.0	< 0.001
	PSG1	Pregnancy specific beta-1-glycoprotein 1	32.9	< 0.001
	PSG8	Pregnancy specific beta-1-glycoprotein 8	21.1	0.006
	PSG9	Pregnancy specific beta-1-glycoprotein 9	20.1	< 0.001
	SLC6A20	Solute carrier family 6 member 20	18.5	< 0.001
	LUM	Lumican	18.1	< 0.001
	PSG11	Pregnancy specific beta-1-glycoprotein 11	14.5	0.006

Table 3: **TOP 5 of biological processes (BP) significantly modulated in Glo1-silenced MDA-MB-231 cells compared to control cells (shNT).**

	Biological process	p-value	Number of modulated genes	Total number of genes in the BP
shGlo1#1	Cell adhesion	< 0.001	89	1067
	Cell migration	< 0.001	89	1073
	Regulation of developmental process	< 0.001	133	1912
	Synapse assembly	< 0.001	21	97
	Extracellular matrix organization	< 0.001	44	385
shGlo1#2	Extracellular matrix organization	< 0.001	44	385
	Cell adhesion	< 0.001	82	1067
	Cell migration	< 0.001	71	1073
	Synapse assembly	< 0.001	16	97
	Cell motility	< 0.001	74	1170

RESULTS

RNA sequencing analysis on Glo1-depleted MDA-MB-231 breast cancer cells highlighted a pro-metastatic signature. In our previous study, we engineered stable Glo1-depleted MDA-MB-231 cells using shRNAs and we observed a significant increase of MG level in these cells. In order to better characterize the effects of MG on cancer cells, messenger RNAs (mRNA) from shGlo1#1 and #2 as well as control (shNT) MDA-MB-231 cells were sequenced using next-generation sequencing analysis. The average number of reads approached or exceeded 20 million in both samples. Alignment of transcripts to the genome indicated that 11653, 11910 and 11813 genes were expressed in the control (shNT) and Glo1-depleted MDA-MB-231 cells shGlo1#1 and #2, respectively. For differential gene expression, absolute fold change >2 and q-value < 0.05 filters were applied. We found 655 and 584 genes significantly upregulated in shGlo1#1 and #2, respectively, when compared to control cells. In addition, 481 and 426 genes were significantly downregulated in shGlo1#1 and #2, respectively. Among these genes, 328 genes were common between the three conditions (Figure 1A). The ten most up- and down-regulated genes are listed in Table 1 and 2, respectively. The expression of 2 genes used as calibrators was not significantly affected by Glo1 affected by Glo1 depletion (GAPDH: 0.9 and 1.1 and ACTB: 0.8 and 0.9 for shGlo1#1 and #2, respectively). As expected, Glo1 level was decreased by 4.9 and 22.6 fold in shGlo1#1 and #2 cells compared with control cells.

Gene ontology analyses were performed using the ToppFun Suite software. The 5 most significantly affected biological processes for each Glo1-depleted clone are listed in Table 3. Interestingly, these analyses revealed that important biological processes related to cancer progression such as cell adhesion, migration and extracellular matrix organization are affected by Glo1-

A.

Gene	Name	Fold change shGlo1#1	Fold change shGlo1#2
CD24	Signal transducer CD24	+ 8.8	+ 7.1
TNC	Tenascin C	+ 5.4	+ 5.3
LUM	Lumican	- 5.2	- 18.1

B.

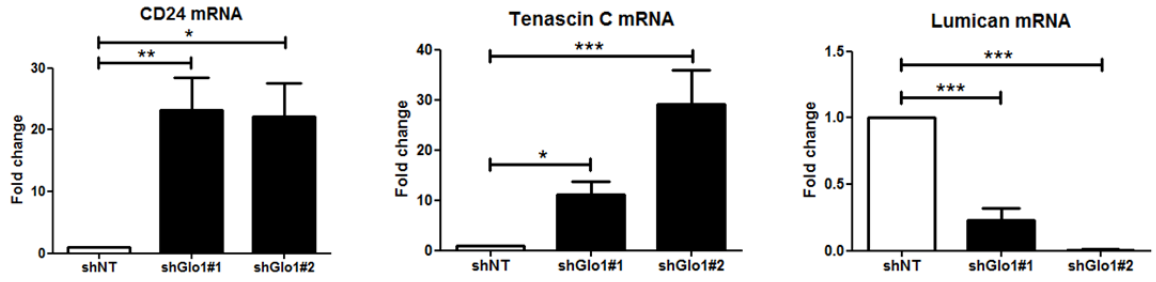

C.

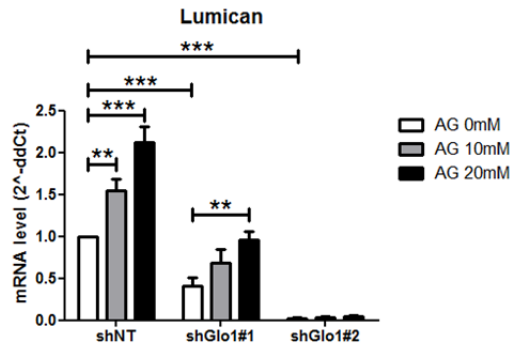

D.

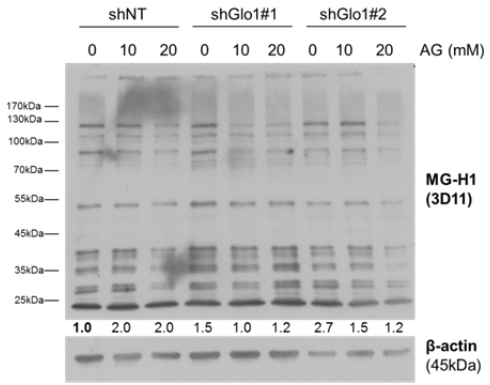

Figure 2: Validation of 3 candidate genes of the pro-metastatic signature obtained from RNA-seq analysis. A. Fold change obtained from RNA-seq analysis of 3 genes (CD24, Tenascin C and Lumican) of the pro-metastatic signature in Glo1-depleted MDA-MB-231 compared to control. **B.** qRT-PCR analysis confirmed the increase of CD24 and Tenascin C mRNA levels as well as the decrease of Lumican mRNA level in Glo1-depleted cells. RNA-seq analysis and validation were performed on distinct RNA isolations. **C.** Lumican mRNA level in Glo1-depleted MDA-MB-231 cells treated with aminoguanidine (0-10-20 mM) during 3 days. **D.** MG-H1 accumulation in MDA-MB-231 cells treated with aminoguanidine (0-10-20 mM) during 3 days using western blot. Immunoblotted data were quantified by densitometric analysis and normalized for β-actin. Data are represented as mean ± SEM of three independent experiments. * $p<0.05$, ** $p<0.01$, *** $p<0.001$.

silencing. Thus the molecular changes occurring in Glo1-depleted breast cancer cells are in good accordance with our previous results linking Glo1 inhibition to tumor growth and metastasis development. We found 140 and 120 significantly modulated genes linked to migration and adhesion processes in shGlo1#1 and #2, respectively. We regrouped the 188 modulated genes linked to cell adhesion and migration, under the name of the pro-metastatic signature of Glo1-depleted cells. A heatmap representing the 47 common genes from the pro-metastatic signature is shown in Figure 1B. Among these genes, we selected 2 candidates *CD24* and *Tenascin C* as well as a third one, *Lumican*, related to extracellular matrix organization biological process (Figure 2A). RT-qPCR analyses were performed to confirm the expression level of these up- or down-regulated genes on independent mRNA samples of Glo1-silenced MDA-MB-231 cells. As shown in Figure 2B, CD24 and Tenascin C mRNA

A.

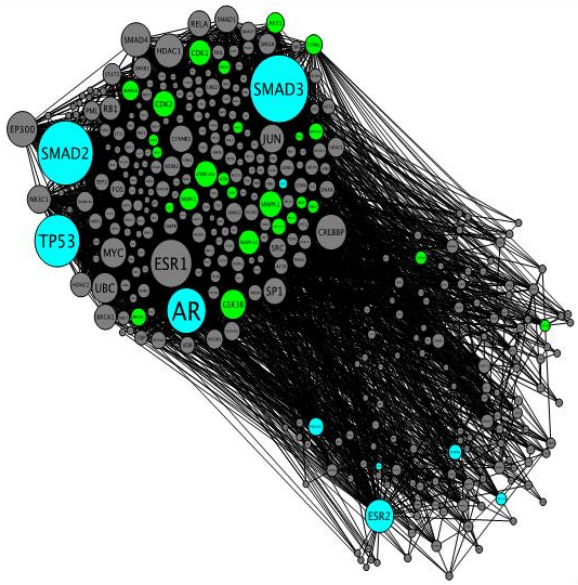

B.

Module	Pathway	Number of genes in network	Number of genes in pathway	p-value
1	**TGFβ signaling pathway**	23	80	< 0.001
2	Coregulation of androgen receptor activity	11	60	< 0.001
3	Glucocorticoid receptor regulatory network	18	77	< 0.001
4	Progesterone-mediated oocyte maturation	12	89	< 0.001
5	p53 pathway	4	57	< 0.001

C.

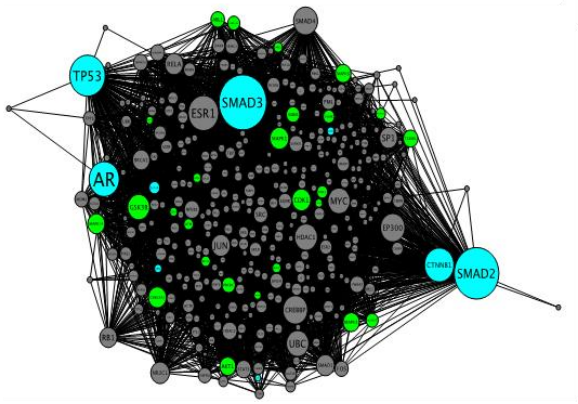

D.

Module	Pathway	Number of genes in network	Number of genes in pathway	p-value
1	**TGFβ signaling pathway**	20	80	< 0.001
2	Glucocorticoid receptor regulatory network	21	77	< 0.001
3	Signaling by ERBB2	19	155	< 0.001
4	p53 pathway	13	57	< 0.001

Figure 3: Transcriptional network associated to the pro-metastatic signature. **A** and **C.** Schematic representation of the transcriptional network significantly associated to the pro-metastatic signature in shGlo1#1 (A) and shGlo1#2 (C) compared to control MDA-MB-231 cells. The nodes represent proteins in the network. The nodes are coloured in cyan when the protein is a transcription factor, in grey when the protein has significant interactions with the identified transcription factors or in green when the protein is a kinase/phosphatase having substrates that are enriched in the network. The size of the nodes depends on how many interactions each node has within the network (node degree). **B** and **D.** List of pathway significantly and with the highest score associated to the pro-metastatic signature for shGlo1#1 (B) and #2 (D). TGFβ signalling pathway components and especially Smad3 represent the major regulator of the pro-metastatic genes in both Glo1-depleted cells.

levels were significantly increased in Glo1-depleted cells while the mRNA level of Lumican was significantly decreased in these cells. Interestingly, the treatment of shGlo1#1 cells with the MG scavenger aminoguanidine reverted Lumican decreased expression to its basal level (Figure 2C). However, aminoguanidine had no effect on Lumican expression in shGlo1#2 (Figure 2C) while aminoguanidine decreased the global level of MG-H1 adducts in these cells (Figure 2D).

Pro-metastatic signature is mediated through Transforming Growth Factor β (TGFβ) signaling pathway in Glo1-depleted cells. In order to determine which molecular pathways are involved in the pro-metastatic signature observed in Glo1-silenced MDA-MB-231 cells, we performed an *in silico* pathway analysis as described under Materials and Methods section. A significant association with the highest score was found for both shGlo1 clones between the 188 genes of the pro-metastatic signature candidate genes and TGFβ signaling pathway (Figure 3A, B, C and D). Among the TGFβ pathway components, Smad3 appeared to be the master regulator of the pro-metastatic signature.

High endogenous MG level increases migratory and invasiveness abilities of breast cancer cells *in vitro*. To explore further the functional aspects of the pro-metastatic signature in Glo1-depleted cancer cells, we performed migration, invasion and adhesion assays. Glo1 silencing significantly increased up to 2.5 fold the migratory ability of MDA-MB-231 cells (Figure 4A and B). The pre-treatment (3 days) with the MG scavenger aminoguanidine decreased the migratory capacity of Glo1-depleted cells to its basal level (Figure 4A and B). These results suggest that increased MG level induced by Glo1 silencing is responsible of the enhanced migratory ability of MDA-MB-231 cells. As shown in Figure 4C, Glo1-depleted cells also showed a significantly increased invasiveness in invasion assays that was efficiently blocked by aminoguanidine pre-treatment. We next analyzed the capacity of Glo1-silenced MDA-MB-231 cells to adhere on collagen, an important component of the extracellular matrix. After 1h, the attachment of shGlo1 cells was significantly reduced compared to control cells (Figure 4E and F). Altogether our data indicate that Glo1 depletion in breast cancer cells resulted in increased migration and invasion and reduced adhesion responses that are compatible with the acquisition of a pro-metastatic phenotype.

DISCUSSION

In this study, we report for the first time that carbonyl stress modulates expression of genes implicated in migration and adhesion processes in cancer cells, potentially through a regulation of the TGFβ signaling pathway.

Metastasis formation is a multistep process where cancer cells breakthrough the basement membrane, enter and resist in the circulation, extravasate in a new organ and proliferate again. In this study, we demonstrated that carbonyl stress enhanced migratory and invasive potential of breast cancer cells. Increased motility and invasiveness are important features of cancer cells to metastasize. Our results also indicate that adhesion to extracellular matrix substrate is affected by MG. Loss of cellular adhesion is the first step of cancer cells in the metastatic process while adhesion to endothelial cells is essential for homing and extravasation of circulating cancer cells [14,15]. Diverse alterations in attachment abilities allow cancer cells to disobey the rules of tissue architecture

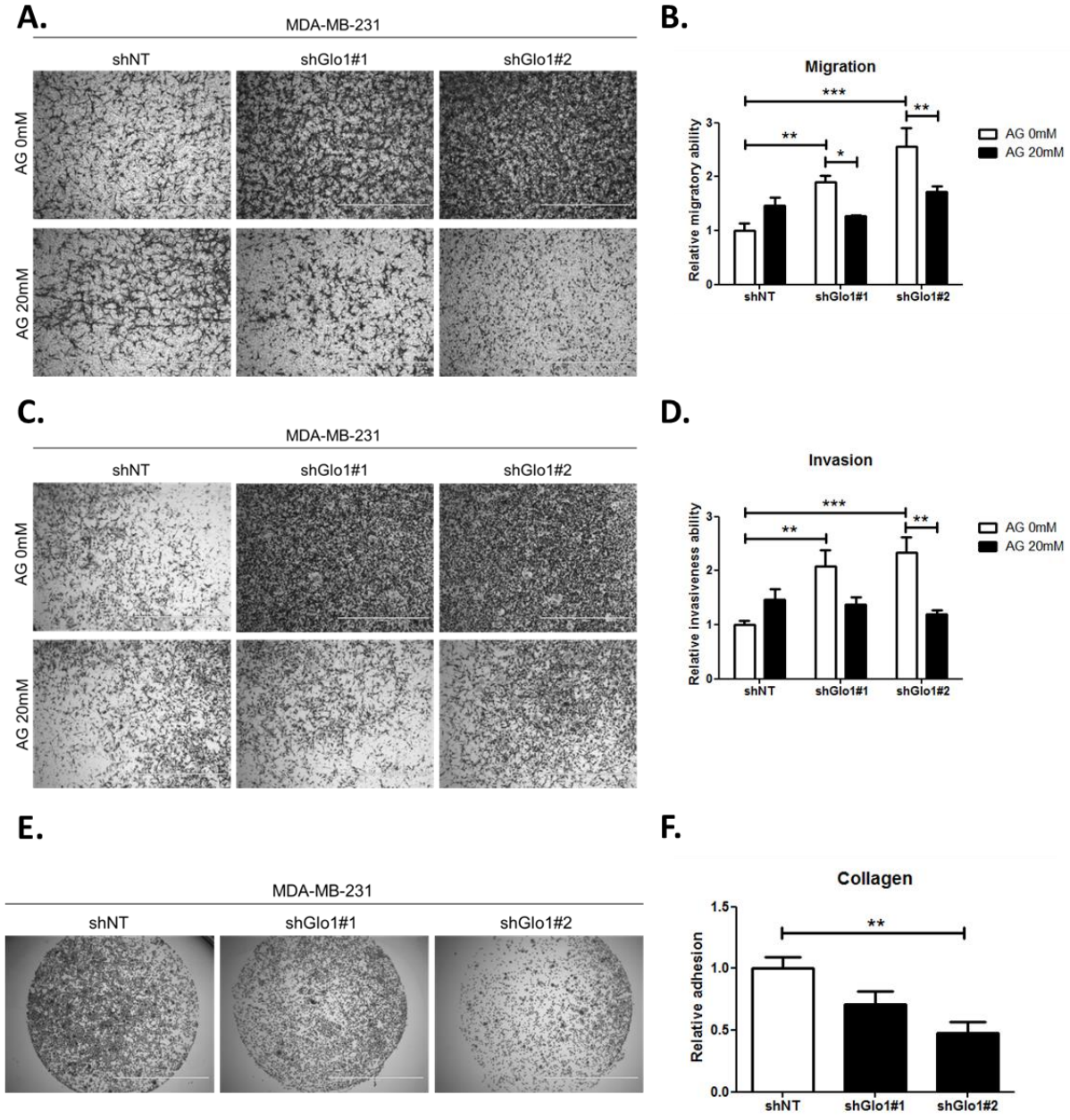

Figure 4: High endogenous MG level increases migratory and invasiveness abilities of breast cancer cells *in vitro*. A. Increased number of migrating cells after 16h of migration toward serum in Go1-depleted MDA-MB-231 cells. Aminoguanidine treatment (20mM) 3 days before migration assay reversed migratory capacity enhancement in shGlo1 cells. White bar represent 1mm. **B.** Quantification of panel A according to the area covered by cells. **C**. Increased number of invading cells after 24h of invasion through matrigel coated insert in Go1-depleted MDA-MB-231 cells. Aminoguanidine treatment (20mM) 3 days before invasion assay reversed invasiveness capacity enhancement in shGlo1 cells. White bar represent 1mm. **D.** Quantification of panel B according to the area covered by cells. **E.** Decreased number of attached cells to collagen after 1h in Glo1-silenced conditions compared to control. White bar represent 2mm. **F.** Quantification of panel E. Data are represented as mean ± SEM of three independant experiments. * p<0.05, ** p<0.01, *** p<0.001.

and to advance in their malignant progression [16]. Depending on time and location context during the metastatic process, adhesion properties of cancer cells can be increased or decreased. It could be interesting to analyze the adhesion capacity of cancer cells at different steps of the metastatic process (primary tumor, circulating and metastasis) and to correlate it with MG levels.

Metastasis is the final step of tumor progression and could be responsible for up to 90% of deaths associated with solid tumors [17]. It has been demonstrated that metastasis formation is not a random

process. For example, breast cancer cells preferentially colonize bones, lungs, liver and brain. Therefore, specific mutations or signaling pathways regulate the acquisition of the metastatic phenotype and the choice of the target organs. TGFβ signaling pathway has been implicated in the dissemination of cancer cells into the body (for review [18]). However, the role of TGFβ signaling pathway is controversial. Indeed, this pathway is considered as a tumor promoting pathway. Increased expression of TGFβ has been correlated with tumor progression [19-22]. In contrast, several studies demonstrated that some components of TGFβ pathway are inactivated through mutation or deletion in several cancer types [23-26]. In breast cancer, few mutations of the key components of the TGFβ pathway have been reported suggesting that this pathway could procure a selective advantage to these cancer cells [18]. In particular, TGFβ pathway activation has been associated with lung and bone metastasis [27,28]. Minn and colleagues established a TGFβ response signature comprising a set of genes whose expression changes upon TGFβ treatment. Interestingly, this signature correlated with lung metastasis development in breast cancer patients [29]. Among the genes in this TGFβ response signature, *Tenascin C* was one of the most regulated genes. Therefore, it is tempting to hypothesize that MG, by regulating key components of the TGFβ signaling pathway such as Smad3, could be an important regulator of the metastatic process. Further experiments are required to understand the molecular mechanism(s) through which MG could regulate TGFβ pathway signalization.

MATERIALS AND METHODS

Cell culture. Human breast cancer cell line MDA-MB-231 was obtained from the American Type Culture Collection (ATCC). Cells were cultured in DMEM (Lonza) containing 10% fetal bovine serum (FBS, ThermoFisher Scientific) and 2mM of L-glutamine (Lonza) and grown in an incubator at 37°C with 5% CO_2.

Aminoguanidine (AG) treatment. The MG scavenger, aminoguanidine, was obtained from Sigma-Aldrich. Glo1-depleted MDA-MB-231 cells were treated with AG 10 and 20mM 3 days with refreshing medium every day.

RNA sequencing analysis. RNA libraries and sequencing were performed on total RNA samples at the GIGA Genomics facility, University of Liège, Belgium. Three biological replicated of each clones (shNT, shGlo1#1 and shGlo1#2) were analyzed. The quality of RNA was checked with BioAnalyser 2100 (Agilent technologies, CA, USA) that indicated a RQI score >8. The libraries were prepared with Truseq® mRNA Sample Prep kit (Illumina, CA, USA) from 1 microgram of total RNA following manufacturer's instructions. mRNAs were isolated by poly-A selection and fragmented (8 minutes at 94°C). Fragmented mRNAs (around 170 nucleotide-long in average) were used for reverse-transcription in the presence of Superscript II (Invitrogen, Oregon, USA) and random primers. After second strand synthesis, end-repair, Atailing and purification, the double strand cDNA fragments were ligated to Truseq® adapters containing the index sequences. Fifteen cycles of PCR in the presence of dedicated PCR primers and PCR master mix were applied to generate the final libraries. Libraries were sequenced in pair-end sequencing runs on the Illumina NextSeq500 in multiplexed 2 × 76 base protocols. The raw data was generated through CASAVA 1.6 suite (Illumina). TopHat (http://ccb.jhu.edu/software/tophat/index.s

html) software was used to align RNA-Seq reads to the reference genome (hg19, UCSA) and discover transcript splice sites. Cufflinks (http://cole-trapnelllab.github.io/cufflinks/) used the resulting alignment files to quantify the gene expression levels, identify up- and down-regulated transcripts. Lists of genes differentially expressed were imported in the ToppGene Suite for analysis [30].

RNA extraction and quantitative reverse transcription-PCR (qRT-PCR). RNAs from cultured cells were isolated using the NucleoSpin RNA kit (Macherey-Nagel) according to manufacturer's protocol. Reverse transcription was done using the RevertAid First Strand cDNA Synthesis Kit (ThermoFisher Scientific). One or three (for CD24) hundred ng of cDNA were mixed with primers, probe (Universal ProbeLibrary System, Roche) and 2x Takyon Master Mix (Eurogentec). Q-PCR experiments were performed using the 7300 Real Time PCR System and the corresponding manufacturer's software (Applied Biosystems). Relative gene expression was normalized to 18S rRNA. Primers were synthesized by IDT and their sequences are detailed in Supplementary Table S1. All data are presented as the mean ± SEM of four independent experiments.

Western Blot. Cells were extracted in SDS 1% buffer containing protease and phosphatase inhibitors (Roche). Protein concentrations were determined using the bicinchoninic acid assay (Pierce). Thirty µg of proteins were separated by 10% SDS-PAGE and transferred to PVDF membranes. After blocking in TBS-Tween 0.1% containing 5% nonfat dried milk (Bio-Rad), membranes were incubated with primary antibodies overnight at 4°C. Anti-MG-H1 antibody (3D11, 1/2000) and anti-β-actin antibody (1/5000) were purchased from Cell Biolabs and Sigma-Aldrich, respectively. Then, the membranes were exposed to anti-mouse secondary antibody (Dako) at RT for 1 hour. The immunoreactive bands were visualized using ECL Western Blotting substrate (Pierce). Immunoblots were quantified by densitometric analysis and normalized for β-actin using ImageJ software [31].

Driving signaling networks. The driving signaling networks were established in collaboration with Prof. Steven van Laere (Antwerp University, Belgium) as previously described [32]. Briefly, a phenome-interactome network was constructed and used to calculate an association score for each candidate gene from RNA sequencing data. Then, association between candidate genes and potential regulators were ranked according to their scores. The phenome-interactome network is established by integrating a phenotype similarity profile, a protein-protein interactions (PPI) network and known association between genes and diseases [32].

Migration and invasion assays. MDA-MB-231 cells ($2x10^5$ cells) were suspended in serum-free DMEM medium (0.1% BSA, 1% penicillin/streptomycin) and seeded into the upper part of a Transwell filter (diameter 6.5mm, pore size 8µm, Costar) for migration assay or a Transwell filter precoated with Matrigel for invasion assay (BD Biosciences). The lower compartment was filled with an attracting medium composed of DMEM containing 1% BSA, 1% pen/strep and 10% BSA. After 16 or 24 hours incubation at 37°C for migration and invasion, respectively, migrating cells were fixed and stained with Diff-Quick kit (Medion Diagnostics). Each insert were scanned at a 10X magnification using the Eclipse Ti microscope (Nikon). The area covered by the migrating/invading cells was further quantified by densitometry using the

ImageJ software. Data are expressed as relative migration/invasion ability compared to control cells. Three biological replicates with two wells per condition were analyzed.

Adhesion assay. Twenty thousand MDA-MB-231 cells were placed in pre-coated 96-well low adherent plate (Greiner) and let to adhere for 1 hour at 37 °C. The coating of the wells was performed using 10µl of collagen (Sigma-Aldrich, 10 µg/ml). Plates were incubated 16h at 4°C and then dried at room temperature. Each well was blocked with a Tris 0.1M pH 7.8 and 1% BSA solution. Subsequently, the cells were washed with PBS and fixed in a 0.5% crystal violet in 20% methanol solution for 5 minutes. Stained cells were rinsed with water and air-dried. Pictures of each insert were taken at a 2X magnification using the EVOS microscope (ThermoFisher Scientific). The colored cells were lysed in 1:1 mixture of absolute ethanol and 0.1M Na-citrate buffer. The cell attachment was evaluated using the Filter Max F5 plate reader (Molecular Devices) at 560 nm. All data are presented as the mean ± SEM of three biological replicates.

REFERENCES

1 Richard, J. P. Mechanism for the formation of methylglyoxal from triosephosphates. *Biochemical Society transactions* **21**, 549-553 (1993).

2 Lo, T. W., Westwood, M. E., McLellan, A. C., Selwood, T. & Thornalley, P. J. Binding and modification of proteins by methylglyoxal under physiological conditions. A kinetic and mechanistic study with N alpha-acetylarginine, N alpha-acetylcysteine, and N alpha-acetyllysine, and bovine serum albumin. *The Journal of biological chemistry* **269**, 32299-32305 (1994).

3 Rabbani, N. & Thornalley, P. J. Methylglyoxal, glyoxalase 1 and the dicarbonyl proteome. *Amino acids* **42**, 1133-1142, doi:10.1007/s00726-010-0783-0 (2012).

4 Chiavarina, B. *et al.* Triple negative tumors accumulate significantly less methylglyoxal specific adducts than other human breast cancer subtypes. *Oncotarget* **5**, 5472-5482 (2014).

5 van Heijst, J. W., Niessen, H. W., Hoekman, K. & Schalkwijk, C. G. Advanced glycation end products in human cancer tissues: detection of Nepsilon-(carboxymethyl)lysine and argpyrimidine. *Annals of the New York Academy of Sciences* **1043**, 725-733, doi:10.1196/annals.1333.084 (2005).

6 Zender, L. *et al.* An oncogenomics-based in vivo RNAi screen identifies tumor suppressors in liver cancer. *Cell* **135**, 852-864, doi:10.1016/j.cell.2008.09.061 (2008).

7 Sakamoto, H. *et al.* Selective activation of apoptosis program by S-p-bromobenzylglutathione cyclopentyl diester in glyoxalase I-overexpressing human lung cancer cells. *Clinical cancer research : an official journal of the American Association for Cancer Research* **7**, 2513-2518 (2001).

8 Zhang, S. *et al.* Glo1 genetic amplification as a potential therapeutic target in hepatocellular carcinoma. *International journal of clinical and experimental pathology* **7**, 2079-2090 (2014).

9 Cheng, W. L. *et al.* Glyoxalase-I is a novel prognosis factor associated with gastric cancer progression. *PloS one* **7**, e34352, doi:10.1371/journal.pone.0034352 (2012).

10 Hosoda, F. *et al.* Integrated genomic and functional analyses reveal glyoxalase I as a novel metabolic oncogene in human gastric cancer. *Oncogene* **34**, 1196-1206, doi:10.1038/onc.2014.57 (2015).

11 Antognelli, C., Mezzasoma, L., Fettucciari, K., Mearini, E. & Talesa, V. N. Role of glyoxalase I in the proliferation and apoptosis control of human LNCaP and PC3 prostate cancer cells. *The Prostate* **73**, 121-132, doi:10.1002/pros.22547 (2013).

12 Fonseca-Sanchez, M. A. *et al.* Breast cancer proteomics reveals a positive correlation between glyoxalase 1 expression and high tumor grade. *International journal of oncology* **41**, 670-680, doi:10.3892/ijo.2012.1478 (2012).

13 Santarius, T. *et al.* GLO1-A novel amplified gene in human cancer. *Genes, chromosomes & cancer* **49**, 711-725, doi:10.1002/gcc.20784 (2010).

14 Chambers, A. F., Groom, A. C. & MacDonald, I. C. Dissemination and growth of cancer cells in metastatic sites. *Nature reviews. Cancer* **2**, 563-572, doi:10.1038/nrc865 (2002).

15 Fidler, I. J. The pathogenesis of cancer metastasis: the 'seed and soil' hypothesis revisited. *Nature reviews. Cancer* **3**, 453-458, doi:10.1038/nrc1098 (2003).

16 Gupta, G. P. & Massague, J. Cancer metastasis: building a framework. *Cell* **127**, 679-695, doi:10.1016/j.cell.2006.11.001 (2006).

17 Hanahan, D. & Weinberg, R. A. Hallmarks of cancer: the next generation. *Cell* **144**, 646-674, doi:10.1016/j.cell.2011.02.013 (2011).

18 Padua, D. & Massague, J. Roles of TGFbeta in metastasis. *Cell research* **19**, 89-102, doi:10.1038/cr.2008.316 (2009).

19 Hasegawa, Y. *et al.* Transforming growth factor-beta1 level correlates with angiogenesis, tumor progression, and prognosis in patients with nonsmall cell lung carcinoma. *Cancer* **91**, 964-971 (2001).

20 Saito, H. *et al.* The expression of transforming growth factor-beta1 is significantly correlated with the expression of vascular endothelial growth factor and poor prognosis of patients with advanced gastric carcinoma. *Cancer* **86**, 1455-1462 (1999).

21 Tsushima, H. *et al.* High levels of transforming growth factor beta 1 in patients with colorectal cancer: association with disease progression. *Gastroenterology* **110**, 375-382 (1996).

22 Wikstrom, P., Stattin, P., Franck-Lissbrant, I., Damber, J. E. & Bergh, A. Transforming growth factor beta1 is associated with angiogenesis, metastasis, and poor clinical outcome in prostate cancer. *The Prostate* **37**, 19-29 (1998).

23 Levy, L. & Hill, C. S. Alterations in components of the TGF-beta superfamily signaling pathways in human cancer. *Cytokine & growth factor reviews* **17**, 41-58, doi:10.1016/j.cytogfr.2005.09.009 (2006).

24 Markowitz, S. *et al.* Inactivation of the type II TGF-beta receptor in colon cancer cells with microsatellite instability. *Science* **268**, 1336-1338 (1995).

25 Hahn, S. A. *et al.* Allelotype of pancreatic adenocarcinoma using xenograft enrichment. *Cancer research* **55**, 4670-4675 (1995).

26 Thiagalingam, S. *et al.* Evaluation of candidate tumour suppressor genes on chromosome 18 in colorectal cancers. *Nature genetics* **13**, 343-346, doi:10.1038/ng0796-343 (1996).

27 Siegel, P. M., Shu, W., Cardiff, R. D., Muller, W. J. & Massague, J. Transforming growth factor beta signaling impairs Neu-induced mammary tumorigenesis while promoting pulmonary metastasis. *Proceedings of the National Academy of Sciences of the United States of America* **100**, 8430-8435, doi:10.1073/pnas.0932636100 (2003).

28 Yin, J. J. *et al.* TGF-beta signaling blockade inhibits PTHrP secretion by breast cancer cells and bone metastases development. *The Journal of clinical investigation* **103**, 197-206, doi:10.1172/JCI3523 (1999).

29 Minn, A. J. *et al.* Genes that mediate breast cancer metastasis to lung. *Nature* **436**, 518-524, doi:10.1038/nature03799 (2005).

30 Chen, J., Bardes, E. E., Aronow, B. J. & Jegga, A. G. ToppGene Suite for gene list enrichment analysis and candidate gene prioritization. *Nucleic acids research* **37**, W305-311, doi:10.1093/nar/gkp427 (2009).

31 Schneider, C. A., Rasband, W. S. & Eliceiri, K. W. NIH Image to ImageJ: 25 years of image analysis. *Nature methods* **9**, 671-675 (2012).

32 Chen, Y., Jiang, T. & Jiang, R. Uncover disease genes by maximizing information flow in the phenome-interactome network. *Bioinformatics* **27**, i167-176, doi:10.1093/bioinformatics/btr213 (2011).

Supplementary Table 1: Primer sequences and probe used for qRT-PCR experiment.

Gene	Fw/Rv	Sequence	Probe (UPL, Roche)
CD24	Fw	5'-TGGATTTGACATTGCATTTGA -3'	37
	Rv	5'-TGGGGGTAGATTCTCATTCATC-3'	
Tenascin C	Fw	5'-CCGGACCAAAACCATCAGT-3'	76
	Rv	5'-GGGATTAATGTCGGAAATGGT-3'	
Lumican	Fw	5'-GAAAGCAGTGTCAAGACAGTAAGG-3'	72
	Rv	5'-GGCCACTGGTACCACCAA-3'	

IV. Discussion and perspectives

IV. Discussion and perspectives

Cancer cells prefer to use aerobic glycolysis rather than oxidative phosphorylation to produce their energy. The elevated glycolytic rate leads unavoidably to an increased MG production. This highly reactive dicarbonyl is mainly detoxified by glyoxalase enzymes into D-lactate. In our study, we have used a silencing Glo1 strategy that strongly suggested a pro-tumorigenic and pro-metastatic role of endogenous MG accumulation *in vivo*. Consistently, a study aimed at functionally identifying tumor suppressor genes in liver cancer identified and validated Glo1 as a tumor suppressor gene. Indeed, the knockdown of Glo1 using shRNAs increased tumor growth in a mouse model (Zender et al. 2008). However, in light of recent studies, Glo1 appears to be a dual mediator for growth regulation in cancer. In 2014, Glo1 knockdown using doxycycline-inducible shRNAs significantly reduced hepatocellular tumor volume in a xenograft mouse model (Zhang et al. 2014). Using intraperitoneal injection of BBGC (a Glo1 inhibitor), Sakamoto and colleagues (Sakamoto et al. 2001) demonstrated a significant decrease of lung and prostate cancer cell growth *in vivo*. As the only function reported to date for Glo1 is the detoxification of MG, both studies attributed tumor volume reduction to the cytotoxic and pro-apoptotic accumulation of MG in cancer cells. Indeed, it is noteworthy that MG was first viewed as a potential therapeutic agent in cancer based on animal studies (Apple and Greenberg 1967, Jerzykowski et al. 1970). Due to high adverse toxic effects of MG, another strategy using Glo1 inhibitors has been suggested for the treatment of cancer patients (Lo and Thornalley 1992, Edwards et al. 1996). In our study, the silencing of Glo1 in breast cancer cells also increased MG level but not to a toxic level. We have associated the increased pro-tumorigenic and pro-metastatic potential of Glo1-depleted breast cancer cells to the accumulation of MG because these effects were abrogated by carnosine. Therefore, long-term Glo1-targeting therapies may select for aggressive cancer cells that will acquire resistance to apoptosis. To experimentally validate this hypothesis, it would be interesting to design inducible Glo1-shRNAs in order to compare acute and chronic exposure of cancer cells to high endogenous MG stress.

We next hypothesized that MG follows a hormetic dose or adaptive stress response principle. Hormesis has been defined as “a process in which exposure to a

low dose of a chemical agent or environmental factor, that is damaging at higher doses, induces an adaptive beneficial effect on the cell or organism" (Figure 49A) (Mattson 2008). This concept was, at least in part, postulated in the 16th century when Paracelsus, the founder of toxicology, observed that "the dose makes the poison". Ongoing experiments conducted in our Laboratory showed that low doses of MG are stimulating and beneficial to the proliferation of cancer cells while at higher concentrations, MG becomes cytotoxic (Figure 49B). These observations have been made by growing U87-MG human glioblastoma cancer cells on the chicken chorioallantoic membrane (CAM assay) in presence of different concentrations of MG (Nokin et al., unpublished data). Ongoing mass spectrometry analysis will help to determine the mechanism(s) through which MG exhibits both pro and anti-tumor effects. In a non-tumoral context, MG dual role has been demonstrated for neurons where low MG levels are favorable to neurons viability and excitability while high MG levels are cytotoxic (Radu et al. 2012). In our hands, different cancer cell types (breast, brain and colon) presented with extreme values of inhibitory concentrations (IC50) ranging from 250 to 3000 µM of MG. These preliminary data suggest that different cancer types with diverse phenotype, particularly Glo1 detoxification abilities and energetic metabolic balance may respond differently to MG exposition. This hypothesis is supported by our observation that highly glycolytic cancer cells reacted to MG by increasing their basal expression and activity of Glo1 while non glycolytic cells did not. A large scale genomic study revealed that Glo1 is amplified in many human cancer cell lines and primary tumors with breast tumors (22%) showing the highest rate (Santarius et al. 2010). If this amplification is associated with high Glo1 expression/activity, it is tempting to speculate that the cells will be more resistant to MG accumulation. Accordingly, it has been demonstrated that cancer cells overexpressing Glo1 are more sensitive to Glo1 inhibition (Sakamoto et al. 2001, Santarius et al. 2010, Zhang et al. 2014). Therefore, Glo1 gene amplification might be a promising biomarker to discriminate those patients that would benefit from Glo1 inhibition therapies.

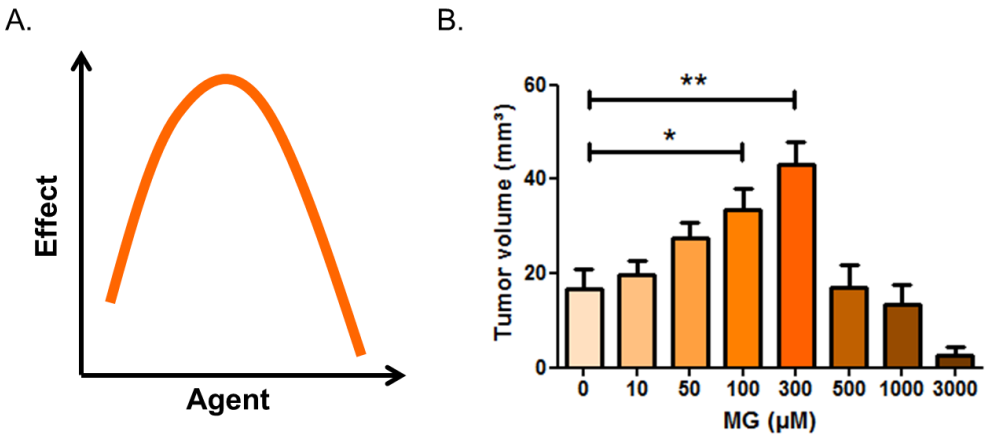

Figure 49: The hormetic model and MG. A. Theoretical graphical representation of the hormesis process where x axis correspond to the level of stressor and y axis correspond to the effect on cell or organism. Hormesis is defined as a biphasic dose response to an agent characterized by low dose stimulation or beneficial effects and high dose inhibitory or toxic effects. **B.** U87-MG cancer cells were grown on CAM and treated every day with different concentrations of MG. The graph of tumor volume against MG concentration adopts the curve profile of the hormetic model (Nokin et al., Unpublished data).

This dual role of MG stress reminds clearly the one established for oxidative stress in cancer cells. At low to moderate levels, Reactive Oxygen Species (ROS) facilitates carcinogenesis notably through acting as signaling molecules or by promoting oncogenic mutation of genomic DNA. At high levels, ROS induce severe cellular damage and cell death. Therefore, cancer cells develop a high antioxidant capacity that maintains ROS to a level beneficial for their proliferation and escape from apoptosis (for review (Gorrini et al. 2013)). Moreover, oxidative stress and carbonyl stress are tightly linked together and may work in tandem to influence tumor development and progression (Figure 50). The formation of ROS and AGEs generates a sequence of reactions mutually enhancing each other in cancer cells (for review, (Kalapos 2008)). Several groups have shown that MG treatment leads to an increase of the levels of various ROS in many cell types (Kalapos et al. 1993, Kikuchi et al. 1999, Du et al. 2001, Chang et al. 2005, Wu 2005). Additionally, overexpression of Glo1 decreased ROS formation in yeast (Morcos et al. 2008) and in human endothelial cells (Yao and Brownlee 2010). Globally, the increased production of ROS by MG has been associated with diabetes and its complications (Rosca et al. 2005, Yao and Brownlee 2010, Vulesevic et al. 2016). More largely, the glycation of proteins is also responsible of ROS generation (Yim et al. 1995, Shumaev et al. 2009). MG reacts with GSH and forms a hemithioacetal intermediate before its detoxification into D-lactate. MG can deplete the amount of GSH, a

powerful antioxidant, at least during short periods of time (Kalapos et al. 1992). As mitochondria are the major source of ROS in cells, increased ROS formation induced by MG could be explained by direct glycation and alteration of mitochondrial respiratory chain proteins (Rosca et al. 2005, Morcos et al. 2008). An inhibition of the activity of antioxidant enzymes such as catalase and superoxide dismutase (SOD) has been shown upon MG treatment in different models (Choudhary et al. 1997, Wu 2005). SOD was found to be highly susceptible to carbonyl-mediated glycation (Arai et al. 1987, Takamiya et al. 2003). Furthermore, ROS are known to favor glucose uptake notably through HIF1α activation and the subsequent increase of glucose transporters expression (Shi et al. 2009, Liemburg-Apers et al. 2015). This increased glycolytic flux inevitably leads to MG production. In cancer cells, the tight control of this vicious cycle between MG and ROS likely may favor tumor progression and metastases development.

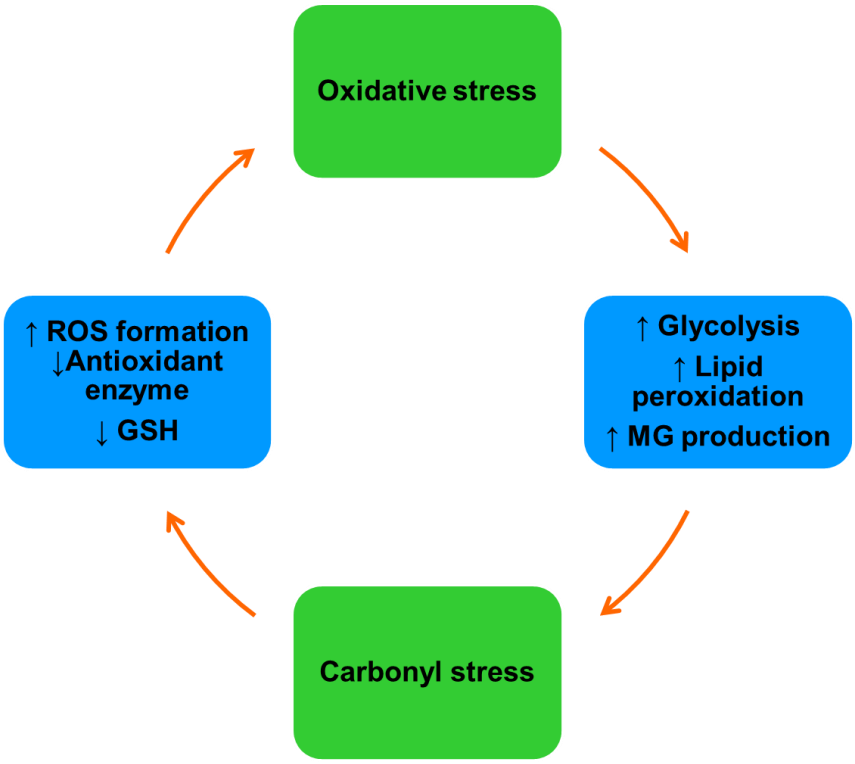

Figure 50: Oxidative stress and carbonyl stress generate a sequence of reactions mutually enhancing each other.

Recent studies indicate that metabolic energy pathways interfere with major signalization routes in cancer cells (DeRan et al. 2014, Enzo et al. 2015). Our data demonstrated for the first time that MG, an endogenously produced metabolite, interferes with the Hippo pathway to confer an aggressive phenotype upon cancer cells. In agreement with this new linked established between carbonyl stress and oncogenic signaling pathways, it is noteworthy that activation of TGFβ pathway components such as Smad3 were observed by high-throughput sequencing analysis of high carbonyl stress cancer cells. The identification and validation of the key target genes affected by MG will contribute to a better understanding of the molecular mechanisms leading the acquisition of a metastatic phenotype by cancer cells exposed to carbonyl stress.

Because MG has been reported to glycate several enzymes involved in glycolysis (Gomes et al. 2006), it was expected that it may affect the glycolytic flux. We observed that high carbonyl stress decreased pyruvate kinase M2 (PKM2) activity in breast cancer cells (Nokin et al., unpublished data). PKM2 acts as a central hub for determining whether glucose is used for ATP generation or building blocks synthesis. It will be critical to understand how MG could favor mitochondrial respiration or the pentose phosphate pathway and to identify the potential direct targets of MG glycation in this context.

Identifying MG-modified proteins in cancer cells represents a major challenge. Our data have shown that MG adducts accumulation is a constant feature of breast cancer cells when compared to non-tumoral counterparts. Our next objective will be to identify MG-modified proteins associated with malignancy. Until now, only Hsp27 has been identified as a target of MG in different cancer cell types. Hsp27 is considered as the major argpyrimidine-modified protein and its MG-modification has been associated with inhibition of apoptosis in cancer cells (Sakamoto et al. 2002, van Heijst et al. 2006, Bair et al. 2010, Oya-Ito et al. 2011). In our study, we observed MG-modifications on Hsp90 and its subsequent decreased activity in breast cancer cells. Hsp90 is overexpressed in several cancer types and is implicated in the correct folding and activity of more than 400 “clients”, many of which are oncoproteins. Our results indicate that LATS1 kinase expression is indirectly affected by MG and suggest that the activity of other kinases may also be regulated under high carbonyl stress conditions. Besides Hsp27 and Hsp90, one may speculate that protein

chaperones could be preferentially targeted by MG. Interestingly, immunohistochemical staining of MG adducts in breast cancer tissues highlighted their accumulation in the nucleus. Cytoplasmic/nuclear protein extraction of different cancer cell lines confirmed the high level of both argpyrimidine and MG-H1 adducts in the nuclear fraction. These results are in good accordance with a previous study showing argpyrimidine adducts in the nucleus of neurons (Nakadate et al. 2009). In order to identify the nuclear MG-modified proteins, we performed immunoprecipitation of nuclear extracts from cancer cells using anti-argpyrimidine antibody followed by mass spectrometry analysis. Our preliminary results suggest that important regulators of mRNA splicing could be targets of MG glycation (Nokin et al., unpublished data). Since the last decade, the role of alternative splicing in cancer has gained an increased interest (Chen and Weiss 2015). To our knowledge, the regulation of the splicing machinery by a glycolytic intermediate has never been demonstrated. Globally, the identification of MG-modified proteins in cancer will contribute to our understanding of the pro- and anti-tumor roles of MG.

Obesity and diabetes represent an alarming global epidemic. In 2014, it has been estimated that over 600 million and 422 million adults were obese and diabetic, respectively, worldwide (World Health Organization). There is growing body of evidence to support a connection between diabetes (principally type 2), obesity and cancer. Both obesity and diabetes have been shown to be associated with increased risk of cancer and mortality (LeRoith et al. 2008). As mentioned previously, the link between carbonyl stress with diabetes and its complications is clearly established (Schalkwijk 2015). Obesity is also more and more associated with carbonyl stress. Indeed, a decrease of Glo1 activity in erythrocytes as well as an increase of MG concentration in whole blood was found in leptin-deficient obese mice compared to controls (Atkins and Thornalley 1989). In visceral adipose tissue of high fat diet feeding mice, an increase of MG level associated with a decrease of Glo1 activity have been demonstrated. These effects were reverted by treatment with MG scavenger pyridoxamine (Maessen et al. 2016). High fat diet feeding of rats increased body weight and serum MG-adducts level (Li et al. 2005). In human, Glo1 gene was added to the obesity gene map updated in 2005 (Rankinen et al. 2006). Incubation of adipocytes with MG results in an increased proliferation rate suggesting that MG carries on the expansion of adipose tissue in obesity (Jia et al. 2012).

Plasma MG concentration was increased of about 35% in obese subjects compared to non-obese healthy subjects placed on an isocaloric diet for 2 weeks (Masania et al. 2016). Interestingly, these MG levels were intermediate between those found in non-obese healthy subjects and type 2 diabetic patients (Rabbani and Thornalley 2014). In obese subjects, the increase of circulating MG could be responsible of protein and DNA glycation throughout the body thus creating a breeding ground for diabetic complications and cancer progression.

Recent studies indicated that cancer in diabetic patients presents with a higher incidence and a poorer prognosis than in non-diabetic subjects (for review (Garg et al. 2014). The association between diabetes and cancer risk and/or mortality was notably shown for breast cancer patients (Michels et al. 2003, Wolf et al. 2006, Larsson et al. 2007, Barone et al. 2008, Duggan et al. 2011, Erickson et al. 2011, De Bruijn et al. 2013). The increased cancer risk has been related to: (a) hyperglycemia, (b) hyperinsulinemia and (c) inflammation linked to increased visceral fat (for review (Gallagher and LeRoith 2015)). Due to the high avidity of cancer cells for glucose, **hyperglycemia** could have an additive effect on tumor growth and progression. Hyperglycemia could also contribute to AGEs formation. Through interaction with the receptor for AGEs (RAGE) present at the surface of cancer cells, AGEs lead to oxidative stress and inflammation which promote tumor growth, angiogenesis and metastasis (Rojas et al. 2011). **Hyperinsulinemia** associated with diabetes could impact upon tumor growth either directly through the activation of insulin-mediated proliferation signaling pathways or indirectly by increasing levels of bioactive insulin growth factor 1, a growth-promoting factor in cancer. **Adipocytes release a range of pro-inflammatory cytokines** such as TNF-α and IL-6. IL-6 has notably been linked to the transformation of breast cancer cells to a more invasive phenotype (Iliopoulos et al. 2009). Both excess of adiposity and insulin resistance may lead to increased levels of free hormones (estrogens and testosterone) which favor tumor growth (Gallagher and LeRoith 2015).

Recent studies reported that anti-diabetic therapies might also modify the risk of cancer (Quinn et al. 2013). Metformin is the most commonly used hypoglycemic therapy in patients with type 2 diabetes. It is noteworthy that diabetic patients treated with metformin have a lower risk of cancer development. Metformin decreased about 20% the incidence of invasive breast cancer compared to other diabetic medications

in type 2 diabetes patients (Bosco et al. 2011). The anti-tumor properties of metformin raised the possibility of its potential use in the non-diabetic population. Indeed, there are currently more than 100 ongoing clinical trials assessing the role of metformin for cancer prevention and therapy (Kasznicki et al. 2014). Metformin may reduce tumor progression by improving systemic metabolism through lowering circulating insulin and glucose levels, or by direct effects on cancer cells. These latters were mainly associated with metformin-mediated inhibition of mitochondrial complex 1 of the respiratory chain, decrease of ATP synthesis and activation of AMP kinase (AMPK). The potent activation of AMPK leads to the inhibition of mTOR pro-proliferation signaling pathway in cancer cells (Chiang and Abraham 2007). Remarkably, Ishibashi and co-workers have shown that metformin inhibits AGE/RAGE effects on tumor cell proliferation by suppressing RAGE expression (Ishibashi et al. 2013). Although metformin proved efficient to reduce systemic MG levels in diabetic patients (Beisswenger et al. 1999), it has been somehow overlooked for its MG scavenging capacities. Recently, carnosine, another MG scavenger, has also been reported to exert anti-tumoral effects (Shen et al. 2014). In our second study, we have shown that the sole supplementation with carnosine significantly lowered the propensity of high MG stress-tumors to metastasize in animals. Our *in vitro* experiments using both carnosine and aminoguanidine provided with an original molecular mechanism implicating MG-mediated induction of YAP oncogenic activity in breast cancer cells. Interestingly, DeRan and collaborators reported that metformin, and its more potent analog phenformin, inhibited YAP activity through AMPK signaling (DeRan et al. 2014). Accordingly, it is not excluded that metformin could have also exerted, at least in part, its inhibitory activity on YAP function through its MG scavenging properties. A multidisciplinary approach is needed to explore the molecular bases that support increased cancer risk for diabetic patients. More studies on the induction of diabetes by specific anti-neoplastic treatments should also be conducted.

Several studies reported that Glo1 expression and activity are increased in different cancer cell types compared to their non-tumoral counterparts (Ranganathan and Tew 1993, Rulli et al. 2001, Wang et al. 2012, Hu et al. 2014). Glo1 has also been considered as a bad prognosis marker (Romanuik et al. 2009, Bair et al. 2010, Cheng et al. 2012, Fonseca-Sanchez et al. 2012). Glo1 overexpression has also

been associated with multidrug resistance in cancer. In response to some anti-tumor agents, cancer cells activate processes of DNA repair which depletes cells of NAD^+, a cofactor for GAPDH enzymatic activity, and increases levels of glycolytic triosephosphates (Godbout et al. 2002). As MG is mainly formed by triosephosphate spontaneous degradation, a consequent dramatic cytotoxic accumulation of MG is expected. However, in response to MG accumulation, aggressive cancer cells increase Glo1 expression/activity which maintains MG at a subtoxic level thus favoring their resistance to chemotherapeutic agents. Remarkably, the combination of chemotherapy and Glo1 inhibitors significantly sensitized chemo-resistant leukemic cells to anti-tumor agents such as Etoposide (Sakamoto et al. 2000). Before starting clinical trials using Glo1 inhibitors, more work is needed to better understand in which specific conditions they could synergize with the cytotoxic activity of anti-tumor drugs by increasing MG concentration in cancer cells.

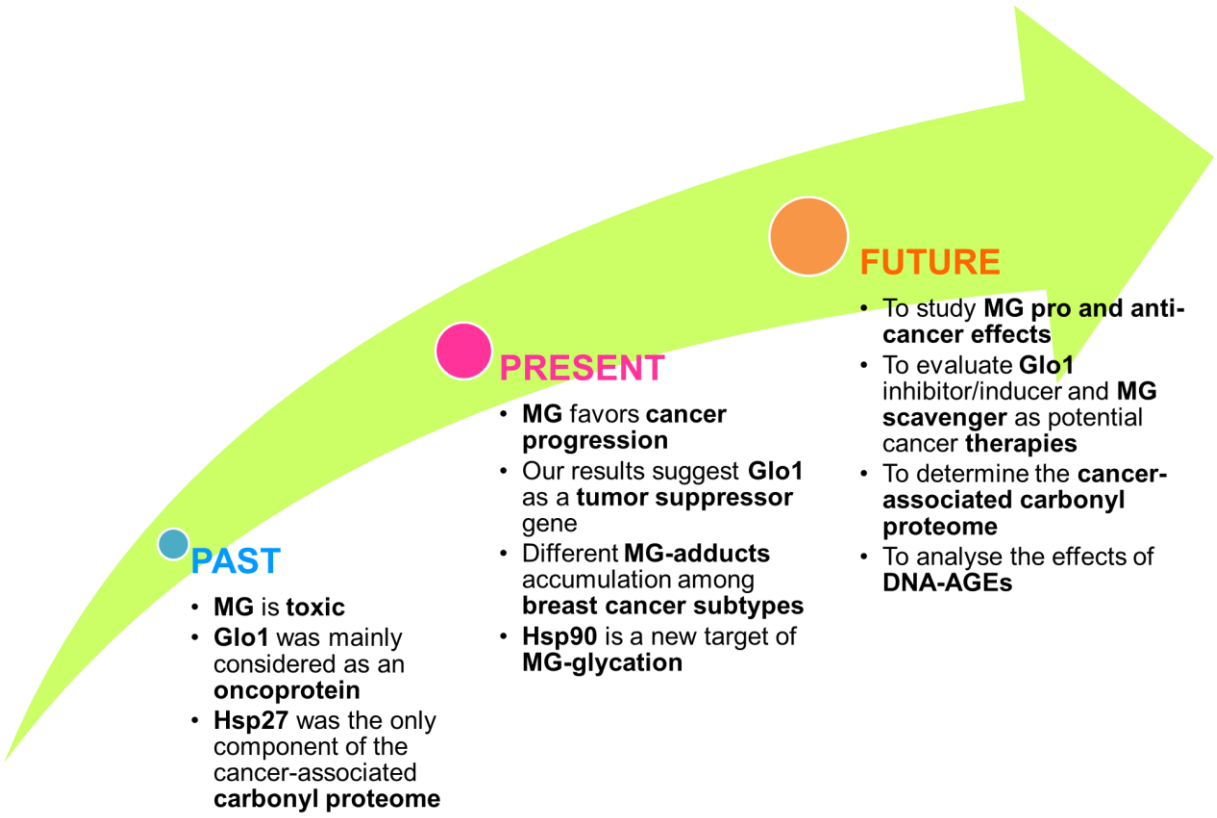

Figure 51: MG and Glo1 in cancer, a summary of what was known at the start of this thesis (past), what we contributed with our original data (present) and what represents the perspectives (future).

In conclusion, going from the existing information available at the start of my thesis and based on the original data that we have generated, new perspectives (Figure 51) are opened up to pursue our contribution to the exciting field of carbonyl stress and cancer.

V. References

V. References

Abordo, E. A., H. S. Minhas and P. J. Thornalley (1999). "Accumulation of alpha-oxoaldehydes during oxidative stress: a role in cytotoxicity." Biochem Pharmacol **58**(4): 641-648.

Ahmed, M. U., E. Brinkmann Frye, T. P. Degenhardt, S. R. Thorpe and J. W. Baynes (1997). "N-epsilon-(carboxyethyl)lysine, a product of the chemical modification of proteins by methylglyoxal, increases with age in human lens proteins." Biochem J **324 (Pt 2)**: 565-570.

Ahmed, M. U., S. R. Thorpe and J. W. Baynes (1986). "Identification of N epsilon-carboxymethyllysine as a degradation product of fructoselysine in glycated protein." J Biol Chem **261**(11): 4889-4894.

Ahmed, N., U. Ahmed, P. J. Thornalley, K. Hager, G. Fleischer and G. Munch (2005). "Protein glycation, oxidation and nitration adduct residues and free adducts of cerebrospinal fluid in Alzheimer's disease and link to cognitive impairment." J Neurochem **92**(2): 255-263.

Ahmed, N., O. K. Argirov, H. S. Minhas, C. A. Cordeiro and P. J. Thornalley (2002). "Assay of advanced glycation endproducts (AGEs): surveying AGEs by chromatographic assay with derivatization by 6-aminoquinolyl-N-hydroxysuccinimidyl-carbamate and application to Nepsilon-carboxymethyl-lysine- and Nepsilon-(1-carboxyethyl)lysine-modified albumin." Biochem J **364**(Pt 1): 1-14.

Ahmed, N., R. Babaei-Jadidi, S. K. Howell, P. J. Beisswenger and P. J. Thornalley (2005). "Degradation products of proteins damaged by glycation, oxidation and nitration in clinical type 1 diabetes." Diabetologia **48**(8): 1590-1603.

Ahmed, N., D. Dobler, M. Dean and P. J. Thornalley (2005). "Peptide mapping identifies hotspot site of modification in human serum albumin by methylglyoxal involved in ligand binding and esterase activity." J Biol Chem **280**(7): 5724-5732.

Ahmed, N. and P. J. Thornalley (2002). "Chromatographic assay of glycation adducts in human serum albumin glycated in vitro by derivatization with 6-aminoquinolyl-N-hydroxysuccinimidyl-carbamate and intrinsic fluorescence." Biochem J **364**(Pt 1): 15-24.

Ahmed, N., P. J. Thornalley, J. Dawczynski, S. Franke, J. Strobel, G. Stein and G. M. Haik (2003). "Methylglyoxal-derived hydroimidazolone advanced glycation end-products of human lens proteins." Invest Ophthalmol Vis Sci **44**(12): 5287-5292.

Ahmed, U., D. Dobler, S. J. Larkin, N. Rabbani and P. J. Thornalley (2008). "Reversal of hyperglycemia-induced angiogenesis deficit of human endothelial cells by overexpression of glyoxalase 1 in vitro." Ann N Y Acad Sci **1126**: 262-264.

Al-Abed, Y., H. Liebich, W. Voelter and R. Bucala (1996). "Hydroxyalkenal formation induced by advanced glycosylation of low density lipoprotein." J Biol Chem **271**(6): 2892-2896.

Alderson, N. L., M. E. Chachich, N. N. Youssef, R. J. Beattie, M. Nachtigal, S. R. Thorpe and J. W. Baynes (2003). "The AGE inhibitor pyridoxamine inhibits lipemia and development of renal and vascular disease in Zucker obese rats." Kidney Int **63**(6): 2123-2133.

Alimova, I. N., B. Liu, Z. Fan, S. M. Edgerton, T. Dillon, S. E. Lind and A. D. Thor (2009). "Metformin inhibits breast cancer cell growth, colony formation and induces cell cycle arrest in vitro." Cell Cycle **8**(6): 909-915.

Amicarelli, F., S. Colafarina, F. Cattani, A. Cimini, C. Di Ilio, M. P. Ceru and M. Miranda (2003). "Scavenging system efficiency is crucial for cell resistance to ROS-mediated methylglyoxal injury." Free Radic Biol Med **35**(8): 856-871.

Andres-Mateos, E., C. Perier, L. Zhang, B. Blanchard-Fillion, T. M. Greco, B. Thomas, H. S. Ko, M. Sasaki, H. Ischiropoulos, S. Przedborski, T. M. Dawson and V. L. Dawson (2007). "DJ-1 gene deletion reveals that DJ-1 is an atypical peroxiredoxin-like peroxidase." Proc Natl Acad Sci U S A **104**(37): 14807-14812.

Antognelli, C., L. Mezzasoma, K. Fettucciari, E. Mearini and V. N. Talesa (2013). "Role of glyoxalase I in the proliferation and apoptosis control of human LNCaP and PC3 prostate cancer cells." Prostate **73**(2): 121-132.
Antognelli, C., L. Mezzasoma, K. Fettucciari and V. N. Talesa (2013). "A novel mechanism of methylglyoxal cytotoxicity in prostate cancer cells." Int J Biochem Cell Biol **45**(4): 836-844.
Apple, M. A. and D. M. Greenberg (1967). "Inhibition of cancer growth in mice by a normal metabolite." Life Sci **6**(20): 2157-2160.
Arai, K., S. Maguchi, S. Fujii, H. Ishibashi, K. Oikawa and N. Taniguchi (1987). "Glycation and inactivation of human Cu-Zn-superoxide dismutase. Identification of the in vitro glycated sites." J Biol Chem **262**(35): 16969-16972.
Arai, M., H. Yuzawa, I. Nohara, T. Ohnishi, N. Obata, Y. Iwayama, S. Haga, T. Toyota, H. Ujike, M. Arai, T. Ichikawa, A. Nishida, Y. Tanaka, A. Furukawa, Y. Aikawa, O. Kuroda, K. Niizato, R. Izawa, K. Nakamura, N. Mori, D. Matsuzawa, K. Hashimoto, M. Iyo, I. Sora, M. Matsushita, Y. Okazaki, T. Yoshikawa, T. Miyata and M. Itokawa (2010). "Enhanced carbonyl stress in a subpopulation of schizophrenia." Arch Gen Psychiatry **67**(6): 589-597.
Aronsson, A. C., E. Marmstal and B. Mannervik (1978). "Glyoxalase I, a zinc metalloenzyme of mammals and yeast." Biochem Biophys Res Commun **81**(4): 1235-1240.
Atkins, T. W. and P. J. Thornalley (1989). "Erythrocyte glyoxalase activity in genetically obese (ob/ob) and streptozotocin diabetic mice." Diabetes Res **11**(3): 125-129.
Auburger, G. and A. Kurz (2011). "The role of glyoxalases for sugar stress and aging, with relevance for dyskinesia, anxiety, dementia and Parkinson's disease." Aging (Albany NY) **3**(1): 5-9.
Bair, W. B., 3rd, C. M. Cabello, K. Uchida, A. S. Bause and G. T. Wondrak (2010). "GLO1 overexpression in human malignant melanoma." Melanoma Res **20**(2): 85-96.
Ballard-Barbash, R., C. M. Friedenreich, K. S. Courneya, S. M. Siddiqi, A. McTiernan and C. M. Alfano (2012). "Physical activity, biomarkers, and disease outcomes in cancer survivors: a systematic review." J Natl Cancer Inst **104**(11): 815-840.
Barati, M. T., M. L. Merchant, A. B. Kain, A. W. Jevans, K. R. McLeish and J. B. Klein (2007). "Proteomic analysis defines altered cellular redox pathways and advanced glycation end-product metabolism in glomeruli of db/db diabetic mice." Am J Physiol Renal Physiol **293**(4): F1157-1165.
Barone, B. B., H. C. Yeh, C. F. Snyder, K. S. Peairs, K. B. Stein, R. L. Derr, A. C. Wolff and F. L. Brancati (2008). "Long-term all-cause mortality in cancer patients with preexisting diabetes mellitus: a systematic review and meta-analysis." JAMA **300**(23): 2754-2764.
Barthel, A., S. T. Okino, J. Liao, K. Nakatani, J. Li, J. P. Whitlock, Jr. and R. A. Roth (1999). "Regulation of GLUT1 gene transcription by the serine/threonine kinase Akt1." J Biol Chem **274**(29): 20281-20286.
Bartlett, G. J., C. T. Porter, N. Borkakoti and J. M. Thornton (2002). "Analysis of catalytic residues in enzyme active sites." J Mol Biol **324**(1): 105-121.
Bartyik, K., S. Turi, F. Orosz and E. Karg (2004). "Methotrexate inhibits the glyoxalase system in vivo in children with acute lymphoid leukaemia." Eur J Cancer **40**(15): 2287-2292.
Baynes, J. W. (1991). "Role of oxidative stress in development of complications in diabetes." Diabetes **40**(4): 405-412.
Beisswenger, P. J., S. K. Howell, K. Smith and B. S. Szwergold (2003). "Glyceraldehyde-3-phosphate dehydrogenase activity as an independent modifier of methylglyoxal levels in diabetes." Biochim Biophys Acta **1637**(1): 98-106.
Beisswenger, P. J., S. K. Howell, A. D. Touchette, S. Lal and B. S. Szwergold (1999). "Metformin reduces systemic methylglyoxal levels in type 2 diabetes." Diabetes **48**(1): 198-202.
Bellia, F., G. Vecchio, S. Cuzzocrea, V. Calabrese and E. Rizzarelli (2011). "Neuroprotective features of carnosine in oxidative driven diseases." Mol Aspects Med **32**(4-6): 258-266.

Ben Sahra, I., K. Laurent, A. Loubat, S. Giorgetti-Peraldi, P. Colosetti, P. Auberger, J. F. Tanti, Y. Le Marchand-Brustel and F. Bost (2008). "The antidiabetic drug metformin exerts an antitumoral effect in vitro and in vivo through a decrease of cyclin D1 level." Oncogene **27**(25): 3576-3586.
Bento, C. F., F. Marques, R. Fernandes and P. Pereira (2010). "Methylglyoxal alters the function and stability of critical components of the protein quality control." PLoS One **5**(9): e13007.
Berner, A. K., O. Brouwers, R. Pringle, I. Klaassen, L. Colhoun, C. McVicar, S. Brockbank, J. W. Curry, T. Miyata, M. Brownlee, R. O. Schlingemann, C. Schalkwijk and A. W. Stitt (2012). "Protection against methylglyoxal-derived AGEs by regulation of glyoxalase 1 prevents retinal neuroglial and vasodegenerative pathology." Diabetologia **55**(3): 845-854.
Bierhaus, A., T. Fleming, S. Stoyanov, A. Leffler, A. Babes, C. Neacsu, S. K. Sauer, M. Eberhardt, M. Schnolzer, F. Lasitschka, W. L. Neuhuber, T. I. Kichko, I. Konrade, R. Elvert, W. Mier, V. Pirags, I. K. Lukic, M. Morcos, T. Dehmer, N. Rabbani, P. J. Thornalley, D. Edelstein, C. Nau, J. Forbes, P. M. Humpert, M. Schwaninger, D. Ziegler, D. M. Stern, M. E. Cooper, U. Haberkorn, M. Brownlee, P. W. Reeh and P. P. Nawroth (2012). "Methylglyoxal modification of Nav1.8 facilitates nociceptive neuron firing and causes hyperalgesia in diabetic neuropathy." Nat Med **18**(6): 926-933.
Bito, A., M. Haider, I. Hadler and M. Breitenbach (1997). "Identification and phenotypic analysis of two glyoxalase II encoding genes from Saccharomyces cerevisiae, GLO2 and GLO4, and intracellular localization of the corresponding proteins." J Biol Chem **272**(34): 21509-21519.
Boldyrev, A., E. Bulygina, T. Leinsoo, I. Petrushanko, S. Tsubone and H. Abe (2004). "Protection of neuronal cells against reactive oxygen species by carnosine and related compounds." Comp Biochem Physiol B Biochem Mol Biol **137**(1): 81-88.
Bond, S. (2011). "New findings from women's health initiative: breast cancer mortality rates higher among combination hormone therapy users." J Midwifery Womens Health **56**(2): 177-178.
Bosco, J. L., S. Antonsen, H. T. Sorensen, L. Pedersen and T. L. Lash (2011). "Metformin and incident breast cancer among diabetic women: a population-based case-control study in Denmark." Cancer Epidemiol Biomarkers Prev **20**(1): 101-111.
Brambilla, G., L. Sciaba, P. Faggin, R. Finollo, A. M. Bassi, M. Ferro and U. M. Marinari (1985). "Methylglyoxal-induced DNA-protein cross-links and cytotoxicity in Chinese hamster ovary cells." Carcinogenesis **6**(5): 683-686.
Broude, N. E. and E. I. Budowsky (1971). "The reaction of glyoxal with nucleic acid components. 3. Kinetics of the reaction with monomers." Biochim Biophys Acta **254**(3): 380-388.
Brownlee, M., H. Vlassara and A. Cerami (1984). "Nonenzymatic glycosylation and the pathogenesis of diabetic complications." Ann Intern Med **101**(4): 527-537.
Brownlee, M., H. Vlassara, A. Kooney, P. Ulrich and A. Cerami (1986). "Aminoguanidine prevents diabetes-induced arterial wall protein cross-linking." Science **232**(4758): 1629-1632.
Bucala, R., Z. Makita, T. Koschinsky, A. Cerami and H. Vlassara (1993). "Lipid advanced glycosylation: pathway for lipid oxidation in vivo." Proc Natl Acad Sci U S A **90**(14): 6434-6438.
Bucala, R., Z. Makita, G. Vega, S. Grundy, T. Koschinsky, A. Cerami and H. Vlassara (1994). "Modification of low density lipoprotein by advanced glycation end products contributes to the dyslipidemia of diabetes and renal insufficiency." Proc Natl Acad Sci U S A **91**(20): 9441-9445.
Buchler, P., H. A. Reber, M. Buchler, S. Shrinkante, M. W. Buchler, H. Friess, G. L. Semenza and O. J. Hines (2003). "Hypoxia-inducible factor 1 regulates vascular endothelial growth factor expression in human pancreatic cancer." Pancreas **26**(1): 56-64.
Buzzai, M., R. G. Jones, R. K. Amaravadi, J. J. Lum, R. J. DeBerardinis, F. Zhao, B. Viollet and C. B. Thompson (2007). "Systemic treatment with the antidiabetic drug metformin selectively impairs p53-deficient tumor cell growth." Cancer Res **67**(14): 6745-6752.

Camargo, F. D., S. Gokhale, J. B. Johnnidis, D. Fu, G. W. Bell, R. Jaenisch and T. R. Brummelkamp (2007). "YAP1 increases organ size and expands undifferentiated progenitor cells." Curr Biol **17**(23): 2054-2060.
Cameron, A. D., B. Olin, M. Ridderstrom, B. Mannervik and T. A. Jones (1997). "Crystal structure of human glyoxalase I--evidence for gene duplication and 3D domain swapping." EMBO J **16**(12): 3386-3395.
Cameron, A. D., M. Ridderstrom, B. Olin and B. Mannervik (1999). "Crystal structure of human glyoxalase II and its complex with a glutathione thiolester substrate analogue." Structure **7**(9): 1067-1078.
Carrard, G., A. L. Bulteau, I. Petropoulos and B. Friguet (2002). "Impairment of proteasome structure and function in aging." Int J Biochem Cell Biol **34**(11): 1461-1474.
Casazza, J. P., M. E. Felver and R. L. Veech (1984). "The metabolism of acetone in rat." J Biol Chem **259**(1): 231-236.
Cefalu, W. T., A. D. Bell-Farrow, Z. Q. Wang, W. E. Sonntag, M. X. Fu, J. W. Baynes and S. R. Thorpe (1995). "Caloric restriction decreases age-dependent accumulation of the glycoxidation products, N epsilon-(carboxymethyl)lysine and pentosidine, in rat skin collagen." J Gerontol A Biol Sci Med Sci **50**(6): B337-341.
Chan, L. H., W. Wang, W. Yeung, Y. Deng, P. Yuan and K. K. Mak (2014). "Hedgehog signaling induces osteosarcoma development through Yap1 and H19 overexpression." Oncogene **33**(40): 4857-4866.
Chang, T., R. Wang and L. Wu (2005). "Methylglyoxal-induced nitric oxide and peroxynitrite production in vascular smooth muscle cells." Free Radic Biol Med **38**(2): 286-293.
Chaplen, F. W., W. E. Fahl and D. C. Cameron (1998). "Evidence of high levels of methylglyoxal in cultured Chinese hamster ovary cells." Proc Natl Acad Sci U S A **95**(10): 5533-5538.
Chen, J. and W. A. Weiss (2015). "Alternative splicing in cancer: implications for biology and therapy." Oncogene **34**(1): 1-14.
Chen, Q., E. J. Vazquez, S. Moghaddas, C. L. Hoppel and E. J. Lesnefsky (2003). "Production of reactive oxygen species by mitochondria: central role of complex III." J Biol Chem **278**(38): 36027-36031.
Cheng, W. L., M. M. Tsai, C. Y. Tsai, Y. H. Huang, C. Y. Chen, H. C. Chi, Y. H. Tseng, I. W. Chao, W. C. Lin, S. M. Wu, Y. Liang, C. J. Liao, Y. H. Lin, I. H. Chung, W. J. Chen, P. Y. Lin, C. S. Wang and K. H. Lin (2012). "Glyoxalase-I is a novel prognosis factor associated with gastric cancer progression." PLoS One **7**(3): e34352.
Chetyrkin, S., M. Mathis, V. Pedchenko, O. A. Sanchez, W. H. McDonald, D. L. Hachey, H. Madu, D. Stec, B. Hudson and P. Voziyan (2011). "Glucose autoxidation induces functional damage to proteins via modification of critical arginine residues." Biochemistry **50**(27): 6102-6112.
Cheung, E. C. and K. H. Vousden (2010). "The role of p53 in glucose metabolism." Curr Opin Cell Biol **22**(2): 186-191.
Chiang, G. G. and R. T. Abraham (2007). "Targeting the mTOR signaling network in cancer." Trends Mol Med **13**(10): 433-442.
Chlebowski, R. T. and G. L. Anderson (2012). "Changing concepts: Menopausal hormone therapy and breast cancer." J Natl Cancer Inst **104**(7): 517-527.
Chlebowski, R. T., G. L. Blackburn, C. A. Thomson, D. W. Nixon, A. Shapiro, M. K. Hoy, M. T. Goodman, A. E. Giuliano, N. Karanja, P. McAndrew, C. Hudis, J. Butler, D. Merkel, A. Kristal, B. Caan, R. Michaelson, V. Vinciguerra, S. Del Prete, M. Winkler, R. Hall, M. Simon, B. L. Winters and R. M. Elashoff (2006). "Dietary fat reduction and breast cancer outcome: interim efficacy results from the Women's Intervention Nutrition Study." J Natl Cancer Inst **98**(24): 1767-1776.
Choudhary, D., D. Chandra and R. K. Kale (1997). "Influence of methylglyoxal on antioxidant enzymes and oxidative damage." Toxicol Lett **93**(2-3): 141-152.

Christofk, H. R., M. G. Vander Heiden, M. H. Harris, A. Ramanathan, R. E. Gerszten, R. Wei, M. D. Fleming, S. L. Schreiber and L. C. Cantley (2008). "The M2 splice isoform of pyruvate kinase is important for cancer metabolism and tumour growth." Nature **452**(7184): 230-233.
Christofk, H. R., M. G. Vander Heiden, N. Wu, J. M. Asara and L. C. Cantley (2008). "Pyruvate kinase M2 is a phosphotyrosine-binding protein." Nature **452**(7184): 181-186.
Clements, C. M., R. S. McNally, B. J. Conti, T. W. Mak and J. P. Ting (2006). "DJ-1, a cancer- and Parkinson's disease-associated protein, stabilizes the antioxidant transcriptional master regulator Nrf2." Proc Natl Acad Sci U S A **103**(41): 15091-15096.
Clugston, S. L., J. F. Barnard, R. Kinach, D. Miedema, R. Ruman, E. Daub and J. F. Honek (1998). "Overproduction and characterization of a dimeric non-zinc glyoxalase I from Escherichia coli: evidence for optimal activation by nickel ions." Biochemistry **37**(24): 8754-8763.
Coller, H. A. (2014). "Is cancer a metabolic disease?" Am J Pathol **184**(1): 4-17.
Conroy, P. J. (1978). "Carcinostatic activity of methylglyoxal and related substances in tumour-bearing mice." Ciba Found Symp(67): 271-300.
Cooper, M. E., V. Thallas, J. Forbes, E. Scalbert, S. Sastra, I. Darby and T. Soulis (2000). "The cross-link breaker, N-phenacylthiazolium bromide prevents vascular advanced glycation end-product accumulation." Diabetologia **43**(5): 660-664.
Cooper, R. A. and A. Anderson (1970). "The formation and catabolism of methylglyoxal during glycolysis in Escherichia coli." FEBS Lett **11**(4): 273-276.
Cordell, P. A., T. S. Futers, P. J. Grant and R. J. Pease (2004). "The Human hydroxyacylglutathione hydrolase (HAGH) gene encodes both cytosolic and mitochondrial forms of glyoxalase II." J Biol Chem **279**(27): 28653-28661.
Cordenonsi, M., F. Zanconato, L. Azzolin, M. Forcato, A. Rosato, C. Frasson, M. Inui, M. Montagner, Anna R. Parenti, A. Poletti, Maria G. Daidone, S. Dupont, G. Basso, S. Bicciato and S. Piccolo (2011). "The Hippo Transducer TAZ Confers Cancer Stem Cell-Related Traits on Breast Cancer Cells." Cell **147**(4): 759-772.
Cui, J. W., J. Wang, K. He, B. F. Jin, H. X. Wang, W. Li, L. H. Kang, M. R. Hu, H. Y. Li, M. Yu, B. F. Shen, G. J. Wang and X. M. Zhang (2004). "Proteomic analysis of human acute leukemia cells: insight into their classification." Clin Cancer Res **10**(20): 6887-6896.
Dairkee, S. H., B. M. Ljung, H. Smith and A. Hackett (1987). "Immunolocalization of a human basal epithelium specific keratin in benign and malignant breast disease." Breast Cancer Res Treat **10**(1): 11-20.
Darby, S., P. McGale, C. Correa, C. Taylor, R. Arriagada, M. Clarke, D. Cutter, C. Davies, M. Ewertz, J. Godwin, R. Gray, L. Pierce, T. Whelan, Y. Wang and R. Peto (2011). "Effect of radiotherapy after breast-conserving surgery on 10-year recurrence and 15-year breast cancer death: meta-analysis of individual patient data for 10,801 women in 17 randomised trials." Lancet **378**(9804): 1707-1716.
Davidson, S. D., J. P. Cherry, M. S. Choudhury, H. Tazaki, C. Mallouh and S. Konno (1999). "Glyoxalase I activity in human prostate cancer: a potential marker and importance in chemotherapy." J Urol **161**(2): 690-691.
Davidson, S. D., D. M. Milanesa, C. Mallouh, M. S. Choudhury, H. Tazaki and S. Konno (2002). "A possible regulatory role of glyoxalase I in cell viability of human prostate cancer." Urol Res **30**(2): 116-121.
Davies, A. A., J. Y. Masson, M. J. McIlwraith, A. Z. Stasiak, A. Stasiak, A. R. Venkitaraman and S. C. West (2001). "Role of BRCA2 in control of the RAD51 recombination and DNA repair protein." Mol Cell **7**(2): 273-282.
De Bruijn, K. M., L. R. Arends, B. E. Hansen, S. Leeflang, R. Ruiter and C. H. van Eijck (2013). "Systematic review and meta-analysis of the association between diabetes mellitus and incidence and mortality in breast and colorectal cancer." Br J Surg **100**(11): 1421-1429.

de Hemptinne, V., D. Rondas, M. Toepoel and K. Vancompernolle (2009). "Phosphorylation on Thr-106 and NO-modification of glyoxalase I suppress the TNF-induced transcriptional activity of NF-kappaB." Mol Cell Biochem **325**(1-2): 169-178.
De Jager, J., A. Kooy, P. Lehert, D. Bets, M. G. Wulffele, T. Teerlink, P. G. Scheffer, C. G. Schalkwijk, A. J. Donker and C. D. Stehouwer (2005). "Effects of short-term treatment with metformin on markers of endothelial function and inflammatory activity in type 2 diabetes mellitus: a randomized, placebo-controlled trial." J Intern Med **257**(1): 100-109.
DeBerardinis, R. J., A. Mancuso, E. Daikhin, I. Nissim, M. Yudkoff, S. Wehrli and C. B. Thompson (2007). "Beyond aerobic glycolysis: transformed cells can engage in glutamine metabolism that exceeds the requirement for protein and nucleotide synthesis." Proc Natl Acad Sci U S A **104**(49): 19345-19350.
Degenhardt, T. P., N. L. Alderson, D. D. Arrington, R. J. Beattie, J. M. Basgen, M. W. Steffes, S. R. Thorpe and J. W. Baynes (2002). "Pyridoxamine inhibits early renal disease and dyslipidemia in the streptozotocin-diabetic rat." Kidney Int **61**(3): 939-950.
Delpierre, G., M. H. Rider, F. Collard, V. Stroobant, F. Vanstapel, H. Santos and E. Van Schaftingen (2000). "Identification, cloning, and heterologous expression of a mammalian fructosamine-3-kinase." Diabetes **49**(10): 1627-1634.
DeRan, M., J. Yang, C. H. Shen, E. C. Peters, J. Fitamant, P. Chan, M. Hsieh, S. Zhu, J. M. Asara, B. Zheng, N. Bardeesy, J. Liu and X. Wu (2014). "Energy stress regulates hippo-YAP signaling involving AMPK-mediated regulation of angiomotin-like 1 protein." Cell Rep **9**(2): 495-503.
Di Ilio, C., G. Del Boccio, R. Casaccia, A. Aceto, F. Di Giacomo and G. Federici (1987). "Selenium level and glutathione-dependent enzyme activities in normal and neoplastic human lung tissues." Carcinogenesis **8**(2): 281-284.
Distler, M. G., L. D. Plant, G. Sokoloff, A. J. Hawk, I. Aneas, G. E. Wuenschell, J. Termini, S. C. Meredith, M. A. Nobrega and A. A. Palmer (2012). "Glyoxalase 1 increases anxiety by reducing GABAA receptor agonist methylglyoxal." J Clin Invest **122**(6): 2306-2315.
Dobler, D., N. Ahmed, L. Song, K. E. Eboigbodin and P. J. Thornalley (2006). "Increased dicarbonyl metabolism in endothelial cells in hyperglycemia induces anoikis and impairs angiogenesis by RGD and GFOGER motif modification." Diabetes **55**(7): 1961-1969.
Dong, J., G. Feldmann, J. Huang, S. Wu, N. Zhang, S. A. Comerford, M. F. Gayyed, R. A. Anders, A. Maitra and D. Pan (2007). "Elucidation of a universal size-control mechanism in Drosophila and mammals." Cell **130**(6): 1120-1133.
Du, J., H. Suzuki, F. Nagase, A. A. Akhand, X. Y. Ma, T. Yokoyama, T. Miyata and I. Nakashima (2001). "Superoxide-mediated early oxidation and activation of ASK1 are important for initiating methylglyoxal-induced apoptosis process." Free Radic Biol Med **31**(4): 469-478.
Du, X., T. Matsumura, D. Edelstein, L. Rossetti, Z. Zsengeller, C. Szabo and M. Brownlee (2003). "Inhibition of GAPDH activity by poly(ADP-ribose) polymerase activates three major pathways of hyperglycemic damage in endothelial cells." J Clin Invest **112**(7): 1049-1057.
Duggan, C., M. L. Irwin, L. Xiao, K. D. Henderson, A. W. Smith, R. N. Baumgartner, K. B. Baumgartner, L. Bernstein, R. Ballard-Barbash and A. McTiernan (2011). "Associations of insulin resistance and adiponectin with mortality in women with breast cancer." J Clin Oncol **29**(1): 32-39.
Dunn, J. A., D. R. McCance, S. R. Thorpe, T. J. Lyons and J. W. Baynes (1991). "Age-dependent accumulation of N epsilon-(carboxymethyl)lysine and N epsilon-(carboxymethyl)hydroxylysine in human skin collagen." Biochemistry **30**(5): 1205-1210.
Dunn, J. A., J. S. Patrick, S. R. Thorpe and J. W. Baynes (1989). "Oxidation of glycated proteins: age-dependent accumulation of N epsilon-(carboxymethyl)lysine in lens proteins." Biochemistry **28**(24): 9464-9468.

Dupont, S., L. Morsut, M. Aragona, E. Enzo, S. Giulitti, M. Cordenonsi, F. Zanconato, J. Le Digabel, M. Forcato, S. Bicciato, N. Elvassore and S. Piccolo (2011). "Role of YAP/TAZ in mechanotransduction." Nature **474**(7350): 179-183.
Edwards, L. G., A. Adesida and P. J. Thornalley (1996). "Inhibition of human leukaemia 60 cell growth by S-D-lactoylglutathione in vitro. Mediation by metabolism to N-D-lactoylcysteine and induction of apoptosis." Leuk Res **20**(1): 17-26.
Egyud, L. G. and A. Szent-Gyorgyi (1966). "Cell division, SH, ketoaldehydes, and cancer." Proc Natl Acad Sci U S A **55**(2): 388-393.
Egyud, L. G. and A. Szent-Gyorgyi (1966). "On the regulation of cell division." Proc Natl Acad Sci U S A **56**(1): 203-207.
Ehmer, U. and J. Sage (2016). "Control of Proliferation and Cancer Growth by the Hippo Signaling Pathway." Mol Cancer Res **14**(2): 127-140.
Elston, C. W. and I. O. Ellis (2002). "Pathological prognostic factors in breast cancer. I. The value of histological grade in breast cancer: experience from a large study with long-term follow-up. C. W. Elston & I. O. Ellis. Histopathology 1991; 19; 403-410." Histopathology **41**(3A): 151-152, discussion 152-153.
Engelen, L., C. D. Stehouwer and C. G. Schalkwijk (2013). "Current therapeutic interventions in the glycation pathway: evidence from clinical studies." Diabetes Obes Metab **15**(8): 677-689.
Enzo, E., G. Santinon, A. Pocaterra, M. Aragona, S. Bresolin, M. Forcato, D. Grifoni, A. Pession, F. Zanconato, G. Guzzo, S. Bicciato and S. Dupont (2015). "Aerobic glycolysis tunes YAP/TAZ transcriptional activity." EMBO J.
Erickson, K., R. E. Patterson, S. W. Flatt, L. Natarajan, B. A. Parker, D. D. Heath, G. A. Laughlin, N. Saquib, C. L. Rock and J. P. Pierce (2011). "Clinically defined type 2 diabetes mellitus and prognosis in early-stage breast cancer." J Clin Oncol **29**(1): 54-60.
Esterbauer, H., K. H. Cheeseman, M. U. Dianzani, G. Poli and T. F. Slater (1982). "Separation and characterization of the aldehydic products of lipid peroxidation stimulated by ADP-Fe2+ in rat liver microsomes." Biochem J **208**(1): 129-140.
Fantin, V. R., J. St-Pierre and P. Leder (2006). "Attenuation of LDH-A expression uncovers a link between glycolysis, mitochondrial physiology, and tumor maintenance." Cancer Cell **9**(6): 425-434.
Ferguson, G. P., S. VanPatten, R. Bucala and Y. Al-Abed (1999). "Detoxification of methylglyoxal by the nucleophilic bidentate, phenylacylthiazolium bromide." Chem Res Toxicol **12**(7): 617-622.
Ferlay, J., E. Steliarova-Foucher, J. Lortet-Tieulent, S. Rosso, J. W. Coebergh, H. Comber, D. Forman and F. Bray (2013). "Cancer incidence and mortality patterns in Europe: estimates for 40 countries in 2012." Eur J Cancer **49**(6): 1374-1403.
Finot, P. A. (2005). "Historical perspective of the Maillard reaction in food science." Ann N Y Acad Sci **1043**: 1-8.
Fischer, K., P. Hoffmann, S. Voelkl, N. Meidenbauer, J. Ammer, M. Edinger, E. Gottfried, S. Schwarz, G. Rothe, S. Hoves, K. Renner, B. Timischl, A. Mackensen, L. Kunz-Schughart, R. Andreesen, S. W. Krause and M. Kreutz (2007). "Inhibitory effect of tumor cell-derived lactic acid on human T cells." Blood **109**(9): 3812-3819.
Fleming, T. H., T. M. Theilen, J. Masania, M. Wunderle, J. Karimi, S. Vittas, R. Bernauer, A. Bierhaus, N. Rabbani, P. J. Thornalley, J. Kroll, J. Tyedmers, R. Nawrotzki, S. Herzig, M. Brownlee and P. P. Nawroth (2013). "Aging-dependent reduction in glyoxalase 1 delays wound healing." Gerontology **59**(5): 427-437.
Fonseca-Sanchez, M. A., S. Rodriguez Cuevas, G. Mendoza-Hernandez, V. Bautista-Pina, E. Arechaga Ocampo, A. Hidalgo Miranda, V. Quintanar Jurado, L. A. Marchat, E. Alvarez-Sanchez, C. Perez Plasencia and C. Lopez-Camarillo (2012). "Breast cancer proteomics reveals a positive correlation between glyoxalase 1 expression and high tumor grade." Int J Oncol **41**(2): 670-680.

Fontana, M., F. Pinnen, G. Lucente and L. Pecci (2002). "Prevention of peroxynitrite-dependent damage by carnosine and related sulphonamido pseudodipeptides." Cell Mol Life Sci **59**(3): 546-551.
Foulkes, W. D., I. E. Smith and J. S. Reis-Filho (2010). "Triple-negative breast cancer." N Engl J Med **363**(20): 1938-1948.
Frickel, E. M., P. Jemth, M. Widersten and B. Mannervik (2001). "Yeast glyoxalase I is a monomeric enzyme with two active sites." J Biol Chem **276**(3): 1845-1849.
Frye, E. B., T. P. Degenhardt, S. R. Thorpe and J. W. Baynes (1998). "Role of the Maillard reaction in aging of tissue proteins. Advanced glycation end product-dependent increase in imidazolium cross-links in human lens proteins." J Biol Chem **273**(30): 18714-18719.
Fujii, M., T. Toyoda, H. Nakanishi, Y. Yatabe, A. Sato, Y. Matsudaira, H. Ito, H. Murakami, Y. Kondo, E. Kondo, T. Hida, T. Tsujimura, H. Osada and Y. Sekido (2012). "TGF-beta synergizes with defects in the Hippo pathway to stimulate human malignant mesothelioma growth." J Exp Med **209**(3): 479-494.
Futerman, A. H. and Y. A. Hannun (2004). "The complex life of simple sphingolipids." EMBO Rep **5**(8): 777-782.
Gallagher, E. J. and D. LeRoith (2015). "Obesity and Diabetes: The Increased Risk of Cancer and Cancer-Related Mortality." Physiol Rev **95**(3): 727-748.
Gallet, X., B. Charloteaux, A. Thomas and R. Brasseur (2000). "A fast method to predict protein interaction sites from sequences." J Mol Biol **302**(4): 917-926.
Gangadhariah, M. H., B. Wang, M. Linetsky, C. Henning, R. Spanneberg, M. A. Glomb and R. H. Nagaraj (2010). "Hydroimidazolone modification of human alphaA-crystallin: Effect on the chaperone function and protein refolding ability." Biochim Biophys Acta **1802**(4): 432-441.
Gao, Y. and Y. Wang (2006). "Site-selective modifications of arginine residues in human hemoglobin induced by methylglyoxal." Biochemistry **45**(51): 15654-15660.
Garg, S. K., H. Maurer, K. Reed and R. Selagamsetty (2014). "Diabetes and cancer: two diseases with obesity as a common risk factor." Diabetes Obes Metab **16**(2): 97-110.
Gatenby, R. A. and R. J. Gillies (2004). "Why do cancers have high aerobic glycolysis?" Nat Rev Cancer **4**(11): 891-899.
Ghosh, A., S. Bera, S. Ray, T. Banerjee and M. Ray (2011). "Methylglyoxal induces mitochondria-dependent apoptosis in sarcoma." Biochemistry (Mosc) **76**(10): 1164-1171.
Giacco, F., X. Du, V. D. D'Agati, R. Milne, G. Sui, M. Geoffrion and M. Brownlee (2014). "Knockdown of glyoxalase 1 mimics diabetic nephropathy in nondiabetic mice." Diabetes **63**(1): 291-299.
Godbout, J. P., J. Pesavento, M. E. Hartman, S. R. Manson and G. G. Freund (2002). "Methylglyoxal enhances cisplatin-induced cytotoxicity by activating protein kinase Cdelta." J Biol Chem **277**(4): 2554-2561.
Gomes, R. A., L. M. Oliveira, M. Silva, C. Ascenso, A. Quintas, G. Costa, A. V. Coelho, M. Sousa Silva, A. E. Ferreira, A. Ponces Freire and C. Cordeiro (2008). "Protein glycation in vivo: functional and structural effects on yeast enolase." Biochem J **416**(3): 317-326.
Gomes, R. A., H. Vicente Miranda, M. S. Silva, G. Graca, A. V. Coelho, A. E. Ferreira, C. Cordeiro and A. P. Freire (2006). "Yeast protein glycation in vivo by methylglyoxal. Molecular modification of glycolytic enzymes and heat shock proteins." FEBS J **273**(23): 5273-5287.
Goodwin, P. J. (2015). "Obesity, insulin resistance and breast cancer outcomes." Breast **24 Suppl 2**: S56-59.
Goodwin, P. J. (2016). "Obesity and Breast Cancer Outcomes: How Much Evidence Is Needed to Change Practice?" J Clin Oncol **34**(7): 646-648.
Goodwin, P. J. and V. Stambolic (2015). "Impact of the obesity epidemic on cancer." Annu Rev Med **66**: 281-296.
Gorrini, C., I. S. Harris and T. W. Mak (2013). "Modulation of oxidative stress as an anticancer strategy." Nat Rev Drug Discov **12**(12): 931-947.

Gotlieb, W. H., J. Saumet, M. C. Beauchamp, J. Gu, S. Lau, M. N. Pollak and I. Bruchim (2008). "In vitro metformin anti-neoplastic activity in epithelial ovarian cancer." Gynecol Oncol **110**(2): 246-250.
Group, T. D. C. a. C. T. R. (1993). "The effect of intensive treatment of diabetes on the development and progression of long-term complications in insulin-dependent diabetes mellitus. The Diabetes Control and Complications Trial Research Group." N Engl J Med **329**(14): 977-986.
Guariguata, L., D. R. Whiting, I. Hambleton, J. Beagley, U. Linnenkamp and J. E. Shaw (2014). "Global estimates of diabetes prevalence for 2013 and projections for 2035." Diabetes Res Clin Pract **103**(2): 137-149.
Haik, G. M., Jr., T. W. Lo and P. J. Thornalley (1994). "Methylglyoxal concentration and glyoxalase activities in the human lens." Exp Eye Res **59**(4): 497-500.
Hamajima, N., K. Hirose, K. Tajima, T. Rohan, E. E. Calle, C. W. Heath, Jr., R. J. Coates, J. M. Liff, R. Talamini, N. Chantarakul, S. Koetsawang, D. Rachawat, A. Morabia, L. Schuman, W. Stewart, M. Szklo, C. Bain, F. Schofield, V. Siskind, P. Band, A. J. Coldman, R. P. Gallagher, T. G. Hislop, P. Yang, L. M. Kolonel, A. M. Nomura, J. Hu, K. C. Johnson, Y. Mao, S. De Sanjose, N. Lee, P. Marchbanks, H. W. Ory, H. B. Peterson, H. G. Wilson, P. A. Wingo, K. Ebeling, D. Kunde, P. Nishan, J. L. Hopper, G. Colditz, V. Gajalanski, N. Martin, T. Pardthaisong, S. Silpisornkosol, C. Theetranont, B. Boosiri, S. Chutivongse, P. Jimakorn, P. Virutamasen, C. Wongsrichanalai, M. Ewertz, H. O. Adami, L. Bergkvist, C. Magnusson, I. Persson, J. Chang-Claude, C. Paul, D. C. Skegg, G. F. Spears, P. Boyle, T. Evstifeeva, J. R. Daling, W. B. Hutchinson, K. Malone, E. A. Noonan, J. L. Stanford, D. B. Thomas, N. S. Weiss, E. White, N. Andrieu, A. Bremond, F. Clavel, B. Gairard, J. Lansac, L. Piana, R. Renaud, A. Izquierdo, P. Viladiu, H. R. Cuevas, P. Ontiveros, A. Palet, S. B. Salazar, N. Aristizabel, A. Cuadros, L. Tryggvadottir, H. Tulinius, A. Bachelot, M. G. Le, J. Peto, S. Franceschi, F. Lubin, B. Modan, E. Ron, Y. Wax, G. D. Friedman, R. A. Hiatt, F. Levi, T. Bishop, K. Kosmelj, M. Primic-Zakelj, B. Ravnihar, J. Stare, W. L. Beeson, G. Fraser, R. D. Bullbrook, J. Cuzick, S. W. Duffy, I. S. Fentiman, J. L. Hayward, D. Y. Wang, A. J. McMichael, K. McPherson, R. L. Hanson, M. C. Leske, M. C. Mahoney, P. C. Nasca, A. O. Varma, A. L. Weinstein, T. R. Moller, H. Olsson, J. Ranstam, R. A. Goldbohm, P. A. van den Brandt, R. A. Apelo, J. Baens, J. R. de la Cruz, B. Javier, L. B. Lacaya, C. A. Ngelangel, C. La Vecchia, E. Negri, E. Marubini, M. Ferraroni, M. Gerber, S. Richardson, C. Segala, D. Gatei, P. Kenya, A. Kungu, J. G. Mati, L. A. Brinton, R. Hoover, C. Schairer, R. Spirtas, H. P. Lee, M. A. Rookus, F. E. van Leeuwen, J. A. Schoenberg, M. McCredie, M. D. Gammon, E. A. Clarke, L. Jones, A. Neil, M. Vessey, D. Yeates, P. Appleby, E. Banks, V. Beral, D. Bull, B. Crossley, A. Goodill, J. Green, C. Hermon, T. Key, N. Langston, C. Lewis, G. Reeves, R. Collins, R. Doll, R. Peto, K. Mabuchi, D. Preston, P. Hannaford, C. Kay, L. Rosero-Bixby, Y. T. Gao, F. Jin, J. M. Yuan, H. Y. Wei, T. Yun, C. Zhiheng, G. Berry, J. Cooper Booth, T. Jelihovsky, R. MacLennan, R. Shearman, Q. S. Wang, C. J. Baines, A. B. Miller, C. Wall, E. Lund, H. Stalsberg, X. O. Shu, W. Zheng, K. Katsouyanni, A. Trichopoulou, D. Trichopoulos, A. Dabancens, L. Martinez, R. Molina, O. Salas, F. E. Alexander, K. Anderson, A. R. Folsom, B. S. Hulka, L. Bernstein, S. Enger, R. W. Haile, A. Paganini-Hill, M. C. Pike, R. K. Ross, G. Ursin, M. C. Yu, M. P. Longnecker, P. Newcomb, L. Bergkvist, A. Kalache, T. M. Farley, S. Holck, O. Meirik and C. Collaborative Group on Hormonal Factors in Breast (2002). "Alcohol, tobacco and breast cancer--collaborative reanalysis of individual data from 53 epidemiological studies, including 58,515 women with breast cancer and 95,067 women without the disease." Br J Cancer **87**(11): 1234-1245.
Hamelin, M., J. Mary, M. Vostry, B. Friguet and H. Bakala (2007). "Glycation damage targets glutamate dehydrogenase in the rat liver mitochondrial matrix during aging." FEBS J **274**(22): 5949-5961.
Hammes, H. P., X. Du, D. Edelstein, T. Taguchi, T. Matsumura, Q. Ju, J. Lin, A. Bierhaus, P. Nawroth, D. Hannak, M. Neumaier, R. Bergfeld, I. Giardino and M. Brownlee (2003).

"Benfotiamine blocks three major pathways of hyperglycemic damage and prevents experimental diabetic retinopathy." Nat Med **9**(3): 294-299.
Hammes, H. P., S. Martin, K. Federlin, K. Geisen and M. Brownlee (1991). "Aminoguanidine treatment inhibits the development of experimental diabetic retinopathy." Proc Natl Acad Sci U S A **88**(24): 11555-11558.
Hanahan, D. and R. A. Weinberg (2011). "Hallmarks of cancer: the next generation." Cell **144**(5): 646-674.
Hanssen, N. M., K. Wouters, M. S. Huijberts, M. J. Gijbels, J. C. Sluimer, J. L. Scheijen, S. Heeneman, E. A. Biessen, M. J. Daemen, M. Brownlee, D. P. de Kleijn, C. D. Stehouwer, G. Pasterkamp and C. G. Schalkwijk (2014). "Higher levels of advanced glycation endproducts in human carotid atherosclerotic plaques are associated with a rupture-prone phenotype." Eur Heart J **35**(17): 1137-1146.
Hao, Y., A. Chun, K. Cheung, B. Rashidi and X. Yang (2008). "Tumor suppressor LATS1 is a negative regulator of oncogene YAP." J Biol Chem **283**(9): 5496-5509.
He, X., P. E. Brenchley, G. C. Jayson, L. Hampson, J. Davies and I. N. Hampson (2004). "Hypoxia increases heparanase-dependent tumor cell invasion, which can be inhibited by antiheparanase antibodies." Cancer Res **64**(11): 3928-3933.
Hiemer, S. E., A. D. Szymaniak and X. Varelas (2014). "The transcriptional regulators TAZ and YAP direct transforming growth factor beta-induced tumorigenic phenotypes in breast cancer cells." J Biol Chem **289**(19): 13461-13474.
Hipkiss, A. R. (2005). "Glycation, ageing and carnosine: are carnivorous diets beneficial?" Mech Ageing Dev **126**(10): 1034-1039.
Hipkiss, A. R. (2014). "Aging risk factors and Parkinson's disease: contrasting roles of common dietary constituents." Neurobiol Aging **35**(6): 1469-1472.
Hipkiss, A. R. and H. Chana (1998). "Carnosine protects proteins against methylglyoxal-mediated modifications." Biochem Biophys Res Commun **248**(1): 28-32.
Hirsch, H. A., D. Iliopoulos, P. N. Tsichlis and K. Struhl (2009). "Metformin selectively targets cancer stem cells, and acts together with chemotherapy to block tumor growth and prolong remission." Cancer Res **69**(19): 7507-7511.
Hisaoka, M., A. Tanaka and H. Hashimoto (2002). "Molecular alterations of h-warts/LATS1 tumor suppressor in human soft tissue sarcoma." Lab Invest **82**(10): 1427-1435.
Hitosugi, T., S. Kang, M. G. Vander Heiden, T. W. Chung, S. Elf, K. Lythgoe, S. Dong, S. Lonial, X. Wang, G. Z. Chen, J. Xie, T. L. Gu, R. D. Polakiewicz, J. L. Roesel, T. J. Boggon, F. R. Khuri, D. G. Gilliland, L. C. Cantley, J. Kaufman and J. Chen (2009). "Tyrosine phosphorylation inhibits PKM2 to promote the Warburg effect and tumor growth." Sci Signal **2**(97): ra73.
Hodge, J. E. (1955). "The Amadori rearrangement." Adv Carbohydr Chem **10**: 169-205.
Holliday, R. and G. A. McFarland (1996). "Inhibition of the growth of transformed and neoplastic cells by the dipeptide carnosine." Br J Cancer **73**(8): 966-971.
Honey, N. K. and T. B. Shows (1981). "Assignment of the glyoxalase II gene (HAGH) to human chromosome 16." Hum Genet **58**(4): 358-361.
Hooper, N. I., M. J. Tisdale and P. J. Thornalley (1987). "Glyoxalase activity during differentiation of human leukaemia cells in vitro." Leuk Res **11**(12): 1141-1148.
Hopkins, F. G. and E. J. Morgan (1945). "On the distribution of glyoxalase and glutathione." Biochem J **39**(4): 320-324.
Horii, Y., J. Shen, Y. Fujisaki, K. Yoshida and K. Nagai (2012). "Effects of L-carnosine on splenic sympathetic nerve activity and tumor proliferation." Neurosci Lett **510**(1): 1-5.
Hosoda, F., Y. Arai, N. Okada, H. Shimizu, M. Miyamoto, N. Kitagawa, H. Katai, H. Taniguchi, K. Yanagihara, I. Imoto, J. Inazawa, M. Ohki and T. Shibata (2015). "Integrated genomic and functional analyses reveal glyoxalase I as a novel metabolic oncogene in human gastric cancer." Oncogene **34**(9): 1196-1206.

Hovatta, I., R. S. Tennant, R. Helton, R. A. Marr, O. Singer, J. M. Redwine, J. A. Ellison, E. E. Schadt, I. M. Verma, D. J. Lockhart and C. Barlow (2005). "Glyoxalase 1 and glutathione reductase 1 regulate anxiety in mice." Nature **438**(7068): 662-666.
Hu, X., X. Yang, Q. He, Q. Chen and L. Yu (2014). "Glyoxalase 1 is up-regulated in hepatocellular carcinoma and is essential for HCC cell proliferation." Biotechnol Lett **36**(2): 257-263.
Huen, M. S., S. M. Sy and J. Chen (2010). "BRCA1 and its toolbox for the maintenance of genome integrity." Nat Rev Mol Cell Biol **11**(2): 138-148.
Huntoon, C. J., M. D. Nye, L. Geng, K. L. Peterson, K. S. Flatten, P. Haluska, S. H. Kaufmann and L. M. Karnitz (2010). "Heat shock protein 90 inhibition depletes LATS1 and LATS2, two regulators of the mammalian hippo tumor suppressor pathway." Cancer Res **70**(21): 8642-8650.
Iliopoulos, D., H. A. Hirsch and K. Struhl (2009). "An epigenetic switch involving NF-kappaB, Lin28, Let-7 MicroRNA, and IL6 links inflammation to cell transformation." Cell **139**(4): 693-706.
Iovine, B., M. L. Iannella, F. Nocella, M. R. Pricolo and M. A. Bevilacqua (2012). "Carnosine inhibits KRAS-mediated HCT116 proliferation by affecting ATP and ROS production." Cancer Lett **315**(2): 122-128.
Ishibashi, Y., T. Matsui, M. Takeuchi and S. Yamagishi (2013). "Metformin inhibits advanced glycation end products (AGEs)-induced growth and VEGF expression in MCF-7 breast cancer cells by suppressing AGEs receptor expression via AMP-activated protein kinase." Horm Metab Res **45**(5): 387-390.
Iyengar, N. M., C. A. Hudis and A. J. Dannenberg (2015). "Obesity and cancer: local and systemic mechanisms." Annu Rev Med **66**: 297-309.
Iyengar, N. M., X. K. Zhou, A. Gucalp, P. G. Morris, L. R. Howe, D. D. Giri, M. Morrow, H. Wang, M. Pollak, L. W. Jones, C. A. Hudis and A. J. Dannenberg (2016). "Systemic Correlates of White Adipose Tissue Inflammation in Early-Stage Breast Cancer." Clin Cancer Res **22**(9): 2283-2289.
Iyer, N. V., L. E. Kotch, F. Agani, S. W. Leung, E. Laughner, R. H. Wenger, M. Gassmann, J. D. Gearhart, A. M. Lawler, A. Y. Yu and G. L. Semenza (1998). "Cellular and developmental control of O2 homeostasis by hypoxia-inducible factor 1 alpha." Genes Dev **12**(2): 149-162.
Izaguirre, G., A. Kikonyogo and R. Pietruszko (1998). "Methylglyoxal as substrate and inhibitor of human aldehyde dehydrogenase: comparison of kinetic properties among the three isozymes." Comp Biochem Physiol B Biochem Mol Biol **119**(4): 747-754.
Jerzykowski, T., W. Matuszewski, N. Otrzonsek and R. Winter (1970). "Antineoplastic action of methylglyoxal." Neoplasma **17**(1): 25-35.
Jia, X., T. Chang, T. W. Wilson and L. Wu (2012). "Methylglyoxal mediates adipocyte proliferation by increasing phosphorylation of Akt1." PLoS One **7**(5): e36610.
Jia, X., D. J. Olson, A. R. Ross and L. Wu (2006). "Structural and functional changes in human insulin induced by methylglyoxal." FASEB J **20**(9): 1555-1557.
Jiang, Z., X. Li, J. Hu, W. Zhou, Y. Jiang, G. Li and D. Lu (2006). "Promoter hypermethylation-mediated down-regulation of LATS1 and LATS2 in human astrocytoma." Neurosci Res **56**(4): 450-458.
Jones, M. B., H. Krutzsch, H. Shu, Y. Zhao, L. A. Liotta, E. C. Kohn and E. F. Petricoin, 3rd (2002). "Proteomic analysis and identification of new biomarkers and therapeutic targets for invasive ovarian cancer." Proteomics **2**(1): 76-84.
Jowett, M. and J. H. Quastel (1933). "The glyoxalase activity of the red blood cell: The function of glutathione." Biochem J **27**(2): 486-498.
Junn, E., H. Taniguchi, B. S. Jeong, X. Zhao, H. Ichijo and M. M. Mouradian (2005). "Interaction of DJ-1 with Daxx inhibits apoptosis signal-regulating kinase 1 activity and cell death." Proc Natl Acad Sci U S A **102**(27): 9691-9696.
Kalapos, M. P. (2008). "The tandem of free radicals and methylglyoxal." Chem Biol Interact **171**(3): 251-271.

Kalapos, M. P., T. Garzo, F. Antoni and J. Mandl (1992). "Accumulation of S-D-lactoylglutathione and transient decrease of glutathione level caused by methylglyoxal load in isolated hepatocytes." Biochim Biophys Acta **1135**(2): 159-164.
Kalapos, M. P., A. Littauer and H. de Groot (1993). "Has reactive oxygen a role in methylglyoxal toxicity? A study on cultured rat hepatocytes." Arch Toxicol **67**(5): 369-372.
Kalembeyi, I., H. Inada, R. Nishiura, K. Imanaka-Yoshida, T. Sakakura and T. Yoshida (2003). "Tenascin-C upregulates matrix metalloproteinase-9 in breast cancer cells: direct and synergistic effects with transforming growth factor beta1." Int J Cancer **105**(1): 53-60.
Kamei, A. (1993). "Glutathione levels of the human crystalline lens in aging and its antioxidant effect against the oxidation of lens proteins." Biol Pharm Bull **16**(9): 870-875.
Kamei, J., M. Ohsawa, S. Miyata and S. Tanaka (2008). "Preventive effect of L-carnosine on changes in the thermal nociceptive threshold in streptozotocin-induced diabetic mice." Eur J Pharmacol **600**(1-3): 83-86.
Kang, J. H. (2003). "Modification and inactivation of human Cu,Zn-superoxide dismutase by methylglyoxal." Mol Cells **15**(2): 194-199.
Kang, Y., L. G. Edwards and P. J. Thornalley (1996). "Effect of methylglyoxal on human leukaemia 60 cell growth: modification of DNA G1 growth arrest and induction of apoptosis." Leuk Res **20**(5): 397-405.
Karuman, P., O. Gozani, R. D. Odze, X. C. Zhou, H. Zhu, R. Shaw, T. P. Brien, C. D. Bozzuto, D. Ooi, L. C. Cantley and J. Yuan (2001). "The Peutz-Jegher gene product LKB1 is a mediator of p53-dependent cell death." Mol Cell **7**(6): 1307-1319.
Kasznicki, J., A. Sliwinska and J. Drzewoski (2014). "Metformin in cancer prevention and therapy." Ann Transl Med **2**(6): 57.
Kavarana, M. J., E. G. Kovaleva, D. J. Creighton, M. B. Wollman and J. L. Eiseman (1999). "Mechanism-based competitive inhibitors of glyoxalase I: intracellular delivery, in vitro antitumor activities, and stabilities in human serum and mouse serum." J Med Chem **42**(2): 221-228.
Kelsey, J. L., M. D. Gammon and E. M. John (1993). "Reproductive factors and breast cancer." Epidemiol Rev **15**(1): 36-47.
Kender, Z., T. Fleming, S. Kopf, P. Torzsa, V. Grolmusz, S. Herzig, E. Schleicher, K. Racz, P. Reismann and P. P. Nawroth (2014). "Effect of metformin on methylglyoxal metabolism in patients with type 2 diabetes." Exp Clin Endocrinol Diabetes **122**(5): 316-319.
Kihara, M., J. D. Schmelzer, J. F. Poduslo, G. L. Curran, K. K. Nickander and P. A. Low (1991). "Aminoguanidine effects on nerve blood flow, vascular permeability, electrophysiology, and oxygen free radicals." Proc Natl Acad Sci U S A **88**(14): 6107-6111.
Kikuchi, S., K. Shinpo, F. Moriwaka, Z. Makita, T. Miyata and K. Tashiro (1999). "Neurotoxicity of methylglyoxal and 3-deoxyglucosone on cultured cortical neurons: synergism between glycation and oxidative stress, possibly involved in neurodegenerative diseases." J Neurosci Res **57**(2): 280-289.
Kim, J. W., I. Tchernyshyov, G. L. Semenza and C. V. Dang (2006). "HIF-1-mediated expression of pyruvate dehydrogenase kinase: a metabolic switch required for cellular adaptation to hypoxia." Cell Metab **3**(3): 177-185.
Kirk, J. E. (1960). "The glyoxalase I activity of arterial tissue in individuals of various ages." J Gerontol **15**: 139-141.
Kisfalvi, K., G. Eibl, J. Sinnett-Smith and E. Rozengurt (2009). "Metformin disrupts crosstalk between G protein-coupled receptor and insulin receptor signaling systems and inhibits pancreatic cancer growth." Cancer Res **69**(16): 6539-6545.
Kislinger, T., C. Fu, B. Huber, W. Qu, A. Taguchi, S. Du Yan, M. Hofmann, S. F. Yan, M. Pischetsrieder, D. Stern and A. M. Schmidt (1999). "N(epsilon)-(carboxymethyl)lysine adducts of proteins are ligands for receptor for advanced glycation end products that activate cell signaling pathways and modulate gene expression." J Biol Chem **274**(44): 31740-31749.

Kitaura, Y., N. Chikazawa, T. Tasaka, K. Nakano, M. Tanaka, H. Onishi and M. Katano (2011). "Transforming growth factor beta1 contributes to the invasiveness of pancreatic ductal adenocarcinoma cells through the regulation of CD24 expression." Pancreas **40**(7): 1034-1042.
Knight, R. J., K. F. Kofoed, H. R. Schelbert and D. B. Buxton (1996). "Inhibition of glyceraldehyde-3-phosphate dehydrogenase in post-ischaemic myocardium." Cardiovasc Res **32**(6): 1016-1023.
Kompf, J. and S. Bissbort (1976). "Confirmation of linkage between the loci for HL-A and glyoxalase I." Hum Genet **32**(2): 197-198.
Kondoh, H. (2008). "Cellular life span and the Warburg effect." Exp Cell Res **314**(9): 1923-1928.
Koppenol, W. H., P. L. Bounds and C. V. Dang (2011). "Otto Warburg's contributions to current concepts of cancer metabolism." Nat Rev Cancer **11**(5): 325-337.
Krogh, A. (1919). "The rate of diffusion of gases through animal tissues, with some remarks on the coefficient of invasion." J Physiol **52**(6): 391-408.
Kromer, S. A., M. S. Kessler, D. Milfay, I. N. Birg, M. Bunck, L. Czibere, M. Panhuysen, B. Putz, J. M. Deussing, F. Holsboer, R. Landgraf and C. W. Turck (2005). "Identification of glyoxalase-I as a protein marker in a mouse model of extremes in trait anxiety." J Neurosci **25**(17): 4375-4384.
Kuhla, B., K. Boeck, H. J. Luth, A. Schmidt, B. Weigle, M. Schmitz, V. Ogunlade, G. Munch and T. Arendt (2006). "Age-dependent changes of glyoxalase I expression in human brain." Neurobiol Aging **27**(6): 815-822.
Kuhla, B., K. Boeck, A. Schmidt, V. Ogunlade, T. Arendt, G. Munch and H. J. Luth (2007). "Age- and stage-dependent glyoxalase I expression and its activity in normal and Alzheimer's disease brains." Neurobiol Aging **28**(1): 29-41.
Kuniyasu, H., N. Oue, A. Wakikawa, H. Shigeishi, N. Matsutani, K. Kuraoka, R. Ito, H. Yokozaki and W. Yasui (2002). "Expression of receptors for advanced glycation end-products (RAGE) is closely associated with the invasive and metastatic activity of gastric cancer." J Pathol **196**(2): 163-170.
Kunkel, M., T. E. Reichert, P. Benz, H. A. Lehr, J. H. Jeong, S. Wieand, P. Bartenstein, W. Wagner and T. L. Whiteside (2003). "Overexpression of Glut-1 and increased glucose metabolism in tumors are associated with a poor prognosis in patients with oral squamous cell carcinoma." Cancer **97**(4): 1015-1024.
Kurz, A., N. Rabbani, M. Walter, M. Bonin, P. Thornalley, G. Auburger and S. Gispert (2011). "Alpha-synuclein deficiency leads to increased glyoxalase I expression and glycation stress." Cell Mol Life Sci **68**(4): 721-733.
Lal, S., W. C. Randall, A. H. Taylor, F. Kappler, M. Walker, T. R. Brown and B. S. Szwergold (1997). "Fructose-3-phosphate production and polyol pathway metabolism in diabetic rat hearts." Metabolism **46**(11): 1333-1338.
Larsen, K., A. C. Aronsson, E. Marmstal and B. Mannervik (1985). "Immunological comparison of glyoxalase I from yeast and mammals and quantitative determination of the enzyme in human tissues by radioimmunoassay." Comp Biochem Physiol B **82**(4): 625-638.
Larsson, S. C., C. S. Mantzoros and A. Wolk (2007). "Diabetes mellitus and risk of breast cancer: a meta-analysis." Int J Cancer **121**(4): 856-862.
Lederer, M. O. and R. G. Klaiber (1999). "Cross-linking of proteins by Maillard processes: characterization and detection of lysine-arginine cross-links derived from glyoxal and methylglyoxal." Bioorg Med Chem **7**(11): 2499-2507.
Lee, H. J., S. K. Howell, R. J. Sanford and P. J. Beisswenger (2005). "Methylglyoxal can modify GAPDH activity and structure." Ann N Y Acad Sci **1043**: 135-145.
Lee, J. Y., J. Song, K. Kwon, S. Jang, C. Kim, K. Baek, J. Kim and C. Park (2012). "Human DJ-1 and its homologs are novel glyoxalases." Hum Mol Genet **21**(14): 3215-3225.

Lee, K. M., J. H. Ju, K. Jang, W. Yang, J. Y. Yi, D. Y. Noh and I. Shin (2012). "CD24 regulates cell proliferation and transforming growth factor beta-induced epithelial to mesenchymal transition through modulation of integrin beta1 stability." Cell Signal **24**(11): 2132-2142.
Lejeune, D., N. Delsaux, B. Charloteaux, A. Thomas and R. Brasseur (2005). "Protein-nucleic acid recognition: statistical analysis of atomic interactions and influence of DNA structure." Proteins **61**(2): 258-271.
LeRoith, D., R. Novosyadlyy, E. J. Gallagher, D. Lann, A. Vijayakumar and S. Yakar (2008). "Obesity and type 2 diabetes are associated with an increased risk of developing cancer and a worse prognosis; epidemiological and mechanistic evidence." Exp Clin Endocrinol Diabetes **116 Suppl 1**: S4-6.
Levine, A. J. and A. M. Puzio-Kuter (2010). "The control of the metabolic switch in cancers by oncogenes and tumor suppressor genes." Science **330**(6009): 1340-1344.
Li, S. Y., Y. Liu, V. K. Sigmon, A. McCort and J. Ren (2005). "High-fat diet enhances visceral advanced glycation end products, nuclear O-Glc-Nac modification, p38 mitogen-activated protein kinase activation and apoptosis." Diabetes Obes Metab **7**(4): 448-454.
Li, X. H., J. Z. Xie, X. Jiang, B. L. Lv, X. S. Cheng, L. L. Du, J. Y. Zhang, J. Z. Wang and X. W. Zhou (2012). "Methylglyoxal induces tau hyperphosphorylation via promoting AGEs formation." Neuromolecular Med **14**(4): 338-348.
Liemburg-Apers, D. C., P. H. Willems, W. J. Koopman and S. Grefte (2015). "Interactions between mitochondrial reactive oxygen species and cellular glucose metabolism." Arch Toxicol **89**(8): 1209-1226.
Lindstad, R. I. and J. S. McKinley-McKee (1993). "Methylglyoxal and the polyol pathway. Three-carbon compounds are substrates for sheep liver sorbitol dehydrogenase." FEBS Lett **330**(1): 31-35.
Lis, H. and N. Sharon (1993). "Protein glycosylation. Structural and functional aspects." Eur J Biochem **218**(1): 1-27.
Liu, B., M. Bhat, A. K. Padival, D. G. Smith and R. H. Nagaraj (2004). "Effect of dicarbonyl modification of fibronectin on retinal capillary pericytes." Invest Ophthalmol Vis Sci **45**(6): 1983-1995.
Liu, B., Z. Fan, S. M. Edgerton, X. S. Deng, I. N. Alimova, S. E. Lind and A. D. Thor (2009). "Metformin induces unique biological and molecular responses in triple negative breast cancer cells." Cell Cycle **8**(13): 2031-2040.
Lo, T. W., T. Selwood and P. J. Thornalley (1994). "The reaction of methylglyoxal with aminoguanidine under physiological conditions and prevention of methylglyoxal binding to plasma proteins." Biochem Pharmacol **48**(10): 1865-1870.
Lo, T. W. and P. J. Thornalley (1992). "Inhibition of proliferation of human leukaemia 60 cells by diethyl esters of glyoxalase inhibitors in vitro." Biochem Pharmacol **44**(12): 2357-2363.
Lo, T. W., M. E. Westwood, A. C. McLellan, T. Selwood and P. J. Thornalley (1994). "Binding and modification of proteins by methylglyoxal under physiological conditions. A kinetic and mechanistic study with N alpha-acetylarginine, N alpha-acetylcysteine, and N alpha-acetyllysine, and bovine serum albumin." J Biol Chem **269**(51): 32299-32305.
Lunt, S. Y. and M. G. Vander Heiden (2011). "Aerobic glycolysis: meeting the metabolic requirements of cell proliferation." Annu Rev Cell Dev Biol **27**: 441-464.
Luth, H. J., V. Ogunlade, B. Kuhla, R. Kientsch-Engel, P. Stahl, J. Webster, T. Arendt and G. Munch (2005). "Age- and stage-dependent accumulation of advanced glycation end products in intracellular deposits in normal and Alzheimer's disease brains." Cereb Cortex **15**(2): 211-220.
Lyles, G. A. and J. Chalmers (1992). "The metabolism of aminoacetone to methylglyoxal by semicarbazide-sensitive amine oxidase in human umbilical artery." Biochem Pharmacol **43**(7): 1409-1414.
Maessen, D. E., O. Brouwers, K. H. Gaens, K. Wouters, J. P. Cleutjens, B. J. Janssen, T. Miyata, C. D. Stehouwer and C. G. Schalkwijk (2016). "Delayed Intervention With Pyridoxamine

Improves Metabolic Function and Prevents Adipose Tissue Inflammation and Insulin Resistance in High-Fat Diet-Induced Obese Mice." Diabetes **65**(4): 956-966.
Maessen, D. E., C. D. Stehouwer and C. G. Schalkwijk (2015). "The role of methylglyoxal and the glyoxalase system in diabetes and other age-related diseases." Clin Sci (Lond) **128**(12): 839-861.
Martinez-Zaguilan, R., R. M. Lynch, G. M. Martinez and R. J. Gillies (1993). "Vacuolar-type H(+)-ATPases are functionally expressed in plasma membranes of human tumor cells." Am J Physiol **265**(4 Pt 1): C1015-1029.
Masania, J., M. Malczewska-Malec, U. Razny, J. Goralska, A. Zdzienicka, B. Kiec-Wilk, A. Gruca, J. Stancel-Mozwillo, A. Dembinska-Kiec, N. Rabbani and P. J. Thornalley (2016). "Dicarbonyl stress in clinical obesity." Glycoconj J.
Maschler, S., S. Grunert, A. Danielopol, H. Beug and G. Wirl (2004). "Enhanced tenascin-C expression and matrix deposition during Ras/TGF-beta-induced progression of mammary tumor cells." Oncogene **23**(20): 3622-3633.
Mattson, M. P. (2008). "Hormesis defined." Ageing Res Rev **7**(1): 1-7.
Mayr, W. R., D. Mayr, J. Kompf, S. Bissbort and H. Ritter (1976). "Possible linkage of HL-A and GLO." Hum Genet **31**(2): 241-242.
Mazurek, S., C. B. Boschek, F. Hugo and E. Eigenbrodt (2005). "Pyruvate kinase type M2 and its role in tumor growth and spreading." Semin Cancer Biol **15**(4): 300-308.
McClung, J. A., N. Naseer, M. Saleem, G. P. Rossi, M. B. Weiss, N. G. Abraham and A. Kappas (2005). "Circulating endothelial cells are elevated in patients with type 2 diabetes mellitus independently of HbA(1)c." Diabetologia **48**(2): 345-350.
McFarland, G. A. and R. Holliday (1994). "Retardation of the senescence of cultured human diploid fibroblasts by carnosine." Exp Cell Res **212**(2): 167-175.
McKinney, G. R. and R. W. Rundles (1956). "Lactate formation and glyoxalase activity in normal and leukemic human leukocytes in vitro." Cancer Res **16**(1): 67-69.
McLean, L. A., J. Roscoe, N. K. Jorgensen, F. A. Gorin and P. M. Cala (2000). "Malignant gliomas display altered pH regulation by NHE1 compared with nontransformed astrocytes." Am J Physiol Cell Physiol **278**(4): C676-688.
McLellan, A. C. and P. J. Thornalley (1989). "Glyoxalase activity in human red blood cells fractioned by age." Mech Ageing Dev **48**(1): 63-71.
McLellan, A. C., P. J. Thornalley, J. Benn and P. H. Sonksen (1994). "Glyoxalase system in clinical diabetes mellitus and correlation with diabetic complications." Clin Sci (Lond) **87**(1): 21-29.
McPherson, K., C. M. Steel and J. M. Dixon (2000). "ABC of breast diseases. Breast cancer-epidemiology, risk factors, and genetics." BMJ **321**(7261): 624-628.
Mearini, E., R. Romani, L. Mearini, C. Antognelli, A. Zucchi, T. Baroni, M. Porena and V. N. Talesa (2002). "Differing expression of enzymes of the glyoxalase system in superficial and invasive bladder carcinomas." Eur J Cancer **38**(14): 1946-1950.
Metz, T. O., N. L. Alderson, S. R. Thorpe and J. W. Baynes (2003). "Pyridoxamine, an inhibitor of advanced glycation and lipoxidation reactions: a novel therapy for treatment of diabetic complications." Arch Biochem Biophys **419**(1): 41-49.
Michels, K. B., C. G. Solomon, F. B. Hu, B. A. Rosner, S. E. Hankinson, G. A. Colditz, J. E. Manson and S. Nurses' Health (2003). "Type 2 diabetes and subsequent incidence of breast cancer in the Nurses' Health Study." Diabetes Care **26**(6): 1752-1758.
Migliore, L., R. Barale, E. Bosco, F. Giorgelli, M. Minunni, R. Scarpato and N. Loprieno (1990). "Genotoxicity of methylglyoxal: cytogenetic damage in human lymphocytes in vitro and in intestinal cells of mice." Carcinogenesis **11**(9): 1503-1507.
Miki, Y., J. Swensen, D. Shattuck-Eidens, P. A. Futreal, K. Harshman, S. Tavtigian, Q. Liu, C. Cochran, L. M. Bennett, W. Ding and et al. (1994). "A strong candidate for the breast and ovarian cancer susceptibility gene BRCA1." Science **266**(5182): 66-71.

Milanesa, D. M., M. S. Choudhury, C. Mallouh, H. Tazaki and S. Konno (2000). "Methylglyoxal-induced apoptosis in human prostate carcinoma: potential modality for prostate cancer treatment." Eur Urol **37**(6): 728-734.
Minn, A. J., G. P. Gupta, P. M. Siegel, P. D. Bos, W. Shu, D. D. Giri, A. Viale, A. B. Olshen, W. L. Gerald and J. Massague (2005). "Genes that mediate breast cancer metastasis to lung." Nature **436**(7050): 518-524.
Misra, K., A. B. Banerjee, S. Ray and M. Ray (1995). "Glyoxalase III from Escherichia coli: a single novel enzyme for the conversion of methylglyoxal into D-lactate without reduced glutathione." Biochem J **305 (Pt 3)**: 999-1003.
Mo, J. S., Z. Meng, Y. C. Kim, H. W. Park, C. G. Hansen, S. Kim, D. S. Lim and K. L. Guan (2015). "Cellular energy stress induces AMPK-mediated regulation of YAP and the Hippo pathway." Nat Cell Biol **17**(4): 500-510.
Mochiki, E., H. Kuwano, H. Katoh, T. Asao, N. Oriuchi and K. Endo (2004). "Evaluation of 18F-2-deoxy-2-fluoro-D-glucose positron emission tomography for gastric cancer." World J Surg **28**(3): 247-253.
Monder, C. (1967). "Alpha-keto aldehyde dehydrogenase, an enzyme that catalyzes the enzymic oxidation of methylglyoxal to pyruvate." J Biol Chem **242**(20): 4603-4609.
Montcourrier, P., I. Silver, R. Farnoud, I. Bird and H. Rochefort (1997). "Breast cancer cells have a high capacity to acidify extracellular milieu by a dual mechanism." Clin Exp Metastasis **15**(4): 382-392.
Morcos, M., X. Du, F. Pfisterer, H. Hutter, A. A. Sayed, P. Thornalley, N. Ahmed, J. Baynes, S. Thorpe, G. Kukudov, A. Schlotterer, F. Bozorgmehr, R. A. El Baki, D. Stern, F. Moehrlen, Y. Ibrahim, D. Oikonomou, A. Hamann, C. Becker, M. Zeier, V. Schwenger, N. Miftari, P. Humpert, H. P. Hammes, M. Buechler, A. Bierhaus, M. Brownlee and P. P. Nawroth (2008). "Glyoxalase-1 prevents mitochondrial protein modification and enhances lifespan in Caenorhabditis elegans." Aging Cell **7**(2): 260-269.
Moreno-Sanchez, R., S. Rodriguez-Enriquez, A. Marin-Hernandez and E. Saavedra (2007). "Energy metabolism in tumor cells." FEBS J **274**(6): 1393-1418.
Morgan, P. E., R. T. Dean and M. J. Davies (2002). "Inactivation of cellular enzymes by carbonyls and protein-bound glycation/glycoxidation products." Arch Biochem Biophys **403**(2): 259-269.
Morin-Kensicki, E. M., B. N. Boone, M. Howell, J. R. Stonebraker, J. Teed, J. G. Alb, T. R. Magnuson, W. O'Neal and S. L. Milgram (2006). "Defects in yolk sac vasculogenesis, chorioallantoic fusion, and embryonic axis elongation in mice with targeted disruption of Yap65." Mol Cell Biol **26**(1): 77-87.
Morita, T., T. Nagaki, I. Fukuda and K. Okumura (1992). "Clastogenicity of low pH to various cultured mammalian cells." Mutat Res **268**(2): 297-305.
Mulvihill, M. M., D. I. Benjamin, X. Ji, E. Le Scolan, S. M. Louie, A. Shieh, M. Green, T. Narasimhalu, P. J. Morris, K. Luo and D. K. Nomura (2014). "Metabolic profiling reveals PAFAH1B3 as a critical driver of breast cancer pathogenicity." Chem Biol **21**(7): 831-840.
Murata-Kamiya, N. and H. Kamiya (2001). "Methylglyoxal, an endogenous aldehyde, crosslinks DNA polymerase and the substrate DNA." Nucleic Acids Res **29**(16): 3433-3438.
Murthy, N. S., T. Bakeris, M. J. Kavarana, D. S. Hamilton, Y. Lan and D. J. Creighton (1994). "S-(N-aryl-N-hydroxycarbamoyl)glutathione derivatives are tight-binding inhibitors of glyoxalase I and slow substrates for glyoxalase II." J Med Chem **37**(14): 2161-2166.
Nagaraj, R. H., T. Oya-Ito, P. S. Padayatti, R. Kumar, S. Mehta, K. West, B. Levison, J. Sun, J. W. Crabb and A. K. Padival (2003). "Enhancement of chaperone function of alpha-crystallin by methylglyoxal modification." Biochemistry **42**(36): 10746-10755.
Nagaraj, R. H., P. Sarkar, A. Mally, K. M. Biemel, M. O. Lederer and P. S. Padayatti (2002). "Effect of pyridoxamine on chemical modification of proteins by carbonyls in diabetic rats:

characterization of a major product from the reaction of pyridoxamine and methylglyoxal." Arch Biochem Biophys **402**(1): 110-119.
Nagaraj, R. H., I. N. Shipanova and F. M. Faust (1996). "Protein cross-linking by the Maillard reaction. Isolation, characterization, and in vivo detection of a lysine-lysine cross-link derived from methylglyoxal." J Biol Chem **271**(32): 19338-19345.
Nakadate, Y., K. Uchida, K. Shikata, S. Yoshimura, M. Azuma, T. Hirata, H. Konishi, H. Kiyama and T. Tachibana (2009). "The formation of argpyrimidine, a methylglyoxal-arginine adduct, in the nucleus of neural cells." Biochem Biophys Res Commun **378**(2): 209-212.
Nakamura, T., Y. Furukawa, H. Nakagawa, T. Tsunoda, H. Ohigashi, K. Murata, O. Ishikawa, K. Ohgaki, N. Kashimura, M. Miyamoto, S. Hirano, S. Kondo, H. Katoh, Y. Nakamura and T. Katagiri (2004). "Genome-wide cDNA microarray analysis of gene expression profiles in pancreatic cancers using populations of tumor cells and normal ductal epithelial cells selected for purity by laser microdissection." Oncogene **23**(13): 2385-2400.
Neckers, L. and P. Workman (2012). "Hsp90 molecular chaperone inhibitors: are we there yet?" Clin Cancer Res **18**(1): 64-76.
Nicolay, J. P., J. Schneider, O. M. Niemoeller, F. Artunc, M. Portero-Otin, G. Haik, Jr., P. J. Thornalley, E. Schleicher, T. Wieder and F. Lang (2006). "Stimulation of suicidal erythrocyte death by methylglyoxal." Cell Physiol Biochem **18**(4-5): 223-232.
Nikitovic, D., A. Berdiaki, A. Zafiropoulos, P. Katonis, A. Tsatsakis, N. K. Karamanos and G. N. Tzanakakis (2008). "Lumican expression is positively correlated with the differentiation and negatively with the growth of human osteosarcoma cells." FEBS J **275**(2): 350-361.
Nikitovic, D., G. Chalkiadaki, A. Berdiaki, J. Aggelidakis, P. Katonis, N. K. Karamanos and G. N. Tzanakakis (2011). "Lumican regulates osteosarcoma cell adhesion by modulating TGFbeta2 activity." Int J Biochem Cell Biol **43**(6): 928-935.
Ober, S. S. and A. B. Pardee (1987). "Intracellular pH is increased after transformation of Chinese hamster embryo fibroblasts." Proc Natl Acad Sci U S A **84**(9): 2766-2770.
Ogretmen, B. and Y. A. Hannun (2004). "Biologically active sphingolipids in cancer pathogenesis and treatment." Nat Rev Cancer **4**(8): 604-616.
Oimomi, M., F. Hata, N. Igaki, T. Nakamichi, S. Baba and H. Kato (1989). "Purification of alpha-ketoaldehyde dehydrogenase from the human liver and its possible significance in the control of glycation." Experientia **45**(5): 463-466.
Okamoto, T., S. Yamagishi, Y. Inagaki, S. Amano, K. Koga, R. Abe, M. Takeuchi, S. Ohno, A. Yoshimura and Z. Makita (2002). "Angiogenesis induced by advanced glycation end products and its prevention by cerivastatin." FASEB J **16**(14): 1928-1930.
Olsson, H., H. Jernstrom, P. Alm, H. Kreipe, C. Ingvar, P. E. Jonsson and S. Ryden (1996). "Proliferation of the breast epithelium in relation to menstrual cycle phase, hormonal use, and reproductive factors." Breast Cancer Res Treat **40**(2): 187-196.
Orr, W. C., S. N. Radyuk, L. Prabhudesai, D. Toroser, J. J. Benes, J. M. Luchak, R. J. Mockett, I. Rebrin, J. G. Hubbard and R. S. Sohal (2005). "Overexpression of glutamate-cysteine ligase extends life span in Drosophila melanogaster." J Biol Chem **280**(45): 37331-37338.
Oskarsson, T., S. Acharyya, X. H. Zhang, S. Vanharanta, S. F. Tavazoie, P. G. Morris, R. J. Downey, K. Manova-Todorova, E. Brogi and J. Massague (2011). "Breast cancer cells produce tenascin C as a metastatic niche component to colonize the lungs." Nat Med **17**(7): 867-874.
Oya-Ito, T., B. F. Liu and R. H. Nagaraj (2006). "Effect of methylglyoxal modification and phosphorylation on the chaperone and anti-apoptotic properties of heat shock protein 27." J Cell Biochem **99**(1): 279-291.
Oya-Ito, T., Y. Naito, T. Takagi, O. Handa, H. Matsui, M. Yamada, K. Shima and T. Yoshikawa (2011). "Heat-shock protein 27 (Hsp27) as a target of methylglyoxal in gastrointestinal cancer." Biochim Biophys Acta **1812**(7): 769-781.

Oya, T., N. Hattori, Y. Mizuno, S. Miyata, S. Maeda, T. Osawa and K. Uchida (1999). "Methylglyoxal modification of protein. Chemical and immunochemical characterization of methylglyoxal-arginine adducts." J Biol Chem **274**(26): 18492-18502.
Padival, A. K., J. W. Crabb and R. H. Nagaraj (2003). "Methylglyoxal modifies heat shock protein 27 in glomerular mesangial cells." FEBS Lett **551**(1-3): 113-118.
Pamplona, R., M. J. Bellmunt, M. Portero, D. Riba and J. Prat (1995). "Chromatographic evidence for Amadori product formation in rat liver aminophospholipids." Life Sci **57**(9): 873-879.
Papandreou, I., R. A. Cairns, L. Fontana, A. L. Lim and N. C. Denko (2006). "HIF-1 mediates adaptation to hypoxia by actively downregulating mitochondrial oxygen consumption." Cell Metab **3**(3): 187-197.
Papoulis, A., Y. al-Abed and R. Bucala (1995). "Identification of N2-(1-carboxyethyl)guanine (CEG) as a guanine advanced glycosylation end product." Biochemistry **34**(2): 648-655.
Park, H. J., J. C. Lyons, T. Ohtsubo and C. W. Song (1999). "Acidic environment causes apoptosis by increasing caspase activity." Br J Cancer **80**(12): 1892-1897.
Pedchenko, V., R. Zent and B. G. Hudson (2004). "Alpha(v)beta3 and alpha(v)beta5 integrins bind both the proximal RGD site and non-RGD motifs within noncollagenous (NC1) domain of the alpha3 chain of type IV collagen: implication for the mechanism of endothelia cell adhesion." J Biol Chem **279**(4): 2772-2780.
Pedchenko, V. K., S. V. Chetyrkin, P. Chuang, A. J. Ham, M. A. Saleem, P. W. Mathieson, B. G. Hudson and P. A. Voziyan (2005). "Mechanism of perturbation of integrin-mediated cell-matrix interactions by reactive carbonyl compounds and its implication for pathogenesis of diabetic nephropathy." Diabetes **54**(10): 2952-2960.
Pelucchi, C., I. Tramacere, P. Boffetta, E. Negri and C. La Vecchia (2011). "Alcohol consumption and cancer risk." Nutr Cancer **63**(7): 983-990.
Penault-Llorca, F. and G. Viale (2012). "Pathological and molecular diagnosis of triple-negative breast cancer: a clinical perspective." Ann Oncol **23 Suppl 6**: vi19-22.
Perou, C. M., T. Sorlie, M. B. Eisen, M. van de Rijn, S. S. Jeffrey, C. A. Rees, J. R. Pollack, D. T. Ross, H. Johnsen, L. A. Akslen, O. Fluge, A. Pergamenschikov, C. Williams, S. X. Zhu, P. E. Lonning, A. L. Borresen-Dale, P. O. Brown and D. Botstein (2000). "Molecular portraits of human breast tumours." Nature **406**(6797): 747-752.
Pfeiffer, T., S. Schuster and S. Bonhoeffer (2001). "Cooperation and competition in the evolution of ATP-producing pathways." Science **292**(5516): 504-507.
Pfister, F., E. Riedl, Q. Wang, F. vom Hagen, M. Deinzer, M. C. Harmsen, G. Molema, B. Yard, Y. Feng and H. P. Hammes (2011). "Oral carnosine supplementation prevents vascular damage in experimental diabetic retinopathy." Cell Physiol Biochem **28**(1): 125-136.
Phillips, S. A. and P. J. Thornalley (1993). "The formation of methylglyoxal from triose phosphates. Investigation using a specific assay for methylglyoxal." Eur J Biochem **212**(1): 101-105.
Piccart-Gebhart, M. J., M. Procter, B. Leyland-Jones, A. Goldhirsch, M. Untch, I. Smith, L. Gianni, J. Baselga, R. Bell, C. Jackisch, D. Cameron, M. Dowsett, C. H. Barrios, G. Steger, C. S. Huang, M. Andersson, M. Inbar, M. Lichinitser, I. Lang, U. Nitz, H. Iwata, C. Thomssen, C. Lohrisch, T. M. Suter, J. Ruschoff, T. Suto, V. Greatorex, C. Ward, C. Straehle, E. McFadden, M. S. Dolci, R. D. Gelber and T. Herceptin Adjuvant Trial Study (2005). "Trastuzumab after adjuvant chemotherapy in HER2-positive breast cancer." N Engl J Med **353**(16): 1659-1672.
Piccolo, S., S. Dupont and M. Cordenonsi (2014). "The biology of YAP/TAZ: hippo signaling and beyond." Physiol Rev **94**(4): 1287-1312.
Pierobon, M. and C. L. Frankenfeld (2013). "Obesity as a risk factor for triple-negative breast cancers: a systematic review and meta-analysis." Breast Cancer Res Treat **137**(1): 307-314.
Pischetsrieder, M., W. Seidel, G. Munch and R. Schinzel (1999). "N(2)-(1-Carboxyethyl)deoxyguanosine, a nonenzymatic glycation adduct of DNA, induces single-strand breaks and increases mutation frequencies." Biochem Biophys Res Commun **264**(2): 544-549.

Porporato, P. E., V. L. Payen, J. Perez-Escuredo, C. J. De Saedeleer, P. Danhier, T. Copetti, S. Dhup, M. Tardy, T. Vazeille, C. Bouzin, O. Feron, C. Michiels, B. Gallez and P. Sonveaux (2014). "A mitochondrial switch promotes tumor metastasis." Cell Rep **8**(3): 754-766.
Postovit, L. M., M. A. Adams, G. E. Lash, J. P. Heaton and C. H. Graham (2002). "Oxygen-mediated regulation of tumor cell invasiveness. Involvement of a nitric oxide signaling pathway." J Biol Chem **277**(38): 35730-35737.
Postovit, L. M., M. A. Adams, G. E. Lash, J. P. Heaton and C. H. Graham (2004). "Nitric oxide-mediated regulation of hypoxia-induced B16F10 melanoma metastasis." Int J Cancer **108**(1): 47-53.
Protani, M., M. Coory and J. H. Martin (2010). "Effect of obesity on survival of women with breast cancer: systematic review and meta-analysis." Breast Cancer Res Treat **123**(3): 627-635.
Queisser, M. A., D. Yao, S. Geisler, H. P. Hammes, G. Lochnit, E. D. Schleicher, M. Brownlee and K. T. Preissner (2010). "Hyperglycemia impairs proteasome function by methylglyoxal." Diabetes **59**(3): 670-678.
Quinn, B. J., H. Kitagawa, R. M. Memmott, J. J. Gills and P. A. Dennis (2013). "Repositioning metformin for cancer prevention and treatment." Trends Endocrinol Metab **24**(9): 469-480.
Rabbani, N., M. V. Chittari, C. W. Bodmer, D. Zehnder, A. Ceriello and P. J. Thornalley (2010). "Increased glycation and oxidative damage to apolipoprotein B100 of LDL cholesterol in patients with type 2 diabetes and effect of metformin." Diabetes **59**(4): 1038-1045.
Rabbani, N., L. Godfrey, M. Xue, F. Shaheen, M. Geoffrion, R. Milne and P. J. Thornalley (2011). "Glycation of LDL by methylglyoxal increases arterial atherogenicity: a possible contributor to increased risk of cardiovascular disease in diabetes." Diabetes **60**(7): 1973-1980.
Rabbani, N. and P. J. Thornalley (2011). "Glyoxalase in diabetes, obesity and related disorders." Semin Cell Dev Biol **22**(3): 309-317.
Rabbani, N. and P. J. Thornalley (2012). "Glycation research in amino acids: a place to call home." Amino Acids **42**(4): 1087-1096.
Rabbani, N. and P. J. Thornalley (2012). "Methylglyoxal, glyoxalase 1 and the dicarbonyl proteome." Amino Acids **42**(4): 1133-1142.
Rabbani, N. and P. J. Thornalley (2014). "Dicarbonyl proteome and genome damage in metabolic and vascular disease." Biochem Soc Trans **42**(2): 425-432.
Rabbani, N. and P. J. Thornalley (2014). "Measurement of methylglyoxal by stable isotopic dilution analysis LC-MS/MS with corroborative prediction in physiological samples." Nat Protoc **9**(8): 1969-1979.
Rabbani, N. and P. J. Thornalley (2015). "Dicarbonyl stress in cell and tissue dysfunction contributing to ageing and disease." Biochem Biophys Res Commun **458**(2): 221-226.
Racker, E. (1951). "The mechanism of action of glyoxalase." J Biol Chem **190**(2): 685-696.
Racker, E. (1952). "Spectrophotometric measurements of the metabolic formation and degradation of thiol esters and enediol compounds." Biochim Biophys Acta **9**(5): 577-578.
Radu, B. M., D. I. Dumitrescu, C. C. Mustaciosu and M. Radu (2012). "Dual effect of methylglyoxal on the intracellular Ca2+ signaling and neurite outgrowth in mouse sensory neurons." Cell Mol Neurobiol **32**(6): 1047-1057.
Rahman, A., Shahabuddin and S. M. Hadi (1990). "Formation of strand breaks and interstrand cross-links in DNA by methylglyoxal." J Biochem Toxicol **5**(3): 161-166.
Ranganathan, S., P. J. Ciaccio, E. S. Walsh and K. D. Tew (1999). "Genomic sequence of human glyoxalase-I: analysis of promoter activity and its regulation." Gene **240**(1): 149-155.
Ranganathan, S. and K. D. Tew (1993). "Analysis of glyoxalase-I from normal and tumor tissue from human colon." Biochim Biophys Acta **1182**(3): 311-316.
Ranganathan, S., E. S. Walsh, A. K. Godwin and K. D. Tew (1993). "Cloning and characterization of human colon glyoxalase-I." J Biol Chem **268**(8): 5661-5667.

Rankinen, T., A. Zuberi, Y. C. Chagnon, S. J. Weisnagel, G. Argyropoulos, B. Walts, L. Perusse and C. Bouchard (2006). "The human obesity gene map: the 2005 update." Obesity (Silver Spring) **14**(4): 529-644.
Ratliff, D. M., D. J. Vander Jagt, R. P. Eaton and D. L. Vander Jagt (1996). "Increased levels of methylglyoxal-metabolizing enzymes in mononuclear and polymorphonuclear cells from insulin-dependent diabetic patients with diabetic complications: aldose reductase, glyoxalase I, and glyoxalase II--a clinical research center study." J Clin Endocrinol Metab **81**(2): 488-492.
Renner, C., N. Zemitzsch, B. Fuchs, K. D. Geiger, M. Hermes, J. Hengstler, R. Gebhardt, J. Meixensberger and F. Gaunitz (2010). "Carnosine retards tumor growth in vivo in an NIH3T3-HER2/neu mouse model." Mol Cancer **9**: 2.
Requena, J. R., M. U. Ahmed, C. W. Fountain, T. P. Degenhardt, S. Reddy, C. Perez, T. J. Lyons, A. J. Jenkins, J. W. Baynes and S. R. Thorpe (1997). "Carboxymethylethanolamine, a biomarker of phospholipid modification during the maillard reaction in vivo." J Biol Chem **272**(28): 17473-17479.
Reynolds, P. (2013). "Smoking and breast cancer." J Mammary Gland Biol Neoplasia **18**(1): 15-23.
Richard, J. P. (1993). "Mechanism for the formation of methylglyoxal from triosephosphates." Biochem Soc Trans **21**(2): 549-553.
Richarme, G., M. Mihoub, J. Dairou, L. C. Bui, T. Leger and A. Lamouri (2015). "Parkinsonism-associated protein DJ-1/Park7 is a major protein deglycase that repairs methylglyoxal- and glyoxal-glycated cysteine, arginine, and lysine residues." J Biol Chem **290**(3): 1885-1897.
Riedl, E., F. Pfister, M. Braunagel, P. Brinkkotter, P. Sternik, M. Deinzer, S. J. Bakker, R. H. Henning, J. van den Born, B. K. Kramer, G. Navis, H. P. Hammes, B. Yard and H. Koeppel (2011). "Carnosine prevents apoptosis of glomerular cells and podocyte loss in STZ diabetic rats." Cell Physiol Biochem **28**(2): 279-288.
Riley, M. L. and J. J. Harding (1995). "The reaction of methylglyoxal with human and bovine lens proteins." Biochim Biophys Acta **1270**(1): 36-43.
Riordan, J. F., K. D. McElvany and C. L. Borders, Jr. (1977). "Arginyl residues: anion recognition sites in enzymes." Science **195**(4281): 884-886.
Rofstad, E. K. and T. Danielsen (1999). "Hypoxia-induced metastasis of human melanoma cells: involvement of vascular endothelial growth factor-mediated angiogenesis." Br J Cancer **80**(11): 1697-1707.
Rogalla, T., M. Ehrnsperger, X. Preville, A. Kotlyarov, G. Lutsch, C. Ducasse, C. Paul, M. Wieske, A. P. Arrigo, J. Buchner and M. Gaestel (1999). "Regulation of Hsp27 oligomerization, chaperone function, and protective activity against oxidative stress/tumor necrosis factor alpha by phosphorylation." J Biol Chem **274**(27): 18947-18956.
Rojas, A., I. Gonzalez, E. Morales, R. Perez-Castro, J. Romero and H. Figueroa (2011). "Diabetes and cancer: Looking at the multiligand/RAGE axis." World J Diabetes **2**(7): 108-113.
Romanuik, T. L., T. Ueda, N. Le, S. Haile, T. M. Yong, T. Thomson, R. L. Vessella and M. D. Sadar (2009). "Novel biomarkers for prostate cancer including noncoding transcripts." Am J Pathol **175**(6): 2264-2276.
Romond, E. H., E. A. Perez, J. Bryant, V. J. Suman, C. E. Geyer, Jr., N. E. Davidson, E. Tan-Chiu, S. Martino, S. Paik, P. A. Kaufman, S. M. Swain, T. M. Pisansky, L. Fehrenbacher, L. A. Kutteh, V. G. Vogel, D. W. Visscher, G. Yothers, R. B. Jenkins, A. M. Brown, S. R. Dakhil, E. P. Mamounas, W. L. Lingle, P. M. Klein, J. N. Ingle and N. Wolmark (2005). "Trastuzumab plus adjuvant chemotherapy for operable HER2-positive breast cancer." N Engl J Med **353**(16): 1673-1684.
Rosca, M. G., T. G. Mustata, M. T. Kinter, A. M. Ozdemir, T. S. Kern, L. I. Szweda, M. Brownlee, V. M. Monnier and M. F. Weiss (2005). "Glycation of mitochondrial proteins from diabetic rat kidney is associated with excess superoxide formation." Am J Physiol Renal Physiol **289**(2): F420-430.

Ruggiero-Lopez, D., M. Lecomte, G. Moinet, G. Patereau, M. Lagarde and N. Wiernsperger (1999). "Reaction of metformin with dicarbonyl compounds. Possible implication in the inhibition of advanced glycation end product formation." Biochem Pharmacol **58**(11): 1765-1773.
Rulli, A., L. Carli, R. Romani, T. Baroni, E. Giovannini, G. Rosi and V. Talesa (2001). "Expression of glyoxalase I and II in normal and breast cancer tissues." Breast Cancer Res Treat **66**(1): 67-72.
Ruoslahti, E. (1996). "RGD and other recognition sequences for integrins." Annu Rev Cell Dev Biol **12**: 697-715.
Sakamoto, H., T. Mashima, A. Kizaki, S. Dan, Y. Hashimoto, M. Naito and T. Tsuruo (2000). "Glyoxalase I is involved in resistance of human leukemia cells to antitumor agent-induced apoptosis." Blood **95**(10): 3214-3218.
Sakamoto, H., T. Mashima, S. Sato, Y. Hashimoto, T. Yamori and T. Tsuruo (2001). "Selective activation of apoptosis program by S-p-bromobenzylglutathione cyclopentyl diester in glyoxalase I-overexpressing human lung cancer cells." Clin Cancer Res **7**(8): 2513-2518.
Sakamoto, H., T. Mashima, K. Yamamoto and T. Tsuruo (2002). "Modulation of heat-shock protein 27 (Hsp27) anti-apoptotic activity by methylglyoxal modification." J Biol Chem **277**(48): 45770-45775.
Samadi, A. A., S. A. Fullerton, D. G. Tortorelis, G. B. Johnson, S. D. Davidson, M. S. Choudhury, C. Mallouh, H. Tazaki and S. Konno (2001). "Glyoxalase I phenotype as a potential risk factor for prostate carcinoma." Urology **57**(1): 183-187.
Santarius, T., G. R. Bignell, C. D. Greenman, S. Widaa, L. Chen, C. L. Mahoney, A. Butler, S. Edkins, S. Waris, P. J. Thornalley, P. A. Futreal and M. R. Stratton (2010). "GLO1-A novel amplified gene in human cancer." Genes Chromosomes Cancer **49**(8): 711-725.
Santel, T., G. Pflug, N. Y. Hemdan, A. Schafer, M. Hollenbach, M. Buchold, A. Hintersdorf, I. Lindner, A. Otto, M. Bigl, I. Oerlecke, A. Hutschenreuther, U. Sack, K. Huse, M. Groth, C. Birkemeyer, W. Schellenberger, R. Gebhardt, M. Platzer, T. Weiss, M. A. Vijayalakshmi, M. Kruger and G. Birkenmeier (2008). "Curcumin inhibits glyoxalase 1: a possible link to its anti-inflammatory and anti-tumor activity." PLoS One **3**(10): e3508.
Santini, D., C. Ceccarelli, M. Taffurelli, S. Pileri and D. Marrano (1996). "Differentiation pathways in primary invasive breast carcinoma as suggested by intermediate filament and biopathological marker expression." J Pathol **179**(4): 386-391.
Schalkwijk, C. G. (2015). "Vascular AGE-ing by methylglyoxal: the past, the present and the future." Diabetologia **58**(8): 1715-1719.
Schalkwijk, C. G., J. van Bezu, R. C. van der Schors, K. Uchida, C. D. Stehouwer and V. W. van Hinsbergh (2006). "Heat-shock protein 27 is a major methylglyoxal-modified protein in endothelial cells." FEBS Lett **580**(6): 1565-1570.
Schleicher, E., T. Deufel and O. H. Wieland (1981). "Non-enzymatic glycosylation of human serum lipoproteins. Elevated epsilon-lysine glycosylated low density lipoprotein in diabetic patients." FEBS Lett **129**(1): 1-4.
Schmidt, A. M., O. Hori, J. X. Chen, J. F. Li, J. Crandall, J. Zhang, R. Cao, S. D. Yan, J. Brett and D. Stern (1995). "Advanced glycation endproducts interacting with their endothelial receptor induce expression of vascular cell adhesion molecule-1 (VCAM-1) in cultured human endothelial cells and in mice. A potential mechanism for the accelerated vasculopathy of diabetes." J Clin Invest **96**(3): 1395-1403.
Schneider, M. B., H. Matsuzaki, J. Haorah, A. Ulrich, J. Standop, X. Z. Ding, T. E. Adrian and P. M. Pour (2001). "Prevention of pancreatic cancer induction in hamsters by metformin." Gastroenterology **120**(5): 1263-1270.
Scire, A., F. Tanfani, F. Saccucci, E. Bertoli and G. Principato (2000). "Specific interaction of cytosolic and mitochondrial glyoxalase II with acidic phospholipids in form of liposomes results in the inhibition of the cytosolic enzyme only." Proteins **41**(1): 33-39.

Seitz, H. K., C. Pelucchi, V. Bagnardi and C. La Vecchia (2012). "Epidemiology and pathophysiology of alcohol and breast cancer: Update 2012." Alcohol Alcohol **47**(3): 204-212.
Sell, D. R. and V. M. Monnier (2012). "Molecular basis of arterial stiffening: role of glycation - a mini-review." Gerontology **58**(3): 227-237.
Sellin, S., L. E. Eriksson, A. C. Aronsson and B. Mannervik (1983). "Octahedral metal coordination in the active site of glyoxalase I as evidenced by the properties of Co(II)-glyoxalase I." J Biol Chem **258**(4): 2091-2093.
Sellin, S. and B. Mannervik (1983). "Reversal of the reaction catalyzed by glyoxalase I. Calculation of the equilibrium constant for the enzymatic reaction." J Biol Chem **258**(14): 8872-8875.
Semenza, G. L. (1998). "Hypoxia-inducible factor 1 and the molecular physiology of oxygen homeostasis." J Lab Clin Med **131**(3): 207-214.
Semenza, G. L., P. H. Roth, H. M. Fang and G. L. Wang (1994). "Transcriptional regulation of genes encoding glycolytic enzymes by hypoxia-inducible factor 1." J Biol Chem **269**(38): 23757-23763.
Sen, S., T. Bose, A. Roy and A. S. Chakraborti (2007). "Effect of non-enzymatic glycation on esterase activities of hemoglobin and myoglobin." Mol Cell Biochem **301**(1-2): 251-257.
Sena, L. A. and N. S. Chandel (2012). "Physiological roles of mitochondrial reactive oxygen species." Mol Cell **48**(2): 158-167.
Shapiro, R., B. I. Cohen, S. J. Shiuey and H. Maurer (1969). "On the reaction of guanine with glyoxal, pyruvaldehyde, and kethoxal, and the structure of the acylguanines. A new synthesis of N2-alkylguanines." Biochemistry **8**(1): 238-245.
Shapiro, R. and J. Hachmann (1966). "The reaction of guanine derivatives with 1,2-dicarbonyl compounds." Biochemistry **5**(9): 2799-2807.
Sharkey, E. M., H. B. O'Neill, M. J. Kavarana, H. Wang, D. J. Creighton, D. L. Sentz and J. L. Eiseman (2000). "Pharmacokinetics and antitumor properties in tumor-bearing mice of an enediol analogue inhibitor of glyoxalase I." Cancer Chemother Pharmacol **46**(2): 156-166.
Sharma-Luthra, R. and R. K. Kale (1994). "Age related changes in the activity of the glyoxalase system." Mech Ageing Dev **73**(1): 39-45.
Shen, Y., J. Yang, J. Li, X. Shi, L. Ouyang, Y. Tian and J. Lu (2014). "Carnosine inhibits the proliferation of human gastric cancer SGC-7901 cells through both of the mitochondrial respiration and glycolysis pathways." PLoS One **9**(8): e104632.
Shendelman, S., A. Jonason, C. Martinat, T. Leete and A. Abeliovich (2004). "DJ-1 is a redox-dependent molecular chaperone that inhibits alpha-synuclein aggregate formation." PLoS Biol **2**(11): e362.
Shi, D. Y., F. Z. Xie, C. Zhai, J. S. Stern, Y. Liu and S. L. Liu (2009). "The role of cellular oxidative stress in regulating glycolysis energy metabolism in hepatoma cells." Mol Cancer **8**: 32.
Shim, H., C. Dolde, B. C. Lewis, C. S. Wu, G. Dang, R. A. Jungmann, R. Dalla-Favera and C. V. Dang (1997). "c-Myc transactivation of LDH-A: implications for tumor metabolism and growth." Proc Natl Acad Sci U S A **94**(13): 6658-6663.
Shinohara, M., P. J. Thornalley, I. Giardino, P. Beisswenger, S. R. Thorpe, J. Onorato and M. Brownlee (1998). "Overexpression of glyoxalase-I in bovine endothelial cells inhibits intracellular advanced glycation endproduct formation and prevents hyperglycemia-induced increases in macromolecular endocytosis." J Clin Invest **101**(5): 1142-1147.
Shipanova, I. N., M. A. Glomb and R. H. Nagaraj (1997). "Protein modification by methylglyoxal: chemical nature and synthetic mechanism of a major fluorescent adduct." Arch Biochem Biophys **344**(1): 29-36.
Shumaev, K. B., S. A. Gubkina, E. M. Kumskova, G. S. Shepelkova, E. K. Ruuge and V. Z. Lankin (2009). "Superoxide formation as a result of interaction of L-lysine with dicarbonyl compounds and its possible mechanism." Biochemistry (Mosc) **74**(4): 461-466.

Smith-Beckerman, D. M., K. W. Fung, K. E. Williams, N. Auersperg, A. K. Godwin and A. L. Burlingame (2005). "Proteome changes in ovarian epithelial cells derived from women with BRCA1 mutations and family histories of cancer." Mol Cell Proteomics **4**(2): 156-168.
Smith, I., M. Procter, R. D. Gelber, S. Guillaume, A. Feyereislova, M. Dowsett, A. Goldhirsch, M. Untch, G. Mariani, J. Baselga, M. Kaufmann, D. Cameron, R. Bell, J. Bergh, R. Coleman, A. Wardley, N. Harbeck, R. I. Lopez, P. Mallmann, K. Gelmon, N. Wilcken, E. Wist, P. Sanchez Rovira, M. J. Piccart-Gebhart and H. s. team (2007). "2-year follow-up of trastuzumab after adjuvant chemotherapy in HER2-positive breast cancer: a randomised controlled trial." Lancet **369**(9555): 29-36.
Smith, M. A., S. Taneda, P. L. Richey, S. Miyata, S. D. Yan, D. Stern, L. M. Sayre, V. M. Monnier and G. Perry (1994). "Advanced Maillard reaction end products are associated with Alzheimer disease pathology." Proc Natl Acad Sci U S A **91**(12): 5710-5714.
Snow, L. M., N. A. Fugere and L. V. Thompson (2007). "Advanced glycation end-product accumulation and associated protein modification in type II skeletal muscle with aging." J Gerontol A Biol Sci Med Sci **62**(11): 1204-1210.
Sonveaux, P., F. Vegran, T. Schroeder, M. C. Wergin, J. Verrax, Z. N. Rabbani, C. J. De Saedeleer, K. M. Kennedy, C. Diepart, B. F. Jordan, M. J. Kelley, B. Gallez, M. L. Wahl, O. Feron and M. W. Dewhirst (2008). "Targeting lactate-fueled respiration selectively kills hypoxic tumor cells in mice." J Clin Invest **118**(12): 3930-3942.
Sooparb, S., S. R. Price, J. Shaoguang and H. A. Franch (2004). "Suppression of chaperone-mediated autophagy in the renal cortex during acute diabetes mellitus." Kidney Int **65**(6): 2135-2144.
Soulis-Liparota, T., M. Cooper, D. Papazoglou, B. Clarke and G. Jerums (1991). "Retardation by aminoguanidine of development of albuminuria, mesangial expansion, and tissue fluorescence in streptozocin-induced diabetic rat." Diabetes **40**(10): 1328-1334.
Soulis, T., M. E. Cooper, D. Vranes, R. Bucala and G. Jerums (1996). "Effects of aminoguanidine in preventing experimental diabetic nephropathy are related to the duration of treatment." Kidney Int **50**(2): 627-634.
Sousa Silva, M., R. A. Gomes, A. E. Ferreira, A. Ponces Freire and C. Cordeiro (2013). "The glyoxalase pathway: the first hundred years... and beyond." Biochem J **453**(1): 1-15.
Speer, O., S. Morkunaite-Haimi, J. Liobikas, M. Franck, L. Hensbo, M. D. Linder, P. K. Kinnunen, T. Wallimann and O. Eriksson (2003). "Rapid suppression of mitochondrial permeability transition by methylglyoxal. Role of reversible arginine modification." J Biol Chem **278**(37): 34757-34763.
Sudol, M. (1994). "Yes-associated protein (YAP65) is a proline-rich phosphoprotein that binds to the SH3 domain of the Yes proto-oncogene product." Oncogene **9**(8): 2145-2152.
Szent-Gyorgyi, A. and L. Egyud (1966). "On regulators of cell division." Science **152**(3722): 676-677.
Szent-Gyorgyi, A., L. G. Egyud and J. A. McLaughlin (1967). "Keto-aldehydes and cell division." Science **155**(3762): 539-541.
Tajes, M., A. Eraso-Pichot, F. Rubio-Moscardo, B. Guivernau, M. Bosch-Morato, V. Valls-Comamala and F. J. Munoz (2014). "Methylglyoxal reduces mitochondrial potential and activates Bax and caspase-3 in neurons: Implications for Alzheimer's disease." Neurosci Lett **580**: 78-82.
Takada, M., T. Koizumi, H. Toyama, Y. Suzuki and Y. Kuroda (2001). "Differential expression of RAGE in human pancreatic carcinoma cells." Hepatogastroenterology **48**(42): 1577-1578.
Takahashi, K. (1968). "The reaction of phenylglyoxal with arginine residues in proteins." J Biol Chem **243**(23): 6171-6179.
Takahashi, Y., Y. Miyoshi, C. Takahata, N. Irahara, T. Taguchi, Y. Tamaki and S. Noguchi (2005). "Down-regulation of LATS1 and LATS2 mRNA expression by promoter hypermethylation and its association with biologically aggressive phenotype in human breast cancers." Clin Cancer Res **11**(4): 1380-1385.

Takamiya, R., M. Takahashi, T. Myint, Y. S. Park, N. Miyazawa, T. Endo, N. Fujiwara, H. Sakiyama, Y. Misonou, Y. Miyamoto, J. Fujii and N. Taniguchi (2003). "Glycation proceeds faster in mutated Cu, Zn-superoxide dismutases related to familial amyotrophic lateral sclerosis." FASEB J **17**(8): 938-940.
Takanashi, M., T. Sakurai and S. Tsuchiya (1992). "Identification of the carboxymethyllysine residue in the advanced stage of glycated human serum albumin." Chem Pharm Bull (Tokyo) **40**(3): 705-708.
Takiyama, Y., T. Harumi, J. Watanabe, Y. Fujita, J. Honjo, N. Shimizu, Y. Makino and M. Haneda (2011). "Tubular injury in a rat model of type 2 diabetes is prevented by metformin: a possible role of HIF-1alpha expression and oxygen metabolism." Diabetes **60**(3): 981-992.
Talesa, V., L. Uotila, M. Koivusalo, G. Principato, E. Giovannini and G. Rosi (1988). "Demonstration of glyoxalase II in rat liver mitochondria. Partial purification and occurrence in multiple forms." Biochim Biophys Acta **955**(1): 103-110.
Tanimoto, M., T. Gohda, S. Kaneko, S. Hagiwara, M. Murakoshi, T. Aoki, K. Yamada, T. Ito, M. Matsumoto, S. Horikoshi and Y. Tomino (2007). "Effect of pyridoxamine (K-163), an inhibitor of advanced glycation end products, on type 2 diabetic nephropathy in KK-A(y)/Ta mice." Metabolism **56**(2): 160-167.
Tao, X. and L. Tong (2003). "Crystal structure of human DJ-1, a protein associated with early onset Parkinson's disease." J Biol Chem **278**(33): 31372-31379.
Thangarajah, H., D. Yao, E. I. Chang, Y. Shi, L. Jazayeri, I. N. Vial, R. D. Galiano, X. L. Du, R. Grogan, M. G. Galvez, M. Januszyk, M. Brownlee and G. C. Gurtner (2009). "The molecular basis for impaired hypoxia-induced VEGF expression in diabetic tissues." Proc Natl Acad Sci U S A **106**(32): 13505-13510.
Thimmulappa, R. K., K. H. Mai, S. Srisuma, T. W. Kensler, M. Yamamoto and S. Biswal (2002). "Identification of Nrf2-regulated genes induced by the chemopreventive agent sulforaphane by oligonucleotide microarray." Cancer Res **62**(18): 5196-5203.
Thornalley, P. J. (1988). "Modification of the glyoxalase system in human red blood cells by glucose in vitro." Biochem J **254**(3): 751-755.
Thornalley, P. J. (1990). "The glyoxalase system: new developments towards functional characterization of a metabolic pathway fundamental to biological life." Biochem J **269**(1): 1-11.
Thornalley, P. J. (1993). "The glyoxalase system in health and disease." Mol Aspects Med **14**(4): 287-371.
Thornalley, P. J. (1994). "Methylglyoxal, glyoxalases and the development of diabetic complications." Amino Acids **6**(1): 15-23.
Thornalley, P. J. (1996). "Pharmacology of methylglyoxal: formation, modification of proteins and nucleic acids, and enzymatic detoxification--a role in pathogenesis and antiproliferative chemotherapy." Gen Pharmacol **27**(4): 565-573.
Thornalley, P. J. (2003). "Protecting the genome: defence against nucleotide glycation and emerging role of glyoxalase I overexpression in multidrug resistance in cancer chemotherapy." Biochem Soc Trans **31**(Pt 6): 1372-1377.
Thornalley, P. J. (2003). "Use of aminoguanidine (Pimagedine) to prevent the formation of advanced glycation endproducts." Arch Biochem Biophys **419**(1): 31-40.
Thornalley, P. J. (2005). "Dicarbonyl intermediates in the maillard reaction." Ann N Y Acad Sci **1043**: 111-117.
Thornalley, P. J. (2008). "Protein and nucleotide damage by glyoxal and methylglyoxal in physiological systems--role in ageing and disease." Drug Metabol Drug Interact **23**(1-2): 125-150.
Thornalley, P. J., S. Battah, N. Ahmed, N. Karachalias, S. Agalou, R. Babaei-Jadidi and A. Dawnay (2003). "Quantitative screening of advanced glycation endproducts in cellular and extracellular proteins by tandem mass spectrometry." Biochem J **375**(Pt 3): 581-592.

Thornalley, P. J., L. G. Edwards, Y. Kang, C. Wyatt, N. Davies, M. J. Ladan and J. Double (1996). "Antitumour activity of S-p-bromobenzylglutathione cyclopentyl diester in vitro and in vivo. Inhibition of glyoxalase I and induction of apoptosis." Biochem Pharmacol **51**(10): 1365-1372.
Thornalley, P. J., N. I. Hooper, P. E. Jennings, C. M. Florkowski, A. F. Jones, J. Lunec and A. H. Barnett (1989). "The human red blood cell glyoxalase system in diabetes mellitus." Diabetes Res Clin Pract **7**(2): 115-120.
Thornalley, P. J., A. Langborg and H. S. Minhas (1999). "Formation of glyoxal, methylglyoxal and 3-deoxyglucosone in the glycation of proteins by glucose." Biochem J **344 Pt 1**: 109-116.
Thornalley, P. J. and H. S. Minhas (1999). "Rapid hydrolysis and slow alpha,beta-dicarbonyl cleavage of an agent proposed to cleave glucose-derived protein cross-links." Biochem Pharmacol **57**(3): 303-307.
Thornalley, P. J. and N. Rabbani (2011). "Glyoxalase in tumourigenesis and multidrug resistance." Semin Cell Dev Biol **22**(3): 318-325.
Thornalley, P. J., M. Strath and R. J. Wilson (1994). "Antimalarial activity in vitro of the glyoxalase I inhibitor diester, S-p-bromobenzylglutathione diethyl ester." Biochem Pharmacol **47**(2): 418-420.
Thornalley, P. J., S. Waris, T. Fleming, T. Santarius, S. J. Larkin, B. M. Winklhofer-Roob, M. R. Stratton and N. Rabbani (2010). "Imidazopurinones are markers of physiological genomic damage linked to DNA instability and glyoxalase 1-associated tumour multidrug resistance." Nucleic Acids Res **38**(16): 5432-5442.
Tikellis, C., R. J. Pickering, D. Tsorotes, O. Huet, M. E. Cooper, K. Jandeleit-Dahm and M. C. Thomas (2014). "Dicarbonyl stress in the absence of hyperglycemia increases endothelial inflammation and atherogenesis similar to that observed in diabetes." Diabetes **63**(11): 3915-3925.
Trepel, J., M. Mollapour, G. Giaccone and L. Neckers (2010). "Targeting the dynamic HSP90 complex in cancer." Nat Rev Cancer **10**(8): 537-549.
Trombley, P. Q., M. S. Horning and L. J. Blakemore (2000). "Interactions between carnosine and zinc and copper: implications for neuromodulation and neuroprotection." Biochemistry (Mosc) **65**(7): 807-816.
Tsujimoto, Y. (1997). "Apoptosis and necrosis: intracellular ATP level as a determinant for cell death modes." Cell Death Differ **4**(6): 429-434.
Uchino, E., T. Fukushima, M. Tsunoda, T. Santa and K. Imai (2004). "Determination of rat blood S-D-lactoylglutathione by a column-switching high-performance liquid chromatography with precolumn fluorescence derivatization with 4-fluoro-7-nitro-2,1,3-benzoxadiazole." Anal Biochem **330**(2): 186-192.
van de Rijn, M., C. M. Perou, R. Tibshirani, P. Haas, O. Kallioniemi, J. Kononen, J. Torhorst, G. Sauter, M. Zuber, O. R. Kochli, F. Mross, H. Dieterich, R. Seitz, D. Ross, D. Botstein and P. Brown (2002). "Expression of cytokeratins 17 and 5 identifies a group of breast carcinomas with poor clinical outcome." Am J Pathol **161**(6): 1991-1996.
van der Brug, M. P., J. Blackinton, J. Chandran, L. Y. Hao, A. Lal, K. Mazan-Mamczarz, J. Martindale, C. Xie, R. Ahmad, K. J. Thomas, A. Beilina, J. R. Gibbs, J. Ding, A. J. Myers, M. Zhan, H. Cai, N. M. Bonini, M. Gorospe and M. R. Cookson (2008). "RNA binding activity of the recessive parkinsonism protein DJ-1 supports involvement in multiple cellular pathways." Proc Natl Acad Sci U S A **105**(29): 10244-10249.
van Heijst, J. W., H. W. Niessen, K. Hoekman and C. G. Schalkwijk (2005). "Advanced glycation end products in human cancer tissues: detection of Nepsilon-(carboxymethyl)lysine and argpyrimidine." Ann N Y Acad Sci **1043**: 725-733.
van Heijst, J. W., H. W. Niessen, R. J. Musters, V. W. van Hinsbergh, K. Hoekman and C. G. Schalkwijk (2006). "Argpyrimidine-modified Heat shock protein 27 in human non-small cell lung cancer: a possible mechanism for evasion of apoptosis." Cancer Lett **241**(2): 309-319.

Van Herreweghe, F., J. Mao, F. W. Chaplen, J. Grooten, K. Gevaert, J. Vandekerckhove and K. Vancompernolle (2002). "Tumor necrosis factor-induced modulation of glyoxalase I activities through phosphorylation by PKA results in cell death and is accompanied by the formation of a specific methylglyoxal-derived AGE." Proc Natl Acad Sci U S A **99**(2): 949-954.
Vander Heiden, M. G., L. C. Cantley and C. B. Thompson (2009). "Understanding the Warburg effect: the metabolic requirements of cell proliferation." Science **324**(5930): 1029-1033.
Vander Heiden, M. G., D. R. Plas, J. C. Rathmell, C. J. Fox, M. H. Harris and C. B. Thompson (2001). "Growth factors can influence cell growth and survival through effects on glucose metabolism." Mol Cell Biol **21**(17): 5899-5912.
Vander Jagt, D. L. (1993). "Glyoxalase II: molecular characteristics, kinetics and mechanism." Biochem Soc Trans **21**(2): 522-527.
Vander Jagt, D. L., L. P. Han and C. H. Lehman (1972). "Kinetic evaluation of substrate specificity in the glyoxalase-I-catalyzed disproportionation of -ketoaldehydes." Biochemistry **11**(20): 3735-3740.
Vander Jagt, D. L., B. Robinson, K. K. Taylor and L. A. Hunsaker (1992). "Reduction of trioses by NADPH-dependent aldo-keto reductases. Aldose reductase, methylglyoxal, and diabetic complications." J Biol Chem **267**(7): 4364-4369.
Vasan, S., P. Foiles and H. Founds (2003). "Therapeutic potential of breakers of advanced glycation end product-protein crosslinks." Arch Biochem Biophys **419**(1): 89-96.
Verzijl, N., J. DeGroot, Z. C. Ben, O. Brau-Benjamin, A. Maroudas, R. A. Bank, J. Mizrahi, C. G. Schalkwijk, S. R. Thorpe, J. W. Baynes, J. W. Bijlsma, F. P. Lafeber and J. M. TeKoppele (2002). "Crosslinking by advanced glycation end products increases the stiffness of the collagen network in human articular cartilage: a possible mechanism through which age is a risk factor for osteoarthritis." Arthritis Rheum **46**(1): 114-123.
Verzijl, N., J. DeGroot, E. Oldehinkel, R. A. Bank, S. R. Thorpe, J. W. Baynes, M. T. Bayliss, J. W. Bijlsma, F. P. Lafeber and J. M. Tekoppele (2000). "Age-related accumulation of Maillard reaction products in human articular cartilage collagen." Biochem J **350 Pt 2**: 381-387.
Verzijl, N., J. DeGroot, S. R. Thorpe, R. A. Bank, J. N. Shaw, T. J. Lyons, J. W. Bijlsma, F. P. Lafeber, J. W. Baynes and J. M. TeKoppele (2000). "Effect of collagen turnover on the accumulation of advanced glycation end products." J Biol Chem **275**(50): 39027-39031.
Vince, R., S. Daluge and W. B. Wadd (1971). "Studies on the inhibition of glyoxalase I by S-substituted glutathiones." J Med Chem **14**(5): 402-404.
Vince, R. and W. B. Wadd (1969). "Glyoxalase inhibitors as potential anticancer agents." Biochem Biophys Res Commun **35**(5): 593-598.
Viollet, B., B. Guigas, N. Sanz Garcia, J. Leclerc, M. Foretz and F. Andreelli (2012). "Cellular and molecular mechanisms of metformin: an overview." Clin Sci (Lond) **122**(6): 253-270.
Vitek, M. P., K. Bhattacharya, J. M. Glendening, E. Stopa, H. Vlassara, R. Bucala, K. Manogue and A. Cerami (1994). "Advanced glycation end products contribute to amyloidosis in Alzheimer disease." Proc Natl Acad Sci U S A **91**(11): 4766-4770.
Viteri, G., G. Carrard, I. Birlouez-Aragon, E. Silva and B. Friguet (2004). "Age-dependent protein modifications and declining proteasome activity in the human lens." Arch Biochem Biophys **427**(2): 197-203.
Voziyan, P. A., T. O. Metz, J. W. Baynes and B. G. Hudson (2002). "A post-Amadori inhibitor pyridoxamine also inhibits chemical modification of proteins by scavenging carbonyl intermediates of carbohydrate and lipid degradation." J Biol Chem **277**(5): 3397-3403.
Vulesevic, B., B. McNeill, F. Giacco, K. Maeda, N. J. Blackburn, M. Brownlee, R. W. Milne and E. J. Suuronen (2016). "Methylglyoxal-Induced Endothelial Cell Loss and Inflammation Contribute to the Development of Diabetic Cardiomyopathy." Diabetes **65**(6): 1699-1713.
Waanders, F., E. van den Berg, R. Nagai, I. van Veen, G. Navis and H. van Goor (2008). "Renoprotective effects of the AGE-inhibitor pyridoxamine in experimental chronic allograft nephropathy in rats." Nephrol Dial Transplant **23**(2): 518-524.

Wang, L. W., Z. S. Li, D. W. Zou, Z. D. Jin, J. Gao and G. M. Xu (2008). "Metformin induces apoptosis of pancreatic cancer cells." World J Gastroenterol **14**(47): 7192-7198.
Wang, T., E. F. Douglass, Jr., K. J. Fitzgerald and D. A. Spiegel (2013). "A "turn-on" fluorescent sensor for methylglyoxal." J Am Chem Soc **135**(33): 12429-12433.
Wang, W., Z. D. Xiao, X. Li, K. E. Aziz, B. Gan, R. L. Johnson and J. Chen (2015). "AMPK modulates Hippo pathway activity to regulate energy homeostasis." Nat Cell Biol **17**(4): 490-499.
Wang, X., M. Chen, J. Zhou and X. Zhang (2014). "HSP27, 70 and 90, anti-apoptotic proteins, in clinical cancer therapy (Review)." Int J Oncol **45**(1): 18-30.
Wang, Y., Y. Kuramitsu, T. Ueno, N. Suzuki, S. Yoshino, N. Iizuka, J. Akada, T. Kitagawa, M. Oka and K. Nakamura (2012). "Glyoxalase I (GLO1) is up-regulated in pancreatic cancerous tissues compared with related non-cancerous tissues." Anticancer Res **32**(8): 3219-3222.
Weigelt, B., J. L. Peterse and L. J. van 't Veer (2005). "Breast cancer metastasis: markers and models." Nat Rev Cancer **5**(8): 591-602.
Weinberg, F., R. Hamanaka, W. W. Wheaton, S. Weinberg, J. Joseph, M. Lopez, B. Kalyanaraman, G. M. Mutlu, G. R. Budinger and N. S. Chandel (2010). "Mitochondrial metabolism and ROS generation are essential for Kras-mediated tumorigenicity." Proc Natl Acad Sci U S A **107**(19): 8788-8793.
Wellen, K. E., C. Lu, A. Mancuso, J. M. Lemons, M. Ryczko, J. W. Dennis, J. D. Rabinowitz, H. A. Coller and C. B. Thompson (2010). "The hexosamine biosynthetic pathway couples growth factor-induced glutamine uptake to glucose metabolism." Genes Dev **24**(24): 2784-2799.
Whitesell, L. and S. L. Lindquist (2005). "HSP90 and the chaperoning of cancer." Nat Rev Cancer **5**(10): 761-772.
Wieman, H. L., J. A. Wofford and J. C. Rathmell (2007). "Cytokine stimulation promotes glucose uptake via phosphatidylinositol-3 kinase/Akt regulation of Glut1 activity and trafficking." Mol Biol Cell **18**(4): 1437-1446.
Williams, A. C., T. J. Collard and C. Paraskeva (1999). "An acidic environment leads to p53 dependent induction of apoptosis in human adenoma and carcinoma cell lines: implications for clonal selection during colorectal carcinogenesis." Oncogene **18**(21): 3199-3204.
Williams, M. E., W. K. Bolton, R. G. Khalifah, T. P. Degenhardt, R. J. Schotzinger and J. B. McGill (2007). "Effects of pyridoxamine in combined phase 2 studies of patients with type 1 and type 2 diabetes and overt nephropathy." Am J Nephrol **27**(6): 605-614.
Wilson, A. F., R. C. Elston, L. D. Tran and R. M. Siervogel (1991). "Use of the robust sib-pair method to screen for single-locus, multiple-locus, and pleiotropic effects: application to traits related to hypertension." Am J Hum Genet **48**(5): 862-872.
Witztum, J. L., E. M. Mahoney, M. J. Branks, M. Fisher, R. Elam and D. Steinberg (1982). "Nonenzymatic glucosylation of low-density lipoprotein alters its biologic activity." Diabetes **31**(4 Pt 1): 283-291.
Wolf, I., S. Sadetzki, I. Gluck, B. Oberman, M. Ben-David, M. Z. Papa, R. Catane and B. Kaufman (2006). "Association between diabetes mellitus and adverse characteristics of breast cancer at presentation." Eur J Cancer **42**(8): 1077-1082.
Wooster, R., G. Bignell, J. Lancaster, S. Swift, S. Seal, J. Mangion, N. Collins, S. Gregory, C. Gumbs and G. Micklem (1995). "Identification of the breast cancer susceptibility gene BRCA2." Nature **378**(6559): 789-792.
Wu, L. (2005). "The pro-oxidant role of methylglyoxal in mesenteric artery smooth muscle cells." Can J Physiol Pharmacol **83**(1): 63-68.
Xia, H., H. Qi, Y. Li, J. Pei, J. Barton, M. Blackstad, T. Xu and W. Tao (2002). "LATS1 tumor suppressor regulates G2/M transition and apoptosis." Oncogene **21**(8): 1233-1241.
Xu, Y. and X. Chen (2006). "Glyoxalase II, a detoxifying enzyme of glycolysis byproduct methylglyoxal and a target of p63 and p73, is a pro-survival factor of the p53 family." J Biol Chem **281**(36): 26702-26713.

Xue, J., R. Ray, D. Singer, D. Bohme, D. S. Burz, V. Rai, R. Hoffmann and A. Shekhtman (2014). "The receptor for advanced glycation end products (RAGE) specifically recognizes methylglyoxal-derived AGEs." Biochemistry **53**(20): 3327-3335.
Xue, M., N. Rabbani, H. Momiji, P. Imbasi, M. M. Anwar, N. Kitteringham, B. K. Park, T. Souma, T. Moriguchi, M. Yamamoto and P. J. Thornalley (2012). "Transcriptional control of glyoxalase 1 by Nrf2 provides a stress-responsive defence against dicarbonyl glycation." Biochem J **443**(1): 213-222.
Xue, M., N. Rabbani and P. J. Thornalley (2011). "Glyoxalase in ageing." Semin Cell Dev Biol **22**(3): 293-301.
Yan, S. D., X. Chen, A. M. Schmidt, J. Brett, G. Godman, Y. S. Zou, C. W. Scott, C. Caputo, T. Frappier, M. A. Smith and et al. (1994). "Glycated tau protein in Alzheimer disease: a mechanism for induction of oxidant stress." Proc Natl Acad Sci U S A **91**(16): 7787-7791.
Yao, D. and M. Brownlee (2010). "Hyperglycemia-induced reactive oxygen species increase expression of the receptor for advanced glycation end products (RAGE) and RAGE ligands." Diabetes **59**(1): 249-255.
Yao, D., T. Taguchi, T. Matsumura, R. Pestell, D. Edelstein, I. Giardino, G. Suske, N. Rabbani, P. J. Thornalley, V. P. Sarthy, H. P. Hammes and M. Brownlee (2007). "High glucose increases angiopoietin-2 transcription in microvascular endothelial cells through methylglyoxal modification of mSin3A." J Biol Chem **282**(42): 31038-31045.
Yasuda, S., H. Fujii, T. Nakahara, N. Nishiumi, W. Takahashi, M. Ide and A. Shohtsu (2001). "18F-FDG PET detection of colonic adenomas." J Nucl Med **42**(7): 989-992.
Yego, E. C. and S. Mohr (2010). "siah-1 Protein is necessary for high glucose-induced glyceraldehyde-3-phosphate dehydrogenase nuclear accumulation and cell death in Muller cells." J Biol Chem **285**(5): 3181-3190.
Yim, H. S., S. O. Kang, Y. C. Hah, P. B. Chock and M. B. Yim (1995). "Free radicals generated during the glycation reaction of amino acids by methylglyoxal. A model study of protein-cross-linked free radicals." J Biol Chem **270**(47): 28228-28233.
Younes, M., L. V. Lechago and J. Lechago (1996). "Overexpression of the human erythrocyte glucose transporter occurs as a late event in human colorectal carcinogenesis and is associated with an increased incidence of lymph node metastases." Clin Cancer Res **2**(7): 1151-1154.
Yun, J., C. Rago, I. Cheong, R. Pagliarini, P. Angenendt, H. Rajagopalan, K. Schmidt, J. K. Willson, S. Markowitz, S. Zhou, L. A. Diaz, Jr., V. E. Velculescu, C. Lengauer, K. W. Kinzler, B. Vogelstein and N. Papadopoulos (2009). "Glucose deprivation contributes to the development of KRAS pathway mutations in tumor cells." Science **325**(5947): 1555-1559.
Zender, L., W. Xue, J. Zuber, C. P. Semighini, A. Krasnitz, B. Ma, P. Zender, S. Kubicka, J. M. Luk, P. Schirmacher, W. R. McCombie, M. Wigler, J. Hicks, G. J. Hannon, S. Powers and S. W. Lowe (2008). "An oncogenomics-based in vivo RNAi screen identifies tumor suppressors in liver cancer." Cell **135**(5): 852-864.
Zhang, D., L. K. Tai, L. L. Wong, L. L. Chiu, S. K. Sethi and E. S. Koay (2005). "Proteomic study reveals that proteins involved in metabolic and detoxification pathways are highly expressed in HER-2/neu-positive breast cancer." Mol Cell Proteomics **4**(11): 1686-1696.
Zhang, H., C. Y. Liu, Z. Y. Zha, B. Zhao, J. Yao, S. Zhao, Y. Xiong, Q. Y. Lei and K. L. Guan (2009). "TEAD transcription factors mediate the function of TAZ in cell growth and epithelial-mesenchymal transition." J Biol Chem **284**(20): 13355-13362.
Zhang, J., G. A. Smolen and D. A. Haber (2008). "Negative regulation of YAP by LATS1 underscores evolutionary conservation of the Drosophila Hippo pathway." Cancer Res **68**(8): 2789-2794.
Zhang, S., X. Liang, X. Zheng, H. Huang, X. Chen, K. Wu, B. Wang and S. Ma (2014). "Glo1 genetic amplification as a potential therapeutic target in hepatocellular carcinoma." Int J Clin Exp Pathol **7**(5): 2079-2090.

Zhao, B., L. Li, Q. Lei and K. L. Guan (2010). "The Hippo-YAP pathway in organ size control and tumorigenesis: an updated version." Genes Dev **24**(9): 862-874.
Zhao, B., X. Ye, J. Yu, L. Li, W. Li, S. Li, J. Yu, J. D. Lin, C. Y. Wang, A. M. Chinnaiyan, Z. C. Lai and K. L. Guan (2008). "TEAD mediates YAP-dependent gene induction and growth control." Genes Dev **22**(14): 1962-1971.
Zhu, P., H. Lin, C. Sun, F. Lin, H. Yu, X. Zhuo, C. Zhou and Z. Deng (2012). "Synergistic effects of telmisartan and pyridoxamine on early renal damage in spontaneously hypertensive rats." Mol Med Rep **5**(3): 655-662.
Zhuang, Y. and W. K. Miskimins (2008). "Cell cycle arrest in Metformin treated breast cancer cells involves activation of AMPK, downregulation of cyclin D1, and requires p27Kip1 or p21Cip1." J Mol Signal **3**: 18.
Zu, X. L. and M. Guppy (2004). "Cancer metabolism: facts, fantasy, and fiction." Biochem Biophys Res Commun **313**(3): 459-465.

VI. Personal bibliography

VI. Personal bibliography

1) Lamour V, **Nokin MJ**, Henry A, Castronovo V, Bellahcène A., SIBLING proteins: molecular tools for tumor progression and angiogenesis, Medecine Sciences, 2013

2) Chiavarina B*, **Nokin MJ***, Durieux F, Bianchi E, Turtoi A, Peulen O, Peixoto P, Irigaray P, Uchida K, Belpomme D, Delvenne P, Castronovo V and Bellahcène A, Triple negative tumors accumulate significantly less arg-pyrimidine, methylglyoxal specific adducts, than other human breast cancer subtypes, Oncotarget, 2014

3) Lamour V, Henry A, Kroonen J, **Nokin MJ**, von Marschall Z, Fisher L W, Chau TL, Chariot A, Sanson M, Delattre JY, Peulen O, Rogister B, Castronovo V and Bellahcène A, Targeting osteopontin suppresses glioblastoma stem-like cell character and tumorigenicity in vivo, International Journal of Cancer, 2015

4) **Nokin MJ**, Durieux F, Peixoto P, Chiavarina B, Peulen O, Blomme A, Turtoi A, Costanza B, Smargiasso N, Baiwir D, Leenders J, De Tullio P, Bianchi E, Thiry M, Uchida K, Spiegel DA, R. Cochrane JR, Hutton CA, De Pauw E, Delvenne P, Belpomme D, Castronovo V and Bellahcène A, Methylglyoxal, a glycolysis side-product, induces Hsp90 post-translational glycation and YAP-mediated breast tumor growth and metastasis, under review at eLife Journal (July 2016)

5) Henry A, **Nokin MJ**, Leroi N, Lallemand F, Lambert J, Goffart N, Roncarati P, Bianchi E, Peixoto P, Blomme A, Turtoi A, Peulen O, Habraken Y, Scholtes F, Martinive P, Delvenne P, Rogister B, Castronovo V and Bellahcène A, New role of osteopontin in DNA repair and impact on human glioblastoma radiosensitivity, under review at Oncotarget Journal (July 2016)

Summary

Several epidemiological, clinical and experimental studies reported the key role of impaired energy metabolism in cancer. This has led us to study methylglyoxal (MG), a glycolysis by-product. This highly reactive dicarbonyl metabolite contributes to the formation of advanced glycation end products (adducts) involved in the development and progression of many diseases such as diabetes and premature aging. Through glycation process, MG modifies the function and/or the stability of proteins, lipids and DNA. All these effects are grouped under the term "carbonyl stress". In order to limit these molecular damages, cells have developed a mechanism for effective MG detoxification composed of two enzymes, the glyoxalases 1 and 2. These enzymes convert MG into D-lactate in presence of reduced glutathione. Similar to oxidative stress, which is well-known to be involved in tumor development, cancer cells could benefit from carbonyl stress to promote tumorigenesis. In a descriptive study using a large cohort of breast adenocarcinoma, we have first demonstrated a strong accumulation of argpyrimidine adducts in cancer cells compared to non-tumoral tissue. These latter results suggest the potential involvement of MG in the development of breast cancers. Several recent studies have established a link between glucose metabolism and the transcription cofactor Yes-associated protein (YAP). In a second study, we demonstrated that MG induces nuclear accumulation of YAP in breast cancer cells through the glycation of the chaperone protein, heat shock protein 90. The nuclear accumulation of this oncoprotein has been correlated with both tumor progression and metastatic dissemination *in vivo*. In the continuity of this work, we have identified a pro-metastatic gene signature in breast cancer cells displaying a high carbonyl stress. Ongoing experiments will help to better understand the role of carbonyl stress in cancer progression and could lead to innovative and original anti-cancer therapeutic approach.

Résumé

De nombreuses études épidémiologiques, cliniques et expérimentales démontrant le rôle clé de l'altération du métabolisme énergétique dans le cancer nous ont conduits à l'étude d'une molécule dérivant de la glycolyse : le méthylglyoxal (MG). Ce dicarbonyl hautement réactif contribue à la formation des produits terminaux de glycation avancée (adduits) impliqués dans le développement et l'aggravation de nombreuses pathologies comme le diabète et le vieillissement prématuré. Le MG inflige des glycations modifiant la fonction et/ou la stabilité des protéines, des lipides et de l'ADN. Tous ces effets sont regroupés sous le terme de « stress carbonyle ». Pour limiter ces agressions moléculaires, la cellule a mis en place un mécanisme enzymatique de détoxification efficace du MG, les glyoxalases 1 et 2. Ces enzymes transforment, en présence de glutathion réduit, le MG en D-lactate qui est inoffensif pour la cellule. A l'instar du stress oxydant, dont l'implication dans le développement tumoral n'est plus à démontrer, les cellules cancéreuses pourraient tirer profit du stress carbonyle pour promouvoir la tumorigenèse. Lors de notre première étude immunohistologique sur une large cohorte d'adénocarcinomes de sein, nous avons mis en évidence une forte accumulation d'adduits argpyrimidine dans les cellules cancéreuses par rapport aux tissus sains associés. Ces résultats suggèrent la participation du MG dans le développement des cancers mammaires. Plusieurs études récentes ont établi un lien entre le métabolisme du glucose et le co-facteur de transcription *Yes-associated Protein* (YAP). Lors de notre seconde étude, nous avons démontré que le MG entraine une accumulation nucléaire de YAP dans les cellules cancéreuses mammaires via la glycation de la *heat shock protein 90*. L'accumulation nucléaire de cette oncoprotéine a été corrélée à une augmentation de la croissance tumorale et au développement de métastases *in vivo.* Dans la continuité de ces travaux, nous avons identifié une signature de gènes pro-métastatiques au sein de cellules cancéreuses mammaires présentant un haut stress carbonyle. Des travaux en cours permettront de mieux comprendre le rôle du MG au cours de la progression cancéreuse et métastatique. Enfin, l'étude de l'implication du stress carbonyle dans le développement et la progression des cancers pourrait aboutir à une approche thérapeutique anti-cancéreuse innovante et originale.